NASA Technical Memorandum 107762

DSMC SIMULATIONS OF MACH 20 NITROGEN FLOWS ABOUT A 70° BLUNTED CONE AND ITS WAKE

James N. Moss

Virendra K. Dogra

Richard G. Wilmoth

August 1993

National Aeronautics and Space Administration

Langley Research Center
Hampton, Virginia 23681-0001

DSMC SIMULATIONS OF MACH 20 NITROGEN FLOWS ABOUT A 70° BLUNTED CONE AND ITS WAKE

James N. Moss
NASA Langley Research Center
Hampton, VA

Virendra K. Dogra
ViGYAN, Inc.
Hampton, VA

and

Richard G. Wilmoth
NASA Langley Research Center
Hampton, VA

Abstract

Numerical results obtained with the direct simulation Monte Carlo (DSMC) method are presented for Mach 20 nitrogen flow about a 70-deg blunted cone. The flow conditions simulated are those that can be obtained in existing low-density hypersonic wind tunnels. Three sets of flow conditions are simulated with freestream Knudsen numbers ranging from 0.03 to 0.001. The focus is to characterize the wake flow under rarefied conditions. This is accomplished by calculating the influence of rarefaction on wake structure along with the impact that an afterbody has on flow features. This data report presents extensive information concerning flowfield features and surface quantities.

Nomenclature

A	base area of cone, $A = \pi d^2/4$
C_D	drag coefficient, $C_D = 2D/\rho_\infty V_\infty^2 A$
C_f	skin friction coefficient, $C_f = 2\tau/\rho_\infty V_\infty^2$

C_H	heat transfer coefficient, $C_H = 2q/\rho_\infty V_\infty^3$
C_p	pressure coefficient, $C_p = 2p/\rho_\infty V_\infty^2$
d	base diameter
dref	molecular diameter at reference temperature
D	drag
Kn	Knudsen number, $Kn = \lambda/d$
M	Mach number
$\overline{M}$	molecular weight, of N_2, $\overline{M} = 28.02$ g/mole
R	gas constant for N_2, $R = 296.7$ J/kgK
R_b	cone base radius
R_c	corner radius
R_n	nose radius
Re	Reynolds number, $Re = \rho V d/\mu$
Re2	total Reynolds number, $Re2 = Re_\infty (\mu_\infty/\mu_0)$
s	distance along the body surface measured from the stagnation point
$\bar{s}$	temperature exponent of the coefficient of viscosity
S	speed ratio, $S = V\sqrt{\overline{M}/2RT}$
T	thermodynamic temperature
T_i	internal kinetic temperature
T_{ov}	overall kinetic temperature
T_r	rotational temperature
T_t	translational
T_w	surface temperature
u	axial velocity
v	radial velocity
V	velocity
x	axial distance from stagnation point measured along symmetry axis

x_b	location of model base plane
x_s	location of wake stagnation point
y	radial distance from symmetry axis
Z_r	rotational collision number
γ	ratio of specific heats, $\gamma = 1.4$
Γ	Gamma function
Δ	size of vortex, $(x_s - x_b)$
λ	mean free path
μ	dynamic viscosity
ρ	density
σ	collision cross section
τ	shear stress

Subscripts

ref	reference value
w	surface values
∞	freestream values

Introduction

There is a lack of both experimental and computational data for providing an understanding of the effects of rarefaction on wake flows. Precise determination of wake closure is a critical issue for aerobrakes since the low lift-to-drag ratio aeroshell designs impose constraints on payload configuration/spacecraft design. The issue is that the payload must fit into the wake in a manner that avoids shear layer impingement in order to minimize heating. A perception exists[1] that the aerothermodynamics of wake flows cannot be accurately predicted. This perception occurs because two complicating phenomena can coexist for aerobraking application. One phenomena is due to rarefaction effects as the

relatively high-density forebody flow expands into the wake. At typical perigees[2], local Knudsen numbers of the order of 0.1 occur in the near wake. Consequently, continuum analyses cannot describe the near wake at the rarefied conditions encountered at substantially higher altitudes. Because of high aerobrake velocities, the second phenomena is the influence of thermochemical nonequilibrium on the wake structure as highly dissociated flow expands into the wake. The combination of these two phenomena brings into question the applicability of several aspects of physical modeling implemented in current computational tools, aspects that have limited testing against experimental data.

Two different approaches are available for simulating wake flows under low-density conditions. One is the continuum approach in which a set of model equations are solved numerically. The second is a molecular approach where a direct physical simulation is achieved by following the motion and interaction of modeled molecules. In the present study, the molecular approach is used to simulate hypersonic wake flows about a 70-deg blunted cone. The molecular simulations are achieved with Bird's[3-5] direct simulation Monte Carlo (DSMC) method. References 6 through 14 are examples of recent applications of the DSMC method to examine the wake structure of blunt bodies. Since the flow conditions selected for simulation are reproducible in low density wind tunnels, the importance of chemical reactions on wake structure is not addressed in the present study.

Objectives of the current study are twofold: first, provide an improved understanding of the effects of rarefaction on blunt body {generic Aeroassisted space transfer vehicles (ASTV's)} wake structure and, second, examine the impact of a model support (sting) on the wake structure. These objectives will be achieved as a part of a continuing[7-12] effort to provide computational information that will help clarify the fluid mechanics of blunt body wakes. Computation for three flow conditions are presented (Kn_∞ = 0.032, 0.011, and 0.001) and for each of

these flow condition three different computational domains were considered: forebody only, forebody and wake, and forebody-wake with a sting/afterbody. Data presented will be primarily for the later configuration highlighting both surface and flowfield quantities.

Computational Method and Boundary Conditions

The direct simulation Monte Carlo (DSMC) method[3-5] provides a numerical capability that acknowledges the discrete nature of a gas and thereby provides a capability of simulating flows across the complete flow spectrum of continuum to free molecular flows. However, the DSMC method is normally applied to the transitional and free molecular flow regimes since the computing requirements can become excessive for continuum applications. The three flow conditions examined (Table 1) include both continuum and transitional forebody flow. The model configurations and computational grid (Case 1) are shown in Figs. 1 and 2, respectively.

The computational domain is large enough so that the upstream and side boundaries can be specified as freestream conditions. The flow at the downstream outflow boundary is supersonic and vacuum conditions are specified. For all computations that included the wake, the outflow boundary was located 2.5 body diameters (0.125 m) downstream of the forebody stagnation point. Figure 1 presents information concerning model configurations and Fig. 2 shows the physical extent of the computational domain (for Case 1) which is subdivided into several unstructured regions with each region subdivided into computational cells. The number of simulated molecules is of the order of 10 per cell. Within a given region, each simulated molecule represents a fixed number of physical or real molecules (a large number on the order of 1.0×10^{10}). The unstructured regions allow one to substantially reduce the number of simulated molecules in

the flow domain and still meet the basic numerical requirements of steady flow problems.

The molecular collisions are simulated using the variable hard sphere (VHS) molecular model. This model employs the simple hard sphere angular scattering law so that all directions are equally possible for post-collision velocity in the center-of-mass frame of reference. However, the collision cross section is a function of the relative energy in the collision. The freestream viscosity and mean free path are evaluated using the VHS collision model with T_{ref} = 300 K, d_{ref} = 4.07×10^{-10} m and $\bar{s}$ = 0.75 (d_{ref} is the molecular diameter at reference temperature T_{ref} and $\bar{s}$ is the temperature exponent of the coefficient of viscosity). The freestream mean free path is calculated from the relation (see Ref. 3)

$$\lambda_\infty = \frac{(T_\infty / T_{ref})^\omega}{[\sqrt{2} n_\infty \sigma_{ref} (2-\omega)^\omega \Gamma(2-\omega)]} \tag{1}$$

$$\omega = \bar{s} - 1/2 \tag{2}$$

Energy exchange between kinetic and internal modes is controlled by the Larsen-Borgnakke[16] statistical model. For the present study, simulations are performed using a nonreacting gas model with one chemical species (N_2) while considering energy exchange between translational, rotational, and vibrational modes (rotational relaxation collision number of 5 and vibrational relaxation collison number of 50).

The effect of grid resolution on computed results is of particular interest for the present study. The results of such a study are included in Appendix A along with the sensitivity of the results to assumptions regarding the rotational collision number (Z_r values of 2.5, 5, and 10), and the fraction of molecule reflected specularly (0 and 20 percent) from the surface.

Freestream and Surface Conditions

The flow conditions and model size (Fig. 1) are those that can be accommodated in existing low-density hypersonic wind tunnels. The specific flow conditions are those for the SR3 tunnel[15] at the Centre National de la Recherche Scientifique (CNRS), and are listed in Table 1. The model surface temperature is assumed to be constant at 300 K and the gas-surface interaction model is diffuse with full thermal accommodation. Because of the relatively low-total temperature, the DSMC simulations model the nitrogen flow as a nonreacting gas with energy exchange between vibrational, rotational, and translational modes.

Results and Discussion

Data for each of the three wind tunnel conditions are presented separately (Case 1, Figs. 2 through 15; Case 2, Figs. 16 through 29; and Case 3, Figs. 30 through 43) followed by data (Figs. 44 through 49) showing the effect of rarefaction on surface and flowfield quantities. Tables 2 and 3 provide tabulated information concerning the aerodynamic forces, heating rates, and wake characterization as influenced by Knudsen number. Table 4 presents values of several of the numerical parameters used in the simulation including the magnitude of the time step (all time values shown are for region 1 [see Fig. 2(a) for example], the time in region 1 at which the overall computational flow domain was assumed to have reached steady state, the time at which the steady state sampling was terminated, the number of time steps between sampling, the number of computational cells, and the number of simulated molecules. The simulations were not time consistent since the computational time step, in general, varied from region to region. The magnitude of the time steps for each of the regions can be inferred from the data included in Tables 5 through 7 by taking the ratio of the time in the region of interest to that of region one and multiplying by the time step

of region one (Table 4). Tables 5 through 7 presents a summary of the freestream conditions and various nondimensional parameters along with a listing of surface coordinates (midpoint of surface element), pressure, skin friction, incident heat flux, reflected heat flux, net heat flux, and the number of simulated nitrogen molecules that have impacted the surface elements during the time averaging interval. The final grouping of information includes the wetted distance from the forebody stagnation point to each surface element centroid (s/R_N); the pressure, skin friction, and heat transfer coefficients; the corresponding free molecular coefficients; and the modified Newtonian pressure coefficient. Tables 5, 6, and 7 are for Cases 1, 2, and 3, respectively, with sting afterbody.

For all calculations, the wall temperature was constant at 300 K and the freestream flow was assumed to be uniform and in thermal equilibrium at the conditions listed in Table 1. The range of flow conditions considered is particularly interesting since the calculations show the absence of a wake vortex for the most rarefied case; however, a well defined and stable vortex exists for the remaining two conditions. With the presence of the sting, a vortex is calculated for all three cases. Specific results for each flow condition will now be discussed. Attention is focused on data obtained with an afterbody sting. The sting extends a distance of 0.115 m downstream of the base of the model (to the end of the computational domain).

Case 1

The grid used for Case 1 contained 13 regions as shown in Fig. 2. Contours and profiles of various flow variable are presented in Figs. 3 through 10 followed by surface data (Figs. 11 through 13).

Flow Structure. As evidenced by the particle traces [Fig. 3(a)], a small stable vortex develops for this condition, but is not present when the sting is absent

[Fig. 3(b)]. The point of separation is on the corner radius [see Fig. 1(a), just before location 4] near the location where the corner radius becomes tangent to the base plane. The minimum surface pressure occurs at or near this location, and this minimum becomes more pronounced for the smaller Knudsen number cases. All this information can be extracted from Tables 5 through 7. The location of the wake stagnation point with a sting is the location where the shear stress experiences a reversal in sign. For Case 1, this location is very close to the base plane as indicated in Table 3. The extent of the rarefaction in the near wake is clearly evident by the magnitude of the velocity slip. An indication of the slip velocity can be inferred from Fig. 4 where a comparison is presented of the axial velocity adjacent (cell center) to the sting and that along the symmetry axis for no sting. Another measure of the wake structure is the sonic line location, and Fig. 5 presents this information along with other selected Mach contours. Velocity vectors for the near wake are displayed in Fig. 6.

The density (Fig. 7) in the near wake is quite low with magnitudes as low as 5 percent of the freestream value near the base plane. Density profiles normal to the sting are presented in Fig. 8 showing the profiles at three locations downstream of the base plane which is located at x = 0.0104m.

The extent of thermal nonequilibrium can be deduced from the contour plots of Figs. 9(a) through 9(c) where the overall kinetic temperature, T_{ov}, (defined for a nonequilibrium gas as the weighted mean of the translational and internal temperatures), translational temperature, and rotational temperature are presented, respectively. For Case 1, most of the flow domain is in thermal nonequilibrium. Along the forebody or compression region, the rotational temperature generally lags the translational temperature. As the flow expands into the near wake region, the rotational temperature is greater than the corresponding translational value for most of the inner portion of the wake. A clearer indication of thermal nonequilibrium for the wake is presented in

Fig. 10(a) where profiles of the difference in translational and internal temperatures normalized by the overall temperature are displayed. The reason that these curves do not become zero at the outer edges of the computational domain is that the outer extent of the temperature disturbance has not been captured. This is not significant since the density field disturbance is adequately captured. The density at the outer computational boundary is within one percent of the freestream density [Fig. 7(a)]. Temperature jump and velocity slip are clearly evident along the sting as shown in Figs. 10(b) and 10(c).

Surface Results. The surface distribution for heating rate, pressure (normal force per unit area) and tangential shear stress are presented in Figs. 11 through 13. These data are presented as a function of nondimensional distance (s/R_n) along the surface measured from the forebody stagnation point. The flow expansion about the corner produces orders of magnitude reductions in surface quantities with respect to their forebody values. The semilog plots give a better perspective of the magnitude of heating and pressure along the base plane. These data show a significant amount of scatter for part of the corner and the base plane surface areas because of the very small sample size in these areas; that is, the number of molecules that have impacted these surface elements range from 20 to 600 rather than the thousand to tens of thousands that occur on other surface elements. (Excessive level of scatter[3] is present unless a macroscopic property is based on a statistically independent sample of the order of 1000.) Along most of the sting, the sample size was in the thousands (see Table 5) and the statistics are much better. The calculated base heating is more than three orders of magnitude less that forebody stagnation point heating with a magnitude of about 3 W/m^2 (0.03 percent of the stagnation value). The heating along the sting increases to a value of about 360 W/m^2 or about 3.6 percent of the forebody stagnation value. There is no evidence of a distinct shear layer impingement along the sting since the surface heating rate increases with distance downstream, reaches a

maximum and then decreases gradually. Qualitative features for the pressure distribution are similar to those for heating rate with the pressure along the sting obtaining a maximum near $s/R_n = 7.15$. The skin friction experiences a maximum (Fig. 13) just after reaching the base corner.

Effect of Sting on Wake. The presence of the sting alters the flow structure in that a small vortex is calculated with the sting [Fig. 3(a)]; however, it is absent without the sting [Fig. 3(b)]. The only region of the flowfield where the sting impacts the density is along the base of the model and along the sting. This is evident in Fig. 14(a) where the radial density profiles with and without the sting are compared at three axial locations. Near the sting and base locations, the sting produces a higher value of density and the surface heating [Fig. 14(a)] and the pressure along the base appears to be somewhat higher with the sting.

Effect of Afterbody on Forebody Solution. The effect of the afterbody or near wake on the forebody results is shown to be insignificant. Figures 15(a) through 15(d) present comparisons of various profiles (density, overall kinetic temperature, axial velocity, and radial velocity) resulting from forebody only solutions (vacuum outflow boundary condition used) and fully coupled results (without a sting) at the same physical location (above and near the maximum body radius). These results suggest that the forebody only results could be used to drive an uncoupled wake analysis as implemented in Ref. 17. In addition, these data show many of the rarefied features of the flow at this location as evidenced by the merger of the shock and shock layer and the sizable temperature jump and velocity slip at the cell center adjacent to the surface [last cell in region 4 adjacent to the surface--see Fig. 2(b)].

Cases 2 and 3

Identical information (presented for Case 1) is displayed in Figs. 16 through 29 for Case 2 and Figs. 30 through 43 for Case 3.

For the smaller Knudsen number cases, the size of the computational domain was reduced in both the radial direction and in the axial direction in front of the blunted cone. Also, the size of the computational cells was reduced, particularly along the forebody (Figs. 16 and 30). The surface sampling statistics are better for these two cases (see Tables 6 and 7) along the corner expansion and base plane, although there are still several surface elements where the sample size (molecules impacting a surface element) is less than one thousand (see Tables 6 and 7).

Effects of Rarefaction

The effects of rarefaction on the forebody flow structure are clearly evident from Fig. 44 where the density profiles along the stagnation streamline are presented for three flow conditions. For Cases 1 and 2 (Kn_∞ = 0.03 and 0.01, respectively), the density profiles show that the shock is very diffuse. However, for Case 3 where Kn_∞ = 0.001, the density profile shows a distinct yet thick shock. Near the stagnation point, a substantial density increase occurs. This is characteristic of hypersonic flows about cold blunt surfaces.

Within the near wake, a stable vortex is calculated for each of the three flow conditions provided there is a sting afterbody. Without the sting, a distinct vortex is evident only for Cases 2 and 3. The size of the vortex, Δ, is shown (Fig. 45) to increase exponentially with decreasing Kn. The magnitude of Δ is the distance measured from the base plane to the wake stagnation point (the point in the wake where the separated flow reattaches and the velocity is zero).

It is normally assumed that the location of the free shear layer in the near wake roughly bounds the usable volume behind an aerobrake available for payload positioning.[2] The concern is that the shear layer impingement may result in high, localized convective heating rates with magnitudes dependent on the severity of the impingement angle, the radius of curvature at the impingement zone, and the degree of rarefaction.

For the present cases, the free shear layer [Figs. 10(c), 24(c) and 38(c)] is not a distinct, narrow region within the wake, but a relatively thick region where the maximum gradients decrease noticeably with distance downstream of the base. Shear layer deflection angles have been measured experimentally and computed computationally for a number of flow conditions (see Ref. 2) at Reynolds number higher than the present flow conditions. The deflection angles were measured from a straight line drawn from the base corner to the measured location of flow attachment (payload/sting oil flow patterns) or to the peak heating point on the payload/sting as measured using phase change paint or heat transfer gages. The value of this angle (relative to the freestream velocity vector) has been measured as 17 deg for blunt axisymmetric bodies tested in the Langley 31-Inch Mach 10 tunnel at Reynolds numbers (based on base diameter) between 133,000 and 333,000.

For the present flow conditions, the calculated locations of reattachment (wake stagnation point) and peak heating on the sting differ substantially. Note that the maximum heating and pressure values along the sting (Figs. 46 and 47) do not occur as a sudden spike, but exists over an appreciable spatial extent that develops asymptotically. In the present results, there is a substantial difference between the wake stagnation point and peak heating locations and this difference increases with increasing Kn_∞. Furthermore, the shear layer deflection angle based on the previously discussed geometric definition and peak heating locations yield values ranging from 19 deg for Case 3 to much higher values for the larger Knudsen number cases.

The current findings are consistent with those reported by Brewer[13] where DSMC simulations were made for a 1.0 m diameter hemisphere with a 0.5 m cylindrical payload/afterbody. These calculations were for reacting air at the following conditions: freestream velocity of 10 km/s and altitudes of 86 to 110 km where the corresponding freestream Knudsen numbers ranged from 0.01 to 0.65.

Results of these calculations show that the wake stagnation point on the payload was quite close to the aerobrake base plane, and the location of peak payload heating was much further downstream of the aerobrake. Consequently, the DSMC results for both wind tunnel and flight conditions show that the heating rate along a sting/payload is quite benign at the wake stagnation point provided the wake flow is in the transitional/rarefied regime. As the Knudsen number decreases, the heating rate at the wake stagnation point location approaches the maximum heating rate along the sting/afterbody.

The maximum sting heating rates (Table 2) nondimensionalized by the forebody stagnation point value increases with decreasing Knudsen number. For Case 1 the ratio is 0.036 while that for Case 3 is 0.057. This trend is even more apparent along the base plane where (approximate values at $y/R_b = 0.5$) the nondimensional heating rate is 0.0003 for Case 1 and 0.008 for Case 3.

The surface heat transfer, pressure, and skin friction coefficients are presented in Figs. 46 through 48 for the three flow conditions. The heat transfer and skin friction coefficients are very sensitive to rarefaction effects. For the pressure coefficient, the data shows a significant sensitivity only along the base plane and sting. These data show that the heat transfer coefficient along the forebody and sting, in general, experiences the same trend in that the fraction of freestream energy ($C_H = 2q/\rho_\infty V_\infty^3$) transferred to the surface increases with increasing rarefaction. The reverse situation occurs along the base plane. In terms of the aerodynamics, we see that the drag coefficient (Table 2) increases with rarefaction and most of this increase is due to an increase in skin friction. The results show that the drag contribution due to friction increases from 2 percent for Case 3 to 8.4 percent for Case 1.

The sensitivity of the near wake flow structure to rarefaction is demonstrated in Figs. 49(a) through 49(d) where radial profiles (density, axial velocity, overall kinetic temperature, and a measure of thermal nonequilibrium) for the three

cases are presented. The profiles are for a x-location of 0.015 m or 4.6 mm downstream of the base plane. The most obvious effect of rarefaction on the radial profiles occurs at the bow shock and in the inner wake regions. As the Knudsen number decreases, the density near the base plane [Fig. 49(a)] becomes a much higher percentage of its freestream value [20 to 30 percent for Case 3 (Fig. 35) rather than 5 percent or less for Case 1 (Fig. 7)].

Reference 14 presented the results of a study comparing DSMC and Navier Stokes solutions for a monatomic gas flowing about a blunted two-dimensional wedge at 8 km/s. The blunted wedge had a 0.425 m nose radius, a 70-deg half angle, a 1.7 m height, and a rounded shoulder. The freestream Knudsen numbers considered were 0.016, 0.049, and 0.146.

The study of Ref. 14 identified a major discrepancy in the two solutions concerning the flow angle in the near wake for the more rarefied conditions. For the 0.16 Knudsen number case, the two methods were in agreement, however for $Kn_\infty = 0.146$, the two solutions predicted vastly different flow angles.

Figures 50 through 51 present flow angle contours for each of the three current cases. Included is an enlarged view of the near wake results. For Case 1 and 2, there exists a significant region of flow near the model base where the flow angle is 40 deg. For case 3, the turning angle is smaller and generally closer to 20 deg rather than 40 deg.

Concluding Remarks

This report provides an extensive amount of data characterizing both the forebody and wake flows about a blunt axisymmetric configuration (generic ASTV's). Specifically, the configuration is that being considered for Mars missions such as the Mars Environmental SURvey (MESUR) Network mission and the MESUR Pathfinder mission. The present study was focused on specific

wind tunnel conditions for which an experiment is planned. Future opportunities will exist for direct comparison with experimental data.

This study is an extension of the work of Ref. 11 where the actual wind tunnel model size is used in the current investigation. Solutions have been obtained with and without a sting afterbody. Three freestream flow conditions have been investigated (Knudsen numbers of 0.03, 0.01, and 0.001). The freestream was nitrogen at Mach 20 conditions. The two smaller Knudsen number cases would normally be considered as continuum flow along blunt forebodies. The present results show that rarefaction effects are very evident as the flow expands into the near wake even for Case 3 ($Kn_\infty = 0.001$). What is clear from the present calculations and those of Ref. 13 is that for both wind tunnel and flight conditions the location of the wake stagnation point and the location of the maximum convective heating rate along a sting/afterbody is not coincident. Furthermore, the separation between the two locations is a function of rarefaction. For wake flows, the convective heating rates near reattachment can be quite benign--only a small fraction of the peak sting/afterbody heating rate. The current results suggests that for aeroassist missions where the wake flow remains transitional, the size of the afterbody/payload could be much larger than that based on smaller Knudsen number experimental/computational data.

The calculated surface data along the base plane is of use in establishing trends but not specific quantitative numbers since the statistical scatter is too large (small sample size). This is particularly true of Case 1. The zonally-decoupled DSMC solution procedure demonstrated in Ref. 17 for the current flow conditions offers the opportunity to obtain quantitative information for the base surface properties in a computationally efficient manner.

References

[1]America at the Threshold, Report of the Synthesis Group on America's Space Exploration Initiative, p. 59, Superintendent of Documents, U.S. Government Printing Office, Washington, D.C., 1991.

[2]Gnoffo, P. A., Price, J. M., and Braun, R. D., "Computation of Near-Wake Aerobrake Flowfields," Journal of Spacecraft and Rockets, Vol. 29, No. 2, March-April 1992, pp. 182-189.

[3]Bird, G. A., Molecular Gas Dynamics, Clarendon Press, Oxford, 1976.

[4]Bird, G. A., "Monte Carlo Simulation in Engineering Context," Rarefied Gas Dynamics, Vol. 74, Part 1, edited by Sam S. Fisher, AIAA New York, 1981, pp. 239-255.

[5]Bird, G. A., "Direct Simulation of Gas Flows at the Molecular Level," Communications in Applied Numerical Method, Vol. 4, 1988, pp. 165-172.

[6]Brewer, E. B., "Direct Simulation of Aerothermal Loads for the Aeroassist Flight Experiment," NAS Technical Summaries, p. 10, March 1990, Feb. 1991.

[7]Moss, J. N. and Price, J. M., "Direct Simulation of AFE Forebody and Wake Flow with Thermal Radiation," Rarefied Gas Dynamics, Vol. 188, edited by E. P. Muntz, D. P. Weaver, and D. H. Campbell, AIAA New York, 1989, pp. 413-431.

[9]Dogra, V. K., Moss, J. N., Wilmoth, R. G., and Price, J. M., "Hypersonic Rarefied Flow Past Spheres Including Wake Structure," AIAA Paper 92-0495, January 1992.

[10]Dogra, V. K., Moss, J. N., Wilmoth, R. G., and Price, J. M., "DSMC Simulations of Hypersonic Low-Density Flow about an ASTV Including Wake Structure," Paper presented at the 18th Rarefied Gas Dynamics Symposium, July 26-31, 1992.

[11]Dogra, V. K., Moss, J. N., and Price, J. M., "Near Wake Structure for a Generic ASTV Configuration," AIAA Paper 93-0271, January 1993.

[12]Moss, J. N., Mitcheltree, R. A.,Dogra, V. K., and Wilmoth, R. G., "Hypersonic Blunt Body Wake Computations Using DSMC and Navier-Stokes Solvers, AIAA Paper 93-2807, July 1993.

[13]Brewer, E. B., "Hypersonic Rarefied Wake Characterization," NASA TP 3327, January 1993.

[14]Lumpkin, F. E., Boyd, I. D., and Venkatapathy, E., "Comparison of Continuum and Partical Simulations of Expanding Rarefied Flows," AIAA paper 93-0728, January 1993.

[15]Allegre, J., "The SR3 Low Density Wind-Tunnel: Facility Capabilities and Research Development," AIAA Paper 92-3972, July 1992.

[16]Borgnakke, C., and Larsen, P. S., "Statistical Collison Model for Monte Carlo Simulation of Polyatomic Gas Mixture," Journal of Computational Physics, Vol. 18, No. 4, 1975, pp. 405-420.

[17]Wilmoth, R. G., Mitcheltree, R. A., Moss, J. N., and Dogra, V. K., "Zonally-Decoupled DSMC Solutions of Hypersonic Blunt Body Wake Flows," AIAA Paper 93-2808, July 1993.

[18]Carnevale, E. H., Cary, C., and Larsen, G., "Ultrasonic Determination of Rotational Collision Numbers and Vibrational Relaxation Times of Polyatomic Gases at High Temperature," J. Chem. Phys., 1967, No. 8, p. 2829.

Appendix A
Effect of Grid Variations, Rotational Collision Number and Surface Reflection on Computed Results

Three aspects of the computations were examined parametrically: two associated with numerics (cell size and time step) and one with physical modeling (rotational energy exchange).

Cell Size

Since the current study was interested in both flowfield and surface results, one has to be particularly sensitive to the importance of cell size, particularly in the direction normal to the surface. Experience has shown that, if the cell size is on the order of one-third of the local mean free path, the results will be grid resolved. For many applications it is neither necessary nor practical to obtain such a grid resolution throughout the flow domain. In such instances, the focus has been to obtain cell dimensions on the order of one-third of the local mean free path in the direction normal to the surface and in the vicinity of the surface. In the direction of flow, provided the gradients are not large, the cell dimensions can be quite large in relation to the local mean free path. Consequently, the cells for two-dimensional and axisymmetric applications often have high aspect ratios (small in the body normal direction and large in the flow direction). Furthermore, as one moves away from the surface, the cell size in the normal direction can often be relaxed without altering the results. This philosophy was used to arrive iteratively at the grids used in the current study. That is, an acceptable grid was selected by trial and adjustment. This was done first for the forebody only. With the forebody grid established, the wake region grid was added and a couple of trail solutions and adjustments made to arrive at the wake grid. Note that, the grid used for the forebody only solutions was the same grid used for the forebody, wake and forebody, and wake with sting configuration [for example, the forebody grid was the same for all three runs for Case 2 (Table 4)].

The cell aspect ratio is quite high for the forebody cells, particularly the cells for Case 3. For most of the results presented in this report, data were obtained with the parameters listed in Table 4 for runs 4 (Case 1), 11 (Case 2), and 16 (Case 3).

For Case 1, the grid refinement was done where the number of cells in certain regions were increased (run 5 in Table 4). As Fig. A1 shows, when the number of computational cells were increased from 6,000 to 8,060, the impact on the calculated surface heating rate was insignificant and the same is true for the flow parameter.

For Case 3, the requirements become more demanding and the cells adjacent to the forebody surface were of the order of one-half of a local mean free path in the body normal direction in the region near the surface. For the corner expansion and along the base, the cells were of the order of a local mean free path. Since Case 3 requires a significant amount of computing time, the effect of altering the grid was investigated in two parts. First, the forebody solution was repeated with approximately three times the number of cells (18,900 rather than the standard 6,630). Figure 2A presents the surface heating rate distributions for these two solutions (runs 12 and 13 in Table 4) and close agreement is evident. The second aspect of the grid refinement study was done in Ref. 17 where a zonally-decoupled methodology was used to examine the sensitivity of only the near wake results to grid size without the sting. Solutions were obtained using the same near wake grid as used herein for run 14 (Table 4) and then with a much finer grid with the number of cells increased by a factor of four (twice as many in both the axial and radial direction). Agreement for the flowfield parameters are excellent (see Ref. 17). Additional calculations will be made to check the sensitivity of the sting heating to grid resolution in the wake for Case 3.

Time Step

Two time aspects were examined; one concerned with the time step and the other concerned with the question of whether we achieved steady flow in the wake. Since the computational domain was subdivided into an arbitrary number of regions and the time step, even though constant within a region, was region dependent, it is important to note that the time step is not completely arbitrary. First, it should satisfy physical constraints in that the time step should be small in relation to the local mean collision time since the DSMC simulation is basically a two step process: move and collide. These two events are simulated as separate and distinct events. During the movement process, collisions are not allowed. Then collisions are calculated on a cell by cell basis. The requirement that the time step be less than the mean collision is assured if

$$\Delta t = \min \left[\frac{\Delta x}{\bar{u}_{max}}, \frac{\Delta y}{\bar{v}_{max}} \right]$$

where

$$\bar{u}_{max} = (u + C'_m)_{max}$$
$$\bar{v}_{max} = (u + C'_m)_{max}$$

and C'_m is the most probable thermal speed. Experience has shown that this can be a conservative guide; that is, the time step can be increased beyond this limit without altering the results. This is demonstrated for each of the three cases in Table 4 where the forebody only solutions were calculated using a more conservative time step and the forebody and wake solutions were done at four to six times the more conservative values. As shown for runs 2 and 3 (Table 4), the effect on overall drag and stagnation heating was insignificant. Comparison of the surface heating rate results show excellent agreement (not shown) for these two runs.

The remaining constraint on the time step is associated with conservation of molecules at region boundaries. The number of physical molecules represented by a simulated molecule is defined by the user for each region. If we define F_{num} = actual molecules/simulated molecules, then F_{num} is specified for each region where the objective is to have on the order of ten molecules per cell. However, the current DSMC algorithm requires that the ratio of $F_{num}/\Delta t$ be the same for all regions so that the fluxes are conserved across region boundaries. Therefore, in the near wake where the density is low, one must use a much smaller F_{num} than in the high density forebody region to adequately populate the cells even through the cells are larger in the wake. This also means that the time step for these regions must also be reduced which is not a requirement imposed by the local mean collision time. Consequently, all solutions that included the wake were obtained with a time step that was at least two orders of magnitude smaller than required based on the mean collision time. This necessitated much larger run time because of the large number of time steps required to achieve steady flow in the wake while continuing to calculate the forebody flow long after it had achieved steady state (see Table 4). Further, a large portion of the near wake is subsonic. The combination of the low speed flow and smaller time step than physically required means that one must be very sensitive to the time required to achieve steady state in the near wake. The zonally-decoupled DSMC methodology demonstrated in Ref. 17 has been shown to be a viable approach for predicting overall mean-flow properties in the near wake for the present flow conditions. The principal advantage of the zonally-decoupled approach is computational efficiency.

The other time issue addressed was whether the flow had achieved steady state. The data listed for runs 14 and 15 (Table 4) were included to demonstrate this point. Note that run 15 is just a continuation of run 14. That is for run 14, the overall flowfield was estimated to be steady prior to a run time of 0.53 ms (time for

region 1). Then the calculation was continued to obtain the time averaged results over the time interval of 0.53 to 1.02 ms producing the results for run 14. Note that the data previously discussed for Case 3 (run 16) used the same time intervals to arrive at the steady state results. Having obtained the results for run 14, the sampling counters were reinitialized and the computation continued to obtain a second time averaged results for the time interval 1.02 to 1.51 ms (run 15). Comparison of the surface heating rate results for these two solutions (Fig. A3) show excellent agreement. Similar agreement in the flowfield parameters for the near wake are demonstrated in Fig. A4 where the radial density profile data are displayed. These data demonstrate that the flow had indeed achieved a steady state and that there were no obvious indication of unsteadiness.

Rotational Energy Exchange

For the calculations presented, a constant rotational collision number, Z_r, of 5 was used even though a temperature dependent option is available. That is, only for one in five collisions is an adjustment made for the rotational energy of the molecules. The measurements of Ref. 18 for nitrogen show a temperature dependence of Z_r that would vary from about 2.5 at 100 K to about 10 at 1000 K. Solutions were obtained for Case 1, the case with the largest degree of thermal nonequilibrium, using three different values of Z_r (2.5, 5, and 10) to examine the sensitivity of the surface and flowfield results to this parameter. The effect on the rotational temperature and density contours is demonstrated in Figs. A5 and A6, and the surface heating in Fig. A7. The impact on the rotational temperature field is qualitatively what one would expect; higher rotational temperatures at a given location in the compression region and lower temperature at a given location in the expanding region (near wake) for the higher rotational collision numbers. The effect on the near wake density field is discernible indicating that a temperature dependent $Z_r(t)$ would be more appropriate. The effect on surface heating rates is insignificant (Fig. A7).

Surface Reflection

The assumed model for the gas surface interaction has been diffuse with full thermal accommodation. Currently, there is no model of gas surface interactions that is adequate for quantitative studies over a wide range of parameters for all combinations of gases and surfaces, and it is unlikely that one will be forthcoming. In the absence of such a model, non-diffuse reflection has most frequently been represented by assuming some fraction of the molecules are reflected spectrally, while the remainder are reflected diffusely. The impact of assuming that 20 percent of the molecules are reflected spectrally is demonstrated in Figs. A8 and A9 for the flowfield density contours and surface heating, respectively.

Table 1. Conditions Used in Simulations*

Case	$\rho_\infty x10^5$, kg/m^3	V_∞, m/s	T_∞, K	M_∞	Kn_∞	Re_∞	Re2
1	1.73	1502	13.3	20.2	0.032	768	28
2	5.19	1502	14.0	19.7	0.011	2,221	84
3	46.67	1633	15.0	20.6	0.001	20,610	726

*Uniform freestream conditions with nitrogen gas in thermal equilibrium at the freestream temperature. Model temperature equal 300 K. Diffuse surface with full thermal accommodation. The characteristic length is taken as the base diamter (0.05m).

Table 2. DSMC Results for Blunted Cone/Sting Configuration

Case	Drag			Heating Rate		
	Force, N	C_D	Percent Due to Friction	Forebody Stagnation Point		Max. to Sting, q,W/cm^2
				q,W/cm^2	C_H	
1	0.064	1.68	8.4	1.0	0.349	0.036
2	0.183	1.59	5.9	1.8	0.202	0.095
3	1.905	1.56	2.0	8.4	0.083	0.476

Table 3. Effect of Rarefaction on Wake Features

Case	Kn_∞	Δ, m	Wake Stagnation Point Location*		Heating Rate Ratio**
			x, m	s/R_N	
1	0.032	0.0007	0.0111	3.69	0.007
2	0.011	0.0082	0.0186	4.29	0.142
3	0.001	0.0340	0.0444	6.36	0.734

*Base plane located at x = 0.0104 m.
**The sting heating rate at the wake stagnation point ratioed to the maximum sting heating rate.

Table 4. Numerical Parameters and Selected Results

Run	Configuration	Time step[a] Δt, ns	Steady State Sampling[a] t_{start}, ms	t_{end}, ms	Time Steps for Flowfield Sampling	Number of Cells	Number of Molecules	C_D	C_H[b]
			Case 1						
1	Forebody	75	0.30	2.24	2	2,720	52,500	1.63	0.345
2	Forebody & Wake	75	3.60	4.80	2	6,020	113,300	1.63	0.353
3	Forebody & Wake	300	4.05	8.10	6	6,020	113,800	1.62	0.350
4	F. W. & Sting[c]	75	3.82	6.11	2	6,000	113,451	1.68	0.348
5	F. W. & Sting	75	3.75	6.18	10	8,060	152,649	1.68	0.344
6	F. W. & Sting[d]	75	3.89	6.89	2	6,000	115,582	1.68	0.343
7	F. W. & Sting[e]	75	4.19	7.79	2	6,000	113,378	1.67	0.352
8	F. W. & Sting[f]	75	3.51	7.80	2	6,000	111,600	1.67	0.312
			Case 2						
9	Forebody	20	0.31	0.77	2	4,680	119,122	1.57	0.202
10	Forebody & Wake	120	1.44	2.64	5	12,476	236,407	1.56	0.203
11	F. W. & Sting	120	1.44	4.14	5	12,476	223,464	1.59	0.202
			Case 3						
12	Forebody	6	0.147	0.219	2	6,630	187,909	1.58	0.086
13	Forebody	6	0.144	0.204	2	18,900	371,804	1.57	0.079
14	Forebody & Wake	30	0.532	1.019	5	14,094	331,740	1.55	0.083
15	Forebody & Wake	30	1.019	1.507	5	14,094	334,364	1.54	0.082
16	F. W. & Sting	30	0.532	1.004	5	14,675	312,671	1.56	0.083

[a]Time information concerning region 1.
[b]Stagnation point heat transfer coefficient.
[c]Forebody and wake with sting.
[d]Rotational collision number = 2.5.
[e]Rotational collision number = 10.0.
[f]Specular surface reflection = 20%

Table 5. Tabulated Quantities Including Surface Data
for Case 1 (Blunted Cone with Sting).

FREESTREAM QUANTITIES

VELOCITY IN X-DIRECTION, M/S	=	1502.0
VELOCITY IN Y-DIRECTION, M/S	=	0.0
MACH NUMBER	=	20.19
SPEED OF SOUND, M/S	=	74.39
SPEED RATIO	=	16.89
MOST PROBABLE SPEED, M/S	=	88.91
TOTAL TEMPERATURE, K	=	1099.46
TEMPERATURE, K	=	13.32
DENSITY, KG/M3	=	0.1729E-04
NUMBER DENSITY, M-3	=	0.3716E+21
PRESSURE, N/M2	=	0.6833E-01
GAMMAF	=	1.40
MOLECULAR WEIGHT	=	28.020
VISCOSITY, PA*S	=	0.1692E-05
REYNOLDS NUMBER	=	0.7676E+03
SHOCK REYNOLDS NUMBER	=	0.2803E+02
V-BAR PARAMETER (M/SQRT(REN))	=	0.729
CHI-BAR PARAMETER (M*3/SQRT(REN)	=	297.14
CHARACTERISTIC LENGTH, M	=	0.5000E-01
MEAN FREE PATH, M	=	0.1588E-02
KNUDSEN NUMBER	=	0.03176

GAS

SPECIES = N2
MOLE FRACTIONS = 1.0000
MOLECULAR WEIGHT = 28.0200
REFERENCE TEMPERATURE,K = 300.00 VISCOSITY-TEMPERATURE-EXPONENT= 0.75

WALL DATA:

TEMPERATURE K = 300.0 FRACTION SPECULAR REFLECTION= 0.0

REGION 1 FROM TIME 0.375E-02 TO TIME 0.619E-02 COLLISIONS:-
0.10247E+09
REGION 2 FROM TIME 0.563E-02 TO TIME 0.929E-02 COLLISIONS:-
0.25429E+08
REGION 3 FROM TIME 0.563E-02 TO TIME 0.929E-02 COLLISIONS:-
0.28496E+07
REGION 4 FROM TIME 0.150E-02 TO TIME 0.248E-02 COLLISIONS:-
0.40263E+07
REGION 5 FROM TIME 0.300E-02 TO TIME 0.495E-02 COLLISIONS:-
0.52054E+07
REGION 6 FROM TIME 0.375E-02 TO TIME 0.619E-02 COLLISIONS:-
0.16795E+07
REGION 7 FROM TIME 0.113E-02 TO TIME 0.186E-02 COLLISIONS:-
0.13682E+07
REGION 8 FROM TIME 0.750E-03 TO TIME 0.124E-02 COLLISIONS:-
0.29456E+06
REGION 9 FROM TIME 0.375E-03 TO TIME 0.619E-03 COLLISIONS:-
0.17538E+05
REGION 10 FROM TIME 0.225E-02 TO TIME 0.371E-02 COLLISIONS:-
0.16238E+07
REGION 11 FROM TIME 0.675E-02 TO TIME 0.111E-01 COLLISIONS:-
0.32043E+07
REGION 12 FROM TIME 0.113E-01 TO TIME 0.186E-01 COLLISIONS:-
0.26991E+08
REGION 13 FROM TIME 0.120E-01 TO TIME 0.198E-01 COLLISIONS:-
0.22949E+08

NUMBER OF MOVE SEGMENTS 0.14734E+11 RATIO 0.10026E+01
TOTAL NUMBER OF ENTERING MOLECULES = 1.67772E+07
0. EXCESS MOLECULE ERRORS 906. REMOVAL ERRORS

TOTAL NUMBER OF SAMPLES 3250

FORCE ON SURFACE IN X DIRECTION, INCIDENT= 0.39018E-01 REFLECTED= 0.25334E-01 TOTAL(N)= 0.64353E-01 CD= 0.16806E+01

152649 MOLECULES

SURFACE PROPERTIES

ELEMENT	X COORD m	Y COORD m	PRESSURE N/m*2	SHEAR ST. N/m*2	INC ENG --	REF ENG --	NET ENG w/m*2	SAMPLE SPECIES 1-
1	0.5396E-05	0.2597E-03	0.3644E+02	0.1146E+00	0.2069E+05	-0.1060E+05	0.1009E+05	0.1091E+06
2	0.2728E-04	0.7822E-03	0.3676E+02	0.4817E+00	0.2086E+05	-0.1071E+05	0.1015E+05	0.1890E+06
3	0.7178E-04	0.1311E-02	0.3681E+02	0.8171E+00	0.2090E+05	-0.1073E+05	0.1017E+05	0.1655E+06
4	0.1398E-03	0.1844E-02	0.3648E+02	0.1062E+01	0.2064E+05	-0.1068E+05	0.9963E+04	0.1505E+06
5	0.2321E-03	0.2382E-02	0.3637E+02	0.1312E+01	0.2055E+05	-0.1062E+05	0.9928E+04	0.1407E+06
6	0.3494E-03	0.2922E-02	0.3609E+02	0.1564E+01	0.2028E+05	-0.1061E+05	0.9666E+04	0.1338E+06
7	0.4926E-03	0.3463E-02	0.3582E+02	0.1858E+01	0.2001E+05	-0.1056E+05	0.9451E+04	0.1284E+06
8	0.6623E-03	0.4005E-02	0.3525E+02	0.1919E+01	0.1951E+05	-0.1049E+05	0.9019E+04	0.1234E+06
9	0.8616E-03	0.4571E-02	0.3475E+02	0.2070E+01	0.1906E+05	-0.1040E+05	0.8655E+04	0.1299E+06
10	0.1078E-02	0.5165E-02	0.3498E+02	0.2098E+01	0.1900E+05	-0.1053E+05	0.8463E+04	0.1271E+06
11	0.1294E-02	0.5760E-02	0.3464E+02	0.2078E+01	0.1865E+05	-0.1048E+05	0.8164E+04	0.1228E+06
12	0.1512E-02	0.6357E-02	0.3457E+02	0.2141E+01	0.1848E+05	-0.1044E+05	0.8038E+04	0.1194E+06
13	0.1730E-02	0.6956E-02	0.3480E+02	0.2185E+01	0.1843E+05	-0.1066E+05	0.7774E+04	0.1183E+06
14	0.1948E-02	0.7557E-02	0.3433E+02	0.2139E+01	0.1815E+05	-0.1048E+05	0.7662E+04	0.1143E+06
15	0.2168E-02	0.8160E-02	0.3425E+02	0.2284E+01	0.1800E+05	-0.1048E+05	0.7513E+04	0.1122E+06
16	0.2388E-02	0.8765E-02	0.3434E+02	0.2333E+01	0.1804E+05	-0.1055E+05	0.7491E+04	0.1107E+06
17	0.2609E-02	0.9371E-02	0.3415E+02	0.2407E+01	0.1786E+05	-0.1051E+05	0.7354E+04	0.1083E+06
18	0.2830E-02	0.9980E-02	0.3391E+02	0.2340E+01	0.1770E+05	-0.1046E+05	0.7242E+04	0.1063E+06
19	0.3052E-02	0.1059E-01	0.3372E+02	0.2448E+01	0.1757E+05	-0.1040E+05	0.7166E+04	0.1044E+06
20	0.3275E-02	0.1120E-01	0.3367E+02	0.2643E+01	0.1744E+05	-0.1043E+05	0.7016E+04	0.1026E+06
21	0.3499E-02	0.1182E-01	0.3342E+02	0.2480E+01	0.1733E+05	-0.1035E+05	0.6981E+04	0.1011E+06
22	0.3723E-02	0.1243E-01	0.3330E+02	0.2680E+01	0.1718E+05	-0.1033E+05	0.6850E+04	0.9936E+05
23	0.3948E-02	0.1305E-01	0.3306E+02	0.2682E+01	0.1701E+05	-0.1024E+05	0.6773E+04	0.9754E+05
24	0.4174E-02	0.1367E-01	0.3306E+02	0.2836E+01	0.1704E+05	-0.1025E+05	0.6784E+04	0.9661E+05
25	0.4400E-02	0.1429E-01	0.3293E+02	0.2907E+01	0.1688E+05	-0.1023E+05	0.6651E+04	0.9533E+05
26	0.4627E-02	0.1492E-01	0.3251E+02	0.2836E+01	0.1667E+05	-0.1011E+05	0.6562E+04	0.9339E+05
27	0.4855E-02	0.1554E-01	0.3224E+02	0.2968E+01	0.1660E+05	-0.1003E+05	0.6570E+04	0.9184E+05
28	0.5083E-02	0.1617E-01	0.3205E+02	0.3016E+01	0.1652E+05	-0.9961E+04	0.6555E+04	0.9045E+05
29	0.5313E-02	0.1680E-01	0.3202E+02	0.3081E+01	0.1637E+05	-0.9953E+04	0.6417E+04	0.8966E+05
30	0.5542E-02	0.1743E-01	0.3157E+02	0.3292E+01	0.1624E+05	-0.9798E+04	0.6441E+04	0.8759E+05
31	0.5773E-02	0.1807E-01	0.3126E+02	0.3376E+01	0.1604E+05	-0.9734E+04	0.6310E+04	0.8615E+05
32	0.6004E-02	0.1870E-01	0.3091E+02	0.3544E+01	0.1596E+05	-0.9614E+04	0.6346E+04	0.8454E+05
33	0.6236E-02	0.1934E-01	0.3071E+02	0.3560E+01	0.1586E+05	-0.9533E+04	0.6329E+04	0.8312E+05
34	0.6469E-02	0.1998E-01	0.3029E+02	0.3845E+01	0.1574E+05	-0.9376E+04	0.6362E+04	0.8115E+05
35	0.6702E-02	0.2062E-01	0.2975E+02	0.4075E+01	0.1554E+05	-0.9181E+04	0.6359E+04	0.7926E+05
36	0.6936E-02	0.2126E-01	0.2953E+02	0.4333E+01	0.1553E+05	-0.9059E+04	0.6473E+04	0.7770E+05
37	0.7171E-02	0.2191E-01	0.2861E+02	0.4520E+01	0.1519E+05	-0.8803E+04	0.6391E+04	0.7467E+05
38	0.7406E-02	0.2255E-01	0.2774E+02	0.4947E+01	0.1492E+05	-0.8481E+04	0.6437E+04	0.7151E+05
39	0.7642E-02	0.2320E-01	0.2656E+02	0.5548E+01	0.1453E+05	-0.8044E+04	0.6488E+04	0.6746E+05
40	0.7879E-02	0.2385E-01	0.2549E+02	0.6412E+01	0.1437E+05	-0.7546E+04	0.6823E+04	0.6305E+05
41	0.8022E-02	0.2424E-01	0.2256E+02	0.6833E+01	0.1315E+05	-0.6602E+04	0.6551E+04	0.1005E+05
42	0.8083E-02	0.2436E-01	0.1976E+02	0.7115E+01	0.1181E+05	-0.5846E+04	0.5968E+04	0.1020E+05
43	0.8166E-02	0.2449E-01	0.1710E+02	0.6730E+01	0.1052E+05	-0.5088E+04	0.5435E+04	0.9943E+04
44	0.8278E-02	0.2462E-01	0.1413E+02	0.6486E+01	0.9077E+04	-0.4293E+04	0.4784E+04	0.9304E+04
45	0.8421E-02	0.2474E-01	0.1086E+02	0.5695E+01	0.7220E+04	-0.3359E+04	0.3862E+04	0.7975E+04
46	0.8597E-02	0.2485E-01	0.7402E+01	0.4302E+01	0.5027E+04	-0.2382E+04	0.2646E+04	0.6163E+04
47	0.8807E-02	0.2494E-01	0.4926E+01	0.3229E+01	0.3500E+04	-0.1649E+04	0.1851E+04	0.4604E+04
48	0.9046E-02	0.2499E-01	0.2986E+01	0.2060E+01	0.2098E+04	-0.1044E+04	0.1054E+04	0.3123E+04
49	0.9224E-02	0.2500E-01	0.1935E+01	0.1472E+01	0.1395E+04	-0.6934E+03	0.7017E+03	0.8630E+03
50	0.9334E-02	0.2499E-01	0.1411E+01	0.1051E+01	0.1008E+04	-0.5191E+03	0.4886E+03	0.6990E+03
51	0.9453E-02	0.2497E-01	0.1005E+01	0.8167E+00	0.7687E+03	-0.3838E+03	0.3849E+03	0.5820E+03
52	0.9582E-02	0.2493E-01	0.7348E+00	0.5506E+00	0.5249E+03	-0.2831E+03	0.2419E+03	0.4800E+03
53	0.9717E-02	0.2487E-01	0.5370E+00	0.3925E+00	0.3614E+03	-0.2205E+03	0.1409E+03	0.3890E+03
54	0.9854E-02	0.2479E-01	0.3054E+00	0.2434E+00	0.2203E+03	-0.1270E+03	0.9333E+02	0.2470E+03
55	0.9990E-02	0.2469E-01	0.1912E+00	0.1387E+00	0.1306E+03	-0.7948E+02	0.5109E+02	0.1680E+03
56	0.1009E-01	0.2460E-01	0.1416E+00	0.1173E+00	0.1040E+03	-0.6036E+02	0.4365E+02	0.6800E+02
57	0.1015E-01	0.2452E-01	0.9800E-01	0.6800E-01	0.5972E+02	-0.4109E+02	0.1863E+02	0.5100E+02
58	0.1022E-01	0.2443E-01	0.7133E-01	0.2434E-01	0.4184E+02	-0.3109E+02	0.1075E+02	0.4400E+02
59	0.1029E-01	0.2431E-01	0.5491E-01	0.2842E-01	0.3180E+02	-0.2326E+02	0.8537E+01	0.4500E+02
60	0.1034E-01	0.2418E-01	0.4700E-01	0.7467E-02	0.2454E+02	-0.1893E+02	0.5611E+01	0.3800E+02
61	0.1039E-01	0.2402E-01	0.3651E-01	-0.4651E-02	0.2111E+02	-0.1641E+02	0.4702E+01	0.3400E+02
62	0.1042E-01	0.2384E-01	0.3335E-01	0.3166E-02	0.2059E+02	-0.1397E+02	0.6627E+01	0.3800E+02
63	0.1042E-01	0.2321E-01	0.4731E-01	-0.1194E-01	0.2222E+02	-0.1843E+02	0.3795E+01	0.2470E+03
64	0.1042E-01	0.2212E-01	0.4940E-01	-0.9638E-02	0.2445E+02	-0.1968E+02	0.4766E+01	0.2570E+03
65	0.1042E-01	0.2102E-01	0.5292E-01	-0.1287E-01	0.2162E+02	-0.2011E+02	0.1513E+01	0.2790E+03
66	0.1042E-01	0.1989E-01	0.5206E-01	-0.1425E-01	0.2259E+02	-0.2044E+02	0.2151E+01	0.2960E+03
67	0.1042E-01	0.1875E-01	0.6127E-01	-0.1358E-01	0.2360E+02	-0.2189E+02	0.1712E+01	0.3310E+03
68	0.1042E-01	0.1759E-01	0.5096E-01	-0.1111E-01	0.2036E+02	-0.1834E+02	0.2018E+01	0.2910E+03
69	0.1042E-01	0.1642E-01	0.5840E-01	-0.1191E-01	0.2418E+02	-0.2106E+02	0.3124E+01	0.3350E+03
70	0.1042E-01	0.1522E-01	0.6012E-01	-0.8943E-02	0.2293E+02	-0.2220E+02	0.7308E+00	0.3690E+03
71	0.1042E-01	0.1401E-01	0.6266E-01	-0.1017E-01	0.2403E+02	-0.2205E+02	0.1978E+01	0.3960E+03
72	0.1042E-01	0.1277E-01	0.6001E-01	-0.7286E-02	0.2405E+02	-0.2164E+02	0.2409E+01	0.4000E+03
73	0.1042E-01	0.1153E-01	0.5886E-01	-0.5105E-02	0.2306E+02	-0.2175E+02	0.1310E+01	0.4070E+03
74	0.1042E-01	0.1026E-01	0.5809E-01	-0.6059E-02	0.2409E+02	-0.2105E+02	0.3039E+01	0.4110E+03
75	0.1042E-01	0.8972E-02	0.5006E-01	-0.5974E-02	0.1844E+02	-0.1742E+02	0.1021E+01	0.3630E+03
76	0.1059E-01	0.7755E-02	0.5193E-01	-0.2097E-02	0.2058E+02	-0.1855E+02	0.2036E+01	0.3790E+03
77	0.1163E-01	0.6717E-02	0.5486E-01	0.2876E-02	0.2301E+02	-0.2002E+02	0.2986E+01	0.6820E+03
78	0.1309E-01	0.6250E-02	0.6672E-01	0.4556E-02	0.2683E+02	-0.2255E+02	0.4272E+01	0.4450E+03
79	0.1426E-01	0.6250E-02	0.8800E-01	0.4540E-02	0.3948E+02	-0.2975E+02	0.9738E+01	0.5730E+03
80	0.1541E-01	0.6250E-02	0.1017E+00	0.1068E-01	0.4389E+02	-0.3247E+02	0.1143E+02	0.6150E+03
81	0.1654E-01	0.6250E-02	0.1167E+00	0.1114E-01	0.5374E+02	-0.3815E+02	0.1559E+02	0.7090E+03
82	0.1764E-01	0.6250E-02	0.1531E+00	0.1582E-01	0.6647E+02	-0.4660E+02	0.1987E+02	0.8320E+03
83	0.1873E-01	0.6250E-02	0.1494E+00	0.2344E-01	0.6856E+02	-0.4708E+02	0.2148E+02	0.8520E+03
84	0.1980E-01	0.6250E-02	0.2260E+00	0.4442E-01	0.1223E+03	-0.6792E+02	0.5436E+02	0.1190E+04
85	0.2084E-01	0.6250E-02	0.2165E+00	0.3928E-01	0.1032E+03	-0.6796E+02	0.3528E+02	0.1120E+04
86	0.2186E-01	0.6250E-02	0.2403E+00	0.5746E-01	0.1096E+03	-0.7416E+02	0.3546E+02	0.1227E+04
87	0.2286E-01	0.6250E-02	0.2843E+00	0.6161E-01	0.1341E+03	-0.8580E+02	0.4833E+02	0.1416E+04

88	0.2384E-01	0.6250E-02	0.2950E+00	0.7941E-01	0.1527E+03	-0.8707E+02	0.6563E+02	0.1384E+04
89	0.2480E-01	0.6250E-02	0.3440E+00	0.1050E+00	0.1813E+03	-0.1043E+03	0.7698E+02	0.1621E+04
90	0.2574E-01	0.6250E-02	0.3693E+00	0.1127E+00	0.1927E+03	-0.1060E+03	0.8669E+02	0.1605E+04
91	0.2666E-01	0.6250E-02	0.3924E+00	0.1412E+00	0.2163E+03	-0.1174E+03	0.9895E+02	0.1713E+04
92	0.2756E-01	0.6250E-02	0.4442E+00	0.1553E+00	0.2233E+03	-0.1319E+03	0.9133E+02	0.1898E+04
93	0.2877E-01	0.6250E-02	0.4397E+00	0.1645E+00	0.2397E+03	-0.1307E+03	0.1090E+03	0.3298E+04
94	0.3031E-01	0.6250E-02	0.5103E+00	0.2281E+00	0.3024E+03	-0.1515E+03	0.1509E+03	0.3832E+04
95	0.3184E-01	0.6250E-02	0.5590E+00	0.2377E+00	0.3186E+03	-0.1669E+03	0.1517E+03	0.4161E+04
96	0.3337E-01	0.6250E-02	0.5885E+00	0.2719E+00	0.3564E+03	-0.1738E+03	0.1825E+03	0.4307E+04
97	0.3489E-01	0.6250E-02	0.6122E+00	0.2980E+00	0.3665E+03	-0.1816E+03	0.1849E+03	0.4522E+04
98	0.3641E-01	0.6250E-02	0.6742E+00	0.3470E+00	0.4114E+03	-0.2047E+03	0.2067E+03	0.5068E+04
99	0.3793E-01	0.6250E-02	0.6956E+00	0.3872E+00	0.4457E+03	-0.2116E+03	0.2341E+03	0.5197E+04
100	0.3944E-01	0.6250E-02	0.6964E+00	0.3951E+00	0.4347E+03	-0.2152E+03	0.2195E+03	0.5212E+04
101	0.4094E-01	0.6250E-02	0.7468E+00	0.4290E+00	0.4791E+03	-0.2258E+03	0.2533E+03	0.5503E+04
102	0.4245E-01	0.6250E-02	0.7405E+00	0.4443E+00	0.4770E+03	-0.2271E+03	0.2499E+03	0.5597E+04
103	0.4394E-01	0.6250E-02	0.7233E+00	0.4528E+00	0.4823E+03	-0.2254E+03	0.2569E+03	0.5501E+04
104	0.4544E-01	0.6250E-02	0.7335E+00	0.4476E+00	0.4839E+03	-0.2290E+03	0.2549E+03	0.5512E+04
105	0.4692E-01	0.6250E-02	0.7943E+00	0.5159E+00	0.5428E+03	-0.2455E+03	0.2973E+03	0.5962E+04
106	0.4841E-01	0.6250E-02	0.7626E+00	0.5000E+00	0.5196E+03	-0.2368E+03	0.2828E+03	0.5751E+04
107	0.4989E-01	0.6250E-02	0.7900E+00	0.5333E+00	0.5431E+03	-0.2482E+03	0.2949E+03	0.5929E+04
108	0.5136E-01	0.6250E-02	0.7897E+00	0.5451E+00	0.5609E+03	-0.2476E+03	0.3133E+03	0.5965E+04
109	0.5283E-01	0.6250E-02	0.7914E+00	0.5682E+00	0.5754E+03	-0.2468E+03	0.3286E+03	0.5915E+04
110	0.5430E-01	0.6250E-02	0.7877E+00	0.5708E+00	0.5670E+03	-0.2472E+03	0.3198E+03	0.5951E+04
111	0.5576E-01	0.6250E-02	0.8015E+00	0.5797E+00	0.5687E+03	-0.2530E+03	0.3157E+03	0.6024E+04
112	0.5722E-01	0.6250E-02	0.8032E+00	0.5743E+00	0.5774E+03	-0.2554E+03	0.3220E+03	0.6030E+04
113	0.5867E-01	0.6250E-02	0.8357E+00	0.6161E+00	0.6148E+03	-0.2644E+03	0.3504E+03	0.6269E+04
114	0.6012E-01	0.6250E-02	0.7935E+00	0.6057E+00	0.5910E+03	-0.2533E+03	0.3377E+03	0.6044E+04
115	0.6156E-01	0.6250E-02	0.8235E+00	0.6204E+00	0.6161E+03	-0.2643E+03	0.3518E+03	0.6244E+04
116	0.6300E-01	0.6250E-02	0.8265E+00	0.6346E+00	0.6182E+03	-0.2620E+03	0.3562E+03	0.6147E+04
117	0.6444E-01	0.6250E-02	0.8188E+00	0.6150E+00	0.5983E+03	-0.2623E+03	0.3360E+03	0.6114E+04
118	0.6587E-01	0.6250E-02	0.7984E+00	0.6327E+00	0.6094E+03	-0.2542E+03	0.3552E+03	0.6029E+04
119	0.6729E-01	0.6250E-02	0.8192E+00	0.6571E+00	0.6265E+03	-0.2633E+03	0.3632E+03	0.6106E+04
120	0.6871E-01	0.6250E-02	0.8350E+00	0.6715E+00	0.6321E+03	-0.2685E+03	0.3636E+03	0.6177E+04
121	0.7013E-01	0.6250E-02	0.7931E+00	0.6389E+00	0.6091E+03	-0.2563E+03	0.3528E+03	0.5905E+04
122	0.7154E-01	0.6250E-02	0.7772E+00	0.6365E+00	0.5946E+03	-0.2559E+03	0.3388E+03	0.5799E+04
123	0.7295E-01	0.6250E-02	0.7749E+00	0.6243E+00	0.5856E+03	-0.2533E+03	0.3324E+03	0.5742E+04
124	0.7436E-01	0.6250E-02	0.8112E+00	0.6695E+00	0.6246E+03	-0.2643E+03	0.3603E+03	0.6031E+04
125	0.7575E-01	0.6250E-02	0.7483E+00	0.6171E+00	0.5746E+03	-0.2459E+03	0.3287E+03	0.5592E+04
126	0.7715E-01	0.6250E-02	0.7352E+00	0.6140E+00	0.5618E+03	-0.2415E+03	0.3203E+03	0.5482E+04
127	0.7854E-01	0.6250E-02	0.7849E+00	0.6680E+00	0.6109E+03	-0.2575E+03	0.3534E+03	0.5795E+04
128	0.7993E-01	0.6250E-02	0.7556E+00	0.6237E+00	0.5806E+03	-0.2449E+03	0.3357E+03	0.5597E+04
129	0.8131E-01	0.6250E-02	0.7722E+00	0.6662E+00	0.6082E+03	-0.2531E+03	0.3550E+03	0.5737E+04
130	0.8268E-01	0.6250E-02	0.7745E+00	0.6735E+00	0.6060E+03	-0.2558E+03	0.3502E+03	0.5683E+04
131	0.8406E-01	0.6250E-02	0.7377E+00	0.6434E+00	0.5832E+03	-0.2411E+03	0.3421E+03	0.5385E+04
132	0.8542E-01	0.6250E-02	0.7199E+00	0.6323E+00	0.5715E+03	-0.2354E+03	0.3361E+03	0.5283E+04
133	0.8679E-01	0.6250E-02	0.6942E+00	0.6110E+00	0.5532E+03	-0.2298E+03	0.3234E+03	0.5166E+04
134	0.8815E-01	0.6250E-02	0.7240E+00	0.6398E+00	0.5789E+03	-0.2370E+03	0.3419E+03	0.5255E+04
135	0.8950E-01	0.6250E-02	0.7394E+00	0.6414E+00	0.5682E+03	-0.2464E+03	0.3218E+03	0.5388E+04
136	0.9085E-01	0.6250E-02	0.7019E+00	0.6344E+00	0.5689E+03	-0.2312E+03	0.3376E+03	0.5103E+04
137	0.9220E-01	0.6250E-02	0.7166E+00	0.6543E+00	0.5902E+03	-0.2343E+03	0.3559E+03	0.5203E+04
138	0.9354E-01	0.6250E-02	0.7203E+00	0.6487E+00	0.5849E+03	-0.2374E+03	0.3475E+03	0.5195E+04
139	0.9487E-01	0.6250E-02	0.6928E+00	0.6381E+00	0.5652E+03	-0.2315E+03	0.3337E+03	0.5041E+04
140	0.9621E-01	0.6250E-02	0.6934E+00	0.6405E+00	0.5578E+03	-0.2328E+03	0.3250E+03	0.5073E+04
141	0.9753E-01	0.6250E-02	0.6740E+00	0.6178E+00	0.5536E+03	-0.2278E+03	0.3258E+03	0.4902E+04
142	0.9886E-01	0.6250E-02	0.6696E+00	0.6119E+00	0.5448E+03	-0.2258E+03	0.3190E+03	0.4822E+04
143	0.1002E+00	0.6250E-02	0.6923E+00	0.6362E+00	0.5700E+03	-0.2289E+03	0.3410E+03	0.4982E+04
144	0.1015E+00	0.6250E-02	0.6725E+00	0.6177E+00	0.5558E+03	-0.2261E+03	0.3297E+03	0.4817E+04
145	0.1028E+00	0.6250E-02	0.6609E+00	0.6150E+00	0.5465E+03	-0.2215E+03	0.3249E+03	0.4708E+04
146	0.1041E+00	0.6250E-02	0.6697E+00	0.6419E+00	0.5698E+03	-0.2219E+03	0.3479E+03	0.4752E+04
147	0.1054E+00	0.6250E-02	0.6673E+00	0.6334E+00	0.5551E+03	-0.2220E+03	0.3331E+03	0.4756E+04
148	0.1067E+00	0.6250E-02	0.6494E+00	0.6178E+00	0.5389E+03	-0.2183E+03	0.3206E+03	0.4595E+04
149	0.1080E+00	0.6250E-02	0.6750E+00	0.6455E+00	0.5643E+03	-0.2266E+03	0.3377E+03	0.4781E+04
150	0.1093E+00	0.6250E-02	0.6279E+00	0.5985E+00	0.5200E+03	-0.2124E+03	0.3077E+03	0.4473E+04
151	0.1106E+00	0.6250E-02	0.6646E+00	0.6445E+00	0.5666E+03	-0.2207E+03	0.3459E+03	0.4660E+04
152	0.1118E+00	0.6250E-02	0.6352E+00	0.6245E+00	0.5436E+03	-0.2129E+03	0.3306E+03	0.4512E+04
153	0.1131E+00	0.6250E-02	0.6294E+00	0.6106E+00	0.5300E+03	-0.2127E+03	0.3173E+03	0.4407E+04
154	0.1144E+00	0.6250E-02	0.6006E+00	0.5969E+00	0.5087E+03	-0.2036E+03	0.3051E+03	0.4255E+04
155	0.1157E+00	0.6250E-02	0.6093E+00	0.6071E+00	0.5163E+03	-0.2049E+03	0.3114E+03	0.4270E+04
156	0.1169E+00	0.6250E-02	0.6055E+00	0.5893E+00	0.5130E+03	-0.2024E+03	0.3105E+03	0.4109E+04
157	0.1182E+00	0.6250E-02	0.5754E+00	0.5851E+00	0.5034E+03	-0.1939E+03	0.3095E+03	0.4001E+04
158	0.1194E+00	0.6250E-02	0.5960E+00	0.6085E+00	0.5126E+03	-0.2033E+03	0.3092E+03	0.4151E+04
159	0.1207E+00	0.6250E-02	0.5720E+00	0.5817E+00	0.4961E+03	-0.1959E+03	0.3002E+03	0.3979E+04
160	0.1219E+00	0.6250E-02	0.5667E+00	0.5688E+00	0.4882E+03	-0.1913E+03	0.2970E+03	0.3869E+04
161	0.1232E+00	0.6250E-02	0.5968E+00	0.6336E+00	0.5311E+03	-0.2039E+03	0.3272E+03	0.4133E+04
162	0.1244E+00	0.6250E-02	0.5777E+00	0.6257E+00	0.5161E+03	-0.1973E+03	0.3188E+03	0.3947E+04

NONDIMENSIONAL SURFACE QUANTITIES

0.5*ROF*UF**2= 0.1950E+02 0.5*ROF*UF**3= 0.2929E+05

ELEMENT	X, m	Y, m	S/Rn	CP	CF	CH	CPFM	CFFM	CHFM	CPMN
1	0.540E-05	0.260E-03	0.208E-01	0.187E+01	0.587E-02	0.344E+00	0.250E+01	0.415E-01	0.775E+00	0.184E+01
2	0.273E-04	0.782E-03	0.626E-01	0.188E+01	0.247E-01	0.346E+00	0.249E+01	0.125E+00	0.774E+00	0.183E+01
3	0.718E-04	0.131E-02	0.105E+00	0.189E+01	0.419E-01	0.347E+00	0.248E+01	0.209E+00	0.771E+00	0.182E+01
4	0.140E-03	0.184E-02	0.148E+00	0.187E+01	0.545E-01	0.340E+00	0.245E+01	0.292E+00	0.767E+00	0.180E+01
5	0.232E-03	0.238E-02	0.192E+00	0.186E+01	0.673E-01	0.339E+00	0.242E+01	0.374E+00	0.761E+00	0.177E+01
6	0.349E-03	0.292E-02	0.236E+00	0.185E+01	0.802E-01	0.330E+00	0.238E+01	0.455E+00	0.754E+00	0.174E+01
7	0.493E-03	0.346E-02	0.281E+00	0.184E+01	0.953E-01	0.323E+00	0.233E+01	0.533E+00	0.745E+00	0.170E+01
8	0.662E-03	0.400E-02	0.326E+00	0.181E+01	0.984E-01	0.308E+00	0.227E+01	0.607E+00	0.735E+00	0.165E+01
9	0.862E-03	0.457E-02	0.374E+00	0.178E+01	0.106E+00	0.295E+00	0.224E+01	0.643E+00	0.729E+00	0.162E+01
10	0.108E-02	0.516E-02	0.425E+00	0.179E+01	0.108E+00	0.289E+00	0.224E+01	0.643E+00	0.729E+00	0.162E+01
11	0.129E-02	0.576E-02	0.475E+00	0.178E+01	0.107E+00	0.279E+00	0.224E+01	0.643E+00	0.729E+00	0.162E+01
12	0.151E-02	0.636E-02	0.526E+00	0.177E+01	0.110E+00	0.274E+00	0.224E+01	0.643E+00	0.729E+00	0.162E+01
13	0.173E-02	0.696E-02	0.577E+00	0.178E+01	0.112E+00	0.265E+00	0.224E+01	0.643E+00	0.729E+00	0.162E+01
14	0.195E-02	0.756E-02	0.628E+00	0.176E+01	0.110E+00	0.262E+00	0.224E+01	0.643E+00	0.729E+00	0.162E+01
15	0.217E-02	0.816E-02	0.680E+00	0.176E+01	0.117E+00	0.256E+00	0.224E+01	0.643E+00	0.729E+00	0.162E+01
16	0.239E-02	0.876E-02	0.731E+00	0.176E+01	0.120E+00	0.256E+00	0.224E+01	0.643E+00	0.729E+00	0.162E+01
17	0.261E-02	0.937E-02	0.783E+00	0.175E+01	0.123E+00	0.251E+00	0.224E+01	0.643E+00	0.729E+00	0.162E+01
18	0.283E-02	0.998E-02	0.835E+00	0.174E+01	0.120E+00	0.247E+00	0.224E+01	0.643E+00	0.729E+00	0.162E+01
19	0.305E-02	0.106E-01	0.887E+00	0.173E+01	0.126E+00	0.245E+00	0.224E+01	0.643E+00	0.729E+00	0.162E+01
20	0.328E-02	0.112E-01	0.939E+00	0.173E+01	0.136E+00	0.240E+00	0.224E+01	0.643E+00	0.729E+00	0.162E+01
21	0.350E-02	0.118E-01	0.991E+00	0.171E+01	0.127E+00	0.238E+00	0.224E+01	0.643E+00	0.729E+00	0.162E+01
22	0.372E-02	0.124E-01	0.104E+01	0.171E+01	0.137E+00	0.234E+00	0.224E+01	0.643E+00	0.729E+00	0.162E+01
23	0.395E-02	0.131E-01	0.110E+01	0.170E+01	0.138E+00	0.231E+00	0.224E+01	0.643E+00	0.729E+00	0.162E+01
24	0.417E-02	0.137E-01	0.115E+01	0.170E+01	0.145E+00	0.232E+00	0.224E+01	0.643E+00	0.729E+00	0.162E+01
25	0.440E-02	0.143E-01	0.120E+01	0.169E+01	0.149E+00	0.227E+00	0.224E+01	0.643E+00	0.729E+00	0.162E+01
26	0.463E-02	0.149E-01	0.125E+01	0.167E+01	0.145E+00	0.224E+00	0.224E+01	0.643E+00	0.729E+00	0.162E+01
27	0.485E-02	0.155E-01	0.131E+01	0.165E+01	0.152E+00	0.224E+00	0.224E+01	0.643E+00	0.729E+00	0.162E+01
28	0.508E-02	0.162E-01	0.136E+01	0.164E+01	0.155E+00	0.224E+00	0.224E+01	0.643E+00	0.729E+00	0.162E+01
29	0.531E-02	0.168E-01	0.142E+01	0.164E+01	0.158E+00	0.219E+00	0.224E+01	0.643E+00	0.729E+00	0.162E+01
30	0.554E-02	0.174E-01	0.147E+01	0.162E+01	0.169E+00	0.220E+00	0.224E+01	0.643E+00	0.729E+00	0.162E+01
31	0.577E-02	0.181E-01	0.152E+01	0.160E+01	0.173E+00	0.215E+00	0.224E+01	0.643E+00	0.729E+00	0.162E+01
32	0.600E-02	0.187E-01	0.158E+01	0.158E+01	0.182E+00	0.217E+00	0.224E+01	0.643E+00	0.729E+00	0.162E+01
33	0.624E-02	0.193E-01	0.163E+01	0.157E+01	0.183E+00	0.216E+00	0.224E+01	0.643E+00	0.729E+00	0.162E+01
34	0.647E-02	0.200E-01	0.169E+01	0.155E+01	0.197E+00	0.217E+00	0.224E+01	0.643E+00	0.729E+00	0.162E+01
35	0.670E-02	0.206E-01	0.174E+01	0.153E+01	0.209E+00	0.217E+00	0.224E+01	0.643E+00	0.729E+00	0.162E+01
36	0.694E-02	0.213E-01	0.180E+01	0.151E+01	0.222E+00	0.221E+00	0.224E+01	0.643E+00	0.729E+00	0.162E+01
37	0.717E-02	0.219E-01	0.185E+01	0.147E+01	0.232E+00	0.218E+00	0.224E+01	0.643E+00	0.729E+00	0.162E+01
38	0.741E-02	0.226E-01	0.190E+01	0.142E+01	0.254E+00	0.220E+00	0.224E+01	0.643E+00	0.729E+00	0.162E+01
39	0.764E-02	0.232E-01	0.196E+01	0.136E+01	0.284E+00	0.221E+00	0.224E+01	0.643E+00	0.729E+00	0.162E+01
40	0.788E-02	0.239E-01	0.202E+01	0.131E+01	0.329E+00	0.233E+00	0.224E+01	0.643E+00	0.729E+00	0.162E+01
41	0.802E-02	0.242E-01	0.205E+01	0.116E+01	0.350E+00	0.224E+00	0.216E+01	0.717E+00	0.714E+00	0.156E+01
42	0.808E-02	0.244E-01	0.206E+01	0.101E+01	0.365E+00	0.204E+00	0.196E+01	0.851E+00	0.677E+00	0.140E+01
43	0.817E-02	0.245E-01	0.207E+01	0.877E+00	0.345E+00	0.186E+00	0.171E+01	0.954E+00	0.625E+00	0.120E+01
44	0.828E-02	0.246E-01	0.209E+01	0.725E+00	0.333E+00	0.163E+00	0.139E+01	0.100E+01	0.556E+00	0.946E+00
45	0.842E-02	0.247E-01	0.210E+01	0.557E+00	0.292E+00	0.132E+00	0.103E+01	0.962E+00	0.468E+00	0.669E+00
46	0.860E-02	0.249E-01	0.212E+01	0.380E+00	0.221E+00	0.903E-01	0.660E+00	0.819E+00	0.358E+00	0.392E+00
47	0.881E-02	0.249E-01	0.214E+01	0.253E+00	0.166E+00	0.632E-01	0.322E+00	0.562E+00	0.228E+00	0.159E+00
48	0.905E-02	0.250E-01	0.215E+01	0.153E+00	0.106E+00	0.360E-01	0.748E-01	0.202E+00	0.789E-01	0.190E-01
49	0.922E-02	0.250E-01	0.217E+01	0.992E-01	0.755E-01	0.240E-01	0.203E-02	0.707E-02	0.272E-02	0.000E+00
50	0.933E-02	0.250E-01	0.218E+01	0.724E-01	0.539E-01	0.167E-01	0.639E-05	0.234E-04	0.889E-05	0.000E+00
51	0.945E-02	0.250E-01	0.219E+01	0.515E-01	0.419E-01	0.131E-01	0.195E-09	0.372E-08	0.147E-08	0.000E+00
52	0.958E-02	0.249E-01	0.220E+01	0.377E-01	0.282E-01	0.826E-02	-0.116E-15	0.138E-14	0.564E-15	0.000E+00
53	0.972E-02	0.249E-01	0.221E+01	0.275E-01	0.201E-01	0.481E-02	-0.156E-25	0.751E-25	0.323E-25	0.000E+00
54	0.985E-02	0.248E-01	0.222E+01	0.157E-01	0.125E-01	0.319E-02	-0.920E-39	0.259E-38	0.120E-38	0.000E+00
55	0.999E-02	0.247E-01	0.224E+01	0.980E-02	0.711E-02	0.174E-02	0.000E+00	0.000E+00	0.000E+00	0.000E+00
56	0.101E-01	0.246E-01	0.225E+01	0.726E-02	0.601E-02	0.149E-02	0.000E+00	0.000E+00	0.000E+00	0.000E+00
57	0.102E-01	0.245E-01	0.226E+01	0.502E-02	0.349E-02	0.636E-03	0.000E+00	0.000E+00	0.000E+00	0.000E+00
58	0.102E-01	0.244E-01	0.226E+01	0.366E-02	0.125E-02	0.367E-03	0.000E+00	0.000E+00	0.000E+00	0.000E+00
59	0.103E-01	0.243E-01	0.228E+01	0.282E-02	0.146E-02	0.291E-03	0.000E+00	0.000E+00	0.000E+00	0.000E+00
60	0.103E-01	0.242E-01	0.229E+01	0.241E-02	0.383E-03	0.192E-03	0.000E+00	0.000E+00	0.000E+00	0.000E+00
61	0.104E-01	0.240E-01	0.230E+01	0.187E-02	-0.238E-03	0.161E-03	0.000E+00	0.000E+00	0.000E+00	0.000E+00
62	0.104E-01	0.238E-01	0.231E+01	0.171E-02	0.162E-03	0.226E-03	0.000E+00	0.000E+00	0.000E+00	0.000E+00
63	0.104E-01	0.232E-01	0.236E+01	0.243E-02	-0.612E-03	0.130E-03	0.000E+00	0.000E+00	0.000E+00	0.000E+00
64	0.104E-01	0.221E-01	0.245E+01	0.253E-02	-0.494E-03	0.163E-03	0.000E+00	0.000E+00	0.000E+00	0.000E+00
65	0.104E-01	0.210E-01	0.254E+01	0.271E-02	-0.660E-03	0.517E-04	0.000E+00	0.000E+00	0.000E+00	0.000E+00
66	0.104E-01	0.199E-01	0.263E+01	0.267E-02	-0.731E-03	0.734E-04	0.000E+00	0.000E+00	0.000E+00	0.000E+00
67	0.104E-01	0.188E-01	0.272E+01	0.314E-02	-0.696E-03	0.584E-04	0.000E+00	0.000E+00	0.000E+00	0.000E+00
68	0.104E-01	0.176E-01	0.281E+01	0.261E-02	-0.570E-03	0.689E-04	0.000E+00	0.000E+00	0.000E+00	0.000E+00
69	0.104E-01	0.164E-01	0.291E+01	0.299E-02	-0.611E-03	0.107E-03	0.000E+00	0.000E+00	0.000E+00	0.000E+00
70	0.104E-01	0.152E-01	0.300E+01	0.308E-02	-0.459E-03	0.249E-04	0.000E+00	0.000E+00	0.000E+00	0.000E+00
71	0.104E-01	0.140E-01	0.310E+01	0.321E-02	-0.522E-03	0.675E-04	0.000E+00	0.000E+00	0.000E+00	0.000E+00
72	0.104E-01	0.128E-01	0.320E+01	0.308E-02	-0.374E-03	0.822E-04	0.000E+00	0.000E+00	0.000E+00	0.000E+00
73	0.104E-01	0.115E-01	0.330E+01	0.302E-02	-0.262E-03	0.447E-04	0.000E+00	0.000E+00	0.000E+00	0.000E+00
74	0.104E-01	0.103E-01	0.340E+01	0.298E-02	-0.311E-03	0.104E-03	0.000E+00	0.000E+00	0.000E+00	0.000E+00
75	0.104E-01	0.897E-02	0.350E+01	0.257E-02	-0.306E-03	0.348E-04	0.000E+00	0.000E+00	0.000E+00	0.000E+00
76	0.106E-01	0.775E-02	0.360E+01	0.266E-02	-0.108E-03	0.695E-04	0.000E+00	0.000E+00	0.000E+00	0.000E+00
77	0.116E-01	0.672E-02	0.372E+01	0.281E-02	0.147E-03	0.102E-03	-0.910E-30	0.355E-29	0.156E-29	0.000E+00
78	0.131E-01	0.625E-02	0.384E+01	0.342E-02	0.234E-03	0.146E-03	0.101E-01	0.334E-01	0.129E-01	0.000E+00
79	0.143E-01	0.625E-02	0.394E+01	0.451E-02	0.233E-03	0.332E-03	0.101E-01	0.334E-01	0.129E-01	0.000E+00
80	0.154E-01	0.625E-02	0.403E+01	0.521E-02	0.548E-03	0.390E-03	0.101E-01	0.334E-01	0.129E-01	0.000E+00
81	0.165E-01	0.625E-02	0.412E+01	0.599E-02	0.571E-03	0.532E-03	0.101E-01	0.334E-01	0.129E-01	0.000E+00
82	0.176E-01	0.625E-02	0.421E+01	0.785E-02	0.811E-03	0.678E-03	0.101E-01	0.334E-01	0.129E-01	0.000E+00
83	0.187E-01	0.625E-02	0.429E+01	0.766E-02	0.120E-02	0.733E-03	0.101E-01	0.334E-01	0.129E-01	0.000E+00
84	0.198E-01	0.625E-02	0.438E+01	0.116E-01	0.228E-02	0.186E-02	0.101E-01	0.334E-01	0.129E-01	0.000E+00
85	0.208E-01	0.625E-02	0.446E+01	0.111E-01	0.201E-02	0.120E-02	0.101E-01	0.334E-01	0.129E-01	0.000E+00
86	0.219E-01	0.625E-02	0.454E+01	0.123E-01	0.295E-02	0.121E-02	0.101E-01	0.334E-01	0.129E-01	0.000E+00
87	0.229E-01	0.625E-02	0.462E+01	0.146E-01	0.316E-02	0.165E-02	0.101E-01	0.334E-01	0.129E-01	0.000E+00

88	0.238E-01	0.625E-02	0.470E+01	0.151E-01	0.407E-02	0.224E-02	0.101E-01	0.334E-01	0.129E-01	0.000E+00
89	0.248E-01	0.625E-02	0.478E+01	0.176E-01	0.538E-02	0.263E-02	0.101E-01	0.334E-01	0.129E-01	0.000E+00
90	0.257E-01	0.625E-02	0.485E+01	0.189E-01	0.578E-02	0.296E-02	0.101E-01	0.334E-01	0.129E-01	0.000E+00
91	0.267E-01	0.625E-02	0.493E+01	0.201E-01	0.724E-02	0.338E-02	0.101E-01	0.334E-01	0.129E-01	0.000E+00
92	0.276E-01	0.625E-02	0.500E+01	0.228E-01	0.797E-02	0.312E-02	0.101E-01	0.334E-01	0.129E-01	0.000E+00
93	0.288E-01	0.625E-02	0.510E+01	0.225E-01	0.843E-02	0.372E-02	0.101E-01	0.334E-01	0.129E-01	0.000E+00
94	0.303E-01	0.625E-02	0.522E+01	0.262E-01	0.117E-01	0.515E-02	0.101E-01	0.334E-01	0.129E-01	0.000E+00
95	0.318E-01	0.625E-02	0.534E+01	0.287E-01	0.122E-01	0.518E-02	0.101E-01	0.334E-01	0.129E-01	0.000E+00
96	0.334E-01	0.625E-02	0.546E+01	0.302E-01	0.139E-01	0.623E-02	0.101E-01	0.334E-01	0.129E-01	0.000E+00
97	0.349E-01	0.625E-02	0.559E+01	0.314E-01	0.153E-01	0.631E-02	0.101E-01	0.334E-01	0.129E-01	0.000E+00
98	0.364E-01	0.625E-02	0.571E+01	0.346E-01	0.178E-01	0.706E-02	0.101E-01	0.334E-01	0.129E-01	0.000E+00
99	0.379E-01	0.625E-02	0.583E+01	0.357E-01	0.199E-01	0.799E-02	0.101E-01	0.334E-01	0.129E-01	0.000E+00
100	0.394E-01	0.625E-02	0.595E+01	0.357E-01	0.203E-01	0.749E-02	0.101E-01	0.334E-01	0.129E-01	0.000E+00
101	0.409E-01	0.625E-02	0.607E+01	0.383E-01	0.220E-01	0.865E-02	0.101E-01	0.334E-01	0.129E-01	0.000E+00
102	0.424E-01	0.625E-02	0.619E+01	0.380E-01	0.228E-01	0.853E-02	0.101E-01	0.334E-01	0.129E-01	0.000E+00
103	0.439E-01	0.625E-02	0.631E+01	0.371E-01	0.232E-01	0.877E-02	0.101E-01	0.334E-01	0.129E-01	0.000E+00
104	0.454E-01	0.625E-02	0.643E+01	0.376E-01	0.230E-01	0.870E-02	0.101E-01	0.334E-01	0.129E-01	0.000E+00
105	0.469E-01	0.625E-02	0.655E+01	0.407E-01	0.265E-01	0.101E-01	0.101E-01	0.334E-01	0.129E-01	0.000E+00
106	0.484E-01	0.625E-02	0.667E+01	0.391E-01	0.256E-01	0.965E-02	0.101E-01	0.334E-01	0.129E-01	0.000E+00
107	0.499E-01	0.625E-02	0.679E+01	0.405E-01	0.273E-01	0.101E-01	0.101E-01	0.334E-01	0.129E-01	0.000E+00
108	0.514E-01	0.625E-02	0.690E+01	0.405E-01	0.280E-01	0.107E-01	0.101E-01	0.334E-01	0.129E-01	0.000E+00
109	0.528E-01	0.625E-02	0.702E+01	0.406E-01	0.291E-01	0.112E-01	0.101E-01	0.334E-01	0.129E-01	0.000E+00
110	0.543E-01	0.625E-02	0.714E+01	0.404E-01	0.293E-01	0.109E-01	0.101E-01	0.334E-01	0.129E-01	0.000E+00
111	0.558E-01	0.625E-02	0.726E+01	0.411E-01	0.297E-01	0.108E-01	0.101E-01	0.334E-01	0.129E-01	0.000E+00
112	0.572E-01	0.625E-02	0.737E+01	0.412E-01	0.294E-01	0.110E-01	0.101E-01	0.334E-01	0.129E-01	0.000E+00
113	0.587E-01	0.625E-02	0.749E+01	0.429E-01	0.316E-01	0.120E-01	0.101E-01	0.334E-01	0.129E-01	0.000E+00
114	0.601E-01	0.625E-02	0.760E+01	0.407E-01	0.311E-01	0.115E-01	0.101E-01	0.334E-01	0.129E-01	0.000E+00
115	0.616E-01	0.625E-02	0.772E+01	0.422E-01	0.318E-01	0.120E-01	0.101E-01	0.334E-01	0.129E-01	0.000E+00
116	0.630E-01	0.625E-02	0.784E+01	0.424E-01	0.325E-01	0.122E-01	0.101E-01	0.334E-01	0.129E-01	0.000E+00
117	0.644E-01	0.625E-02	0.795E+01	0.420E-01	0.315E-01	0.115E-01	0.101E-01	0.334E-01	0.129E-01	0.000E+00
118	0.659E-01	0.625E-02	0.806E+01	0.409E-01	0.324E-01	0.121E-01	0.101E-01	0.334E-01	0.129E-01	0.000E+00
119	0.673E-01	0.625E-02	0.818E+01	0.420E-01	0.337E-01	0.124E-01	0.101E-01	0.334E-01	0.129E-01	0.000E+00
120	0.687E-01	0.625E-02	0.829E+01	0.428E-01	0.344E-01	0.124E-01	0.101E-01	0.334E-01	0.129E-01	0.000E+00
121	0.701E-01	0.625E-02	0.841E+01	0.407E-01	0.328E-01	0.120E-01	0.101E-01	0.334E-01	0.129E-01	0.000E+00
122	0.715E-01	0.625E-02	0.852E+01	0.399E-01	0.326E-01	0.116E-01	0.101E-01	0.334E-01	0.129E-01	0.000E+00
123	0.730E-01	0.625E-02	0.863E+01	0.397E-01	0.320E-01	0.113E-01	0.101E-01	0.334E-01	0.129E-01	0.000E+00
124	0.744E-01	0.625E-02	0.874E+01	0.416E-01	0.343E-01	0.123E-01	0.101E-01	0.334E-01	0.129E-01	0.000E+00
125	0.758E-01	0.625E-02	0.886E+01	0.384E-01	0.316E-01	0.112E-01	0.101E-01	0.334E-01	0.129E-01	0.000E+00
126	0.771E-01	0.625E-02	0.897E+01	0.377E-01	0.315E-01	0.109E-01	0.101E-01	0.334E-01	0.129E-01	0.000E+00
127	0.785E-01	0.625E-02	0.908E+01	0.402E-01	0.343E-01	0.121E-01	0.101E-01	0.334E-01	0.129E-01	0.000E+00
128	0.799E-01	0.625E-02	0.919E+01	0.387E-01	0.320E-01	0.115E-01	0.101E-01	0.334E-01	0.129E-01	0.000E+00
129	0.813E-01	0.625E-02	0.930E+01	0.396E-01	0.342E-01	0.121E-01	0.101E-01	0.334E-01	0.129E-01	0.000E+00
130	0.827E-01	0.625E-02	0.941E+01	0.397E-01	0.345E-01	0.120E-01	0.101E-01	0.334E-01	0.129E-01	0.000E+00
131	0.841E-01	0.625E-02	0.952E+01	0.378E-01	0.330E-01	0.117E-01	0.101E-01	0.334E-01	0.129E-01	0.000E+00
132	0.854E-01	0.625E-02	0.963E+01	0.369E-01	0.324E-01	0.115E-01	0.101E-01	0.334E-01	0.129E-01	0.000E+00
133	0.868E-01	0.625E-02	0.974E+01	0.356E-01	0.313E-01	0.110E-01	0.101E-01	0.334E-01	0.129E-01	0.000E+00
134	0.881E-01	0.625E-02	0.985E+01	0.371E-01	0.328E-01	0.117E-01	0.101E-01	0.334E-01	0.129E-01	0.000E+00
135	0.895E-01	0.625E-02	0.996E+01	0.379E-01	0.329E-01	0.110E-01	0.101E-01	0.334E-01	0.129E-01	0.000E+00
136	0.909E-01	0.625E-02	0.101E+02	0.360E-01	0.325E-01	0.115E-01	0.101E-01	0.334E-01	0.129E-01	0.000E+00
137	0.922E-01	0.625E-02	0.102E+02	0.367E-01	0.335E-01	0.121E-01	0.101E-01	0.334E-01	0.129E-01	0.000E+00
138	0.935E-01	0.625E-02	0.103E+02	0.369E-01	0.333E-01	0.119E-01	0.101E-01	0.334E-01	0.129E-01	0.000E+00
139	0.949E-01	0.625E-02	0.104E+02	0.355E-01	0.327E-01	0.114E-01	0.101E-01	0.334E-01	0.129E-01	0.000E+00
140	0.962E-01	0.625E-02	0.105E+02	0.356E-01	0.328E-01	0.111E-01	0.101E-01	0.334E-01	0.129E-01	0.000E+00
141	0.975E-01	0.625E-02	0.106E+02	0.346E-01	0.317E-01	0.111E-01	0.101E-01	0.334E-01	0.129E-01	0.000E+00
142	0.989E-01	0.625E-02	0.107E+02	0.343E-01	0.314E-01	0.109E-01	0.101E-01	0.334E-01	0.129E-01	0.000E+00
143	0.100E+00	0.625E-02	0.108E+02	0.355E-01	0.326E-01	0.116E-01	0.101E-01	0.334E-01	0.129E-01	0.000E+00
144	0.101E+00	0.625E-02	0.109E+02	0.345E-01	0.317E-01	0.113E-01	0.101E-01	0.334E-01	0.129E-01	0.000E+00
145	0.103E+00	0.625E-02	0.110E+02	0.339E-01	0.315E-01	0.111E-01	0.101E-01	0.334E-01	0.129E-01	0.000E+00
146	0.104E+00	0.625E-02	0.111E+02	0.343E-01	0.329E-01	0.119E-01	0.101E-01	0.334E-01	0.129E-01	0.000E+00
147	0.105E+00	0.625E-02	0.112E+02	0.342E-01	0.325E-01	0.114E-01	0.101E-01	0.334E-01	0.129E-01	0.000E+00
148	0.107E+00	0.625E-02	0.113E+02	0.333E-01	0.317E-01	0.109E-01	0.101E-01	0.334E-01	0.129E-01	0.000E+00
149	0.108E+00	0.625E-02	0.114E+02	0.346E-01	0.331E-01	0.115E-01	0.101E-01	0.334E-01	0.129E-01	0.000E+00
150	0.109E+00	0.625E-02	0.115E+02	0.322E-01	0.307E-01	0.105E-01	0.101E-01	0.334E-01	0.129E-01	0.000E+00
151	0.111E+00	0.625E-02	0.116E+02	0.341E-01	0.330E-01	0.118E-01	0.101E-01	0.334E-01	0.129E-01	0.000E+00
152	0.112E+00	0.625E-02	0.117E+02	0.326E-01	0.320E-01	0.113E-01	0.101E-01	0.334E-01	0.129E-01	0.000E+00
153	0.113E+00	0.625E-02	0.118E+02	0.323E-01	0.313E-01	0.108E-01	0.101E-01	0.334E-01	0.129E-01	0.000E+00
154	0.114E+00	0.625E-02	0.119E+02	0.308E-01	0.306E-01	0.104E-01	0.101E-01	0.334E-01	0.129E-01	0.000E+00
155	0.116E+00	0.625E-02	0.120E+02	0.312E-01	0.311E-01	0.106E-01	0.101E-01	0.334E-01	0.129E-01	0.000E+00
156	0.117E+00	0.625E-02	0.121E+02	0.310E-01	0.302E-01	0.106E-01	0.101E-01	0.334E-01	0.129E-01	0.000E+00
157	0.118E+00	0.625E-02	0.122E+02	0.295E-01	0.300E-01	0.106E-01	0.101E-01	0.334E-01	0.129E-01	0.000E+00
158	0.119E+00	0.625E-02	0.123E+02	0.306E-01	0.312E-01	0.106E-01	0.101E-01	0.334E-01	0.129E-01	0.000E+00
159	0.121E+00	0.625E-02	0.124E+02	0.293E-01	0.298E-01	0.102E-01	0.101E-01	0.334E-01	0.129E-01	0.000E+00
160	0.122E+00	0.625E-02	0.125E+02	0.291E-01	0.292E-01	0.101E-01	0.101E-01	0.334E-01	0.129E-01	0.000E+00
161	0.123E+00	0.625E-02	0.126E+02	0.306E-01	0.325E-01	0.112E-01	0.101E-01	0.334E-01	0.129E-01	0.000E+00
162	0.124E+00	0.625E-02	0.127E+02	0.296E-01	0.321E-01	0.109E-01	0.101E-01	0.334E-01	0.129E-01	0.000E+00

Table 6. Tabulated Quantities Including Surface Data for Case 2 (Blunted Cone with Sting).

FREESTREAM QUANTITIES

VELOCITY IN X-DIRECTION, M/S	= 1502.0
VELOCITY IN Y-DIRECTION, M/S	= 0.0
MACH NUMBER	= 19.70
SPEED OF SOUND, M/S	= 76.26
SPEED RATIO	= 16.48
MOST PROBABLE SPEED, M/S	= 91.15
TOTAL TEMPERATURE, K	= 1100.14
TEMPERATURE, K	= 14.00
DENSITY, KG/M3	= 0.5192E-04
NUMBER DENSITY, M-3	= 0.1116E+22
PRESSURE, N/M2	= 0.2157E+00
GAMMAF	= 1.40
MOLECULAR WEIGHT	= 28.020
VISCOSITY, PA*S	= 0.1756E-05
REYNOLDS NUMBER	= 0.2221E+04
SHOCK REYNOLDS NUMBER	= 0.8414E+02
V-BAR PARAMETER (M/SQRT(REN))	= 0.418
CHI-BAR PARAMETER (M*3/SQRT(REN)	= 162.12
CHARACTERISTIC LENGTH, M	= 0.5000E-01
MEAN FREE PATH, M	= 0.5354E-03
KNUDSEN NUMBER	= 0.01071

GAS

SPECIES = N2
MOLE FRACTIONS = 1.0000
MOLECULAR WEIGHT = 28.0200
REFERENCE TEMPERATURE,K = 300.00 VISCOSITY-TEMPERATURE-EXPONENT= 0.75

WALL DATA:

TEMPERATURE K = 300.0 FRACTION SPECULAR REFLECTION= 0.0

REGION 1 FROM TIME 0.144E-02 TO TIME 0.414E-02 COLLISIONS:- 0.61858E+09
REGION 2 FROM TIME 0.360E-02 TO TIME 0.103E-01 COLLISIONS:- 0.35979E+09
REGION 3 FROM TIME 0.288E-02 TO TIME 0.828E-02 COLLISIONS:- 0.33421E+08
REGION 4 FROM TIME 0.720E-03 TO TIME 0.207E-02 COLLISIONS:- 0.17301E+08
REGION 5 FROM TIME 0.202E-02 TO TIME 0.580E-02 COLLISIONS:- 0.68716E+08
REGION 6 FROM TIME 0.288E-02 TO TIME 0.828E-02 COLLISIONS:- 0.10569E+08
REGION 7 FROM TIME 0.504E-03 TO TIME 0.145E-02 COLLISIONS:- 0.42585E+07
REGION 8 FROM TIME 0.360E-03 TO TIME 0.103E-02 COLLISIONS:- 0.10390E+07
REGION 9 FROM TIME 0.288E-03 TO TIME 0.828E-03 COLLISIONS:- 0.51456E+06
REGION 10 FROM TIME 0.274E-02 TO TIME 0.787E-02 COLLISIONS:- 0.22062E+08
REGION 11 FROM TIME 0.288E-02 TO TIME 0.828E-02 COLLISIONS:- 0.22316E+08
REGION 12 FROM TIME 0.518E-02 TO TIME 0.149E-01 COLLISIONS:- 0.83867E+08
REGION 13 FROM TIME 0.518E-02 TO TIME 0.149E-01 COLLISIONS:- 0.31142E+09
REGION 14 FROM TIME 0.662E-02 TO TIME 0.190E-01 COLLISIONS:- 0.68294E+08

NUMBER OF MOVE SEGMENTS 0.11878E+11 RATIO 0.10097E+01
TOTAL NUMBER OF ENTERING MOLECULES = 1.67772E+07
0. EXCESS MOLECULE ERRORS 3151. REMOVAL ERRORS

TOTAL NUMBER OF SAMPLES 4500

FORCE ON SURFACE IN X DIRECTION, INCIDENT= 0.10409E+00 REFLECTED= 0.78486E-01 TOTAL(N)= 0.18258E+00 CD= 0.15876E+01

223464 MOLECULES

SURFACE PROPERTIES

ELEMENT	X COORD m	Y COORD m	PRESSURE N/m*2	SHEAR ST. N/m*2	INC ENG --	REF ENG --	NET ENG w/m*2	SAMPLE SPECIES 1-
1	0.3454E-05	0.2078E-03	0.1051E+03	-0.1171E+00	0.5139E+05	-0.3361E+05	0.1778E+05	0.3840E+06
2	0.1742E-04	0.6253E-03	0.1069E+03	0.3987E+00	0.5203E+05	-0.3415E+05	0.1788E+05	0.4732E+06
3	0.4572E-04	0.1047E-02	0.1074E+03	0.7445E+00	0.5223E+05	-0.3406E+05	0.1817E+05	0.4109E+06
4	0.8878E-04	0.1472E-02	0.1074E+03	0.1069E+01	0.5223E+05	-0.3423E+05	0.1800E+05	0.3737E+06
5	0.1470E-03	0.1899E-02	0.1073E+03	0.1556E+01	0.5216E+05	-0.3412E+05	0.1804E+05	0.3488E+06
6	0.2209E-03	0.2329E-02	0.1071E+03	0.1981E+01	0.5208E+05	-0.3430E+05	0.1778E+05	0.3312E+06
7	0.3107E-03	0.2761E-02	0.1069E+03	0.2395E+01	0.5186E+05	-0.3422E+05	0.1763E+05	0.3179E+06
8	0.4169E-03	0.3193E-02	0.1060E+03	0.2720E+01	0.5110E+05	-0.3387E+05	0.1723E+05	0.3053E+06
9	0.5397E-03	0.3626E-02	0.1057E+03	0.2764E+01	0.5070E+05	-0.3395E+05	0.1675E+05	0.2963E+06
10	0.6796E-03	0.4059E-02	0.1051E+03	0.3148E+01	0.5005E+05	-0.3378E+05	0.1627E+05	0.2889E+06
11	0.8401E-03	0.4512E-02	0.1046E+03	0.2949E+01	0.4939E+05	-0.3374E+05	0.1565E+05	0.3083E+06
12	0.1013E-02	0.4987E-02	0.1044E+03	0.2985E+01	0.4893E+05	-0.3388E+05	0.1505E+05	0.3005E+06
13	0.1186E-02	0.5462E-02	0.1037E+03	0.3127E+01	0.4830E+05	-0.3364E+05	0.1467E+05	0.2919E+06
14	0.1359E-02	0.5939E-02	0.1037E+03	0.3077E+01	0.4805E+05	-0.3372E+05	0.1433E+05	0.2855E+06
15	0.1533E-02	0.6417E-02	0.1035E+03	0.3102E+01	0.4768E+05	-0.3362E+05	0.1407E+05	0.2797E+06
16	0.1708E-02	0.6897E-02	0.1033E+03	0.3294E+01	0.4745E+05	-0.3364E+05	0.1381E+05	0.2743E+06
17	0.1883E-02	0.7377E-02	0.1030E+03	0.3161E+01	0.4723E+05	-0.3372E+05	0.1351E+05	0.2694E+06
18	0.2058E-02	0.7859E-02	0.1026E+03	0.3384E+01	0.4680E+05	-0.3346E+05	0.1334E+05	0.2644E+06
19	0.2234E-02	0.8342E-02	0.1022E+03	0.3453E+01	0.4652E+05	-0.3347E+05	0.1305E+05	0.2596E+06
20	0.2410E-02	0.8826E-02	0.1019E+03	0.3319E+01	0.4627E+05	-0.3338E+05	0.1288E+05	0.2550E+06
21	0.2587E-02	0.9312E-02	0.1017E+03	0.3798E+01	0.4606E+05	-0.3336E+05	0.1270E+05	0.2514E+06
22	0.2764E-02	0.9798E-02	0.1013E+03	0.3576E+01	0.4575E+05	-0.3314E+05	0.1261E+05	0.2477E+06
23	0.2942E-02	0.1029E-01	0.1012E+03	0.3782E+01	0.4560E+05	-0.3312E+05	0.1248E+05	0.2440E+06
24	0.3120E-02	0.1078E-01	0.1007E+03	0.3747E+01	0.4537E+05	-0.3301E+05	0.1236E+05	0.2405E+06
25	0.3298E-02	0.1127E-01	0.1000E+03	0.3871E+01	0.4507E+05	-0.3283E+05	0.1224E+05	0.2366E+06
26	0.3477E-02	0.1176E-01	0.1003E+03	0.3921E+01	0.4510E+05	-0.3293E+05	0.1217E+05	0.2344E+06
27	0.3656E-02	0.1225E-01	0.9977E+02	0.3972E+01	0.4484E+05	-0.3281E+05	0.1203E+05	0.2317E+06
28	0.3836E-02	0.1274E-01	0.9974E+02	0.4010E+01	0.4473E+05	-0.3283E+05	0.1190E+05	0.2291E+06
29	0.4016E-02	0.1324E-01	0.9886E+02	0.4394E+01	0.4435E+05	-0.3248E+05	0.1187E+05	0.2253E+06
30	0.4197E-02	0.1373E-01	0.9838E+02	0.4091E+01	0.4415E+05	-0.3231E+05	0.1184E+05	0.2224E+06
31	0.4378E-02	0.1423E-01	0.9808E+02	0.4461E+01	0.4399E+05	-0.3223E+05	0.1176E+05	0.2199E+06
32	0.4560E-02	0.1473E-01	0.9777E+02	0.4380E+01	0.4380E+05	-0.3213E+05	0.1167E+05	0.2177E+06
33	0.4741E-02	0.1523E-01	0.9714E+02	0.4704E+01	0.4355E+05	-0.3192E+05	0.1163E+05	0.2146E+06
34	0.4924E-02	0.1573E-01	0.9651E+02	0.4735E+01	0.4322E+05	-0.3170E+05	0.1152E+05	0.2113E+06
35	0.5107E-02	0.1623E-01	0.9592E+02	0.4960E+01	0.4300E+05	-0.3148E+05	0.1151E+05	0.2088E+06
36	0.5290E-02	0.1674E-01	0.9564E+02	0.4923E+01	0.4286E+05	-0.3156E+05	0.1130E+05	0.2066E+06
37	0.5474E-02	0.1724E-01	0.9479E+02	0.5225E+01	0.4254E+05	-0.3126E+05	0.1129E+05	0.2038E+06
38	0.5658E-02	0.1775E-01	0.9429E+02	0.5284E+01	0.4233E+05	-0.3109E+05	0.1124E+05	0.2012E+06
39	0.5843E-02	0.1826E-01	0.9321E+02	0.5627E+01	0.4190E+05	-0.3068E+05	0.1122E+05	0.1975E+06
40	0.6028E-02	0.1877E-01	0.9241E+02	0.5662E+01	0.4161E+05	-0.3041E+05	0.1120E+05	0.1944E+06
41	0.6213E-02	0.1927E-01	0.9175E+02	0.6004E+01	0.4138E+05	-0.3012E+05	0.1126E+05	0.1921E+06
42	0.6399E-02	0.1979E-01	0.9041E+02	0.6205E+01	0.4086E+05	-0.2963E+05	0.1123E+05	0.1881E+06
43	0.6586E-02	0.2030E-01	0.8924E+02	0.6366E+01	0.4046E+05	-0.2926E+05	0.1120E+05	0.1845E+06
44	0.6772E-02	0.2081E-01	0.8839E+02	0.6780E+01	0.4030E+05	-0.2896E+05	0.1134E+05	0.1820E+06
45	0.6960E-02	0.2133E-01	0.8631E+02	0.7356E+01	0.3954E+05	-0.2833E+05	0.1122E+05	0.1763E+06
46	0.7147E-02	0.2184E-01	0.8479E+02	0.7615E+01	0.3908E+05	-0.2766E+05	0.1142E+05	0.1720E+06
47	0.7336E-02	0.2236E-01	0.8256E+02	0.8673E+01	0.3822E+05	-0.2691E+05	0.1130E+05	0.1661E+06
48	0.7524E-02	0.2288E-01	0.7965E+02	0.9228E+01	0.3732E+05	-0.2580E+05	0.1151E+05	0.1590E+06
49	0.7713E-02	0.2340E-01	0.7566E+02	0.1026E+02	0.3590E+05	-0.2444E+05	0.1146E+05	0.1497E+06
50	0.7903E-02	0.2392E-01	0.7146E+02	0.1258E+02	0.3492E+05	-0.2280E+05	0.1212E+05	0.1391E+06
51	0.8017E-02	0.2422E-01	0.6111E+02	0.1428E+02	0.3103E+05	-0.1931E+05	0.1172E+05	0.2172E+05
52	0.8062E-02	0.2432E-01	0.5610E+02	0.1525E+02	0.2891E+05	-0.1784E+05	0.1108E+05	0.2197E+05
53	0.8122E-02	0.2442E-01	0.5021E+02	0.1529E+02	0.2649E+05	-0.1596E+05	0.1053E+05	0.2173E+05
54	0.8198E-02	0.2453E-01	0.4321E+02	0.1450E+02	0.2342E+05	-0.1382E+05	0.9610E+04	0.2048E+05
55	0.8292E-02	0.2463E-01	0.3659E+02	0.1394E+02	0.2037E+05	-0.1182E+05	0.8549E+04	0.1890E+05
56	0.8407E-02	0.2474E-01	0.2928E+02	0.1239E+02	0.1666E+05	-0.9584E+04	0.7081E+04	0.1654E+05
57	0.8542E-02	0.2483E-01	0.2303E+02	0.1095E+02	0.1356E+05	-0.7658E+04	0.5906E+04	0.1410E+05
58	0.8699E-02	0.2490E-01	0.1688E+02	0.8936E+01	0.1026E+05	-0.5740E+04	0.4516E+04	0.1127E+05
59	0.8876E-02	0.2496E-01	0.1199E+02	0.6958E+01	0.7445E+04	-0.4200E+04	0.3245E+04	0.8752E+04
60	0.9071E-02	0.2499E-01	0.7970E+01	0.5106E+01	0.5074E+04	-0.2865E+04	0.2209E+04	0.6320E+04
61	0.9218E-02	0.2500E-01	0.5476E+01	0.3531E+01	0.3540E+04	-0.2024E+04	0.1516E+04	0.1973E+04
62	0.9313E-02	0.2499E-01	0.4391E+01	0.2904E+01	0.2806E+04	-0.1605E+04	0.1201E+04	0.1731E+04
63	0.9416E-02	0.2497E-01	0.3270E+01	0.2365E+01	0.2082E+04	-0.1261E+04	0.8213E+03	0.1488E+04
64	0.9526E-02	0.2495E-01	0.2635E+01	0.1973E+01	0.1780E+04	-0.1025E+04	0.7548E+03	0.1288E+04
65	0.9642E-02	0.2491E-01	0.1914E+01	0.1302E+01	0.1232E+04	-0.7502E+03	0.4814E+03	0.1018E+04
66	0.9761E-02	0.2485E-01	0.1301E+01	0.9628E+00	0.8638E+03	-0.5257E+03	0.3381E+03	0.7680E+03
67	0.9881E-02	0.2478E-01	0.8557E+00	0.5977E+00	0.5374E+03	-0.3503E+03	0.1871E+03	0.5580E+03
68	0.9998E-02	0.2469E-01	0.6278E+00	0.4396E+00	0.4135E+03	-0.2570E+03	0.1566E+03	0.4400E+03
69	0.1008E-01	0.2460E-01	0.4598E+00	0.3037E+00	0.2861E+03	-0.1953E+03	0.9077E+02	0.1650E+03
70	0.1014E-01	0.2454E-01	0.3803E+00	0.1935E+00	0.2248E+03	-0.1578E+03	0.6698E+02	0.1690E+03
71	0.1021E-01	0.2445E-01	0.3209E+00	0.1786E+00	0.1864E+03	-0.1361E+03	0.5033E+02	0.1780E+03
72	0.1027E-01	0.2434E-01	0.2645E+00	0.1050E+00	0.1361E+03	-0.1084E+03	0.2772E+02	0.1690E+03
73	0.1034E-01	0.2420E-01	0.1798E+00	0.3394E-01	0.1083E+03	-0.7893E+02	0.2942E+02	0.1390E+03
74	0.1039E-01	0.2404E-01	0.1541E+00	-0.6656E-02	0.7704E+02	-0.6486E+02	0.1218E+02	0.1280E+03
75	0.1041E-01	0.2385E-01	0.1741E+00	-0.2125E-01	0.8217E+02	-0.6647E+02	0.1570E+02	0.1530E+03
76	0.1042E-01	0.2336E-01	0.2113E+00	-0.4712E-01	0.1044E+03	-0.8033E+02	0.2404E+02	0.6830E+03
77	0.1042E-01	0.2258E-01	0.2429E+00	-0.5600E-01	0.1161E+03	-0.9049E+02	0.2561E+02	0.8180E+03
78	0.1042E-01	0.2178E-01	0.2770E+00	-0.6307E-01	0.1284E+03	-0.1013E+03	0.2714E+02	0.9250E+03
79	0.1042E-01	0.2098E-01	0.3170E+00	-0.7442E-01	0.1398E+03	-0.1169E+03	0.2293E+02	0.1061E+04
80	0.1042E-01	0.2017E-01	0.3374E+00	-0.7732E-01	0.1532E+03	-0.1198E+03	0.3331E+02	0.1145E+04
81	0.1042E-01	0.1935E-01	0.3290E+00	-0.7825E-01	0.1463E+03	-0.1171E+03	0.2919E+02	0.1146E+04
82	0.1042E-01	0.1852E-01	0.3845E+00	-0.7012E-01	0.1727E+03	-0.1331E+03	0.3962E+02	0.1347E+04
83	0.1042E-01	0.1768E-01	0.4001E+00	-0.6913E-01	0.1767E+03	-0.1390E+03	0.3765E+02	0.1457E+04
84	0.1042E-01	0.1683E-01	0.4544E+00	-0.8850E-01	0.1987E+03	-0.1599E+03	0.3885E+02	0.1667E+04
85	0.1042E-01	0.1598E-01	0.4619E+00	-0.7627E-01	0.1973E+03	-0.1604E+03	0.3688E+02	0.1723E+04
86	0.1042E-01	0.1511E-01	0.4853E+00	-0.7102E-01	0.2078E+03	-0.1694E+03	0.3842E+02	0.1868E+04

87	0.1042E-01	0.1424E-01	0.5290E+00	-0.6546E-01	0.2243E+03	-0.1832E+03	0.4115E+02	0.2083E+04
88	0.1042E-01	0.1335E-01	0.5402E+00	-0.8054E-01	0.2252E+03	-0.1867E+03	0.3855E+02	0.2165E+04
89	0.1042E-01	0.1246E-01	0.5921E+00	-0.6374E-01	0.2441E+03	-0.2008E+03	0.4331E+02	0.2426E+04
90	0.1042E-01	0.1156E-01	0.5687E+00	-0.4853E-01	0.2309E+03	-0.1904E+03	0.4049E+02	0.2422E+04
91	0.1042E-01	0.1064E-01	0.6123E+00	-0.4125E-01	0.2490E+03	-0.2076E+03	0.4143E+02	0.2667E+04
92	0.1042E-01	0.9723E-02	0.6199E+00	-0.4933E-01	0.2520E+03	-0.2099E+03	0.4208E+02	0.2845E+04
93	0.1042E-01	0.8792E-02	0.6141E+00	-0.2286E-01	0.2466E+03	-0.2109E+03	0.3571E+02	0.2917E+04
94	0.1059E-01	0.7755E-02	0.6036E+00	-0.4341E-01	0.2438E+03	-0.2052E+03	0.3858E+02	0.3802E+04
95	0.1163E-01	0.6717E-02	0.5947E+00	-0.2543E-01	0.2505E+03	-0.2097E+03	0.4080E+02	0.6636E+04
96	0.1313E-01	0.6250E-02	0.5989E+00	-0.1863E-01	0.2516E+03	-0.2051E+03	0.4656E+02	0.3939E+04
97	0.1438E-01	0.6250E-02	0.6598E+00	-0.2038E-01	0.2792E+03	-0.2222E+03	0.5704E+02	0.4133E+04
98	0.1561E-01	0.6250E-02	0.7142E+00	-0.2927E-01	0.3146E+03	-0.2402E+03	0.7444E+02	0.4362E+04
99	0.1682E-01	0.6250E-02	0.8081E+00	-0.3201E-01	0.3627E+03	-0.2670E+03	0.9565E+02	0.4764E+04
100	0.1800E-01	0.6250E-02	0.9157E+00	-0.1632E-01	0.4181E+03	-0.2938E+03	0.1243E+03	0.5169E+04
101	0.1915E-01	0.6250E-02	0.1038E+01	0.1405E-01	0.4752E+03	-0.3289E+03	0.1463E+03	0.5629E+04
102	0.2029E-01	0.6250E-02	0.1181E+01	0.3110E-01	0.5491E+03	-0.3672E+03	0.1818E+03	0.6168E+04
103	0.2139E-01	0.6250E-02	0.1260E+01	0.5618E-01	0.5930E+03	-0.3950E+03	0.1980E+03	0.6521E+04
104	0.2248E-01	0.6250E-02	0.1400E+01	0.8279E-01	0.6715E+03	-0.4371E+03	0.2343E+03	0.7017E+04
105	0.2353E-01	0.6250E-02	0.1587E+01	0.1171E+00	0.7803E+03	-0.4823E+03	0.2980E+03	0.7649E+04
106	0.2457E-01	0.6250E-02	0.1663E+01	0.1551E+00	0.8130E+03	-0.5069E+03	0.3061E+03	0.7805E+04
107	0.2558E-01	0.6250E-02	0.1872E+01	0.2105E+00	0.9219E+03	-0.5665E+03	0.3553E+03	0.8497E+04
108	0.2656E-01	0.6250E-02	0.2006E+01	0.2495E+00	0.1005E+04	-0.6025E+03	0.4022E+03	0.8900E+04
109	0.2753E-01	0.6250E-02	0.2126E+01	0.2978E+00	0.1075E+04	-0.6382E+03	0.4365E+03	0.9149E+04
110	0.2877E-01	0.6250E-02	0.2305E+01	0.3913E+00	0.1204E+04	-0.6921E+03	0.5122E+03	0.1652E+05
111	0.3031E-01	0.6250E-02	0.2449E+01	0.4702E+00	0.1277E+04	-0.7411E+03	0.5356E+03	0.1763E+05
112	0.3184E-01	0.6250E-02	0.2568E+01	0.5252E+00	0.1342E+04	-0.7802E+03	0.5616E+03	0.1833E+05
113	0.3337E-01	0.6250E-02	0.2765E+01	0.6148E+00	0.1477E+04	-0.8344E+03	0.6422E+03	0.1969E+05
114	0.3489E-01	0.6250E-02	0.2861E+01	0.7096E+00	0.1539E+04	-0.8678E+03	0.6709E+03	0.2046E+05
115	0.3641E-01	0.6250E-02	0.2952E+01	0.7750E+00	0.1593E+04	-0.9018E+03	0.6914E+03	0.2102E+05
116	0.3793E-01	0.6250E-02	0.3120E+01	0.8374E+00	0.1688E+04	-0.9481E+03	0.7398E+03	0.2205E+05
117	0.3944E-01	0.6250E-02	0.3111E+01	0.8948E+00	0.1717E+04	-0.9505E+03	0.7660E+03	0.2209E+05
118	0.4094E-01	0.6250E-02	0.3272E+01	0.9933E+00	0.1823E+04	-0.9965E+03	0.8264E+03	0.2315E+05
119	0.4245E-01	0.6250E-02	0.3275E+01	0.9958E+00	0.1828E+04	-0.1006E+04	0.8223E+03	0.2324E+05
120	0.4394E-01	0.6250E-02	0.3382E+01	0.1095E+01	0.1915E+04	-0.1038E+04	0.8773E+03	0.2392E+05
121	0.4544E-01	0.6250E-02	0.3492E+01	0.1136E+01	0.1978E+04	-0.1073E+04	0.9045E+03	0.2473E+05
122	0.4692E-01	0.6250E-02	0.3494E+01	0.1191E+01	0.1987E+04	-0.1080E+04	0.9070E+03	0.2469E+05
123	0.4841E-01	0.6250E-02	0.3443E+01	0.1208E+01	0.1964E+04	-0.1067E+04	0.8971E+03	0.2440E+05
124	0.4989E-01	0.6250E-02	0.3488E+01	0.1229E+01	0.1987E+04	-0.1077E+04	0.9105E+03	0.2461E+05
125	0.5136E-01	0.6250E-02	0.3467E+01	0.1246E+01	0.2000E+04	-0.1075E+04	0.9256E+03	0.2450E+05
126	0.5283E-01	0.6250E-02	0.3455E+01	0.1279E+01	0.1992E+04	-0.1078E+04	0.9139E+03	0.2444E+05
127	0.5430E-01	0.6250E-02	0.3467E+01	0.1314E+01	0.2015E+04	-0.1076E+04	0.9394E+03	0.2443E+05
128	0.5576E-01	0.6250E-02	0.3542E+01	0.1351E+01	0.2056E+04	-0.1104E+04	0.9520E+03	0.2491E+05
129	0.5722E-01	0.6250E-02	0.3484E+01	0.1385E+01	0.2022E+04	-0.1086E+04	0.9356E+03	0.2446E+05
130	0.5867E-01	0.6250E-02	0.3494E+01	0.1398E+01	0.2033E+04	-0.1087E+04	0.9466E+03	0.2442E+05
131	0.6012E-01	0.6250E-02	0.3456E+01	0.1414E+01	0.2025E+04	-0.1084E+04	0.9411E+03	0.2427E+05
132	0.6156E-01	0.6250E-02	0.3433E+01	0.1439E+01	0.2026E+04	-0.1077E+04	0.9489E+03	0.2407E+05
133	0.6300E-01	0.6250E-02	0.3410E+01	0.1408E+01	0.1996E+04	-0.1070E+04	0.9256E+03	0.2378E+05
134	0.6444E-01	0.6250E-02	0.3440E+01	0.1464E+01	0.2015E+04	-0.1081E+04	0.9340E+03	0.2402E+05
135	0.6587E-01	0.6250E-02	0.3402E+01	0.1462E+01	0.2010E+04	-0.1068E+04	0.9421E+03	0.2354E+05
136	0.6729E-01	0.6250E-02	0.3358E+01	0.1465E+01	0.1997E+04	-0.1062E+04	0.9349E+03	0.2334E+05
137	0.6871E-01	0.6250E-02	0.3362E+01	0.1502E+01	0.1998E+04	-0.1063E+04	0.9354E+03	0.2344E+05
138	0.7013E-01	0.6250E-02	0.3312E+01	0.1474E+01	0.1961E+04	-0.1048E+04	0.9125E+03	0.2286E+05
139	0.7154E-01	0.6250E-02	0.3288E+01	0.1456E+01	0.1949E+04	-0.1039E+04	0.9098E+03	0.2261E+05
140	0.7295E-01	0.6250E-02	0.3254E+01	0.1488E+01	0.1960E+04	-0.1028E+04	0.9327E+03	0.2240E+05
141	0.7436E-01	0.6250E-02	0.3232E+01	0.1508E+01	0.1964E+04	-0.1025E+04	0.9385E+03	0.2219E+05
142	0.7575E-01	0.6250E-02	0.3198E+01	0.1474E+01	0.1929E+04	-0.1008E+04	0.9216E+03	0.2180E+05
143	0.7715E-01	0.6250E-02	0.3196E+01	0.1511E+01	0.1927E+04	-0.1018E+04	0.9094E+03	0.2182E+05
144	0.7854E-01	0.6250E-02	0.3198E+01	0.1521E+01	0.1937E+04	-0.1014E+04	0.9226E+03	0.2182E+05
145	0.7993E-01	0.6250E-02	0.3127E+01	0.1505E+01	0.1893E+04	-0.9957E+03	0.8973E+03	0.2133E+05
146	0.8131E-01	0.6250E-02	0.3165E+01	0.1521E+01	0.1928E+04	-0.1002E+04	0.9265E+03	0.2144E+05
147	0.8268E-01	0.6250E-02	0.3068E+01	0.1483E+01	0.1859E+04	-0.9790E+03	0.8795E+03	0.2083E+05
148	0.8406E-01	0.6250E-02	0.3078E+01	0.1514E+01	0.1882E+04	-0.9787E+03	0.9036E+03	0.2072E+05
149	0.8542E-01	0.6250E-02	0.3003E+01	0.1469E+01	0.1837E+04	-0.9589E+03	0.8786E+03	0.2030E+05
150	0.8679E-01	0.6250E-02	0.2988E+01	0.1496E+01	0.1833E+04	-0.9584E+03	0.8748E+03	0.2021E+05
151	0.8815E-01	0.6250E-02	0.2982E+01	0.1508E+01	0.1840E+04	-0.9501E+03	0.8904E+03	0.1992E+05
152	0.8950E-01	0.6250E-02	0.2976E+01	0.1514E+01	0.1843E+04	-0.9475E+03	0.8957E+03	0.1983E+05
153	0.9085E-01	0.6250E-02	0.2940E+01	0.1508E+01	0.1820E+04	-0.9344E+03	0.8856E+03	0.1952E+05
154	0.9220E-01	0.6250E-02	0.2901E+01	0.1508E+01	0.1804E+04	-0.9233E+03	0.8808E+03	0.1931E+05
155	0.9354E-01	0.6250E-02	0.2806E+01	0.1444E+01	0.1726E+04	-0.8960E+03	0.8303E+03	0.1869E+05
156	0.9487E-01	0.6250E-02	0.2856E+01	0.1469E+01	0.1760E+04	-0.9061E+03	0.8543E+03	0.1880E+05
157	0.9621E-01	0.6250E-02	0.2780E+01	0.1451E+01	0.1730E+04	-0.8874E+03	0.8424E+03	0.1841E+05
158	0.9753E-01	0.6250E-02	0.2734E+01	0.1452E+01	0.1705E+04	-0.8786E+03	0.8264E+03	0.1808E+05
159	0.9886E-01	0.6250E-02	0.2737E+01	0.1442E+01	0.1710E+04	-0.8700E+03	0.8400E+03	0.1798E+05
160	0.1002E+00	0.6250E-02	0.2728E+01	0.1482E+01	0.1709E+04	-0.8713E+03	0.8373E+03	0.1776E+05
161	0.1015E+00	0.6250E-02	0.2668E+01	0.1451E+01	0.1671E+04	-0.8569E+03	0.8144E+03	0.1746E+05
162	0.1028E+00	0.6250E-02	0.2667E+01	0.1424E+01	0.1682E+04	-0.8542E+03	0.8273E+03	0.1730E+05
163	0.1041E+00	0.6250E-02	0.2625E+01	0.1430E+01	0.1662E+04	-0.8413E+03	0.8203E+03	0.1702E+05
164	0.1054E+00	0.6250E-02	0.2600E+01	0.1440E+01	0.1654E+04	-0.8325E+03	0.8215E+03	0.1687E+05
165	0.1067E+00	0.6250E-02	0.2564E+01	0.1400E+01	0.1604E+04	-0.8289E+03	0.7756E+03	0.1659E+05
166	0.1080E+00	0.6250E-02	0.2576E+01	0.1425E+01	0.1636E+04	-0.8290E+03	0.8065E+03	0.1648E+05
167	0.1093E+00	0.6250E-02	0.2593E+01	0.1418E+01	0.1633E+04	-0.8331E+03	0.7995E+03	0.1659E+05
168	0.1106E+00	0.6250E-02	0.2516E+01	0.1402E+01	0.1583E+04	-0.8084E+03	0.7747E+03	0.1605E+05
169	0.1118E+00	0.6250E-02	0.2528E+01	0.1441E+01	0.1618E+04	-0.8098E+03	0.8086E+03	0.1613E+05
170	0.1131E+00	0.6250E-02	0.2486E+01	0.1409E+01	0.1576E+04	-0.8005E+03	0.7753E+03	0.1578E+05
171	0.1144E+00	0.6250E-02	0.2445E+01	0.1437E+01	0.1571E+04	-0.7838E+03	0.7874E+03	0.1546E+05
172	0.1157E+00	0.6250E-02	0.2460E+01	0.1445E+01	0.1583E+04	-0.7927E+03	0.7900E+03	0.1547E+05
173	0.1169E+00	0.6250E-02	0.2394E+01	0.1408E+01	0.1538E+04	-0.7691E+03	0.7689E+03	0.1511E+05
174	0.1182E+00	0.6250E-02	0.2337E+01	0.1403E+01	0.1521E+04	-0.7499E+03	0.7713E+03	0.1468E+05
175	0.1194E+00	0.6250E-02	0.2267E+01	0.1402E+01	0.1484E+04	-0.7265E+03	0.7576E+03	0.1412E+05
176	0.1207E+00	0.6250E-02	0.2218E+01	0.1402E+01	0.1462E+04	-0.7141E+03	0.7483E+03	0.1388E+05
177	0.1219E+00	0.6250E-02	0.2158E+01	0.1390E+01	0.1420E+04	-0.6901E+03	0.7302E+03	0.1338E+05
178	0.1232E+00	0.6250E-02	0.2074E+01	0.1400E+01	0.1393E+04	-0.6695E+03	0.7235E+03	0.1292E+05
179	0.1244E+00	0.6250E-02	0.1963E+01	0.1428E+01	0.1362E+04	-0.6342E+03	0.7280E+03	0.1214E+05

NONDIMENSIONAL SURFACE QUANTITIES

0.5*ROF*UF**2= 0.5857E+02 0.5*ROF*UF**3= 0.8797E+05

ELEMENT	X, m	Y, m	S/Rn	CP	CF	CH	CPFM	CFFM	CHFM	CPMN
1	0.345E-05	0.208E-03	0.166E-01	0.179E+01	-0.200E-02	0.202E+00	0.250E+01	0.332E-01	0.776E+00	0.184E+01
2	0.174E-04	0.625E-03	0.500E-01	0.183E+01	0.681E-02	0.203E+00	0.250E+01	0.999E-01	0.775E+00	0.183E+01
3	0.457E-04	0.105E-02	0.838E-01	0.183E+01	0.127E-01	0.206E+00	0.249E+01	0.167E+00	0.773E+00	0.183E+01
4	0.888E-04	0.147E-02	0.118E+00	0.183E+01	0.183E-01	0.205E+00	0.247E+01	0.234E+00	0.771E+00	0.181E+01
5	0.147E-03	0.190E-02	0.153E+00	0.183E+01	0.266E-01	0.205E+00	0.245E+01	0.300E+00	0.767E+00	0.180E+01
6	0.221E-03	0.233E-02	0.187E+00	0.183E+01	0.338E-01	0.202E+00	0.242E+01	0.366E+00	0.763E+00	0.178E+01
7	0.311E-03	0.276E-02	0.223E+00	0.183E+01	0.409E-01	0.200E+00	0.239E+01	0.431E+00	0.757E+00	0.175E+01
8	0.417E-03	0.319E-02	0.258E+00	0.181E+01	0.464E-01	0.196E+00	0.235E+01	0.494E+00	0.750E+00	0.172E+01
9	0.540E-03	0.363E-02	0.294E+00	0.180E+01	0.472E-01	0.190E+00	0.231E+01	0.555E+00	0.743E+00	0.168E+01
10	0.680E-03	0.406E-02	0.331E+00	0.179E+01	0.537E-01	0.185E+00	0.226E+01	0.614E+00	0.734E+00	0.165E+01
11	0.840E-03	0.451E-02	0.369E+00	0.179E+01	0.504E-01	0.178E+00	0.224E+01	0.643E+00	0.729E+00	0.162E+01
12	0.101E-02	0.499E-02	0.410E+00	0.178E+01	0.510E-01	0.171E+00	0.224E+01	0.643E+00	0.729E+00	0.162E+01
13	0.119E-02	0.546E-02	0.450E+00	0.177E+01	0.534E-01	0.167E+00	0.224E+01	0.643E+00	0.729E+00	0.162E+01
14	0.136E-02	0.594E-02	0.491E+00	0.177E+01	0.525E-01	0.163E+00	0.224E+01	0.643E+00	0.729E+00	0.162E+01
15	0.153E-02	0.642E-02	0.531E+00	0.177E+01	0.530E-01	0.160E+00	0.224E+01	0.643E+00	0.729E+00	0.162E+01
16	0.171E-02	0.690E-02	0.572E+00	0.176E+01	0.562E-01	0.157E+00	0.224E+01	0.643E+00	0.729E+00	0.162E+01
17	0.188E-02	0.738E-02	0.613E+00	0.176E+01	0.540E-01	0.154E+00	0.224E+01	0.643E+00	0.729E+00	0.162E+01
18	0.206E-02	0.786E-02	0.654E+00	0.175E+01	0.578E-01	0.152E+00	0.224E+01	0.643E+00	0.729E+00	0.162E+01
19	0.223E-02	0.834E-02	0.695E+00	0.174E+01	0.590E-01	0.148E+00	0.224E+01	0.643E+00	0.729E+00	0.162E+01
20	0.241E-02	0.883E-02	0.736E+00	0.174E+01	0.567E-01	0.146E+00	0.224E+01	0.643E+00	0.729E+00	0.162E+01
21	0.259E-02	0.931E-02	0.778E+00	0.174E+01	0.648E-01	0.144E+00	0.224E+01	0.643E+00	0.729E+00	0.162E+01
22	0.276E-02	0.980E-02	0.819E+00	0.173E+01	0.611E-01	0.143E+00	0.224E+01	0.643E+00	0.729E+00	0.162E+01
23	0.294E-02	0.103E-01	0.861E+00	0.173E+01	0.646E-01	0.142E+00	0.224E+01	0.643E+00	0.729E+00	0.162E+01
24	0.312E-02	0.108E-01	0.902E+00	0.172E+01	0.640E-01	0.141E+00	0.224E+01	0.643E+00	0.729E+00	0.162E+01
25	0.330E-02	0.113E-01	0.944E+00	0.171E+01	0.661E-01	0.139E+00	0.224E+01	0.643E+00	0.729E+00	0.162E+01
26	0.348E-02	0.118E-01	0.986E+00	0.171E+01	0.670E-01	0.138E+00	0.224E+01	0.643E+00	0.729E+00	0.162E+01
27	0.366E-02	0.122E-01	0.103E+01	0.170E+01	0.678E-01	0.137E+00	0.224E+01	0.643E+00	0.729E+00	0.162E+01
28	0.384E-02	0.127E-01	0.107E+01	0.170E+01	0.685E-01	0.135E+00	0.224E+01	0.643E+00	0.729E+00	0.162E+01
29	0.402E-02	0.132E-01	0.111E+01	0.169E+01	0.750E-01	0.135E+00	0.224E+01	0.643E+00	0.729E+00	0.162E+01
30	0.420E-02	0.137E-01	0.115E+01	0.168E+01	0.698E-01	0.135E+00	0.224E+01	0.643E+00	0.729E+00	0.162E+01
31	0.438E-02	0.142E-01	0.120E+01	0.167E+01	0.762E-01	0.134E+00	0.224E+01	0.643E+00	0.729E+00	0.162E+01
32	0.456E-02	0.147E-01	0.124E+01	0.167E+01	0.748E-01	0.133E+00	0.224E+01	0.643E+00	0.729E+00	0.162E+01
33	0.474E-02	0.152E-01	0.128E+01	0.166E+01	0.803E-01	0.132E+00	0.224E+01	0.643E+00	0.729E+00	0.162E+01
34	0.492E-02	0.157E-01	0.132E+01	0.165E+01	0.808E-01	0.131E+00	0.224E+01	0.643E+00	0.729E+00	0.162E+01
35	0.511E-02	0.162E-01	0.137E+01	0.164E+01	0.847E-01	0.131E+00	0.224E+01	0.643E+00	0.729E+00	0.162E+01
36	0.529E-02	0.167E-01	0.141E+01	0.163E+01	0.841E-01	0.128E+00	0.224E+01	0.643E+00	0.729E+00	0.162E+01
37	0.547E-02	0.172E-01	0.145E+01	0.162E+01	0.892E-01	0.128E+00	0.224E+01	0.643E+00	0.729E+00	0.162E+01
38	0.566E-02	0.177E-01	0.150E+01	0.161E+01	0.902E-01	0.128E+00	0.224E+01	0.643E+00	0.729E+00	0.162E+01
39	0.584E-02	0.183E-01	0.154E+01	0.159E+01	0.961E-01	0.127E+00	0.224E+01	0.643E+00	0.729E+00	0.162E+01
40	0.603E-02	0.188E-01	0.158E+01	0.158E+01	0.967E-01	0.127E+00	0.224E+01	0.643E+00	0.729E+00	0.162E+01
41	0.621E-02	0.193E-01	0.163E+01	0.157E+01	0.103E+00	0.128E+00	0.224E+01	0.643E+00	0.729E+00	0.162E+01
42	0.640E-02	0.198E-01	0.167E+01	0.154E+01	0.106E+00	0.128E+00	0.224E+01	0.643E+00	0.729E+00	0.162E+01
43	0.659E-02	0.203E-01	0.171E+01	0.152E+01	0.109E+00	0.127E+00	0.224E+01	0.643E+00	0.729E+00	0.162E+01
44	0.677E-02	0.208E-01	0.176E+01	0.151E+01	0.116E+00	0.129E+00	0.224E+01	0.643E+00	0.729E+00	0.162E+01
45	0.696E-02	0.213E-01	0.180E+01	0.147E+01	0.126E+00	0.128E+00	0.224E+01	0.643E+00	0.729E+00	0.162E+01
46	0.715E-02	0.218E-01	0.184E+01	0.145E+01	0.130E+00	0.130E+00	0.224E+01	0.643E+00	0.729E+00	0.162E+01
47	0.734E-02	0.224E-01	0.189E+01	0.141E+01	0.148E+00	0.128E+00	0.224E+01	0.643E+00	0.729E+00	0.162E+01
48	0.752E-02	0.229E-01	0.193E+01	0.136E+01	0.158E+00	0.131E+00	0.224E+01	0.643E+00	0.729E+00	0.162E+01
49	0.771E-02	0.234E-01	0.198E+01	0.129E+01	0.175E+00	0.130E+00	0.224E+01	0.643E+00	0.729E+00	0.162E+01
50	0.790E-02	0.239E-01	0.202E+01	0.122E+01	0.215E+00	0.138E+00	0.224E+01	0.643E+00	0.729E+00	0.162E+01
51	0.802E-02	0.242E-01	0.205E+01	0.104E+01	0.244E+00	0.133E+00	0.218E+01	0.703E+00	0.718E+00	0.157E+01
52	0.806E-02	0.243E-01	0.206E+01	0.958E+00	0.260E+00	0.126E+00	0.203E+01	0.814E+00	0.690E+00	0.145E+01
53	0.812E-02	0.244E-01	0.207E+01	0.857E+00	0.261E+00	0.120E+00	0.184E+01	0.909E+00	0.653E+00	0.130E+01
54	0.820E-02	0.245E-01	0.208E+01	0.738E+00	0.248E+00	0.109E+00	0.161E+01	0.976E+00	0.606E+00	0.112E+01
55	0.829E-02	0.246E-01	0.209E+01	0.625E+00	0.238E+00	0.972E-01	0.135E+01	0.100E+01	0.547E+00	0.915E+00
56	0.841E-02	0.247E-01	0.210E+01	0.500E+00	0.212E+00	0.805E-01	0.106E+01	0.969E+00	0.476E+00	0.692E+00
57	0.854E-02	0.248E-01	0.211E+01	0.393E+00	0.187E+00	0.671E-01	0.765E+00	0.872E+00	0.392E+00	0.469E+00
58	0.870E-02	0.249E-01	0.213E+01	0.288E+00	0.153E+00	0.513E-01	0.480E+00	0.702E+00	0.294E+00	0.265E+00
59	0.888E-02	0.250E-01	0.214E+01	0.205E+00	0.119E+00	0.369E-01	0.235E+00	0.461E+00	0.184E+00	0.104E+00
60	0.907E-02	0.250E-01	0.216E+01	0.136E+00	0.872E-01	0.251E-01	0.576E-01	0.163E+00	0.635E-01	0.122E-01
61	0.922E-02	0.250E-01	0.217E+01	0.935E-01	0.603E-01	0.172E-01	0.275E-02	0.948E-02	0.366E-02	0.000E+00
62	0.931E-02	0.250E-01	0.218E+01	0.750E-01	0.496E-01	0.137E-01	0.321E-04	0.117E-03	0.445E-04	0.000E+00
63	0.942E-02	0.250E-01	0.218E+01	0.558E-01	0.404E-01	0.934E-02	0.125E-07	0.430E-07	0.160E-07	0.000E+00
64	0.953E-02	0.249E-01	0.219E+01	0.450E-01	0.337E-01	0.858E-02	-0.403E-12	0.112E-10	0.454E-11	0.000E+00
65	0.964E-02	0.249E-01	0.220E+01	0.327E-01	0.222E-01	0.547E-02	-0.934E-19	0.682E-18	0.285E-18	0.000E+00
66	0.976E-02	0.249E-01	0.221E+01	0.222E-01	0.164E-01	0.384E-02	-0.476E-28	0.189E-27	0.828E-28	0.000E+00
67	0.988E-02	0.248E-01	0.223E+01	0.146E-01	0.102E-01	0.213E-02	-0.111E-39	0.287E-39	0.135E-39	0.000E+00
68	0.100E-01	0.247E-01	0.224E+01	0.107E-01	0.751E-02	0.178E-02	0.000E+00	0.000E+00	0.000E+00	0.000E+00
69	0.101E-01	0.246E-01	0.225E+01	0.785E-02	0.519E-02	0.103E-02	0.000E+00	0.000E+00	0.000E+00	0.000E+00
70	0.101E-01	0.245E-01	0.225E+01	0.649E-02	0.330E-02	0.761E-03	0.000E+00	0.000E+00	0.000E+00	0.000E+00
71	0.102E-01	0.244E-01	0.226E+01	0.548E-02	0.305E-02	0.572E-03	0.000E+00	0.000E+00	0.000E+00	0.000E+00
72	0.103E-01	0.243E-01	0.227E+01	0.452E-02	0.179E-02	0.315E-03	0.000E+00	0.000E+00	0.000E+00	0.000E+00
73	0.103E-01	0.242E-01	0.229E+01	0.307E-02	0.579E-03	0.334E-03	0.000E+00	0.000E+00	0.000E+00	0.000E+00
74	0.104E-01	0.240E-01	0.230E+01	0.263E-02	-0.114E-03	0.138E-03	0.000E+00	0.000E+00	0.000E+00	0.000E+00
75	0.104E-01	0.238E-01	0.231E+01	0.297E-02	-0.363E-03	0.179E-03	0.000E+00	0.000E+00	0.000E+00	0.000E+00
76	0.104E-01	0.234E-01	0.235E+01	0.361E-02	-0.804E-03	0.273E-03	0.000E+00	0.000E+00	0.000E+00	0.000E+00
77	0.104E-01	0.226E-01	0.242E+01	0.415E-02	-0.956E-03	0.291E-03	0.000E+00	0.000E+00	0.000E+00	0.000E+00
78	0.104E-01	0.218E-01	0.248E+01	0.473E-02	-0.108E-02	0.308E-03	0.000E+00	0.000E+00	0.000E+00	0.000E+00
79	0.104E-01	0.210E-01	0.254E+01	0.541E-02	-0.127E-02	0.261E-03	0.000E+00	0.000E+00	0.000E+00	0.000E+00
80	0.104E-01	0.202E-01	0.261E+01	0.576E-02	-0.132E-02	0.379E-03	0.000E+00	0.000E+00	0.000E+00	0.000E+00
81	0.104E-01	0.194E-01	0.267E+01	0.562E-02	-0.134E-02	0.332E-03	0.000E+00	0.000E+00	0.000E+00	0.000E+00
82	0.104E-01	0.185E-01	0.274E+01	0.657E-02	-0.120E-02	0.450E-03	0.000E+00	0.000E+00	0.000E+00	0.000E+00
83	0.104E-01	0.177E-01	0.281E+01	0.683E-02	-0.118E-02	0.428E-03	0.000E+00	0.000E+00	0.000E+00	0.000E+00
84	0.104E-01	0.168E-01	0.288E+01	0.776E-02	-0.151E-02	0.442E-03	0.000E+00	0.000E+00	0.000E+00	0.000E+00
85	0.104E-01	0.160E-01	0.294E+01	0.789E-02	-0.130E-02	0.419E-03	0.000E+00	0.000E+00	0.000E+00	0.000E+00
86	0.104E-01	0.151E-01	0.301E+01	0.829E-02	-0.121E-02	0.437E-03	0.000E+00	0.000E+00	0.000E+00	0.000E+00
87	0.104E-01	0.142E-01	0.308E+01	0.903E-02	-0.112E-02	0.468E-03	0.000E+00	0.000E+00	0.000E+00	0.000E+00

88	0.104E-01	0.134E-01	0.315E+01	0.922E-02	-0.138E-02	0.438E-03	0.000E+00	0.000E+00	0.000E+00	0.000E+00
89	0.104E-01	0.125E-01	0.323E+01	0.101E-01	-0.109E-02	0.492E-03	0.000E+00	0.000E+00	0.000E+00	0.000E+00
90	0.104E-01	0.116E-01	0.330E+01	0.971E-02	-0.829E-03	0.460E-03	0.000E+00	0.000E+00	0.000E+00	0.000E+00
91	0.104E-01	0.106E-01	0.337E+01	0.105E-01	-0.704E-03	0.471E-03	0.000E+00	0.000E+00	0.000E+00	0.000E+00
92	0.104E-01	0.972E-02	0.344E+01	0.106E-01	-0.842E-03	0.478E-03	0.000E+00	0.000E+00	0.000E+00	0.000E+00
93	0.104E-01	0.879E-02	0.352E+01	0.105E-01	-0.390E-03	0.406E-03	0.000E+00	0.000E+00	0.000E+00	0.000E+00
94	0.106E-01	0.775E-02	0.360E+01	0.103E-01	-0.741E-03	0.439E-03	0.000E+00	0.000E+00	0.000E+00	0.000E+00
95	0.116E-01	0.672E-02	0.372E+01	0.102E-01	-0.434E-03	0.464E-03	-0.212E-28	0.826E-28	0.363E-28	0.000E+00
96	0.131E-01	0.625E-02	0.385E+01	0.102E-01	-0.318E-03	0.529E-03	0.104E-01	0.342E-01	0.133E-01	0.000E+00
97	0.144E-01	0.625E-02	0.395E+01	0.113E-01	-0.348E-03	0.648E-03	0.104E-01	0.342E-01	0.133E-01	0.000E+00
98	0.156E-01	0.625E-02	0.404E+01	0.122E-01	-0.500E-03	0.846E-03	0.104E-01	0.342E-01	0.133E-01	0.000E+00
99	0.168E-01	0.625E-02	0.414E+01	0.138E-01	-0.546E-03	0.109E-02	0.104E-01	0.342E-01	0.133E-01	0.000E+00
100	0.180E-01	0.625E-02	0.424E+01	0.156E-01	-0.279E-03	0.141E-02	0.104E-01	0.342E-01	0.133E-01	0.000E+00
101	0.192E-01	0.625E-02	0.433E+01	0.177E-01	0.240E-03	0.166E-02	0.104E-01	0.342E-01	0.133E-01	0.000E+00
102	0.203E-01	0.625E-02	0.442E+01	0.202E-01	0.531E-03	0.207E-02	0.104E-01	0.342E-01	0.133E-01	0.000E+00
103	0.214E-01	0.625E-02	0.451E+01	0.215E-01	0.959E-03	0.225E-02	0.104E-01	0.342E-01	0.133E-01	0.000E+00
104	0.225E-01	0.625E-02	0.459E+01	0.239E-01	0.141E-02	0.266E-02	0.104E-01	0.342E-01	0.133E-01	0.000E+00
105	0.235E-01	0.625E-02	0.468E+01	0.271E-01	0.200E-02	0.339E-02	0.104E-01	0.342E-01	0.133E-01	0.000E+00
106	0.246E-01	0.625E-02	0.476E+01	0.284E-01	0.265E-02	0.348E-02	0.104E-01	0.342E-01	0.133E-01	0.000E+00
107	0.256E-01	0.625E-02	0.484E+01	0.320E-01	0.359E-02	0.404E-02	0.104E-01	0.342E-01	0.133E-01	0.000E+00
108	0.266E-01	0.625E-02	0.492E+01	0.343E-01	0.426E-02	0.457E-02	0.104E-01	0.342E-01	0.133E-01	0.000E+00
109	0.275E-01	0.625E-02	0.500E+01	0.363E-01	0.508E-02	0.496E-02	0.104E-01	0.342E-01	0.133E-01	0.000E+00
110	0.288E-01	0.625E-02	0.510E+01	0.394E-01	0.668E-02	0.582E-02	0.104E-01	0.342E-01	0.133E-01	0.000E+00
111	0.303E-01	0.625E-02	0.522E+01	0.418E-01	0.803E-02	0.609E-02	0.104E-01	0.342E-01	0.133E-01	0.000E+00
112	0.318E-01	0.625E-02	0.534E+01	0.439E-01	0.897E-02	0.638E-02	0.104E-01	0.342E-01	0.133E-01	0.000E+00
113	0.334E-01	0.625E-02	0.546E+01	0.472E-01	0.105E-01	0.730E-02	0.104E-01	0.342E-01	0.133E-01	0.000E+00
114	0.349E-01	0.625E-02	0.559E+01	0.489E-01	0.121E-01	0.763E-02	0.104E-01	0.342E-01	0.133E-01	0.000E+00
115	0.364E-01	0.625E-02	0.571E+01	0.504E-01	0.132E-01	0.786E-02	0.104E-01	0.342E-01	0.133E-01	0.000E+00
116	0.379E-01	0.625E-02	0.583E+01	0.533E-01	0.143E-01	0.841E-02	0.104E-01	0.342E-01	0.133E-01	0.000E+00
117	0.394E-01	0.625E-02	0.595E+01	0.531E-01	0.153E-01	0.871E-02	0.104E-01	0.342E-01	0.133E-01	0.000E+00
118	0.409E-01	0.625E-02	0.607E+01	0.559E-01	0.170E-01	0.939E-02	0.104E-01	0.342E-01	0.133E-01	0.000E+00
119	0.424E-01	0.625E-02	0.619E+01	0.559E-01	0.170E-01	0.935E-02	0.104E-01	0.342E-01	0.133E-01	0.000E+00
120	0.439E-01	0.625E-02	0.631E+01	0.578E-01	0.187E-01	0.997E-02	0.104E-01	0.342E-01	0.133E-01	0.000E+00
121	0.454E-01	0.625E-02	0.643E+01	0.596E-01	0.194E-01	0.103E-01	0.104E-01	0.342E-01	0.133E-01	0.000E+00
122	0.469E-01	0.625E-02	0.655E+01	0.596E-01	0.203E-01	0.103E-01	0.104E-01	0.342E-01	0.133E-01	0.000E+00
123	0.484E-01	0.625E-02	0.667E+01	0.588E-01	0.206E-01	0.102E-01	0.104E-01	0.342E-01	0.133E-01	0.000E+00
124	0.499E-01	0.625E-02	0.679E+01	0.596E-01	0.210E-01	0.104E-01	0.104E-01	0.342E-01	0.133E-01	0.000E+00
125	0.514E-01	0.625E-02	0.690E+01	0.592E-01	0.213E-01	0.105E-01	0.104E-01	0.342E-01	0.133E-01	0.000E+00
126	0.528E-01	0.625E-02	0.702E+01	0.590E-01	0.218E-01	0.104E-01	0.104E-01	0.342E-01	0.133E-01	0.000E+00
127	0.543E-01	0.625E-02	0.714E+01	0.592E-01	0.224E-01	0.107E-01	0.104E-01	0.342E-01	0.133E-01	0.000E+00
128	0.558E-01	0.625E-02	0.726E+01	0.605E-01	0.231E-01	0.108E-01	0.104E-01	0.342E-01	0.133E-01	0.000E+00
129	0.572E-01	0.625E-02	0.737E+01	0.595E-01	0.236E-01	0.106E-01	0.104E-01	0.342E-01	0.133E-01	0.000E+00
130	0.587E-01	0.625E-02	0.749E+01	0.597E-01	0.239E-01	0.108E-01	0.104E-01	0.342E-01	0.133E-01	0.000E+00
131	0.601E-01	0.625E-02	0.760E+01	0.590E-01	0.241E-01	0.107E-01	0.104E-01	0.342E-01	0.133E-01	0.000E+00
132	0.616E-01	0.625E-02	0.772E+01	0.586E-01	0.246E-01	0.108E-01	0.104E-01	0.342E-01	0.133E-01	0.000E+00
133	0.630E-01	0.625E-02	0.784E+01	0.582E-01	0.240E-01	0.105E-01	0.104E-01	0.342E-01	0.133E-01	0.000E+00
134	0.644E-01	0.625E-02	0.795E+01	0.587E-01	0.250E-01	0.106E-01	0.104E-01	0.342E-01	0.133E-01	0.000E+00
135	0.659E-01	0.625E-02	0.806E+01	0.581E-01	0.250E-01	0.107E-01	0.104E-01	0.342E-01	0.133E-01	0.000E+00
136	0.673E-01	0.625E-02	0.818E+01	0.573E-01	0.250E-01	0.106E-01	0.104E-01	0.342E-01	0.133E-01	0.000E+00
137	0.687E-01	0.625E-02	0.829E+01	0.574E-01	0.257E-01	0.106E-01	0.104E-01	0.342E-01	0.133E-01	0.000E+00
138	0.701E-01	0.625E-02	0.841E+01	0.565E-01	0.252E-01	0.104E-01	0.104E-01	0.342E-01	0.133E-01	0.000E+00
139	0.715E-01	0.625E-02	0.852E+01	0.561E-01	0.249E-01	0.103E-01	0.104E-01	0.342E-01	0.133E-01	0.000E+00
140	0.730E-01	0.625E-02	0.863E+01	0.556E-01	0.254E-01	0.106E-01	0.104E-01	0.342E-01	0.133E-01	0.000E+00
141	0.744E-01	0.625E-02	0.874E+01	0.552E-01	0.257E-01	0.107E-01	0.104E-01	0.342E-01	0.133E-01	0.000E+00
142	0.758E-01	0.625E-02	0.886E+01	0.546E-01	0.252E-01	0.105E-01	0.104E-01	0.342E-01	0.133E-01	0.000E+00
143	0.771E-01	0.625E-02	0.897E+01	0.546E-01	0.258E-01	0.103E-01	0.104E-01	0.342E-01	0.133E-01	0.000E+00
144	0.785E-01	0.625E-02	0.908E+01	0.546E-01	0.260E-01	0.105E-01	0.104E-01	0.342E-01	0.133E-01	0.000E+00
145	0.799E-01	0.625E-02	0.919E+01	0.534E-01	0.257E-01	0.102E-01	0.104E-01	0.342E-01	0.133E-01	0.000E+00
146	0.813E-01	0.625E-02	0.930E+01	0.540E-01	0.260E-01	0.105E-01	0.104E-01	0.342E-01	0.133E-01	0.000E+00
147	0.827E-01	0.625E-02	0.941E+01	0.524E-01	0.253E-01	0.100E-01	0.104E-01	0.342E-01	0.133E-01	0.000E+00
148	0.841E-01	0.625E-02	0.952E+01	0.525E-01	0.259E-01	0.103E-01	0.104E-01	0.342E-01	0.133E-01	0.000E+00
149	0.854E-01	0.625E-02	0.963E+01	0.513E-01	0.251E-01	0.999E-02	0.104E-01	0.342E-01	0.133E-01	0.000E+00
150	0.868E-01	0.625E-02	0.974E+01	0.510E-01	0.255E-01	0.994E-02	0.104E-01	0.342E-01	0.133E-01	0.000E+00
151	0.881E-01	0.625E-02	0.985E+01	0.509E-01	0.258E-01	0.101E-01	0.104E-01	0.342E-01	0.133E-01	0.000E+00
152	0.895E-01	0.625E-02	0.996E+01	0.508E-01	0.259E-01	0.102E-01	0.104E-01	0.342E-01	0.133E-01	0.000E+00
153	0.909E-01	0.625E-02	0.101E+02	0.502E-01	0.257E-01	0.101E-01	0.104E-01	0.342E-01	0.133E-01	0.000E+00
154	0.922E-01	0.625E-02	0.102E+02	0.495E-01	0.257E-01	0.100E-01	0.104E-01	0.342E-01	0.133E-01	0.000E+00
155	0.935E-01	0.625E-02	0.103E+02	0.479E-01	0.247E-01	0.944E-02	0.104E-01	0.342E-01	0.133E-01	0.000E+00
156	0.949E-01	0.625E-02	0.104E+02	0.488E-01	0.251E-01	0.971E-02	0.104E-01	0.342E-01	0.133E-01	0.000E+00
157	0.962E-01	0.625E-02	0.105E+02	0.475E-01	0.248E-01	0.958E-02	0.104E-01	0.342E-01	0.133E-01	0.000E+00
158	0.975E-01	0.625E-02	0.106E+02	0.467E-01	0.248E-01	0.939E-02	0.104E-01	0.342E-01	0.133E-01	0.000E+00
159	0.989E-01	0.625E-02	0.107E+02	0.467E-01	0.246E-01	0.955E-02	0.104E-01	0.342E-01	0.133E-01	0.000E+00
160	0.100E+00	0.625E-02	0.108E+02	0.466E-01	0.253E-01	0.952E-02	0.104E-01	0.342E-01	0.133E-01	0.000E+00
161	0.101E+00	0.625E-02	0.109E+02	0.456E-01	0.248E-01	0.926E-02	0.104E-01	0.342E-01	0.133E-01	0.000E+00
162	0.103E+00	0.625E-02	0.110E+02	0.455E-01	0.243E-01	0.940E-02	0.104E-01	0.342E-01	0.133E-01	0.000E+00
163	0.104E+00	0.625E-02	0.111E+02	0.448E-01	0.244E-01	0.932E-02	0.104E-01	0.342E-01	0.133E-01	0.000E+00
164	0.105E+00	0.625E-02	0.112E+02	0.444E-01	0.246E-01	0.934E-02	0.104E-01	0.342E-01	0.133E-01	0.000E+00
165	0.107E+00	0.625E-02	0.113E+02	0.438E-01	0.239E-01	0.882E-02	0.104E-01	0.342E-01	0.133E-01	0.000E+00
166	0.108E+00	0.625E-02	0.114E+02	0.440E-01	0.243E-01	0.917E-02	0.104E-01	0.342E-01	0.133E-01	0.000E+00
167	0.109E+00	0.625E-02	0.115E+02	0.443E-01	0.242E-01	0.909E-02	0.104E-01	0.342E-01	0.133E-01	0.000E+00
168	0.111E+00	0.625E-02	0.116E+02	0.430E-01	0.239E-01	0.881E-02	0.104E-01	0.342E-01	0.133E-01	0.000E+00
169	0.112E+00	0.625E-02	0.117E+02	0.432E-01	0.246E-01	0.919E-02	0.104E-01	0.342E-01	0.133E-01	0.000E+00
170	0.113E+00	0.625E-02	0.118E+02	0.424E-01	0.240E-01	0.881E-02	0.104E-01	0.342E-01	0.133E-01	0.000E+00
171	0.114E+00	0.625E-02	0.119E+02	0.417E-01	0.245E-01	0.895E-02	0.104E-01	0.342E-01	0.133E-01	0.000E+00
172	0.116E+00	0.625E-02	0.120E+02	0.420E-01	0.247E-01	0.898E-02	0.104E-01	0.342E-01	0.133E-01	0.000E+00
173	0.117E+00	0.625E-02	0.121E+02	0.409E-01	0.240E-01	0.874E-02	0.104E-01	0.342E-01	0.133E-01	0.000E+00
174	0.118E+00	0.625E-02	0.122E+02	0.399E-01	0.239E-01	0.877E-02	0.104E-01	0.342E-01	0.133E-01	0.000E+00
175	0.119E+00	0.625E-02	0.123E+02	0.387E-01	0.239E-01	0.861E-02	0.104E-01	0.342E-01	0.133E-01	0.000E+00
176	0.121E+00	0.625E-02	0.124E+02	0.379E-01	0.239E-01	0.851E-02	0.104E-01	0.342E-01	0.133E-01	0.000E+00
177	0.122E+00	0.625E-02	0.125E+02	0.368E-01	0.237E-01	0.830E-02	0.104E-01	0.342E-01	0.133E-01	0.000E+00
178	0.123E+00	0.625E-02	0.126E+02	0.354E-01	0.239E-01	0.822E-02	0.104E-01	0.342E-01	0.133E-01	0.000E+00
179	0.124E+00	0.625E-02	0.127E+02	0.335E-01	0.244E-01	0.828E-02	0.104E-01	0.342E-01	0.133E-01	0.000E+00

Table 7. Tabulated Quantities Including Surface Data for Case 3 (Blunted Cone with Sting).

FREESTREAM QUANTITIES

VELOCITY IN X-DIRECTION, M/S	= 1633.0
VELOCITY IN Y-DIRECTION, M/S	= 0.0
MACH NUMBER	= 20.69
SPEED OF SOUND, M/S	= 78.94
SPEED RATIO	= 17.31
MOST PROBABLE SPEED, M/S	= 94.35
TOTAL TEMPERATURE, K	= 1298.86
TEMPERATURE, K	= 15.00
DENSITY, KG/M3	= 0.4667E-03
NUMBER DENSITY, M-3	= 0.1003E+23
PRESSURE, N/M2	= 0.2077E+01
GAMMAF	= 1.40
MOLECULAR WEIGHT	= 28.020
VISCOSITY, PA*S	= 0.1849E-05
REYNOLDS NUMBER	= 0.2061E+05
SHOCK REYNOLDS NUMBER	= 0.7259E+03
V-BAR PARAMETER (M/SQRT(REN))	= 0.144
CHI-BAR PARAMETER (M*3/SQRT(REN)	= 61.67
CHARACTERISTIC LENGTH, M	= 0.5000E-01
MEAN FREE PATH, M	= 0.6060E-04
KNUDSEN NUMBER	= 0.00121

GAS

SPECIES = N2
MOLE FRACTIONS = 1.0000
MOLECULAR WEIGHT = 28.0200
REFERENCE TEMPERATURE,K = 300.00 VISCOSITY-TEMPERATURE-EXPONENT= 0.75

WALL DATA:

TEMPERATURE K = 300.0 FRACTION SPECULAR REFLECTION= 0.0

REGION 1 FROM TIME 0.533E-03 TO TIME 0.100E-02 COLLISIONS:- 0.15294E+10
REGION 2 FROM TIME 0.213E-02 TO TIME 0.402E-02 COLLISIONS:- 0.26560E+10
REGION 3 FROM TIME 0.213E-02 TO TIME 0.402E-02 COLLISIONS:- 0.53771E+09
REGION 4 FROM TIME 0.160E-03 TO TIME 0.301E-03 COLLISIONS:- 0.29027E+08
REGION 5 FROM TIME 0.959E-03 TO TIME 0.181E-02 COLLISIONS:- 0.41938E+09
REGION 6 FROM TIME 0.186E-02 TO TIME 0.352E-02 COLLISIONS:- 0.12911E+09
REGION 7 FROM TIME 0.160E-03 TO TIME 0.301E-03 COLLISIONS:- 0.79031E+07
REGION 8 FROM TIME 0.133E-03 TO TIME 0.251E-03 COLLISIONS:- 0.11287E+07
REGION 9 FROM TIME 0.160E-03 TO TIME 0.301E-03 COLLISIONS:- 0.21883E+07
REGION 10 FROM TIME 0.266E-02 TO TIME 0.502E-02 COLLISIONS:- 0.20433E+09
REGION 11 FROM TIME 0.213E-02 TO TIME 0.402E-02 COLLISIONS:- 0.82370E+08
REGION 12 FROM TIME 0.373E-02 TO TIME 0.704E-02 COLLISIONS:- 0.27810E+09
REGION 13 FROM TIME 0.532E-02 TO TIME 0.100E-01 COLLISIONS:- 0.58340E+09
REGION 14 FROM TIME 0.799E-02 TO TIME 0.151E-01 COLLISIONS:- 0.18359E+10

NUMBER OF MOVE SEGMENTS 0.14731E+11 RATIO 0.10050E+01
TOTAL NUMBER OF ENTERING MOLECULES = 1.67772E+07
0. EXCESS MOLECULE ERRORS 1734. REMOVAL ERRORS

TOTAL NUMBER OF SAMPLES 3150

FORCE ON SURFACE IN X DIRECTION, INCIDENT= 0.10066E+01 REFLECTED= 0.89856E+00 TOTAL(N)= 0.19052E+01 CD= 0.15594E+01

312671 MOLECULES

SURFACE PROPERTIES

ELEMENT	X COORD m	Y COORD m	PRESSURE N/m*2	SHEAR ST. N/m*2	INC ENG --	REF ENG --	NET ENG w/m*2	SAMPLE SPECIES 1-
1	0.3770E-05	0.2171E-03	0.1075E+04	0.1530E+01	0.4482E+06	-0.3643E+06	0.8389E+05	0.3247E+06
2	0.1886E-04	0.6511E-03	0.1134E+04	0.3044E+01	0.4693E+06	-0.3841E+06	0.8515E+05	0.3390E+06
3	0.4907E-04	0.1085E-02	0.1150E+04	0.5564E+01	0.4748E+06	-0.3906E+06	0.8419E+05	0.2955E+06
4	0.9440E-04	0.1518E-02	0.1146E+04	0.4896E+01	0.4716E+06	-0.3900E+06	0.8161E+05	0.2661E+06
5	0.1549E-03	0.1949E-02	0.1153E+04	0.9382E+01	0.4726E+06	-0.3928E+06	0.7980E+05	0.2497E+06
6	0.2304E-03	0.2379E-02	0.1139E+04	0.7479E+01	0.4652E+06	-0.3870E+06	0.7816E+05	0.2326E+06
7	0.3210E-03	0.2806E-02	0.1138E+04	0.8501E+01	0.4627E+06	-0.3874E+06	0.7526E+05	0.2212E+06
8	0.4266E-03	0.3230E-02	0.1129E+04	0.1034E+02	0.4586E+06	-0.3851E+06	0.7349E+05	0.2112E+06
9	0.5471E-03	0.3651E-02	0.1125E+04	0.1007E+02	0.4545E+06	-0.3843E+06	0.7014E+05	0.2033E+06
10	0.6825E-03	0.4068E-02	0.1117E+04	0.1025E+02	0.4504E+06	-0.3824E+06	0.6798E+05	0.1962E+06
11	0.8439E-03	0.4523E-02	0.1116E+04	0.1134E+02	0.4471E+06	-0.3820E+06	0.6514E+05	0.2283E+06
12	0.1024E-02	0.5018E-02	0.1115E+04	0.9658E+01	0.4458E+06	-0.3832E+06	0.6254E+05	0.2220E+06
13	0.1204E-02	0.5513E-02	0.1110E+04	0.1002E+02	0.4425E+06	-0.3815E+06	0.6094E+05	0.2144E+06
14	0.1385E-02	0.6009E-02	0.1111E+04	0.1059E+02	0.4419E+06	-0.3824E+06	0.5948E+05	0.2094E+06
15	0.1565E-02	0.6504E-02	0.1104E+04	0.1077E+02	0.4394E+06	-0.3797E+06	0.5973E+05	0.2030E+06
16	0.1745E-02	0.7000E-02	0.1112E+04	0.1135E+02	0.4413E+06	-0.3831E+06	0.5816E+05	0.2007E+06
17	0.1926E-02	0.7496E-02	0.1106E+04	0.1250E+02	0.4384E+06	-0.3790E+06	0.5943E+05	0.1954E+06
18	0.2106E-02	0.7991E-02	0.1105E+04	0.1225E+02	0.4371E+06	-0.3796E+06	0.5751E+05	0.1917E+06
19	0.2287E-02	0.8487E-02	0.1101E+04	0.8762E+01	0.4352E+06	-0.3789E+06	0.5632E+05	0.1882E+06
20	0.2468E-02	0.8984E-02	0.1098E+04	0.1243E+02	0.4339E+06	-0.3778E+06	0.5610E+05	0.1845E+06
21	0.2648E-02	0.9480E-02	0.1094E+04	0.1325E+02	0.4315E+06	-0.3751E+06	0.5643E+05	0.1807E+06
22	0.2829E-02	0.9976E-02	0.1093E+04	0.1160E+02	0.4313E+06	-0.3770E+06	0.5423E+05	0.1781E+06
23	0.3010E-02	0.1047E-01	0.1088E+04	0.1316E+02	0.4284E+06	-0.3757E+06	0.5275E+05	0.1749E+06
24	0.3190E-02	0.1097E-01	0.1080E+04	0.1227E+02	0.4258E+06	-0.3724E+06	0.5334E+05	0.1712E+06
25	0.3371E-02	0.1147E-01	0.1084E+04	0.1356E+02	0.4259E+06	-0.3742E+06	0.5171E+05	0.1694E+06
26	0.3552E-02	0.1196E-01	0.1076E+04	0.1476E+02	0.4234E+06	-0.3715E+06	0.5188E+05	0.1661E+06
27	0.3733E-02	0.1246E-01	0.1072E+04	0.1395E+02	0.4217E+06	-0.3699E+06	0.5186E+05	0.1635E+06
28	0.3914E-02	0.1296E-01	0.1074E+04	0.1673E+02	0.4224E+06	-0.3705E+06	0.5193E+05	0.1617E+06
29	0.4095E-02	0.1345E-01	0.1063E+04	0.1591E+02	0.4187E+06	-0.3673E+06	0.5139E+05	0.1587E+06
30	0.4276E-02	0.1395E-01	0.1060E+04	0.1633E+02	0.4171E+06	-0.3657E+06	0.5145E+05	0.1566E+06
31	0.4457E-02	0.1445E-01	0.1065E+04	0.1717E+02	0.4183E+06	-0.3675E+06	0.5083E+05	0.1560E+06
32	0.4638E-02	0.1495E-01	0.1049E+04	0.1485E+02	0.4125E+06	-0.3629E+06	0.4968E+05	0.1522E+06
33	0.4819E-02	0.1545E-01	0.1045E+04	0.1667E+02	0.4109E+06	-0.3603E+06	0.5061E+05	0.1498E+06
34	0.5001E-02	0.1594E-01	0.1042E+04	0.1653E+02	0.4088E+06	-0.3597E+06	0.4904E+05	0.1480E+06
35	0.5182E-02	0.1644E-01	0.1036E+04	0.1824E+02	0.4068E+06	-0.3566E+06	0.5019E+05	0.1459E+06
36	0.5363E-02	0.1694E-01	0.1029E+04	0.1762E+02	0.4050E+06	-0.3543E+06	0.5071E+05	0.1437E+06
37	0.5545E-02	0.1744E-01	0.1023E+04	0.1783E+02	0.4026E+06	-0.3534E+06	0.4924E+05	0.1416E+06
38	0.5726E-02	0.1794E-01	0.1018E+04	0.1822E+02	0.4012E+06	-0.3511E+06	0.5012E+05	0.1398E+06
39	0.5908E-02	0.1843E-01	0.1010E+04	0.2024E+02	0.3977E+06	-0.3475E+06	0.5020E+05	0.1377E+06
40	0.6089E-02	0.1893E-01	0.1000E+04	0.2194E+02	0.3945E+06	-0.3441E+06	0.5034E+05	0.1352E+06
41	0.6271E-02	0.1943E-01	0.9948E+03	0.2103E+02	0.3927E+06	-0.3433E+06	0.4936E+05	0.1332E+06
42	0.6452E-02	0.1993E-01	0.9880E+03	0.2197E+02	0.3905E+06	-0.3405E+06	0.5007E+05	0.1312E+06
43	0.6634E-02	0.2043E-01	0.9776E+03	0.2369E+02	0.3868E+06	-0.3366E+06	0.5013E+05	0.1291E+06
44	0.6816E-02	0.2093E-01	0.9561E+03	0.2653E+02	0.3778E+06	-0.3293E+06	0.4851E+05	0.1250E+06
45	0.6997E-02	0.2143E-01	0.9416E+03	0.2474E+02	0.3750E+06	-0.3240E+06	0.5093E+05	0.1223E+06
46	0.7179E-02	0.2193E-01	0.9323E+03	0.2774E+02	0.3724E+06	-0.3201E+06	0.5230E+05	0.1201E+06
47	0.7361E-02	0.2243E-01	0.9179E+03	0.3162E+02	0.3672E+06	-0.3146E+06	0.5260E+05	0.1174E+06
48	0.7543E-02	0.2293E-01	0.8866E+03	0.3800E+02	0.3579E+06	-0.3035E+06	0.5439E+05	0.1126E+06
49	0.7725E-02	0.2343E-01	0.8562E+03	0.4111E+02	0.3476E+06	-0.2913E+06	0.5623E+05	0.1077E+06
50	0.7907E-02	0.2393E-01	0.8103E+03	0.5282E+02	0.3334E+06	-0.2756E+06	0.5784E+05	0.1006E+06
51	0.8021E-02	0.2423E-01	0.6457E+03	0.6868E+02	0.2723E+06	-0.2180E+06	0.5428E+05	0.1811E+05
52	0.8074E-02	0.2434E-01	0.5657E+03	0.7539E+02	0.2417E+06	-0.1899E+06	0.5181E+05	0.1588E+05
53	0.8137E-02	0.2445E-01	0.4912E+03	0.7729E+02	0.2145E+06	-0.1648E+06	0.4972E+05	0.1390E+05
54	0.8211E-02	0.2455E-01	0.4175E+03	0.7422E+02	0.1849E+06	-0.1408E+06	0.4412E+05	0.1197E+05
55	0.8296E-02	0.2464E-01	0.3506E+03	0.7831E+02	0.1575E+06	-0.1181E+06	0.3938E+05	0.1016E+05
56	0.8390E-02	0.2472E-01	0.2954E+03	0.7016E+02	0.1336E+06	-0.9945E+05	0.3415E+05	0.8578E+04
57	0.8493E-02	0.2480E-01	0.2401E+03	0.6711E+02	0.1114E+06	-0.8124E+05	0.3018E+05	0.7052E+04
58	0.8604E-02	0.2486E-01	0.1913E+03	0.5685E+02	0.9064E+05	-0.6461E+05	0.2603E+05	0.5704E+04
59	0.8722E-02	0.2491E-01	0.1532E+03	0.5367E+02	0.7343E+05	-0.5237E+05	0.2106E+05	0.4580E+04
60	0.8845E-02	0.2495E-01	0.1194E+03	0.4640E+02	0.5831E+05	-0.4139E+05	0.1692E+05	0.3683E+04
61	0.8974E-02	0.2498E-01	0.9324E+02	0.3972E+02	0.4632E+05	-0.3253E+05	0.1379E+05	0.2951E+04
62	0.9106E-02	0.2500E-01	0.6585E+02	0.3093E+02	0.3365E+05	-0.2360E+05	0.1005E+05	0.2124E+04
63	0.9213E-02	0.2500E-01	0.5250E+02	0.3015E+02	0.2766E+05	-0.1884E+05	0.8818E+04	0.1032E+04
64	0.9297E-02	0.2499E-01	0.4602E+02	0.2682E+02	0.2450E+05	-0.1655E+05	0.7957E+04	0.9660E+03
65	0.9387E-02	0.2498E-01	0.3445E+02	0.1991E+02	0.1877E+05	-0.1291E+05	0.5861E+04	0.8190E+03
66	0.9483E-02	0.2496E-01	0.2820E+02	0.1841E+02	0.1624E+05	-0.1076E+05	0.5481E+04	0.7330E+03
67	0.9584E-02	0.2493E-01	0.1924E+02	0.1304E+02	0.1072E+05	-0.7397E+04	0.3324E+04	0.5450E+03
68	0.9689E-02	0.2489E-01	0.1574E+02	0.1114E+02	0.8887E+04	-0.6123E+04	0.2764E+04	0.4770E+03
69	0.9795E-02	0.2483E-01	0.1148E+02	0.7717E+01	0.6387E+04	-0.4608E+04	0.1778E+04	0.3840E+03
70	0.9901E-02	0.2476E-01	0.6675E+01	0.4899E+01	0.3786E+04	-0.2609E+04	0.1176E+04	0.2390E+03
71	0.1001E-01	0.2468E-01	0.4384E+01	0.3267E+01	0.2425E+04	-0.1823E+04	0.6022E+03	0.1650E+03
72	0.1007E-01	0.2462E-01	0.3357E+01	0.1919E+01	0.1638E+04	-0.1493E+04	0.1448E+03	0.4600E+02
73	0.1011E-01	0.2457E-01	0.2339E+01	0.1591E+01	0.1235E+04	-0.9883E+03	0.2471E+03	0.4400E+02
74	0.1016E-01	0.2451E-01	0.1833E+01	0.1468E+01	0.1178E+04	-0.7427E+03	0.4353E+03	0.5200E+02
75	0.1022E-01	0.2443E-01	0.2204E+01	0.1244E+01	0.1142E+04	-0.9378E+03	0.2038E+03	0.7100E+02
76	0.1028E-01	0.2432E-01	0.1679E+01	0.2950E+00	0.7504E+03	-0.6376E+03	0.1128E+03	0.6100E+02
77	0.1034E-01	0.2419E-01	0.1468E+01	0.4760E+00	0.7704E+03	-0.6002E+03	0.1702E+03	0.6700E+02
78	0.1039E-01	0.2403E-01	0.1711E+01	-0.2222E+00	0.7743E+03	-0.6688E+03	0.1055E+03	0.8400E+02
79	0.1041E-01	0.2385E-01	0.2081E+01	-0.3109E+00	0.9501E+03	-0.7996E+03	0.1505E+03	0.1110E+03
80	0.1042E-01	0.2349E-01	0.3186E+01	-0.4286E+00	0.1414E+04	-0.1201E+04	0.2131E+03	0.4390E+03
81	0.1042E-01	0.2297E-01	0.4416E+01	-0.1029E+01	0.1894E+04	-0.1647E+04	0.2467E+03	0.6000E+03
82	0.1042E-01	0.2244E-01	0.5316E+01	-0.1063E+01	0.2223E+04	-0.1878E+04	0.3448E+03	0.7030E+03
83	0.1042E-01	0.2191E-01	0.6242E+01	-0.8789E+00	0.2575E+04	-0.2202E+04	0.3733E+03	0.8330E+03
84	0.1042E-01	0.2138E-01	0.7114E+01	-0.1091E+01	0.2959E+04	-0.2524E+04	0.4347E+03	0.9620E+03
85	0.1042E-01	0.2084E-01	0.7873E+01	-0.1195E+01	0.3349E+04	-0.2700E+04	0.6495E+03	0.1053E+04
86	0.1042E-01	0.2030E-01	0.8416E+01	-0.1163E+01	0.3398E+04	-0.2902E+04	0.4956E+03	0.1145E+04

87	0.1042E-01	0.1976E-01	0.9662E+01	-0.1079E+01	0.3867E+04	-0.3316E+04	0.5507E+03	0.1313E+04
88	0.1042E-01	0.1921E-01	0.9346E+01	-0.1132E+01	0.3760E+04	-0.3187E+04	0.5727E+03	0.1302E+04
89	0.1042E-01	0.1865E-01	0.9671E+01	-0.1165E+01	0.3853E+04	-0.3331E+04	0.5219E+03	0.1348E+04
90	0.1042E-01	0.1810E-01	0.1071E+02	-0.1362E+01	0.4195E+04	-0.3655E+04	0.5393E+03	0.1525E+04
91	0.1042E-01	0.1754E-01	0.1088E+02	-0.1434E+01	0.4348E+04	-0.3757E+04	0.5911E+03	0.1603E+04
92	0.1042E-01	0.1697E-01	0.1116E+02	-0.9381E+00	0.4471E+04	-0.3791E+04	0.6800E+03	0.1657E+04
93	0.1042E-01	0.1640E-01	0.1186E+02	-0.1422E+01	0.4765E+04	-0.4065E+04	0.7000E+03	0.1801E+04
94	0.1042E-01	0.1583E-01	0.1158E+02	-0.1398E+01	0.4564E+04	-0.4036E+04	0.5287E+03	0.1814E+04
95	0.1042E-01	0.1525E-01	0.1221E+02	-0.1325E+01	0.4803E+04	-0.4261E+04	0.5423E+03	0.1953E+04
96	0.1042E-01	0.1467E-01	0.1296E+02	-0.1280E+01	0.5121E+04	-0.4479E+04	0.6411E+03	0.2075E+04
97	0.1042E-01	0.1408E-01	0.1318E+02	-0.8982E+00	0.5133E+04	-0.4464E+04	0.6688E+03	0.2128E+04
98	0.1042E-01	0.1349E-01	0.1343E+02	-0.1059E+01	0.5365E+04	-0.4531E+04	0.8336E+03	0.2238E+04
99	0.1042E-01	0.1290E-01	0.1406E+02	-0.1005E+01	0.5458E+04	-0.4860E+04	0.5984E+03	0.2379E+04
100	0.1042E-01	0.1230E-01	0.1397E+02	-0.7371E+00	0.5523E+04	-0.4755E+04	0.7681E+03	0.2454E+04
101	0.1042E-01	0.1170E-01	0.1395E+02	-0.8956E+00	0.5295E+04	-0.4863E+04	0.4322E+03	0.2479E+04
102	0.1042E-01	0.1110E-01	0.1441E+02	-0.4686E+00	0.5627E+04	-0.4949E+04	0.6776E+03	0.2610E+04
103	0.1042E-01	0.1049E-01	0.1437E+02	-0.4319E+00	0.5578E+04	-0.4865E+04	0.7132E+03	0.2655E+04
104	0.1042E-01	0.9875E-02	0.1429E+02	-0.2607E+00	0.5508E+04	-0.4857E+04	0.6513E+03	0.2707E+04
105	0.1042E-01	0.9258E-02	0.1465E+02	-0.4000E+00	0.5633E+04	-0.5073E+04	0.5599E+03	0.2922E+04
106	0.1042E-01	0.8637E-02	0.1428E+02	0.8699E-02	0.5457E+04	-0.4979E+04	0.4786E+03	0.2925E+04
107	0.1046E-01	0.7979E-02	0.1416E+02	-0.2767E+00	0.5238E+04	-0.4985E+04	0.2529E+03	0.3335E+04
108	0.1075E-01	0.7287E-02	0.1391E+02	0.4988E-01	0.5221E+04	-0.4906E+04	0.3149E+03	0.3878E+04
109	0.1172E-01	0.6596E-02	0.1392E+02	-0.2766E+00	0.5265E+04	-0.4915E+04	0.3503E+03	0.8351E+04
110	0.1272E-01	0.6250E-02	0.1368E+02	-0.2719E+00	0.5154E+04	-0.4764E+04	0.3902E+03	0.2012E+04
111	0.1316E-01	0.6250E-02	0.1276E+02	-0.4151E+00	0.4781E+04	-0.4481E+04	0.3007E+03	0.1865E+04
112	0.1360E-01	0.6250E-02	0.1373E+02	-0.2091E+00	0.5271E+04	-0.4791E+04	0.4805E+03	0.2029E+04
113	0.1403E-01	0.6250E-02	0.1378E+02	-0.5811E+00	0.5300E+04	-0.4770E+04	0.5297E+03	0.2001E+04
114	0.1447E-01	0.6250E-02	0.1274E+02	-0.7378E+00	0.4948E+04	-0.4434E+04	0.5137E+03	0.1893E+04
115	0.1491E-01	0.6250E-02	0.1378E+02	-0.8828E+00	0.5459E+04	-0.4807E+04	0.6513E+03	0.2009E+04
116	0.1535E-01	0.6250E-02	0.1345E+02	-0.8871E+00	0.5437E+04	-0.4630E+04	0.8076E+03	0.1941E+04
117	0.1578E-01	0.6250E-02	0.1339E+02	-0.8576E+00	0.5358E+04	-0.4661E+04	0.6970E+03	0.1962E+04
118	0.1681E-01	0.6250E-02	0.1306E+02	-0.1130E+01	0.5283E+04	-0.4543E+04	0.7404E+03	0.7114E+04
119	0.1842E-01	0.6250E-02	0.1374E+02	-0.1604E+01	0.5611E+04	-0.4717E+04	0.8947E+03	0.7443E+04
120	0.2003E-01	0.6250E-02	0.1444E+02	-0.1653E+01	0.5984E+04	-0.4941E+04	0.1043E+04	0.7708E+04
121	0.2163E-01	0.6250E-02	0.1521E+02	-0.1781E+01	0.6319E+04	-0.5160E+04	0.1159E+04	0.8048E+04
122	0.2323E-01	0.6250E-02	0.1642E+02	-0.1960E+01	0.6866E+04	-0.5531E+04	0.1335E+04	0.8559E+04
123	0.2483E-01	0.6250E-02	0.1781E+02	-0.2161E+01	0.7575E+04	-0.6020E+04	0.1556E+04	0.9341E+04
124	0.2642E-01	0.6250E-02	0.1953E+02	-0.2051E+01	0.8244E+04	-0.6563E+04	0.1681E+04	0.1010E+05
125	0.2800E-01	0.6250E-02	0.2050E+02	-0.2036E+01	0.8747E+04	-0.6876E+04	0.1871E+04	0.1062E+05
126	0.2959E-01	0.6250E-02	0.2177E+02	-0.1974E+01	0.9391E+04	-0.7366E+04	0.2024E+04	0.1123E+05
127	0.3116E-01	0.6250E-02	0.2425E+02	-0.2053E+01	0.1043E+05	-0.8172E+04	0.2255E+04	0.1243E+05
128	0.3274E-01	0.6250E-02	0.2586E+02	-0.1876E+01	0.1101E+05	-0.8654E+04	0.2353E+04	0.1320E+05
129	0.3431E-01	0.6250E-02	0.2775E+02	-0.1617E+01	0.1169E+05	-0.9328E+04	0.2363E+04	0.1413E+05
130	0.3587E-01	0.6250E-02	0.2941E+02	-0.1349E+01	0.1259E+05	-0.9844E+04	0.2745E+04	0.1500E+05
131	0.3743E-01	0.6250E-02	0.3076E+02	-0.1192E+01	0.1310E+05	-0.1028E+05	0.2827E+04	0.1551E+05
132	0.3899E-01	0.6250E-02	0.3270E+02	-0.1216E+01	0.1392E+05	-0.1092E+05	0.2996E+04	0.1641E+05
133	0.4054E-01	0.6250E-02	0.3407E+02	-0.6863E+00	0.1448E+05	-0.1141E+05	0.3074E+04	0.1726E+05
134	0.4209E-01	0.6250E-02	0.3562E+02	-0.5277E+00	0.1513E+05	-0.1194E+05	0.3192E+04	0.1792E+05
135	0.4363E-01	0.6250E-02	0.3790E+02	-0.1009E+00	0.1613E+05	-0.1270E+05	0.3439E+04	0.1897E+05
136	0.4517E-01	0.6250E-02	0.3883E+02	0.1039E+00	0.1652E+05	-0.1300E+05	0.3527E+04	0.1941E+05
137	0.4670E-01	0.6250E-02	0.3963E+02	0.5347E+00	0.1682E+05	-0.1317E+05	0.3644E+04	0.1976E+05
138	0.4823E-01	0.6250E-02	0.4137E+02	0.3829E+00	0.1758E+05	-0.1378E+05	0.3806E+04	0.2054E+05
139	0.4976E-01	0.6250E-02	0.4264E+02	0.1079E+01	0.1806E+05	-0.1434E+05	0.3730E+04	0.2116E+05
140	0.5128E-01	0.6250E-02	0.4337E+02	0.1388E+01	0.1850E+05	-0.1450E+05	0.3999E+04	0.2140E+05
141	0.5279E-01	0.6250E-02	0.4422E+02	0.1435E+01	0.1891E+05	-0.1479E+05	0.4121E+04	0.2194E+05
142	0.5431E-01	0.6250E-02	0.4553E+02	0.1783E+01	0.1936E+05	-0.1523E+05	0.4128E+04	0.2245E+05
143	0.5581E-01	0.6250E-02	0.4595E+02	0.1710E+01	0.1958E+05	-0.1537E+05	0.4209E+04	0.2252E+05
144	0.5732E-01	0.6250E-02	0.4662E+02	0.2425E+01	0.1990E+05	-0.1556E+05	0.4340E+04	0.2280E+05
145	0.5882E-01	0.6250E-02	0.4753E+02	0.2231E+01	0.2027E+05	-0.1591E+05	0.4355E+04	0.2326E+05
146	0.6031E-01	0.6250E-02	0.4758E+02	0.2606E+01	0.2029E+05	-0.1597E+05	0.4326E+04	0.2315E+05
147	0.6180E-01	0.6250E-02	0.4871E+02	0.2920E+01	0.2068E+05	-0.1634E+05	0.4339E+04	0.2367E+05
148	0.6329E-01	0.6250E-02	0.4842E+02	0.3433E+01	0.2068E+05	-0.1617E+05	0.4503E+04	0.2349E+05
149	0.6477E-01	0.6250E-02	0.4892E+02	0.3766E+01	0.2087E+05	-0.1638E+05	0.4495E+04	0.2358E+05
150	0.6625E-01	0.6250E-02	0.4857E+02	0.3405E+01	0.2069E+05	-0.1628E+05	0.4414E+04	0.2345E+05
151	0.6772E-01	0.6250E-02	0.4903E+02	0.3995E+01	0.2102E+05	-0.1641E+05	0.4615E+04	0.2351E+05
152	0.6919E-01	0.6250E-02	0.4948E+02	0.3765E+01	0.2112E+05	-0.1653E+05	0.4590E+04	0.2371E+05
153	0.7065E-01	0.6250E-02	0.4876E+02	0.3900E+01	0.2082E+05	-0.1636E+05	0.4465E+04	0.2327E+05
154	0.7211E-01	0.6250E-02	0.4879E+02	0.4106E+01	0.2074E+05	-0.1640E+05	0.4341E+04	0.2336E+05
155	0.7357E-01	0.6250E-02	0.4971E+02	0.4061E+01	0.2140E+05	-0.1664E+05	0.4755E+04	0.2368E+05
156	0.7502E-01	0.6250E-02	0.4932E+02	0.4848E+01	0.2109E+05	-0.1660E+05	0.4488E+04	0.2332E+05
157	0.7647E-01	0.6250E-02	0.4967E+02	0.4571E+01	0.2124E+05	-0.1675E+05	0.4490E+04	0.2365E+05
158	0.7791E-01	0.6250E-02	0.4935E+02	0.4869E+01	0.2112E+05	-0.1651E+05	0.4611E+04	0.2323E+05
159	0.7935E-01	0.6250E-02	0.4935E+02	0.4768E+01	0.2104E+05	-0.1656E+05	0.4477E+04	0.2320E+05
160	0.8078E-01	0.6250E-02	0.4751E+02	0.4973E+01	0.2024E+05	-0.1601E+05	0.4231E+04	0.2238E+05
161	0.8221E-01	0.6250E-02	0.4748E+02	0.5164E+01	0.2042E+05	-0.1589E+05	0.4531E+04	0.2218E+05
162	0.8363E-01	0.6250E-02	0.4766E+02	0.5025E+01	0.2049E+05	-0.1595E+05	0.4542E+04	0.2217E+05
163	0.8506E-01	0.6250E-02	0.4698E+02	0.4782E+01	0.2023E+05	-0.1571E+05	0.4520E+04	0.2180E+05
164	0.8647E-01	0.6250E-02	0.4721E+02	0.5225E+01	0.2035E+05	-0.1580E+05	0.4541E+04	0.2181E+05
165	0.8788E-01	0.6250E-02	0.4563E+02	0.5079E+01	0.1957E+05	-0.1528E+05	0.4287E+04	0.2106E+05
166	0.8929E-01	0.6250E-02	0.4676E+02	0.5336E+01	0.2005E+05	-0.1563E+05	0.4416E+04	0.2143E+05
167	0.9069E-01	0.6250E-02	0.4542E+02	0.5216E+01	0.1941E+05	-0.1527E+05	0.4143E+04	0.2086E+05
168	0.9209E-01	0.6250E-02	0.4517E+02	0.5776E+01	0.1939E+05	-0.1512E+05	0.4274E+04	0.2070E+05
169	0.9349E-01	0.6250E-02	0.4454E+02	0.5472E+01	0.1911E+05	-0.1492E+05	0.4192E+04	0.2035E+05
170	0.9488E-01	0.6250E-02	0.4366E+02	0.5309E+01	0.1874E+05	-0.1471E+05	0.4025E+04	0.1987E+05
171	0.9626E-01	0.6250E-02	0.4395E+02	0.5689E+01	0.1894E+05	-0.1475E+05	0.4189E+04	0.1991E+05
172	0.9764E-01	0.6250E-02	0.4307E+02	0.5550E+01	0.1871E+05	-0.1444E+05	0.4276E+04	0.1950E+05
173	0.9902E-01	0.6250E-02	0.4252E+02	0.5616E+01	0.1834E+05	-0.1418E+05	0.4159E+04	0.1908E+05
174	0.1004E+00	0.6250E-02	0.4163E+02	0.5110E+01	0.1796E+05	-0.1395E+05	0.4010E+04	0.1872E+05
175	0.1018E+00	0.6250E-02	0.4182E+02	0.5608E+01	0.1805E+05	-0.1401E+05	0.4044E+04	0.1871E+05
176	0.1031E+00	0.6250E-02	0.4101E+02	0.5662E+01	0.1765E+05	-0.1370E+05	0.3955E+04	0.1830E+05
177	0.1045E+00	0.6250E-02	0.3984E+02	0.5277E+01	0.1728E+05	-0.1329E+05	0.3999E+04	0.1774E+05
178	0.1058E+00	0.6250E-02	0.3993E+02	0.5284E+01	0.1715E+05	-0.1341E+05	0.3744E+04	0.1775E+05
179	0.1072E+00	0.6250E-02	0.3939E+02	0.5301E+01	0.1699E+05	-0.1324E+05	0.3749E+04	0.1743E+05

180	0.1085E+00	0.6250E-02	0.3911E+02	0.5335E+01	0.1686E+05	-0.1315E+05	0.3707E+04	0.1733E+05
181	0.1099E+00	0.6250E-02	0.3833E+02	0.5445E+01	0.1650E+05	-0.1286E+05	0.3649E+04	0.1690E+05
182	0.1112E+00	0.6250E-02	0.3785E+02	0.5379E+01	0.1642E+05	-0.1277E+05	0.3651E+04	0.1667E+05
183	0.1126E+00	0.6250E-02	0.3760E+02	0.5269E+01	0.1628E+05	-0.1266E+05	0.3622E+04	0.1652E+05
184	0.1139E+00	0.6250E-02	0.3673E+02	0.5479E+01	0.1592E+05	-0.1238E+05	0.3542E+04	0.1604E+05
185	0.1152E+00	0.6250E-02	0.3589E+02	0.5398E+01	0.1557E+05	-0.1206E+05	0.3514E+04	0.1555E+05
186	0.1165E+00	0.6250E-02	0.3538E+02	0.5483E+01	0.1529E+05	-0.1191E+05	0.3374E+04	0.1529E+05
187	0.1178E+00	0.6250E-02	0.3477E+02	0.5487E+01	0.1527E+05	-0.1163E+05	0.3640E+04	0.1498E+05
188	0.1192E+00	0.6250E-02	0.3352E+02	0.5678E+01	0.1467E+05	-0.1120E+05	0.3472E+04	0.1446E+05
189	0.1205E+00	0.6250E-02	0.3276E+02	0.5889E+01	0.1444E+05	-0.1100E+05	0.3436E+04	0.1407E+05
190	0.1218E+00	0.6250E-02	0.3117E+02	0.6232E+01	0.1384E+05	-0.1041E+05	0.3430E+04	0.1325E+05
191	0.1231E+00	0.6250E-02	0.2875E+02	0.6775E+01	0.1296E+05	-0.9586E+04	0.3376E+04	0.1220E+05
192	0.1244E+00	0.6250E-02	0.2518E+02	0.8075E+01	0.1192E+05	-0.8353E+04	0.3569E+04	0.1061E+05

NONDIMENSIONAL SURFACE QUANTITIES

0.5*ROF*UF**2= 0.6222E+03 0.5*ROF*UF**3= 0.1016E+07

ELEMENT	X, m	Y, m	S/Rn	CP	CF	CH	CPFM	CFFM	CHFM	CPMN
1	0.377E-05	0.217E-03	0.174E-01	0.173E+01	0.246E-02	0.826E-01	0.246E+01	0.347E-01	0.811E+00	0.184E+01
2	0.189E-04	0.651E-03	0.521E-01	0.182E+01	0.489E-02	0.838E-01	0.246E+01	0.104E+00	0.810E+00	0.183E+01
3	0.491E-04	0.108E-02	0.869E-01	0.185E+01	0.894E-02	0.829E-01	0.244E+01	0.173E+00	0.808E+00	0.183E+01
4	0.944E-04	0.152E-02	0.122E+00	0.184E+01	0.787E-02	0.803E-01	0.243E+01	0.241E+00	0.805E+00	0.181E+01
5	0.155E-03	0.195E-02	0.157E+00	0.185E+01	0.151E-01	0.785E-01	0.241E+01	0.308E+00	0.801E+00	0.179E+01
6	0.230E-03	0.238E-02	0.191E+00	0.183E+01	0.120E-01	0.769E-01	0.238E+01	0.374E+00	0.797E+00	0.177E+01
7	0.321E-03	0.281E-02	0.226E+00	0.183E+01	0.137E-01	0.741E-01	0.235E+01	0.438E+00	0.791E+00	0.175E+01
8	0.427E-03	0.323E-02	0.261E+00	0.181E+01	0.166E-01	0.723E-01	0.231E+01	0.499E+00	0.784E+00	0.172E+01
9	0.547E-03	0.365E-02	0.296E+00	0.181E+01	0.162E-01	0.690E-01	0.227E+01	0.559E+00	0.776E+00	0.168E+01
10	0.682E-03	0.407E-02	0.331E+00	0.179E+01	0.165E-01	0.669E-01	0.222E+01	0.616E+00	0.767E+00	0.164E+01
11	0.844E-03	0.452E-02	0.370E+00	0.179E+01	0.182E-01	0.641E-01	0.220E+01	0.643E+00	0.762E+00	0.162E+01
12	0.102E-02	0.502E-02	0.412E+00	0.179E+01	0.155E-01	0.615E-01	0.220E+01	0.643E+00	0.762E+00	0.162E+01
13	0.120E-02	0.551E-02	0.454E+00	0.178E+01	0.161E-01	0.600E-01	0.220E+01	0.643E+00	0.762E+00	0.162E+01
14	0.138E-02	0.601E-02	0.497E+00	0.179E+01	0.170E-01	0.585E-01	0.220E+01	0.643E+00	0.762E+00	0.162E+01
15	0.157E-02	0.650E-02	0.539E+00	0.177E+01	0.173E-01	0.588E-01	0.220E+01	0.643E+00	0.762E+00	0.162E+01
16	0.175E-02	0.700E-02	0.581E+00	0.179E+01	0.182E-01	0.572E-01	0.220E+01	0.643E+00	0.762E+00	0.162E+01
17	0.193E-02	0.750E-02	0.623E+00	0.178E+01	0.201E-01	0.585E-01	0.220E+01	0.643E+00	0.762E+00	0.162E+01
18	0.211E-02	0.799E-02	0.665E+00	0.178E+01	0.197E-01	0.566E-01	0.220E+01	0.643E+00	0.762E+00	0.162E+01
19	0.229E-02	0.849E-02	0.708E+00	0.177E+01	0.141E-01	0.554E-01	0.220E+01	0.643E+00	0.762E+00	0.162E+01
20	0.247E-02	0.898E-02	0.750E+00	0.176E+01	0.200E-01	0.552E-01	0.220E+01	0.643E+00	0.762E+00	0.162E+01
21	0.265E-02	0.948E-02	0.792E+00	0.176E+01	0.213E-01	0.555E-01	0.220E+01	0.643E+00	0.762E+00	0.162E+01
22	0.283E-02	0.998E-02	0.834E+00	0.176E+01	0.186E-01	0.534E-01	0.220E+01	0.643E+00	0.762E+00	0.162E+01
23	0.301E-02	0.105E-01	0.877E+00	0.175E+01	0.212E-01	0.519E-01	0.220E+01	0.643E+00	0.762E+00	0.162E+01
24	0.319E-02	0.110E-01	0.919E+00	0.174E+01	0.197E-01	0.525E-01	0.220E+01	0.643E+00	0.762E+00	0.162E+01
25	0.337E-02	0.115E-01	0.961E+00	0.174E+01	0.218E-01	0.509E-01	0.220E+01	0.643E+00	0.762E+00	0.162E+01
26	0.355E-02	0.120E-01	0.100E+01	0.173E+01	0.237E-01	0.511E-01	0.220E+01	0.643E+00	0.762E+00	0.162E+01
27	0.373E-02	0.125E-01	0.105E+01	0.172E+01	0.224E-01	0.510E-01	0.220E+01	0.643E+00	0.762E+00	0.162E+01
28	0.391E-02	0.130E-01	0.109E+01	0.173E+01	0.269E-01	0.511E-01	0.220E+01	0.643E+00	0.762E+00	0.162E+01
29	0.409E-02	0.135E-01	0.113E+01	0.171E+01	0.256E-01	0.506E-01	0.220E+01	0.643E+00	0.762E+00	0.162E+01
30	0.428E-02	0.140E-01	0.117E+01	0.170E+01	0.263E-01	0.506E-01	0.220E+01	0.643E+00	0.762E+00	0.162E+01
31	0.446E-02	0.144E-01	0.122E+01	0.171E+01	0.276E-01	0.500E-01	0.220E+01	0.643E+00	0.762E+00	0.162E+01
32	0.464E-02	0.149E-01	0.126E+01	0.169E+01	0.239E-01	0.489E-01	0.220E+01	0.643E+00	0.762E+00	0.162E+01
33	0.482E-02	0.154E-01	0.130E+01	0.168E+01	0.268E-01	0.498E-01	0.220E+01	0.643E+00	0.762E+00	0.162E+01
34	0.500E-02	0.159E-01	0.134E+01	0.167E+01	0.266E-01	0.483E-01	0.220E+01	0.643E+00	0.762E+00	0.162E+01
35	0.518E-02	0.164E-01	0.138E+01	0.167E+01	0.293E-01	0.494E-01	0.220E+01	0.643E+00	0.762E+00	0.162E+01
36	0.536E-02	0.169E-01	0.143E+01	0.165E+01	0.283E-01	0.499E-01	0.220E+01	0.643E+00	0.762E+00	0.162E+01
37	0.554E-02	0.174E-01	0.147E+01	0.164E+01	0.287E-01	0.485E-01	0.220E+01	0.643E+00	0.762E+00	0.162E+01
38	0.573E-02	0.179E-01	0.151E+01	0.164E+01	0.293E-01	0.493E-01	0.220E+01	0.643E+00	0.762E+00	0.162E+01
39	0.591E-02	0.184E-01	0.155E+01	0.162E+01	0.325E-01	0.494E-01	0.220E+01	0.643E+00	0.762E+00	0.162E+01
40	0.609E-02	0.189E-01	0.160E+01	0.161E+01	0.353E-01	0.495E-01	0.220E+01	0.643E+00	0.762E+00	0.162E+01
41	0.627E-02	0.194E-01	0.164E+01	0.160E+01	0.338E-01	0.486E-01	0.220E+01	0.643E+00	0.762E+00	0.162E+01
42	0.645E-02	0.199E-01	0.168E+01	0.159E+01	0.353E-01	0.493E-01	0.220E+01	0.643E+00	0.762E+00	0.162E+01
43	0.663E-02	0.204E-01	0.172E+01	0.157E+01	0.381E-01	0.493E-01	0.220E+01	0.643E+00	0.762E+00	0.162E+01
44	0.682E-02	0.209E-01	0.177E+01	0.154E+01	0.426E-01	0.477E-01	0.220E+01	0.643E+00	0.762E+00	0.162E+01
45	0.700E-02	0.214E-01	0.181E+01	0.151E+01	0.398E-01	0.501E-01	0.220E+01	0.643E+00	0.762E+00	0.162E+01
46	0.718E-02	0.219E-01	0.185E+01	0.150E+01	0.446E-01	0.515E-01	0.220E+01	0.643E+00	0.762E+00	0.162E+01
47	0.736E-02	0.224E-01	0.189E+01	0.148E+01	0.508E-01	0.518E-01	0.220E+01	0.643E+00	0.762E+00	0.162E+01
48	0.754E-02	0.229E-01	0.194E+01	0.142E+01	0.611E-01	0.535E-01	0.220E+01	0.643E+00	0.762E+00	0.162E+01
49	0.772E-02	0.234E-01	0.198E+01	0.138E+01	0.661E-01	0.553E-01	0.220E+01	0.643E+00	0.762E+00	0.162E+01
50	0.791E-02	0.239E-01	0.202E+01	0.130E+01	0.849E-01	0.569E-01	0.220E+01	0.643E+00	0.762E+00	0.162E+01
51	0.802E-02	0.242E-01	0.205E+01	0.104E+01	0.110E+00	0.534E-01	0.213E+01	0.714E+00	0.748E+00	0.156E+01
52	0.807E-02	0.243E-01	0.206E+01	0.909E+00	0.121E+00	0.510E-01	0.196E+01	0.836E+00	0.714E+00	0.142E+01
53	0.814E-02	0.244E-01	0.207E+01	0.789E+00	0.124E+00	0.489E-01	0.176E+01	0.927E+00	0.673E+00	0.126E+01
54	0.821E-02	0.245E-01	0.208E+01	0.671E+00	0.119E+00	0.434E-01	0.154E+01	0.983E+00	0.625E+00	0.109E+01
55	0.830E-02	0.246E-01	0.209E+01	0.563E+00	0.126E+00	0.388E-01	0.131E+01	0.100E+01	0.570E+00	0.907E+00
56	0.839E-02	0.247E-01	0.210E+01	0.475E+00	0.113E+00	0.336E-01	0.108E+01	0.977E+00	0.509E+00	0.722E+00
57	0.849E-02	0.248E-01	0.211E+01	0.386E+00	0.108E+00	0.297E-01	0.845E+00	0.913E+00	0.442E+00	0.545E+00
58	0.860E-02	0.249E-01	0.212E+01	0.307E+00	0.914E-01	0.256E-01	0.627E+00	0.811E+00	0.370E+00	0.382E+00
59	0.872E-02	0.249E-01	0.213E+01	0.246E+00	0.863E-01	0.207E-01	0.429E+00	0.673E+00	0.293E+00	0.240E+00
60	0.885E-02	0.250E-01	0.214E+01	0.192E+00	0.746E-01	0.167E-01	0.260E+00	0.505E+00	0.212E+00	0.126E+00
61	0.897E-02	0.250E-01	0.215E+01	0.150E+00	0.638E-01	0.136E-01	0.127E+00	0.314E+00	0.129E+00	0.464E-01
62	0.911E-02	0.250E-01	0.216E+01	0.106E+00	0.497E-01	0.989E-02	0.342E-01	0.110E+00	0.447E-01	0.523E-02
63	0.921E-02	0.250E-01	0.217E+01	0.844E-01	0.485E-01	0.868E-02	0.268E-02	0.997E-02	0.403E-02	0.000E+00
64	0.930E-02	0.250E-01	0.218E+01	0.740E-01	0.431E-01	0.783E-02	0.502E-04	0.197E-03	0.788E-04	0.000E+00
65	0.939E-02	0.250E-01	0.218E+01	0.554E-01	0.320E-01	0.577E-02	0.549E-07	0.217E-06	0.857E-07	0.000E+00
66	0.948E-02	0.250E-01	0.219E+01	0.453E-01	0.296E-01	0.539E-02	-0.557E-11	0.269E-09	0.112E-09	0.000E+00
67	0.958E-02	0.249E-01	0.220E+01	0.309E-01	0.210E-01	0.327E-02	-0.231E-16	0.216E-15	0.927E-16	0.000E+00
68	0.969E-02	0.249E-01	0.221E+01	0.253E-01	0.179E-01	0.272E-02	-0.347E-24	0.171E-23	0.762E-24	0.000E+00
69	0.979E-02	0.248E-01	0.222E+01	0.184E-01	0.124E-01	0.175E-02	-0.399E-34	0.128E-33	0.598E-34	0.000E+00
70	0.990E-02	0.248E-01	0.223E+01	0.107E-01	0.787E-02	0.116E-02	0.000E+00	0.000E+00	0.000E+00	0.000E+00
71	0.100E-01	0.247E-01	0.224E+01	0.705E-02	0.525E-02	0.593E-03	0.000E+00	0.000E+00	0.000E+00	0.000E+00
72	0.101E-01	0.246E-01	0.225E+01	0.540E-02	0.308E-02	0.142E-03	0.000E+00	0.000E+00	0.000E+00	0.000E+00
73	0.101E-01	0.246E-01	0.225E+01	0.376E-02	0.256E-02	0.243E-03	0.000E+00	0.000E+00	0.000E+00	0.000E+00
74	0.102E-01	0.245E-01	0.226E+01	0.295E-02	0.236E-02	0.428E-03	0.000E+00	0.000E+00	0.000E+00	0.000E+00
75	0.102E-01	0.244E-01	0.227E+01	0.354E-02	0.200E-02	0.201E-03	0.000E+00	0.000E+00	0.000E+00	0.000E+00

76	0.103E-01	0.243E-01	0.227E+01	0.270E-02	0.474E-03	0.111E-03	0.000E+00	0.000E+00	0.000E+00	0.000E+00
77	0.103E-01	0.242E-01	0.229E+01	0.236E-02	0.765E-03	0.168E-03	0.000E+00	0.000E+00	0.000E+00	0.000E+00
78	0.104E-01	0.240E-01	0.230E+01	0.275E-02	-0.357E-03	0.104E-03	0.000E+00	0.000E+00	0.000E+00	0.000E+00
79	0.104E-01	0.238E-01	0.231E+01	0.334E-02	-0.500E-03	0.148E-03	0.000E+00	0.000E+00	0.000E+00	0.000E+00
80	0.104E-01	0.235E-01	0.234E+01	0.512E-02	-0.689E-03	0.210E-03	0.000E+00	0.000E+00	0.000E+00	0.000E+00
81	0.104E-01	0.230E-01	0.238E+01	0.710E-02	-0.165E-02	0.243E-03	0.000E+00	0.000E+00	0.000E+00	0.000E+00
82	0.104E-01	0.224E-01	0.243E+01	0.854E-02	-0.171E-02	0.339E-03	0.000E+00	0.000E+00	0.000E+00	0.000E+00
83	0.104E-01	0.219E-01	0.247E+01	0.100E-01	-0.141E-02	0.367E-03	0.000E+00	0.000E+00	0.000E+00	0.000E+00
84	0.104E-01	0.214E-01	0.251E+01	0.114E-01	-0.175E-02	0.428E-03	0.000E+00	0.000E+00	0.000E+00	0.000E+00
85	0.104E-01	0.208E-01	0.255E+01	0.127E-01	-0.192E-02	0.639E-03	0.000E+00	0.000E+00	0.000E+00	0.000E+00
86	0.104E-01	0.203E-01	0.260E+01	0.135E-01	-0.187E-02	0.488E-03	0.000E+00	0.000E+00	0.000E+00	0.000E+00
87	0.104E-01	0.198E-01	0.264E+01	0.155E-01	-0.173E-02	0.542E-03	0.000E+00	0.000E+00	0.000E+00	0.000E+00
88	0.104E-01	0.192E-01	0.269E+01	0.150E-01	-0.182E-02	0.564E-03	0.000E+00	0.000E+00	0.000E+00	0.000E+00
89	0.104E-01	0.187E-01	0.273E+01	0.155E-01	-0.187E-02	0.514E-03	0.000E+00	0.000E+00	0.000E+00	0.000E+00
90	0.104E-01	0.181E-01	0.277E+01	0.172E-01	-0.219E-02	0.531E-03	0.000E+00	0.000E+00	0.000E+00	0.000E+00
91	0.104E-01	0.175E-01	0.282E+01	0.175E-01	-0.230E-02	0.582E-03	0.000E+00	0.000E+00	0.000E+00	0.000E+00
92	0.104E-01	0.170E-01	0.286E+01	0.179E-01	-0.151E-02	0.669E-03	0.000E+00	0.000E+00	0.000E+00	0.000E+00
93	0.104E-01	0.164E-01	0.291E+01	0.191E-01	-0.228E-02	0.689E-03	0.000E+00	0.000E+00	0.000E+00	0.000E+00
94	0.104E-01	0.158E-01	0.296E+01	0.186E-01	-0.225E-02	0.520E-03	0.000E+00	0.000E+00	0.000E+00	0.000E+00
95	0.104E-01	0.153E-01	0.300E+01	0.196E-01	-0.213E-02	0.534E-03	0.000E+00	0.000E+00	0.000E+00	0.000E+00
96	0.104E-01	0.147E-01	0.305E+01	0.208E-01	-0.206E-02	0.631E-03	0.000E+00	0.000E+00	0.000E+00	0.000E+00
97	0.104E-01	0.141E-01	0.310E+01	0.212E-01	-0.144E-02	0.658E-03	0.000E+00	0.000E+00	0.000E+00	0.000E+00
98	0.104E-01	0.135E-01	0.314E+01	0.216E-01	-0.170E-02	0.820E-03	0.000E+00	0.000E+00	0.000E+00	0.000E+00
99	0.104E-01	0.129E-01	0.319E+01	0.226E-01	-0.162E-02	0.589E-03	0.000E+00	0.000E+00	0.000E+00	0.000E+00
100	0.104E-01	0.123E-01	0.324E+01	0.225E-01	-0.118E-02	0.756E-03	0.000E+00	0.000E+00	0.000E+00	0.000E+00
101	0.104E-01	0.117E-01	0.329E+01	0.224E-01	-0.144E-02	0.425E-03	0.000E+00	0.000E+00	0.000E+00	0.000E+00
102	0.104E-01	0.111E-01	0.333E+01	0.232E-01	-0.753E-03	0.667E-03	0.000E+00	0.000E+00	0.000E+00	0.000E+00
103	0.104E-01	0.105E-01	0.338E+01	0.231E-01	-0.694E-03	0.702E-03	0.000E+00	0.000E+00	0.000E+00	0.000E+00
104	0.104E-01	0.988E-02	0.343E+01	0.230E-01	-0.419E-03	0.641E-03	0.000E+00	0.000E+00	0.000E+00	0.000E+00
105	0.104E-01	0.926E-02	0.348E+01	0.236E-01	-0.643E-03	0.551E-03	0.000E+00	0.000E+00	0.000E+00	0.000E+00
106	0.104E-01	0.864E-02	0.353E+01	0.230E-01	0.140E-04	0.471E-03	0.000E+00	0.000E+00	0.000E+00	0.000E+00
107	0.105E-01	0.798E-02	0.358E+01	0.228E-01	-0.445E-03	0.249E-03	0.000E+00	0.000E+00	0.000E+00	0.000E+00
108	0.107E-01	0.729E-02	0.364E+01	0.224E-01	0.802E-04	0.310E-03	0.000E+00	0.000E+00	0.000E+00	0.000E+00
109	0.117E-01	0.660E-02	0.374E+01	0.224E-01	-0.444E-03	0.345E-03	-0.121E-23	0.616E-23	0.273E-23	0.000E+00
110	0.127E-01	0.625E-02	0.382E+01	0.220E-01	-0.437E-03	0.384E-03	0.913E-02	0.326E-01	0.132E-01	0.000E+00
111	0.132E-01	0.625E-02	0.386E+01	0.205E-01	-0.667E-03	0.296E-03	0.913E-02	0.326E-01	0.132E-01	0.000E+00
112	0.136E-01	0.625E-02	0.389E+01	0.221E-01	-0.336E-03	0.473E-03	0.913E-02	0.326E-01	0.132E-01	0.000E+00
113	0.140E-01	0.625E-02	0.393E+01	0.221E-01	-0.934E-03	0.521E-03	0.913E-02	0.326E-01	0.132E-01	0.000E+00
114	0.145E-01	0.625E-02	0.396E+01	0.205E-01	-0.119E-02	0.506E-03	0.913E-02	0.326E-01	0.132E-01	0.000E+00
115	0.149E-01	0.625E-02	0.400E+01	0.221E-01	-0.142E-02	0.641E-03	0.913E-02	0.326E-01	0.132E-01	0.000E+00
116	0.153E-01	0.625E-02	0.403E+01	0.216E-01	-0.143E-02	0.795E-03	0.913E-02	0.326E-01	0.132E-01	0.000E+00
117	0.158E-01	0.625E-02	0.407E+01	0.215E-01	-0.138E-02	0.686E-03	0.913E-02	0.326E-01	0.132E-01	0.000E+00
118	0.168E-01	0.625E-02	0.415E+01	0.210E-01	-0.182E-02	0.729E-03	0.913E-02	0.326E-01	0.132E-01	0.000E+00
119	0.184E-01	0.625E-02	0.428E+01	0.221E-01	-0.258E-02	0.881E-03	0.913E-02	0.326E-01	0.132E-01	0.000E+00
120	0.200E-01	0.625E-02	0.441E+01	0.232E-01	-0.266E-02	0.103E-02	0.913E-02	0.326E-01	0.132E-01	0.000E+00
121	0.216E-01	0.625E-02	0.454E+01	0.244E-01	-0.286E-02	0.114E-02	0.913E-02	0.326E-01	0.132E-01	0.000E+00
122	0.232E-01	0.625E-02	0.466E+01	0.264E-01	-0.315E-02	0.131E-02	0.913E-02	0.326E-01	0.132E-01	0.000E+00
123	0.248E-01	0.625E-02	0.479E+01	0.286E-01	-0.347E-02	0.153E-02	0.913E-02	0.326E-01	0.132E-01	0.000E+00
124	0.264E-01	0.625E-02	0.492E+01	0.314E-01	-0.330E-02	0.165E-02	0.913E-02	0.326E-01	0.132E-01	0.000E+00
125	0.280E-01	0.625E-02	0.505E+01	0.329E-01	-0.327E-02	0.184E-02	0.913E-02	0.326E-01	0.132E-01	0.000E+00
126	0.296E-01	0.625E-02	0.517E+01	0.350E-01	-0.317E-02	0.199E-02	0.913E-02	0.326E-01	0.132E-01	0.000E+00
127	0.312E-01	0.625E-02	0.530E+01	0.390E-01	-0.330E-02	0.222E-02	0.913E-02	0.326E-01	0.132E-01	0.000E+00
128	0.327E-01	0.625E-02	0.542E+01	0.416E-01	-0.301E-02	0.232E-02	0.913E-02	0.326E-01	0.132E-01	0.000E+00
129	0.343E-01	0.625E-02	0.555E+01	0.446E-01	-0.260E-02	0.233E-02	0.913E-02	0.326E-01	0.132E-01	0.000E+00
130	0.359E-01	0.625E-02	0.568E+01	0.473E-01	-0.217E-02	0.270E-02	0.913E-02	0.326E-01	0.132E-01	0.000E+00
131	0.374E-01	0.625E-02	0.580E+01	0.494E-01	-0.192E-02	0.278E-02	0.913E-02	0.326E-01	0.132E-01	0.000E+00
132	0.390E-01	0.625E-02	0.592E+01	0.526E-01	-0.195E-02	0.295E-02	0.913E-02	0.326E-01	0.132E-01	0.000E+00
133	0.405E-01	0.625E-02	0.605E+01	0.548E-01	-0.110E-02	0.303E-02	0.913E-02	0.326E-01	0.132E-01	0.000E+00
134	0.421E-01	0.625E-02	0.617E+01	0.573E-01	-0.848E-03	0.314E-02	0.913E-02	0.326E-01	0.132E-01	0.000E+00
135	0.436E-01	0.625E-02	0.630E+01	0.609E-01	-0.162E-03	0.339E-02	0.913E-02	0.326E-01	0.132E-01	0.000E+00
136	0.452E-01	0.625E-02	0.642E+01	0.624E-01	0.167E-03	0.347E-02	0.913E-02	0.326E-01	0.132E-01	0.000E+00
137	0.467E-01	0.625E-02	0.654E+01	0.637E-01	0.859E-03	0.359E-02	0.913E-02	0.326E-01	0.132E-01	0.000E+00
138	0.482E-01	0.625E-02	0.666E+01	0.665E-01	0.615E-03	0.375E-02	0.913E-02	0.326E-01	0.132E-01	0.000E+00
139	0.498E-01	0.625E-02	0.679E+01	0.685E-01	0.173E-02	0.367E-02	0.913E-02	0.326E-01	0.132E-01	0.000E+00
140	0.513E-01	0.625E-02	0.691E+01	0.697E-01	0.223E-02	0.394E-02	0.913E-02	0.326E-01	0.132E-01	0.000E+00
141	0.528E-01	0.625E-02	0.703E+01	0.711E-01	0.231E-02	0.406E-02	0.913E-02	0.326E-01	0.132E-01	0.000E+00
142	0.543E-01	0.625E-02	0.715E+01	0.732E-01	0.286E-02	0.406E-02	0.913E-02	0.326E-01	0.132E-01	0.000E+00
143	0.558E-01	0.625E-02	0.727E+01	0.738E-01	0.275E-02	0.414E-02	0.913E-02	0.326E-01	0.132E-01	0.000E+00
144	0.573E-01	0.625E-02	0.739E+01	0.749E-01	0.390E-02	0.427E-02	0.913E-02	0.326E-01	0.132E-01	0.000E+00
145	0.588E-01	0.625E-02	0.751E+01	0.764E-01	0.359E-02	0.429E-02	0.913E-02	0.326E-01	0.132E-01	0.000E+00
146	0.603E-01	0.625E-02	0.763E+01	0.765E-01	0.419E-02	0.426E-02	0.913E-02	0.326E-01	0.132E-01	0.000E+00
147	0.618E-01	0.625E-02	0.775E+01	0.783E-01	0.469E-02	0.427E-02	0.913E-02	0.326E-01	0.132E-01	0.000E+00
148	0.633E-01	0.625E-02	0.787E+01	0.778E-01	0.552E-02	0.443E-02	0.913E-02	0.326E-01	0.132E-01	0.000E+00
149	0.648E-01	0.625E-02	0.799E+01	0.786E-01	0.605E-02	0.442E-02	0.913E-02	0.326E-01	0.132E-01	0.000E+00
150	0.662E-01	0.625E-02	0.811E+01	0.781E-01	0.547E-02	0.434E-02	0.913E-02	0.326E-01	0.132E-01	0.000E+00
151	0.677E-01	0.625E-02	0.822E+01	0.788E-01	0.642E-02	0.454E-02	0.913E-02	0.326E-01	0.132E-01	0.000E+00
152	0.692E-01	0.625E-02	0.834E+01	0.795E-01	0.605E-02	0.452E-02	0.913E-02	0.326E-01	0.132E-01	0.000E+00
153	0.707E-01	0.625E-02	0.846E+01	0.784E-01	0.627E-02	0.439E-02	0.913E-02	0.326E-01	0.132E-01	0.000E+00
154	0.721E-01	0.625E-02	0.857E+01	0.784E-01	0.660E-02	0.427E-02	0.913E-02	0.326E-01	0.132E-01	0.000E+00
155	0.736E-01	0.625E-02	0.869E+01	0.799E-01	0.653E-02	0.468E-02	0.913E-02	0.326E-01	0.132E-01	0.000E+00
156	0.750E-01	0.625E-02	0.881E+01	0.793E-01	0.779E-02	0.442E-02	0.913E-02	0.326E-01	0.132E-01	0.000E+00
157	0.765E-01	0.625E-02	0.892E+01	0.798E-01	0.735E-02	0.442E-02	0.913E-02	0.326E-01	0.132E-01	0.000E+00
158	0.779E-01	0.625E-02	0.904E+01	0.793E-01	0.783E-02	0.454E-02	0.913E-02	0.326E-01	0.132E-01	0.000E+00
159	0.793E-01	0.625E-02	0.915E+01	0.793E-01	0.766E-02	0.441E-02	0.913E-02	0.326E-01	0.132E-01	0.000E+00
160	0.808E-01	0.625E-02	0.927E+01	0.764E-01	0.799E-02	0.416E-02	0.913E-02	0.326E-01	0.132E-01	0.000E+00
161	0.822E-01	0.625E-02	0.938E+01	0.763E-01	0.830E-02	0.446E-02	0.913E-02	0.326E-01	0.132E-01	0.000E+00
162	0.836E-01	0.625E-02	0.950E+01	0.766E-01	0.808E-02	0.447E-02	0.913E-02	0.326E-01	0.132E-01	0.000E+00
163	0.851E-01	0.625E-02	0.961E+01	0.755E-01	0.768E-02	0.445E-02	0.913E-02	0.326E-01	0.132E-01	0.000E+00
164	0.865E-01	0.625E-02	0.972E+01	0.759E-01	0.840E-02	0.447E-02	0.913E-02	0.326E-01	0.132E-01	0.000E+00
165	0.879E-01	0.625E-02	0.984E+01	0.733E-01	0.816E-02	0.422E-02	0.913E-02	0.326E-01	0.132E-01	0.000E+00
166	0.893E-01	0.625E-02	0.995E+01	0.751E-01	0.858E-02	0.435E-02	0.913E-02	0.326E-01	0.132E-01	0.000E+00
167	0.907E-01	0.625E-02	0.101E+02	0.730E-01	0.838E-02	0.408E-02	0.913E-02	0.326E-01	0.132E-01	0.000E+00
168	0.921E-01	0.625E-02	0.102E+02	0.726E-01	0.928E-02	0.421E-02	0.913E-02	0.326E-01	0.132E-01	0.000E+00

169	0.935E-01	0.625E-02	0.103E+02	0.716E-01	0.879E-02	0.413E-02	0.913E-02	0.326E-01	0.132E-01	0.000E+00
170	0.949E-01	0.625E-02	0.104E+02	0.702E-01	0.853E-02	0.396E-02	0.913E-02	0.326E-01	0.132E-01	0.000E+00
171	0.963E-01	0.625E-02	0.105E+02	0.706E-01	0.914E-02	0.412E-02	0.913E-02	0.326E-01	0.132E-01	0.000E+00
172	0.976E-01	0.625E-02	0.106E+02	0.692E-01	0.892E-02	0.421E-02	0.913E-02	0.326E-01	0.132E-01	0.000E+00
173	0.990E-01	0.625E-02	0.107E+02	0.683E-01	0.903E-02	0.409E-02	0.913E-02	0.326E-01	0.132E-01	0.000E+00
174	0.100E+00	0.625E-02	0.108E+02	0.669E-01	0.821E-02	0.395E-02	0.913E-02	0.326E-01	0.132E-01	0.000E+00
175	0.102E+00	0.625E-02	0.109E+02	0.672E-01	0.901E-02	0.398E-02	0.913E-02	0.326E-01	0.132E-01	0.000E+00
176	0.103E+00	0.625E-02	0.111E+02	0.659E-01	0.910E-02	0.389E-02	0.913E-02	0.326E-01	0.132E-01	0.000E+00
177	0.104E+00	0.625E-02	0.112E+02	0.640E-01	0.848E-02	0.394E-02	0.913E-02	0.326E-01	0.132E-01	0.000E+00
178	0.106E+00	0.625E-02	0.113E+02	0.642E-01	0.849E-02	0.368E-02	0.913E-02	0.326E-01	0.132E-01	0.000E+00
179	0.107E+00	0.625E-02	0.114E+02	0.633E-01	0.852E-02	0.369E-02	0.913E-02	0.326E-01	0.132E-01	0.000E+00
180	0.109E+00	0.625E-02	0.115E+02	0.629E-01	0.858E-02	0.365E-02	0.913E-02	0.326E-01	0.132E-01	0.000E+00
181	0.110E+00	0.625E-02	0.116E+02	0.616E-01	0.875E-02	0.359E-02	0.913E-02	0.326E-01	0.132E-01	0.000E+00
182	0.111E+00	0.625E-02	0.117E+02	0.608E-01	0.865E-02	0.359E-02	0.913E-02	0.326E-01	0.132E-01	0.000E+00
183	0.113E+00	0.625E-02	0.118E+02	0.604E-01	0.847E-02	0.356E-02	0.913E-02	0.326E-01	0.132E-01	0.000E+00
184	0.114E+00	0.625E-02	0.119E+02	0.590E-01	0.881E-02	0.349E-02	0.913E-02	0.326E-01	0.132E-01	0.000E+00
185	0.115E+00	0.625E-02	0.120E+02	0.577E-01	0.868E-02	0.346E-02	0.913E-02	0.326E-01	0.132E-01	0.000E+00
186	0.117E+00	0.625E-02	0.121E+02	0.569E-01	0.881E-02	0.332E-02	0.913E-02	0.326E-01	0.132E-01	0.000E+00
187	0.118E+00	0.625E-02	0.122E+02	0.559E-01	0.882E-02	0.358E-02	0.913E-02	0.326E-01	0.132E-01	0.000E+00
188	0.119E+00	0.625E-02	0.123E+02	0.539E-01	0.913E-02	0.342E-02	0.913E-02	0.326E-01	0.132E-01	0.000E+00
189	0.120E+00	0.625E-02	0.124E+02	0.527E-01	0.946E-02	0.338E-02	0.913E-02	0.326E-01	0.132E-01	0.000E+00
190	0.122E+00	0.625E-02	0.125E+02	0.501E-01	0.100E-01	0.338E-02	0.913E-02	0.326E-01	0.132E-01	0.000E+00
191	0.123E+00	0.625E-02	0.127E+02	0.462E-01	0.109E-01	0.332E-02	0.913E-02	0.326E-01	0.132E-01	0.000E+00
192	0.124E+00	0.625E-02	0.128E+02	0.405E-01	0.130E-01	0.351E-02	0.913E-02	0.326E-01	0.132E-01	0.000E+00

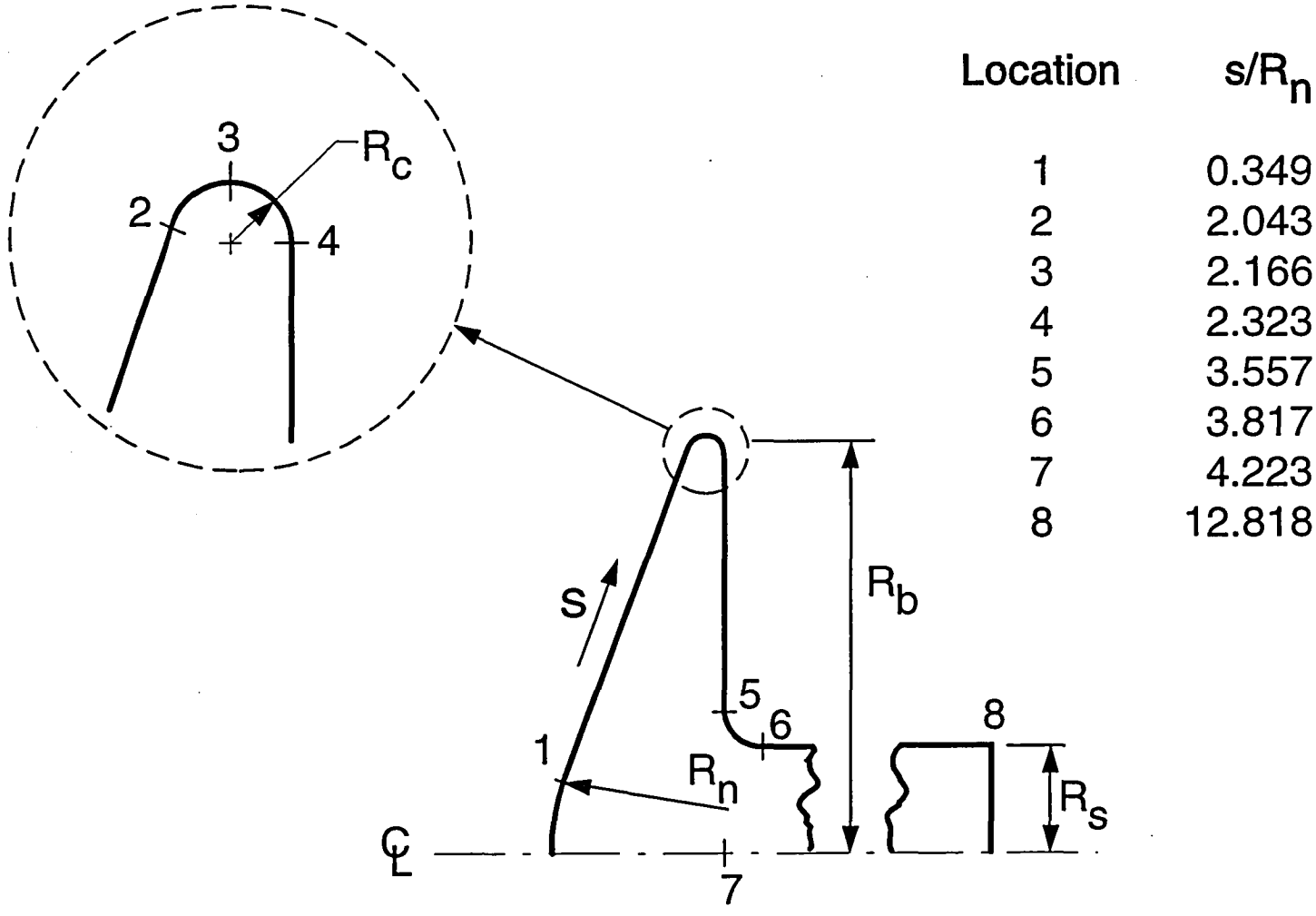

Location	s/R_n
1	0.349
2	2.043
3	2.166
4	2.323
5	3.557
6	3.817
7	4.223
8	12.818

(a) 70° blunted cone/sting (base-sting fillet radius = 0.083 R_b and $R_s/R_b = 0.25$)

Fig. 1 Model configuration with $R_b = 2.50$ cm, $R_n/R_b = 0.50$, and $R_c/R_b = 0.05$.

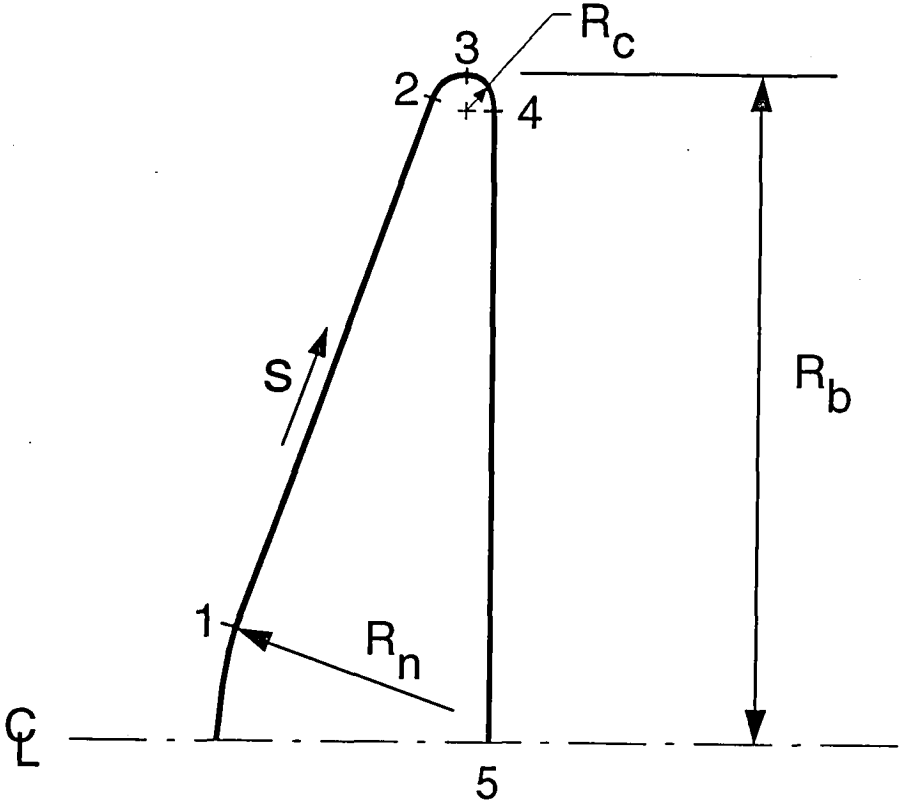

Location	s/R_n
1	0.349
2	2.043
3	2.165
4	2.322
5	4.222

(b) 70° blunted cone

Fig. 1 Concluded.

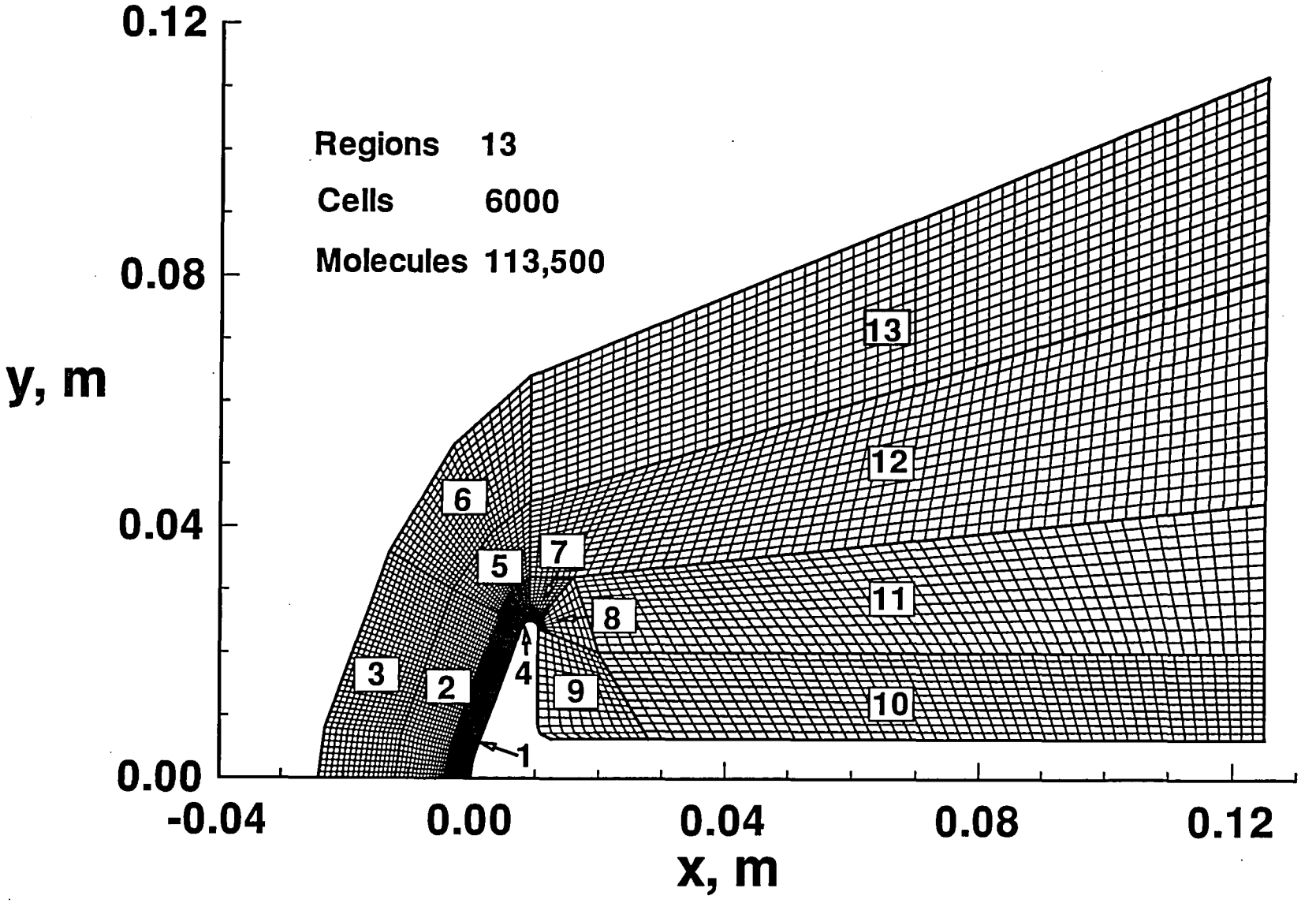

(a) Overall grid

Fig. 2 Computational domain and grid for Case 1.

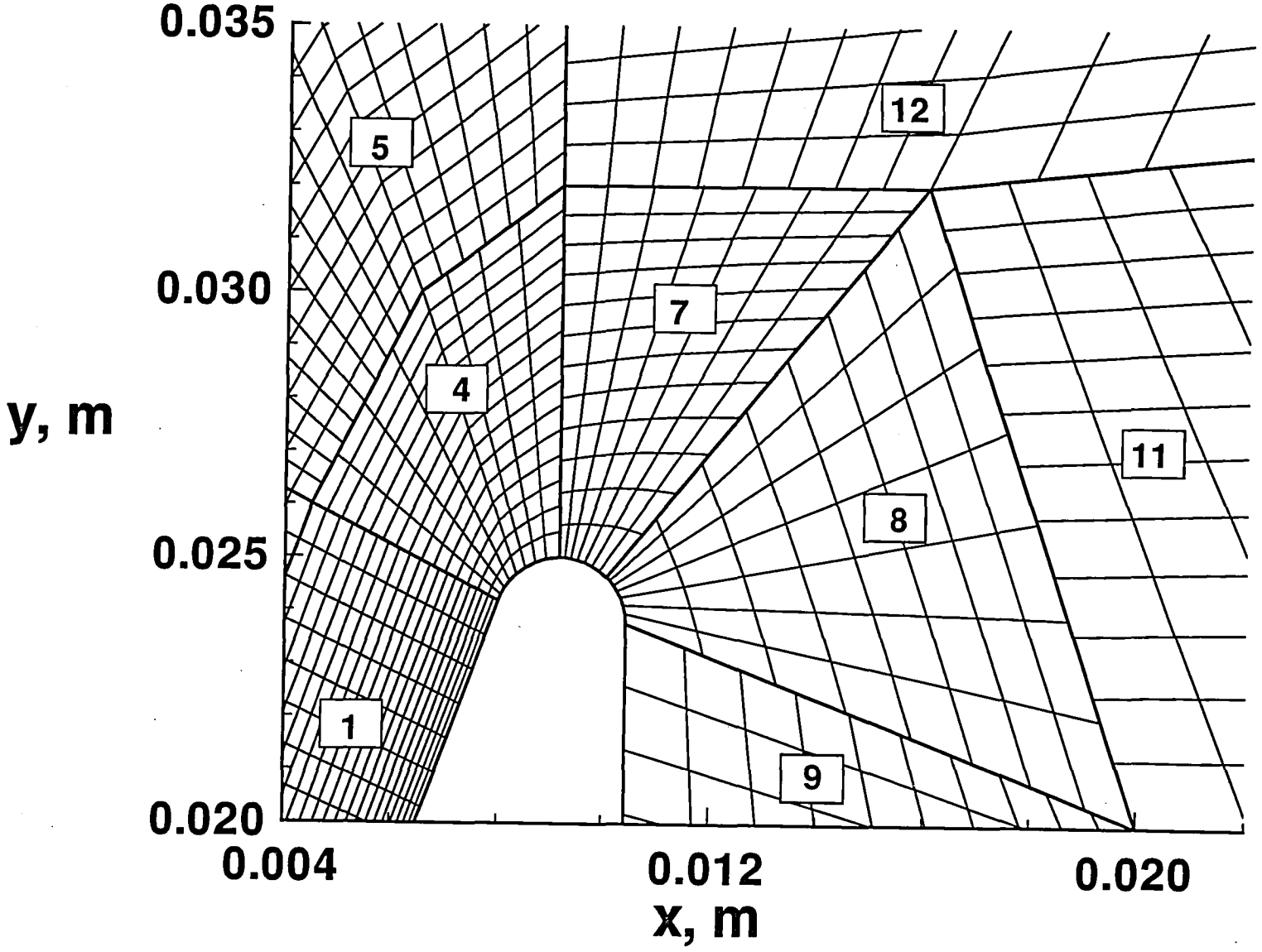

(b) Exploded view of grid for corner expansion

Fig. 2 Concluded.

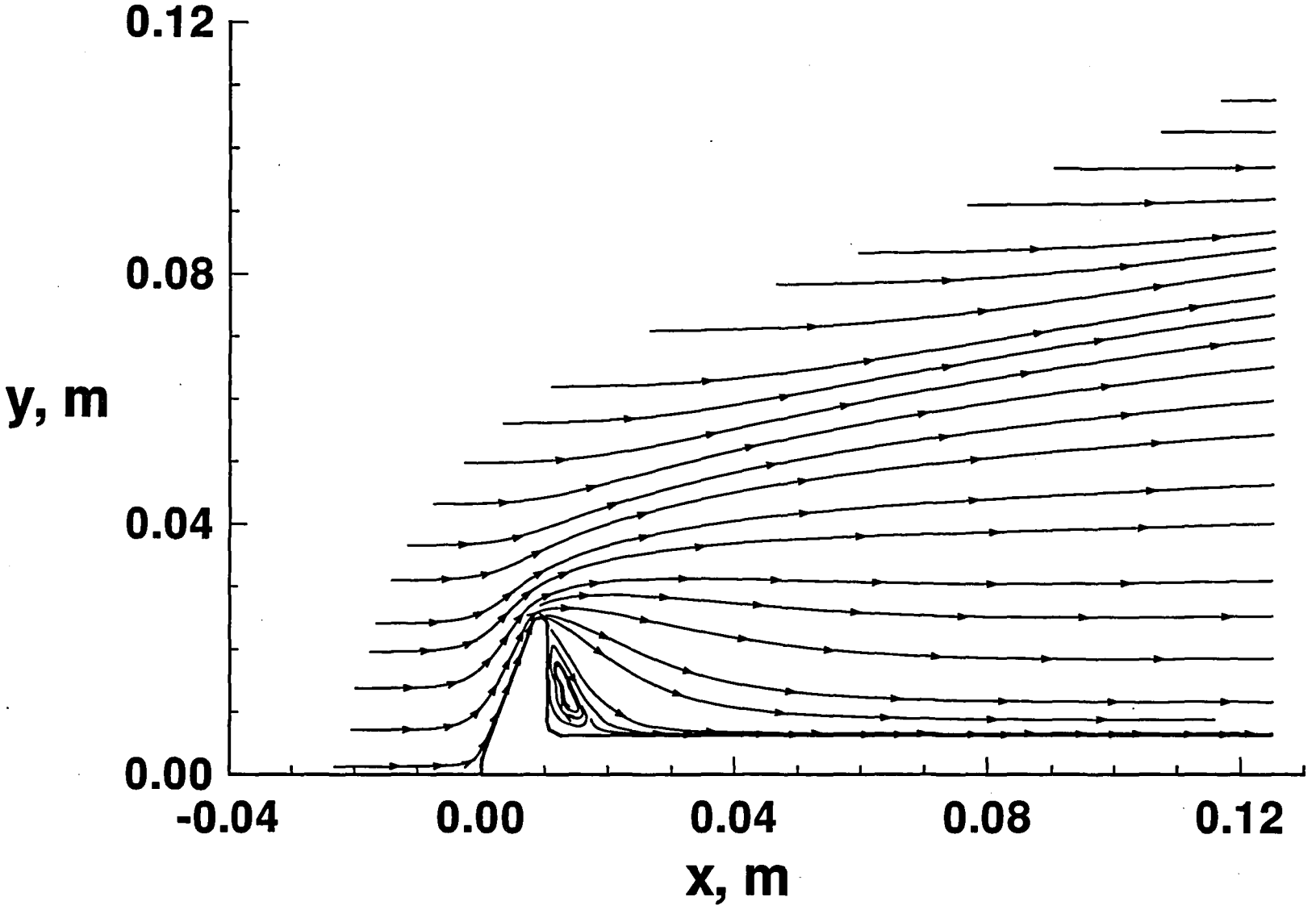

(a) With sting

Fig. 3 Particle traces for Case 1.

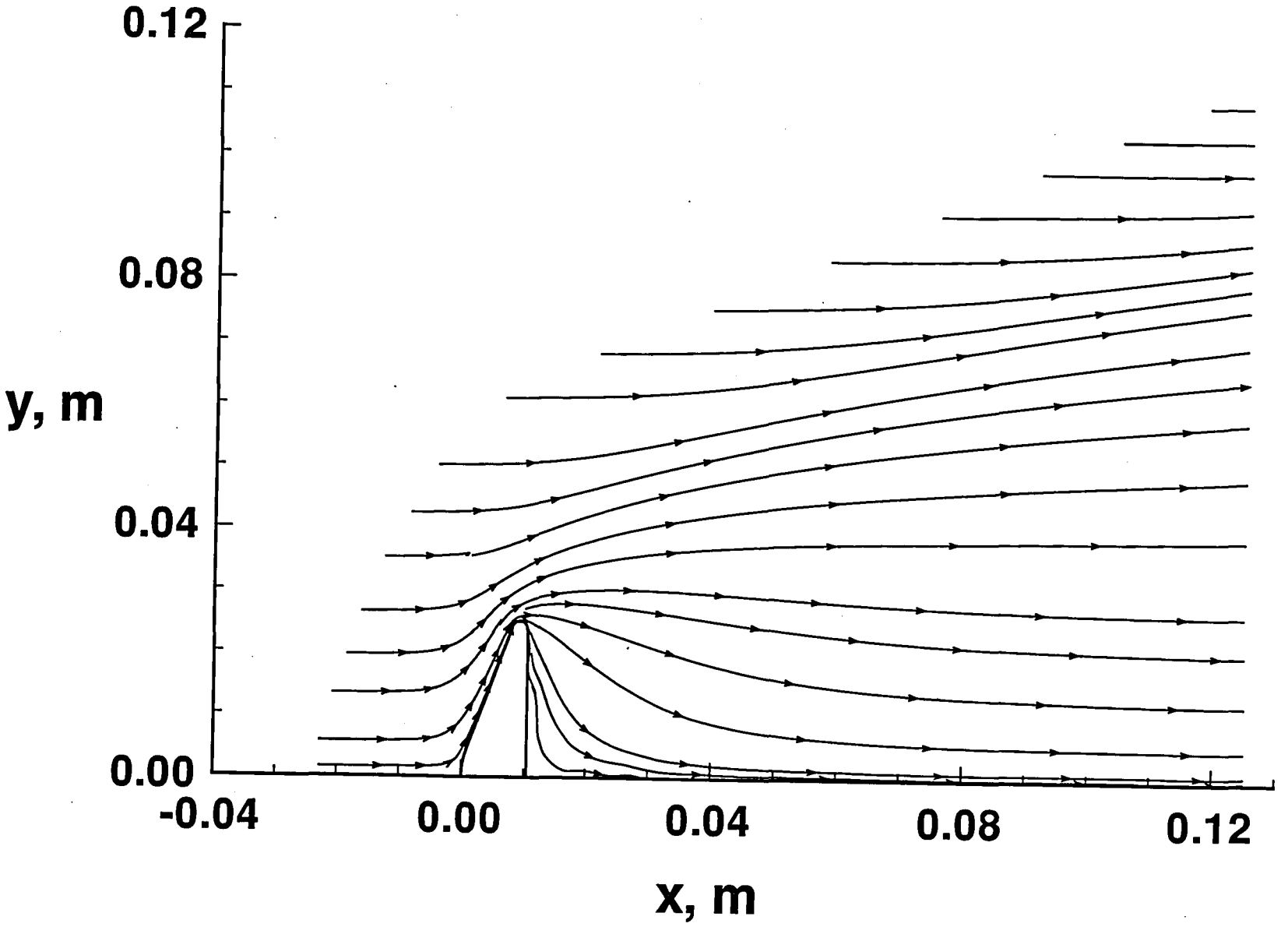

(b) Without sting

Fig. 3 Concluded.

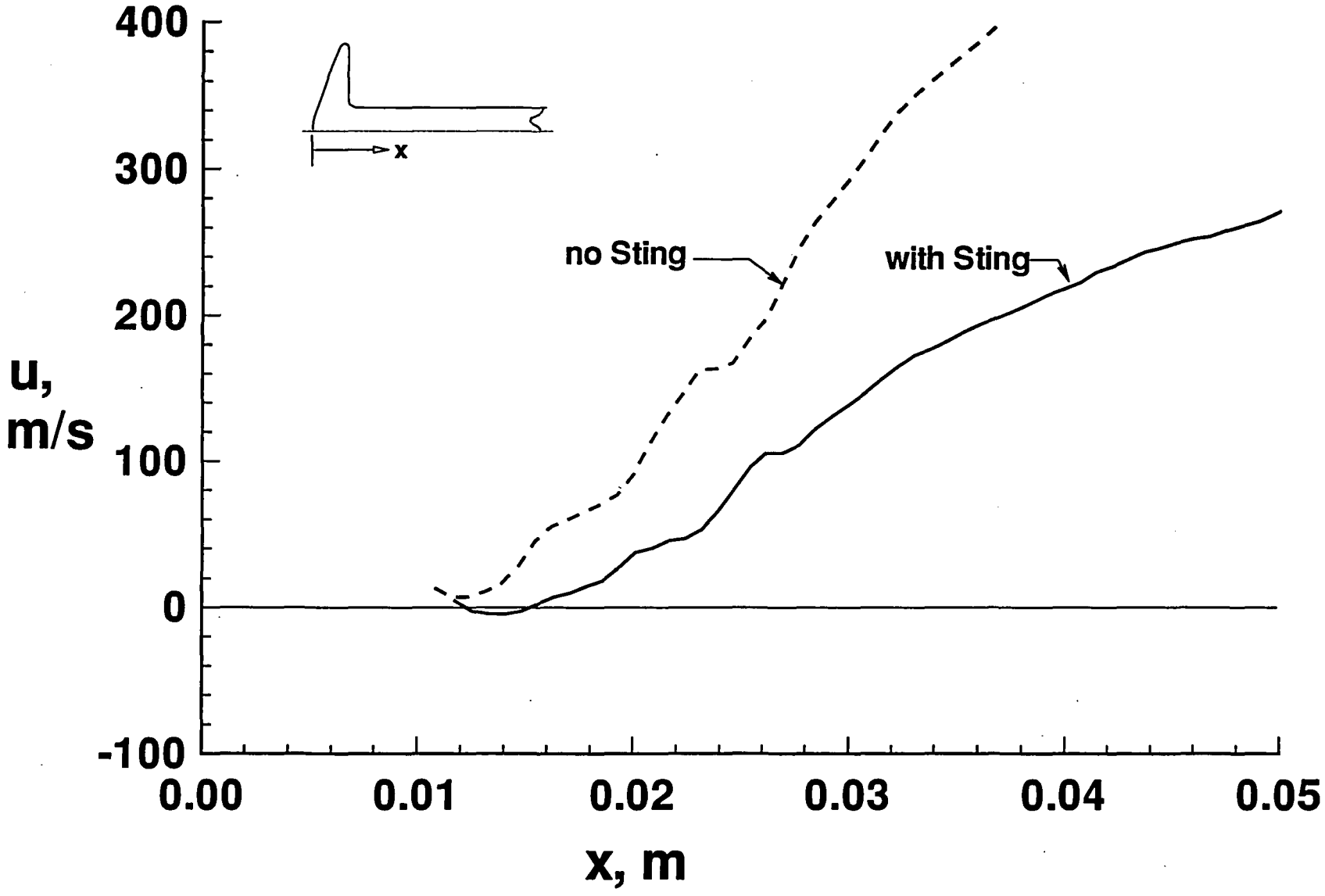

Fig. 4 Axial velocity for Case 1 along symmetry axis (no sting) and cells adjacent to surface (with sting).

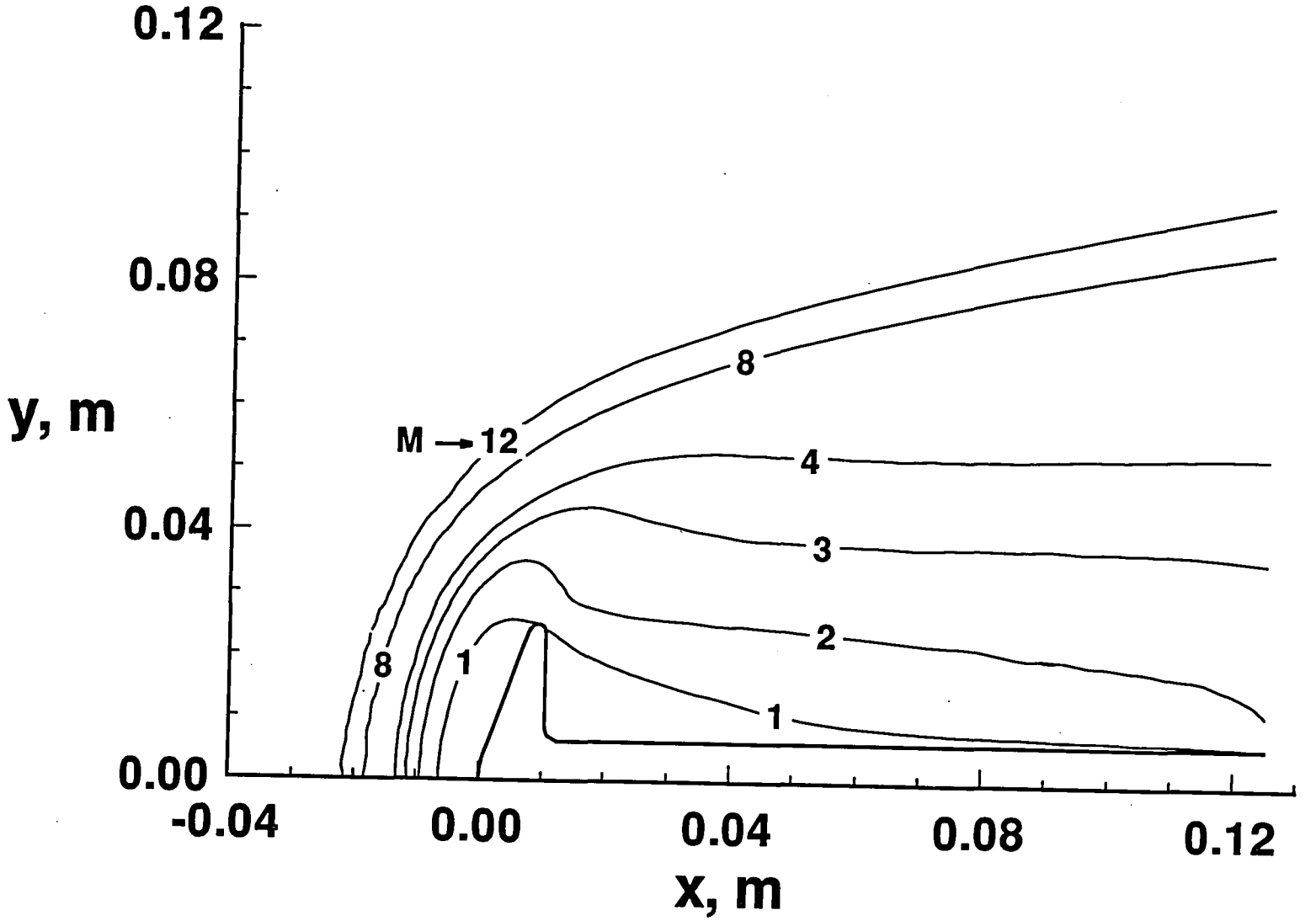

Fig. 5 Mach contours for Case 1

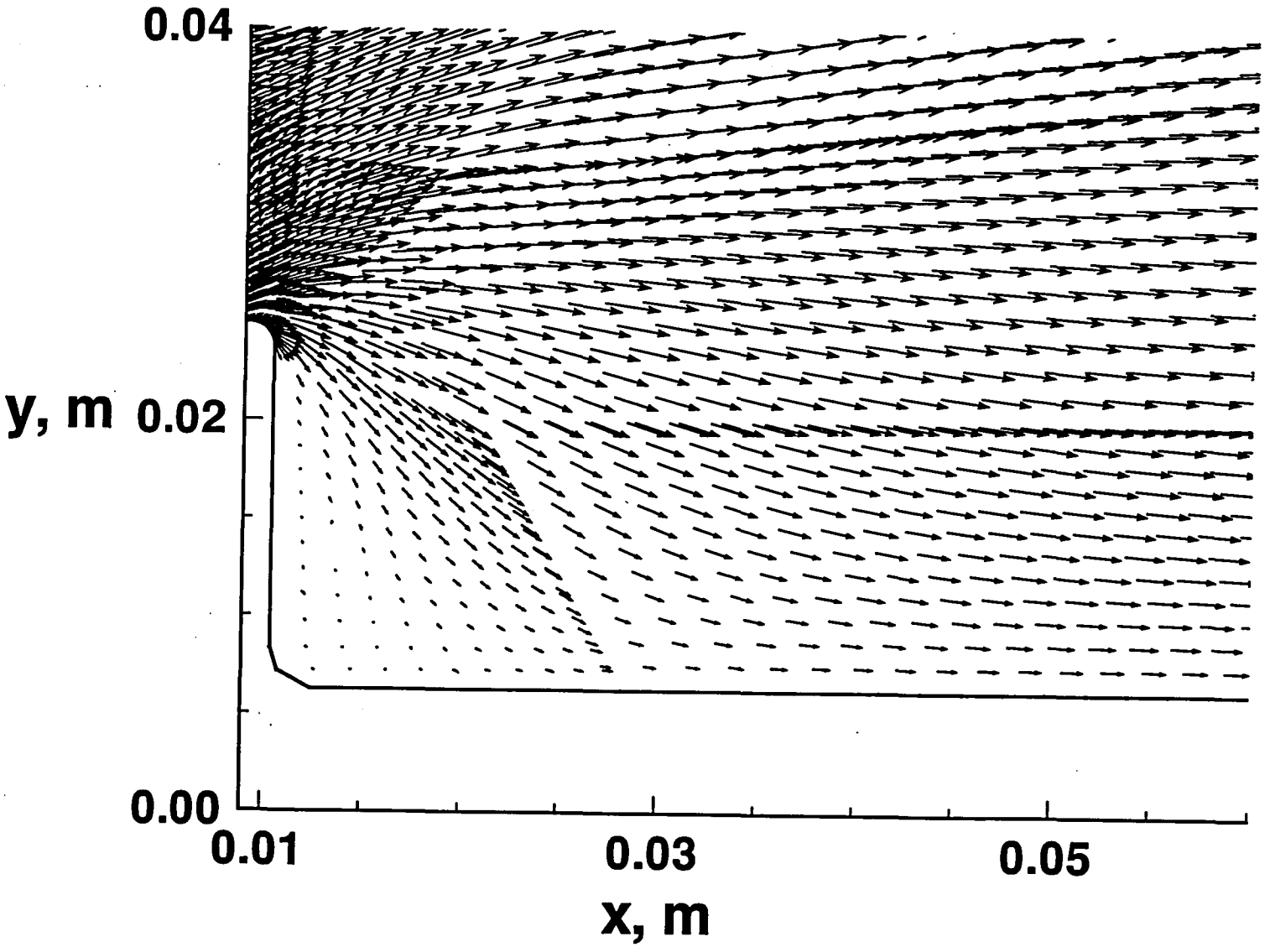

Fig. 6 Velocity vectors in near wake region for Case 1.

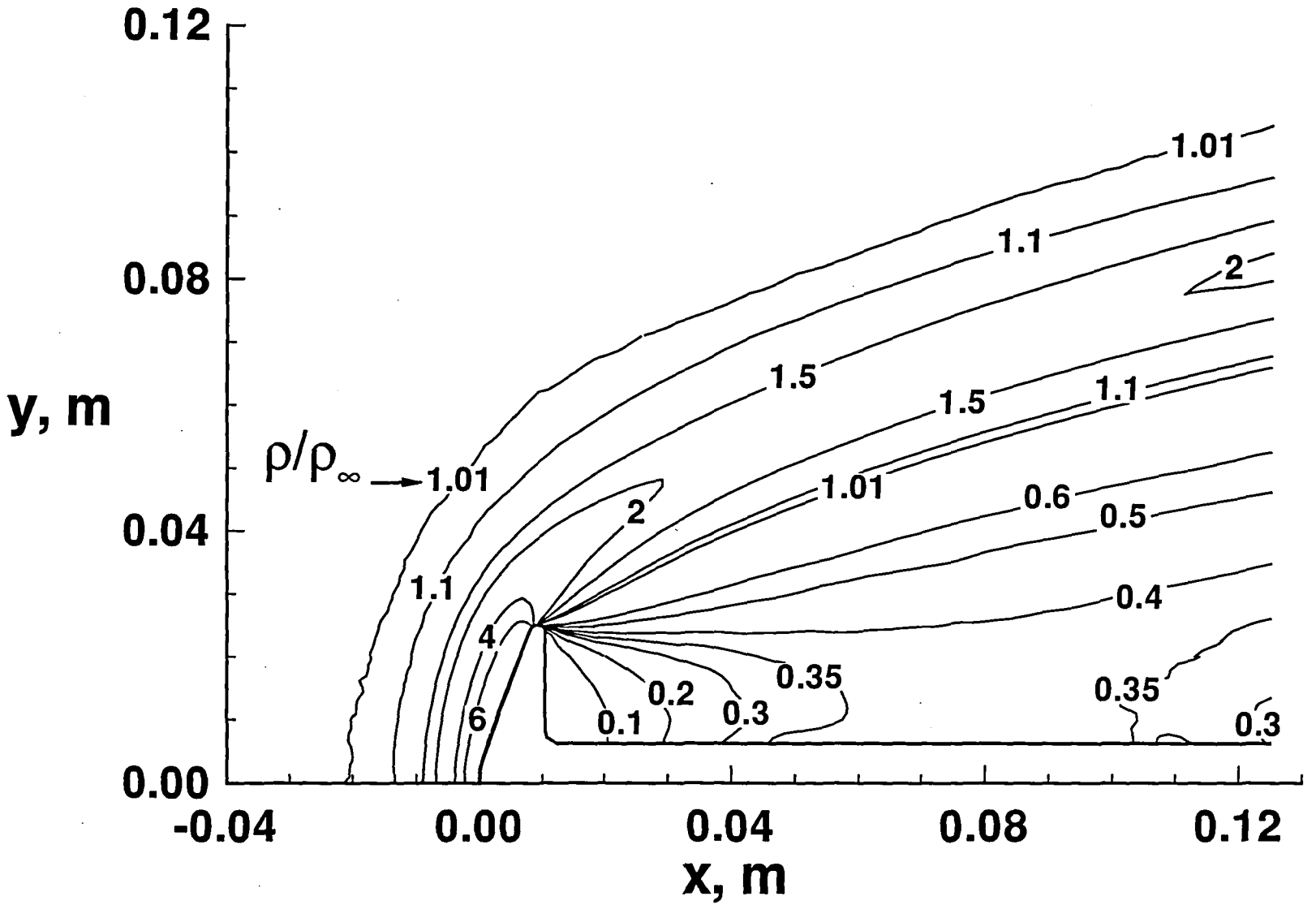

(a) Overall view

Fig 7 Nondimensional density contours for Case 1 (ρ_∞ = 1.729 x 10^{-5} kg/m^3).

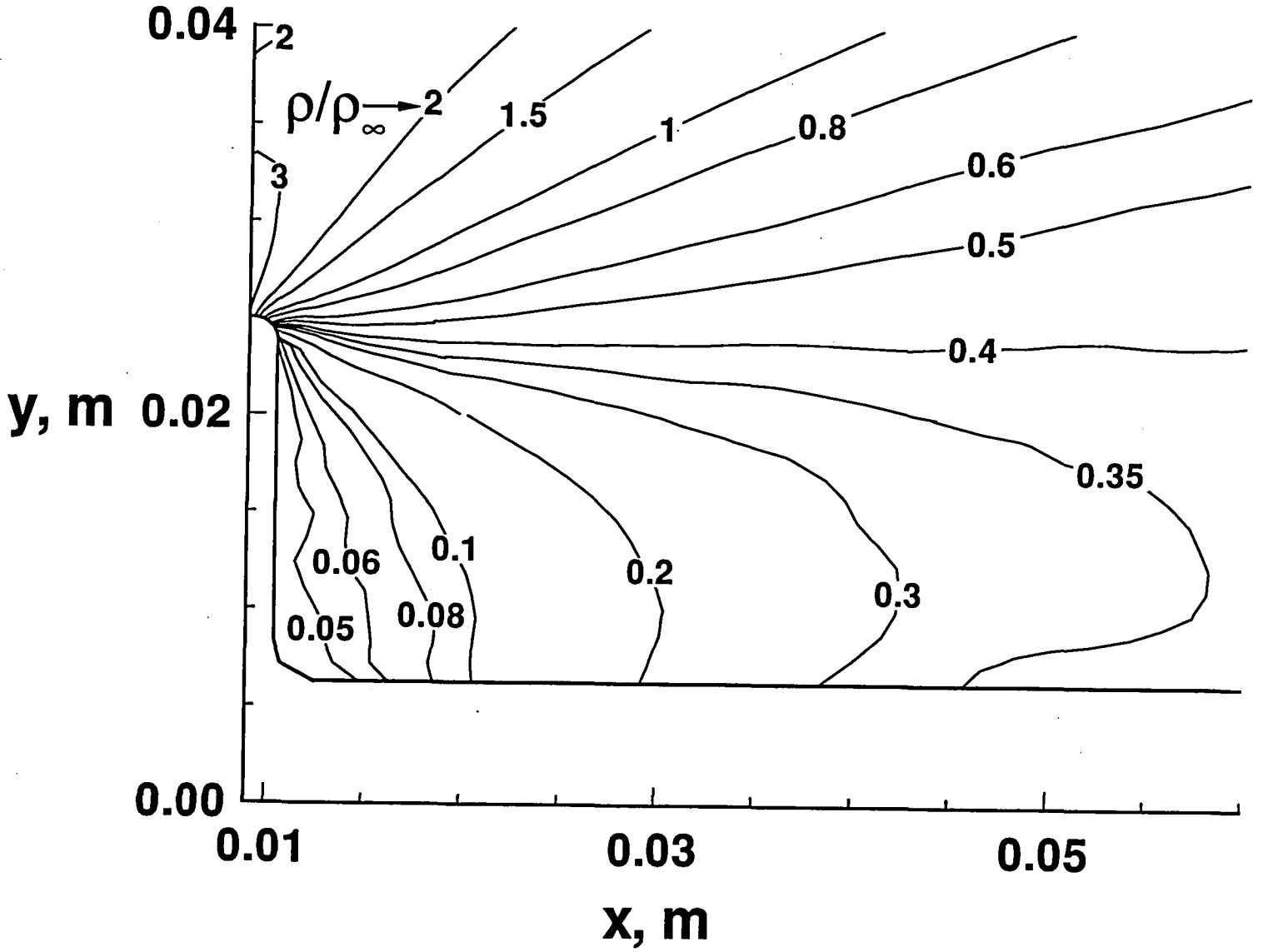

(b) Near wake region

Fig. 7 Concluded.

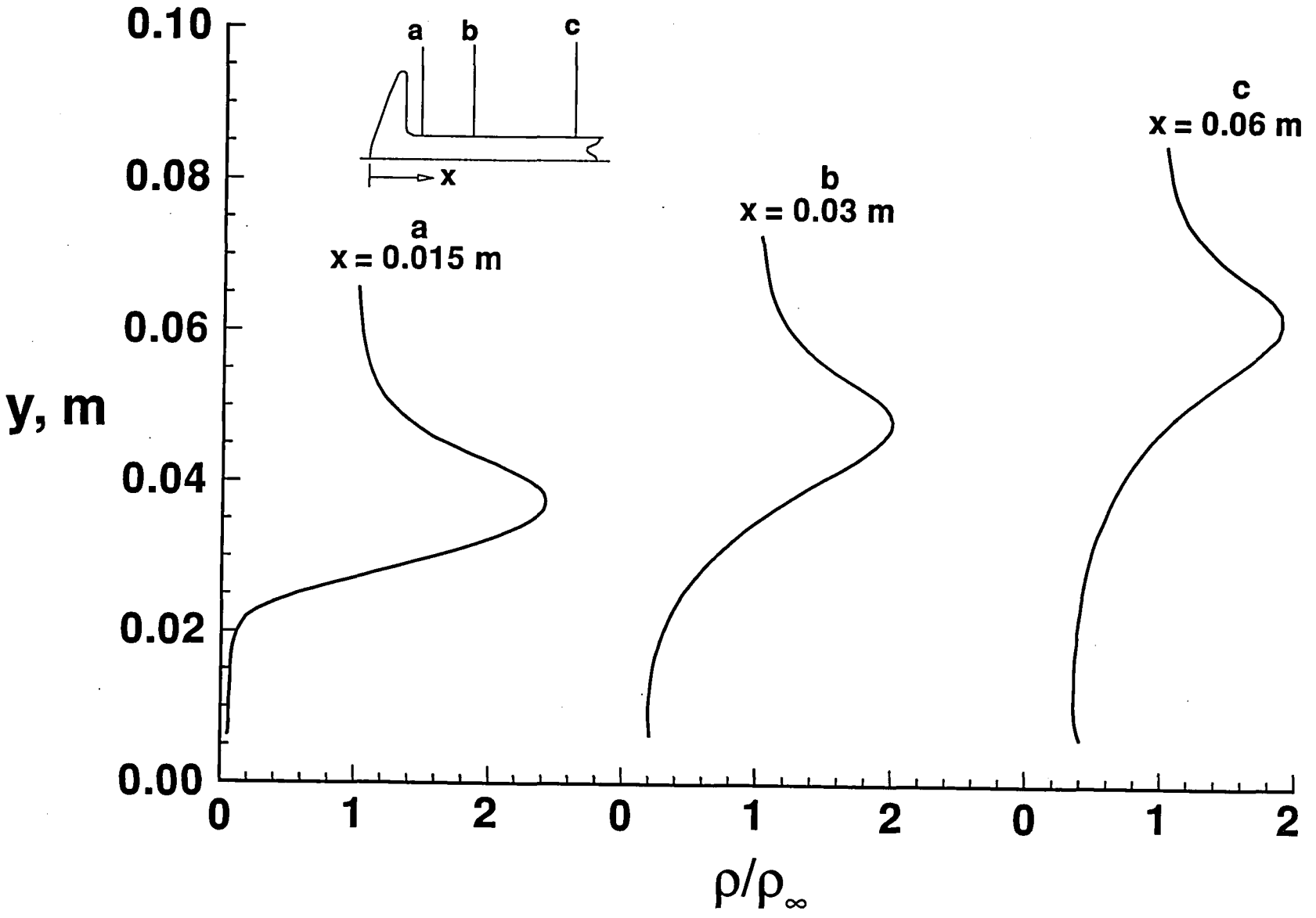

Fig. 8 Wake density profiles for Case 1.

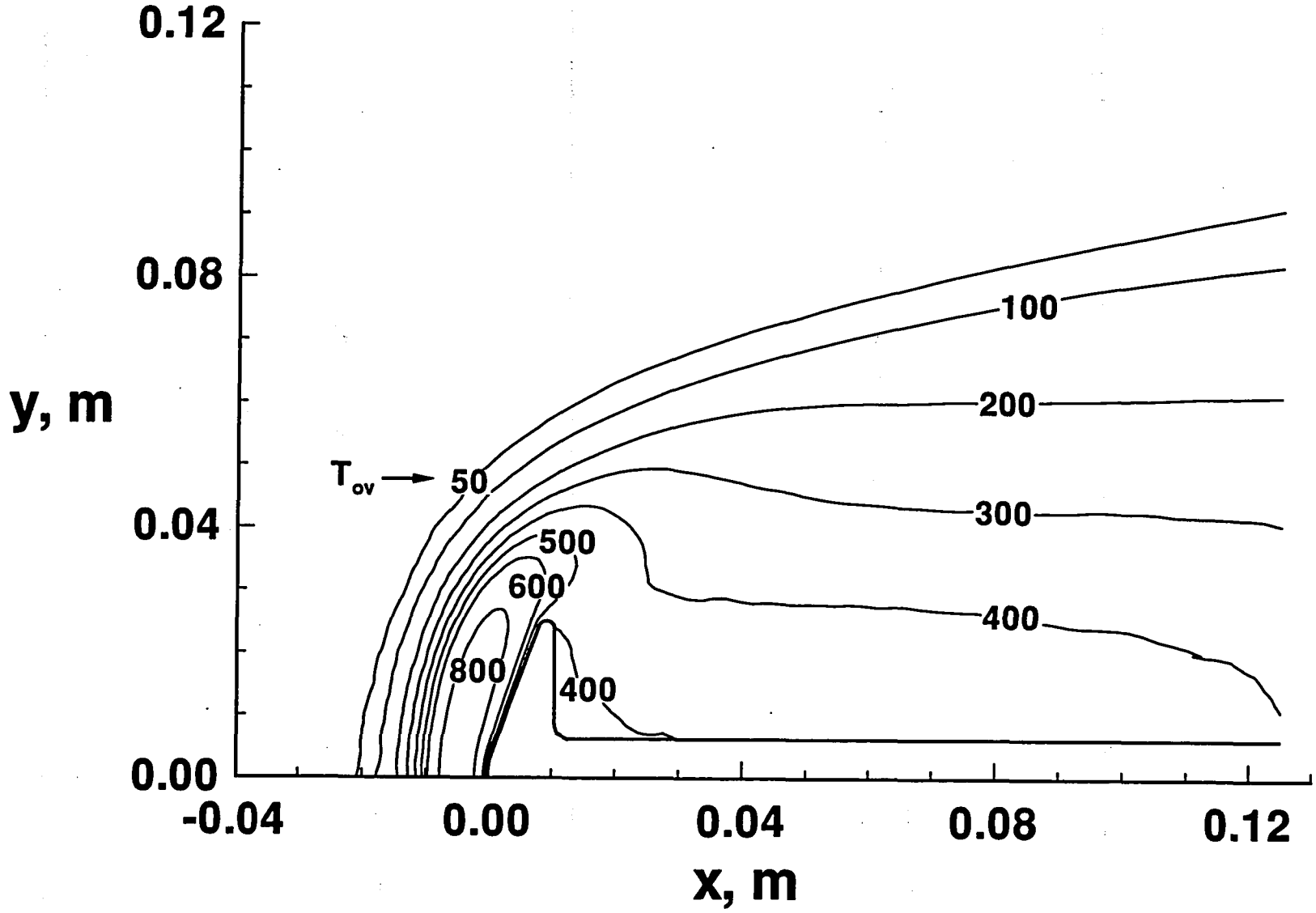

(a) Overall kinetic temperature.

Fig. 9 Temperature contours for Case 1.

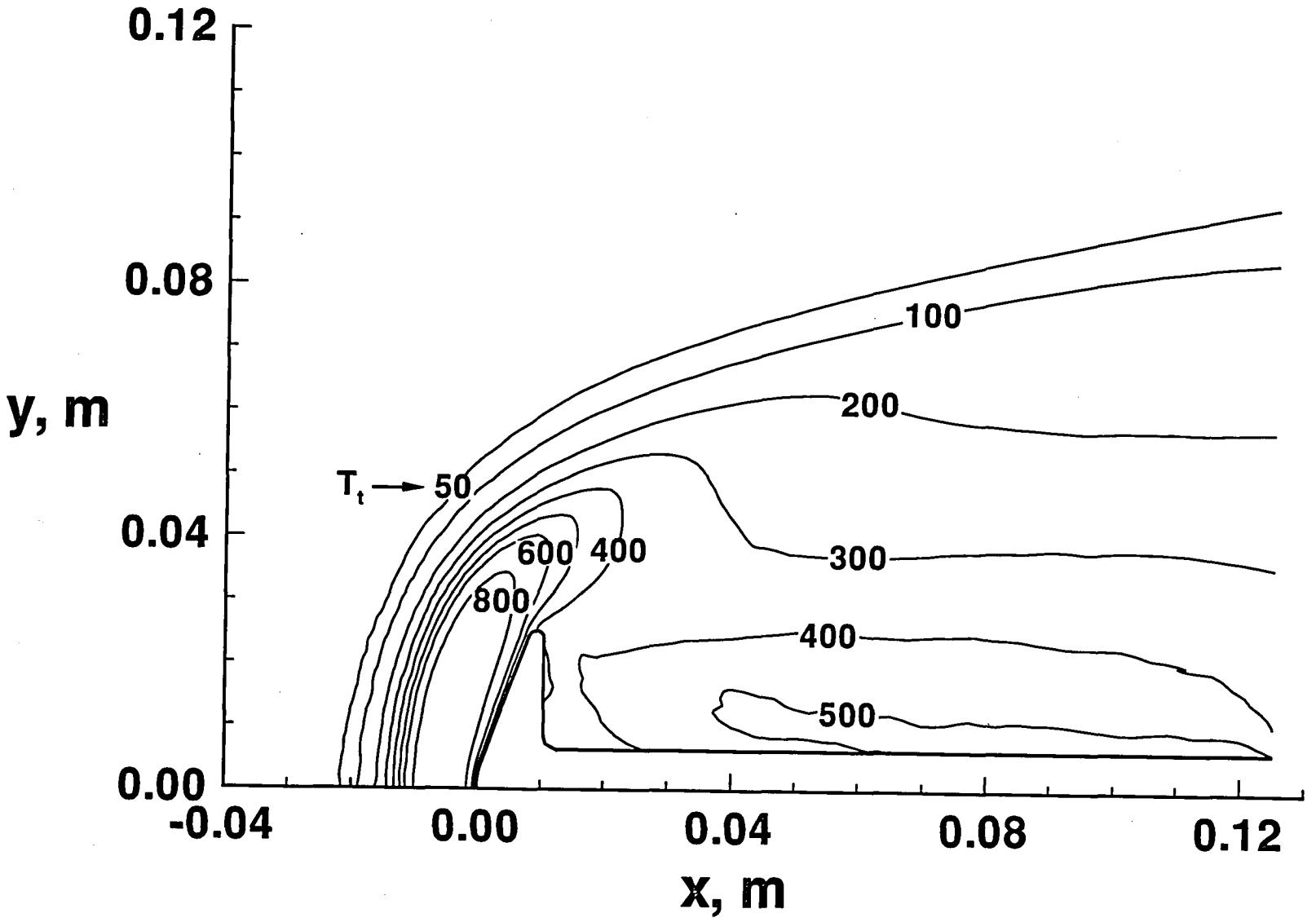

(b) Translational temperature

Fig. 9 Continued.

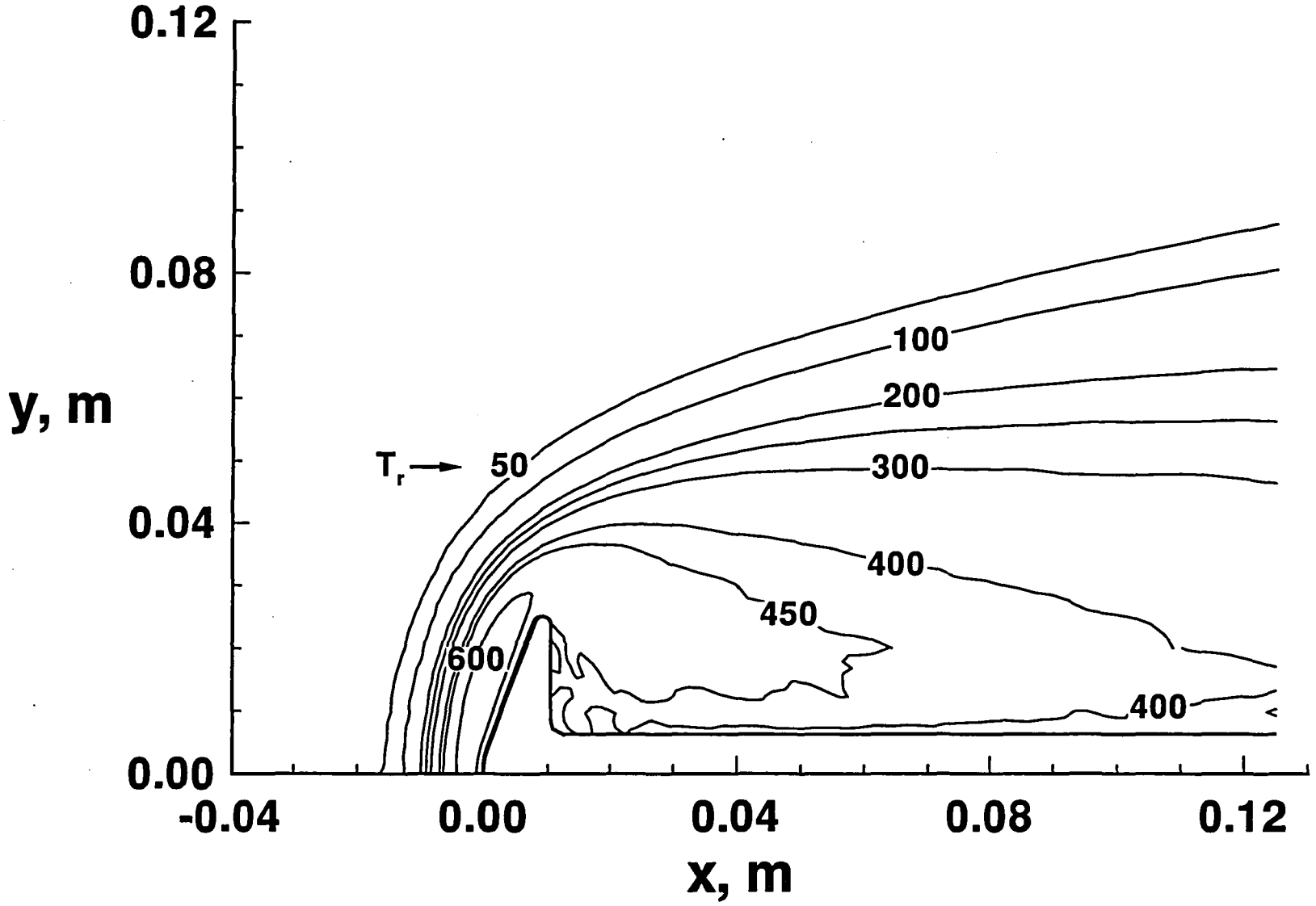

(c) Rotational temperature

Fig. 9 Concluded.

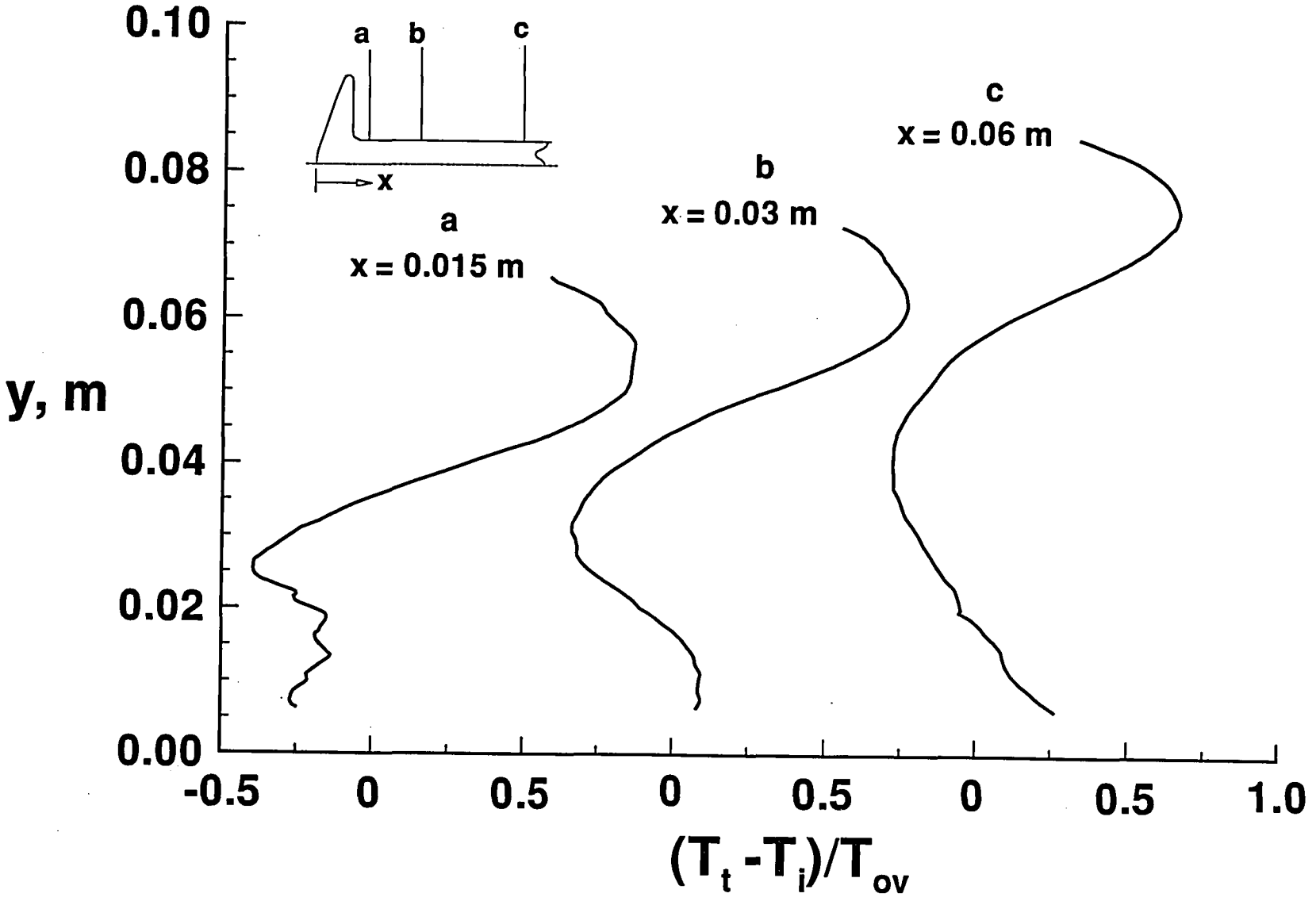

(a) Extent of thermal nonequilibrium.

Fig. 10 Wake profiles for Case 1.

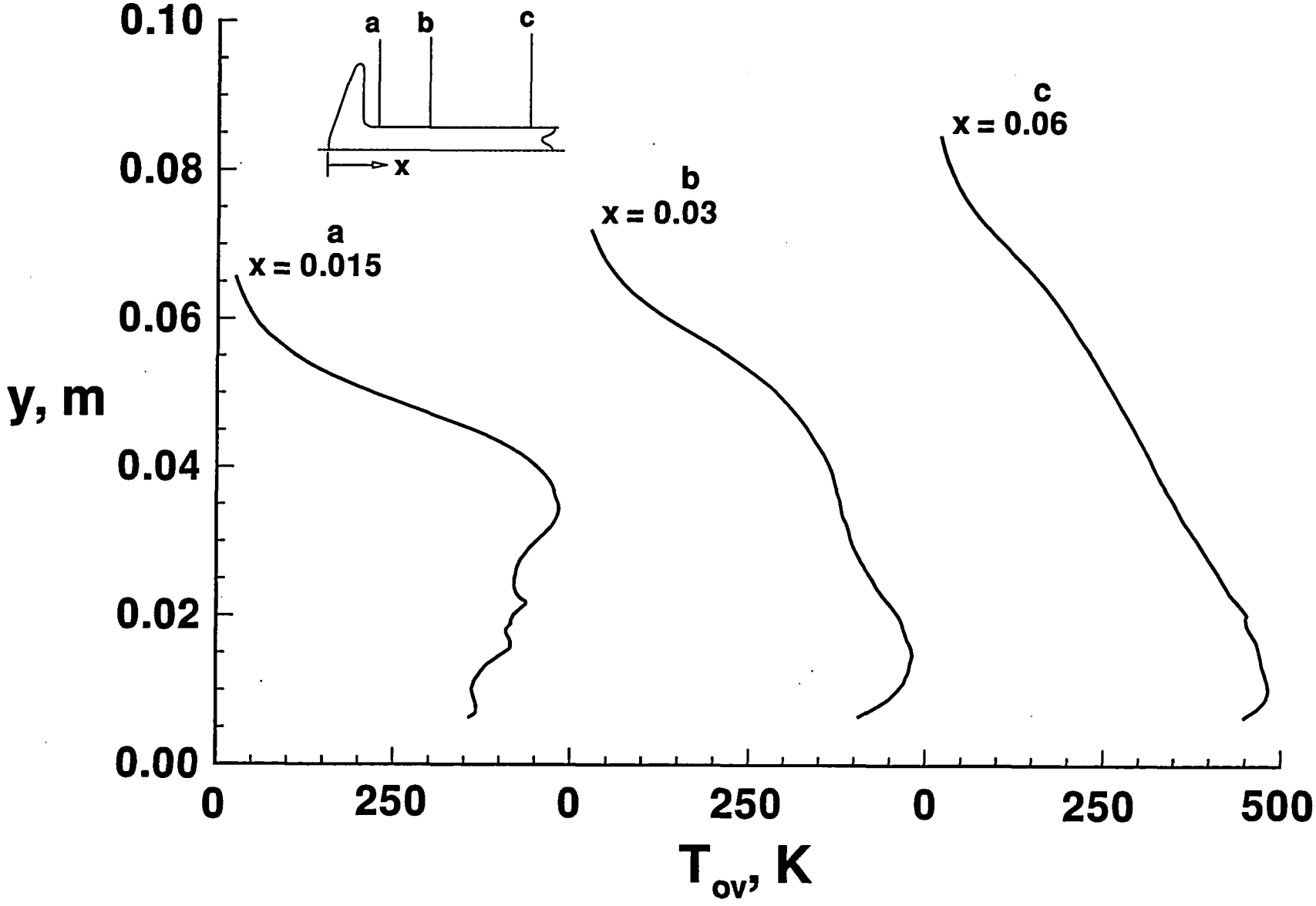

(b) Overall kinetic temperature

Fig. 10 Continued.

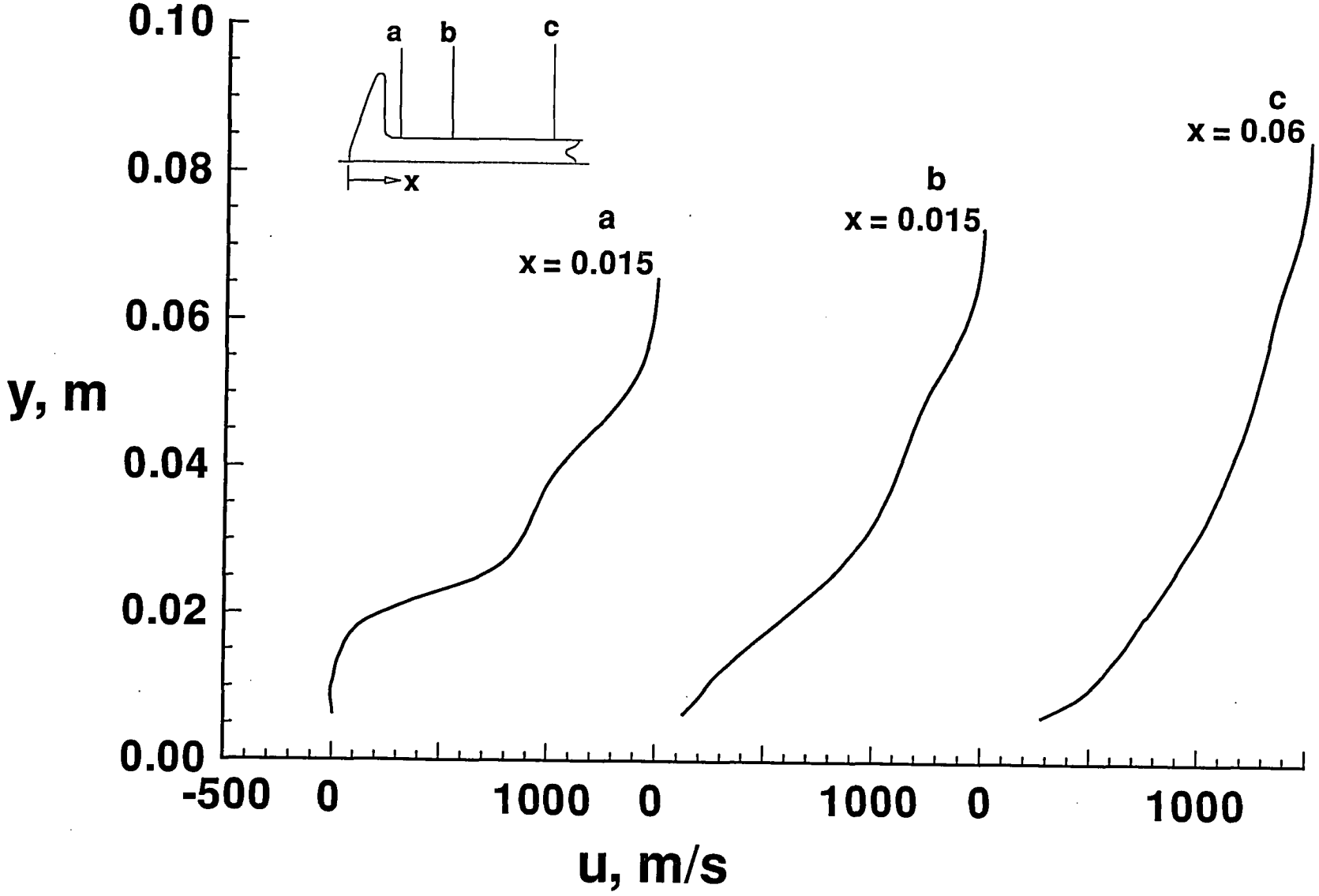

(c) Axial velocity

Fig. 10 Concluded.

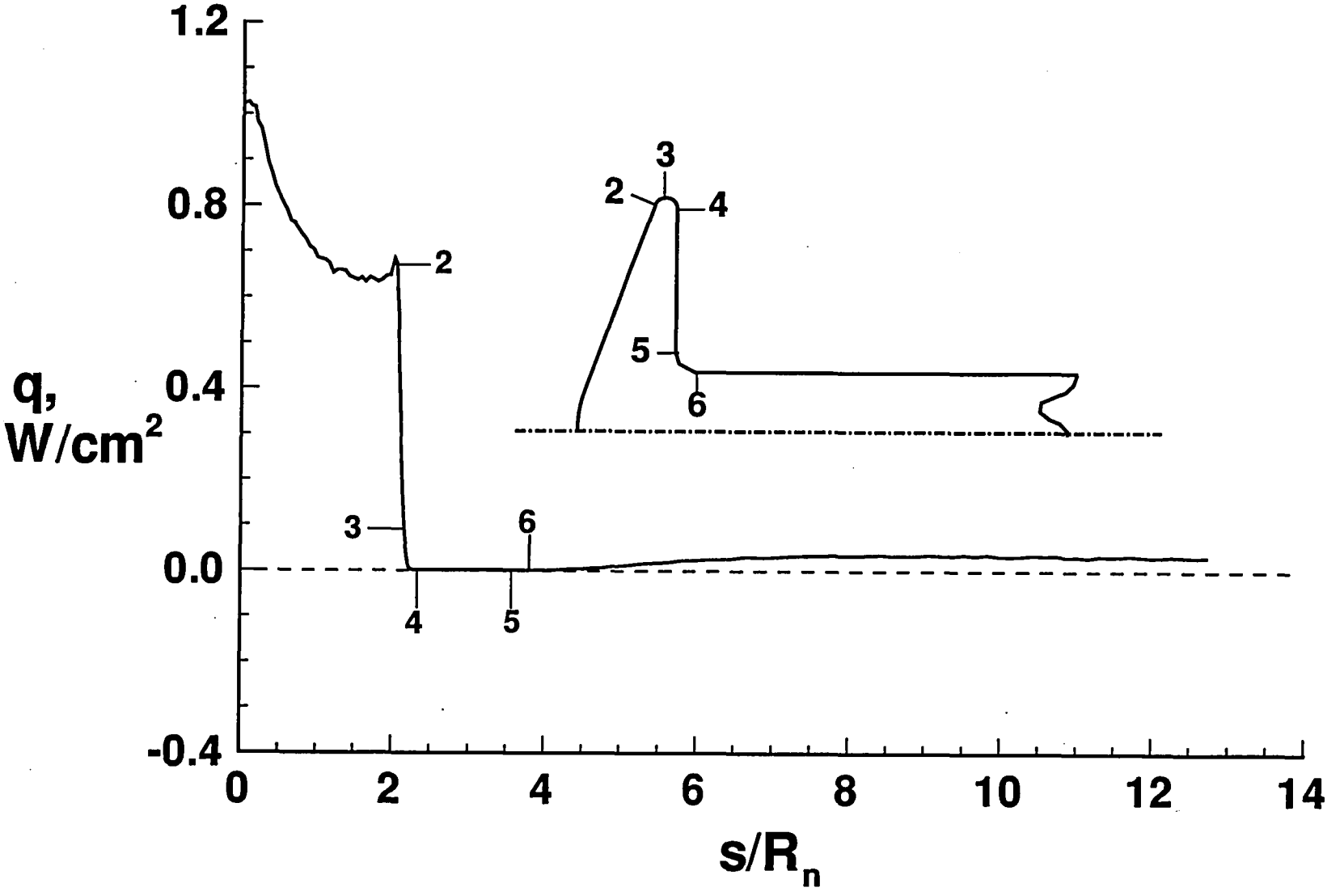

(a) Cartesian plot

Fig. 11 Surface heating rate distribution for Case 1.

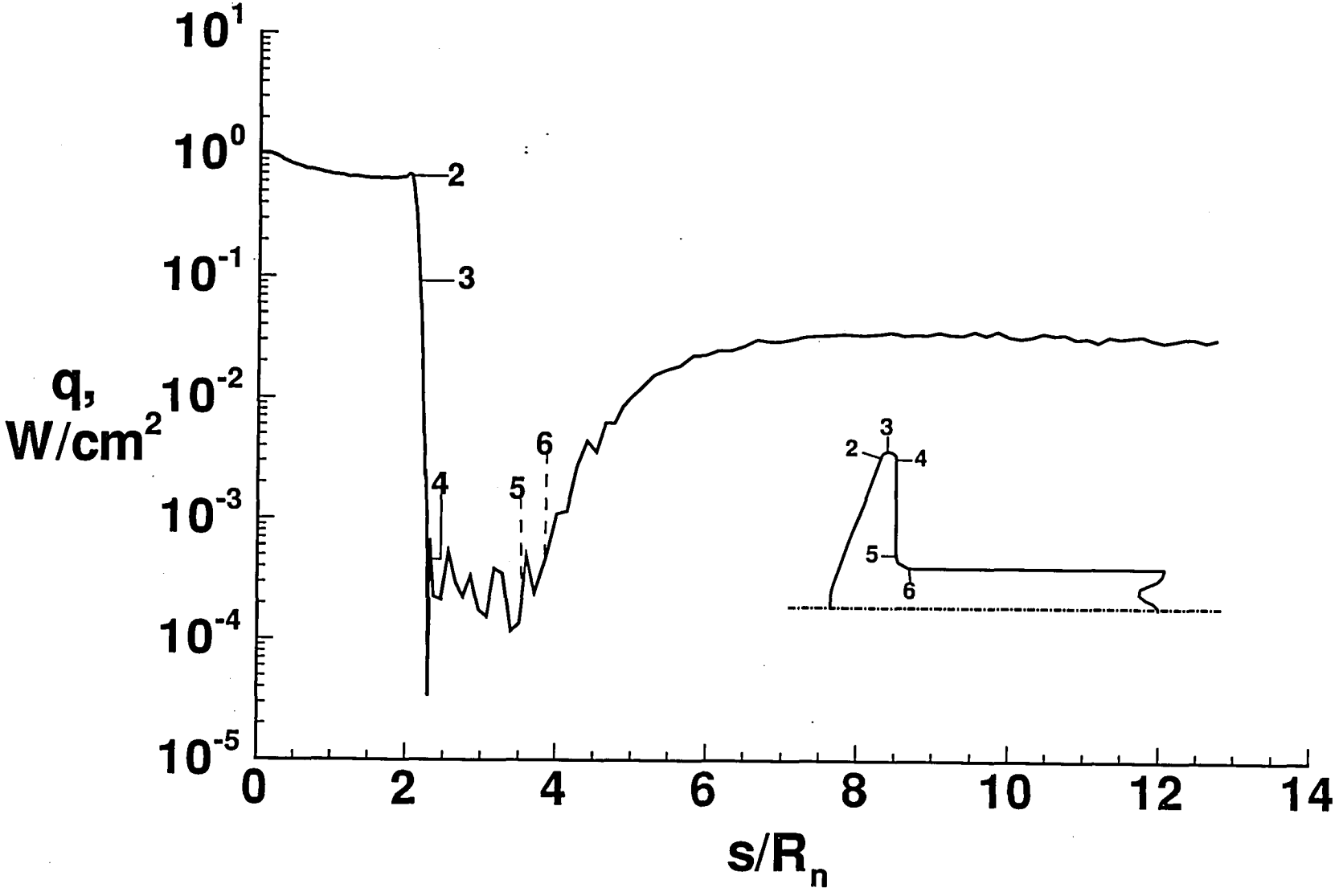

(b) Semilog plot

Fig. 11 Concluded

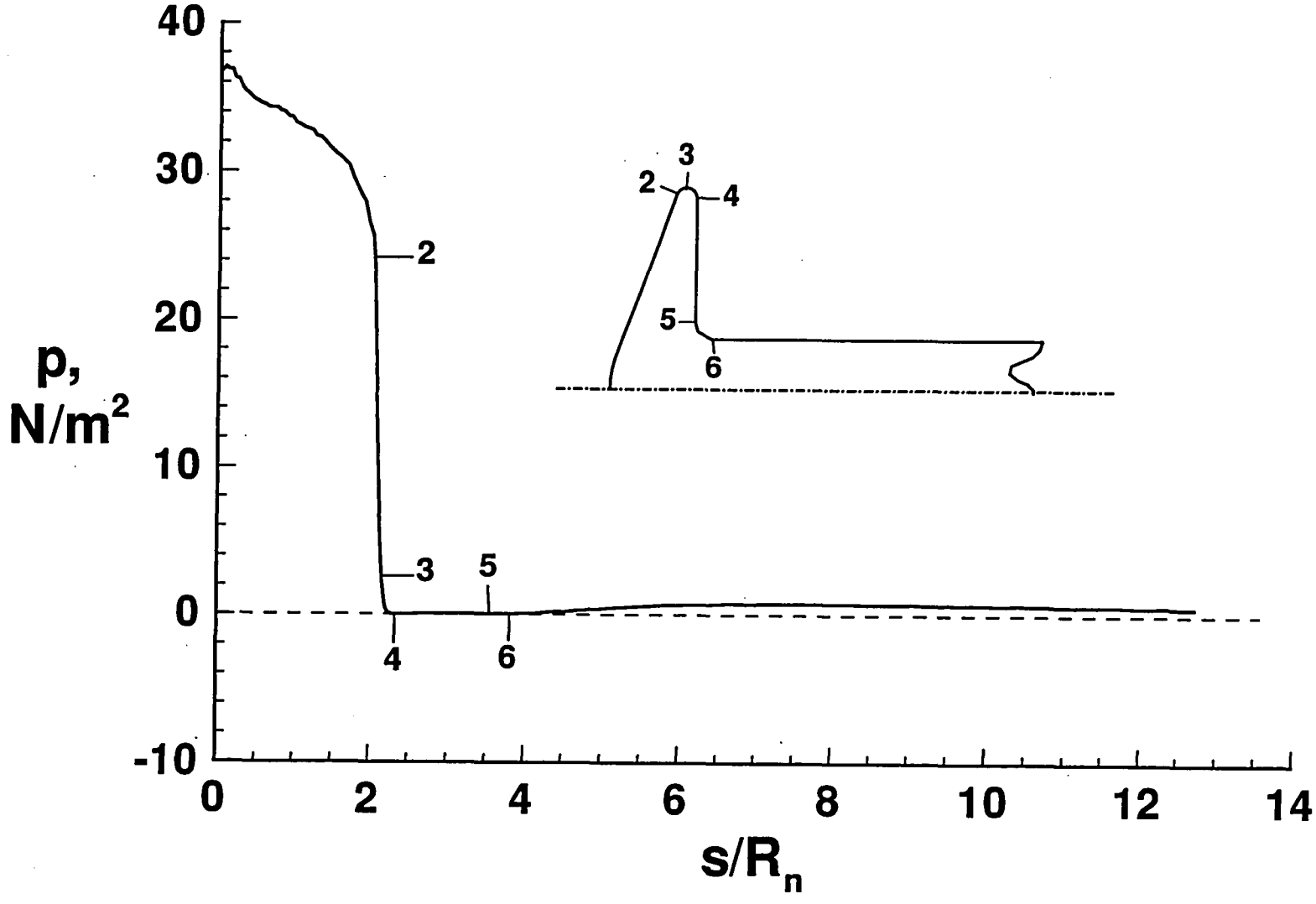

(a) Cartesian plot

Fig. 12 Surface pressure distribution for Case 1.

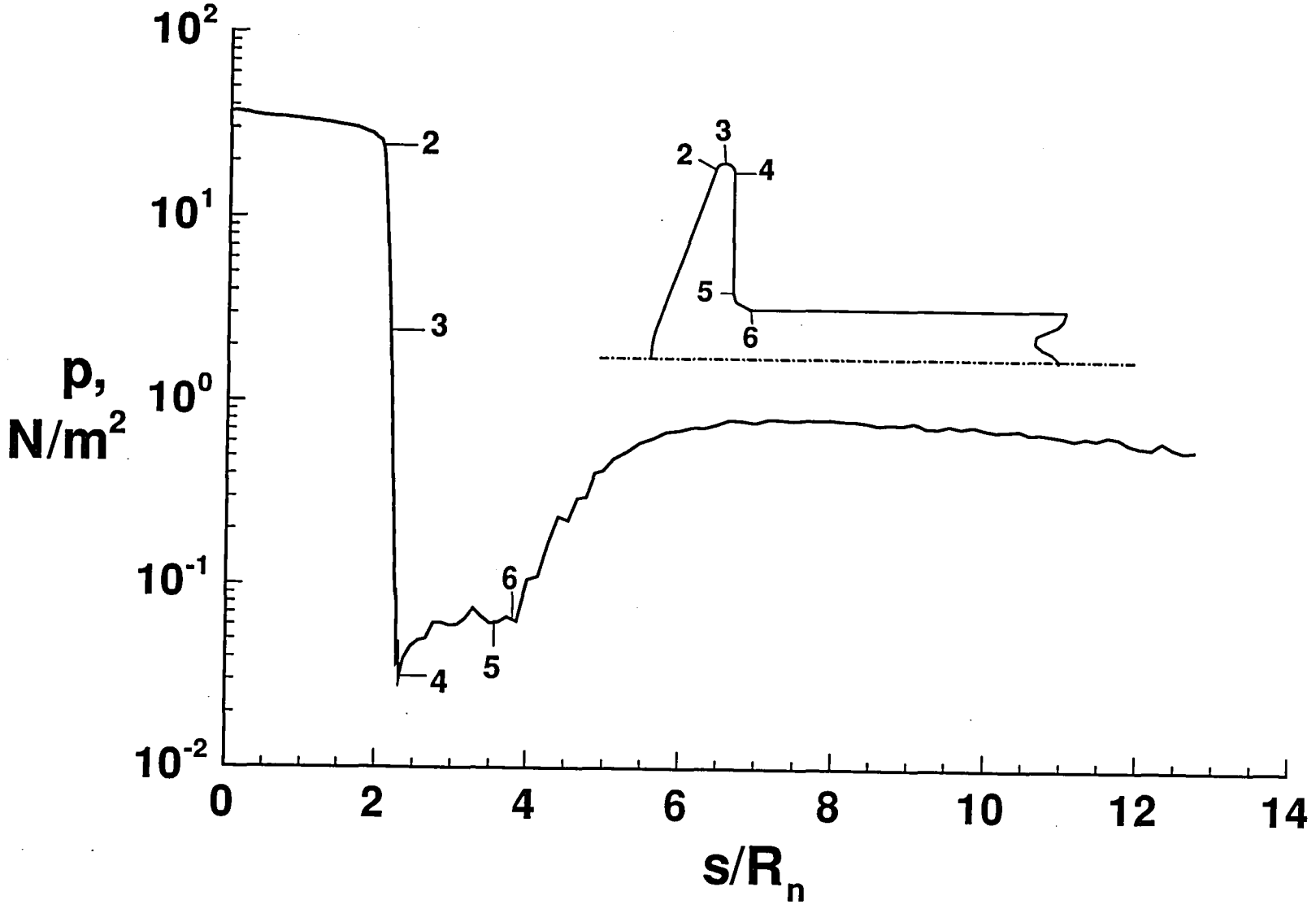

(b) Semilog plot

Fig. 12 Concluded.

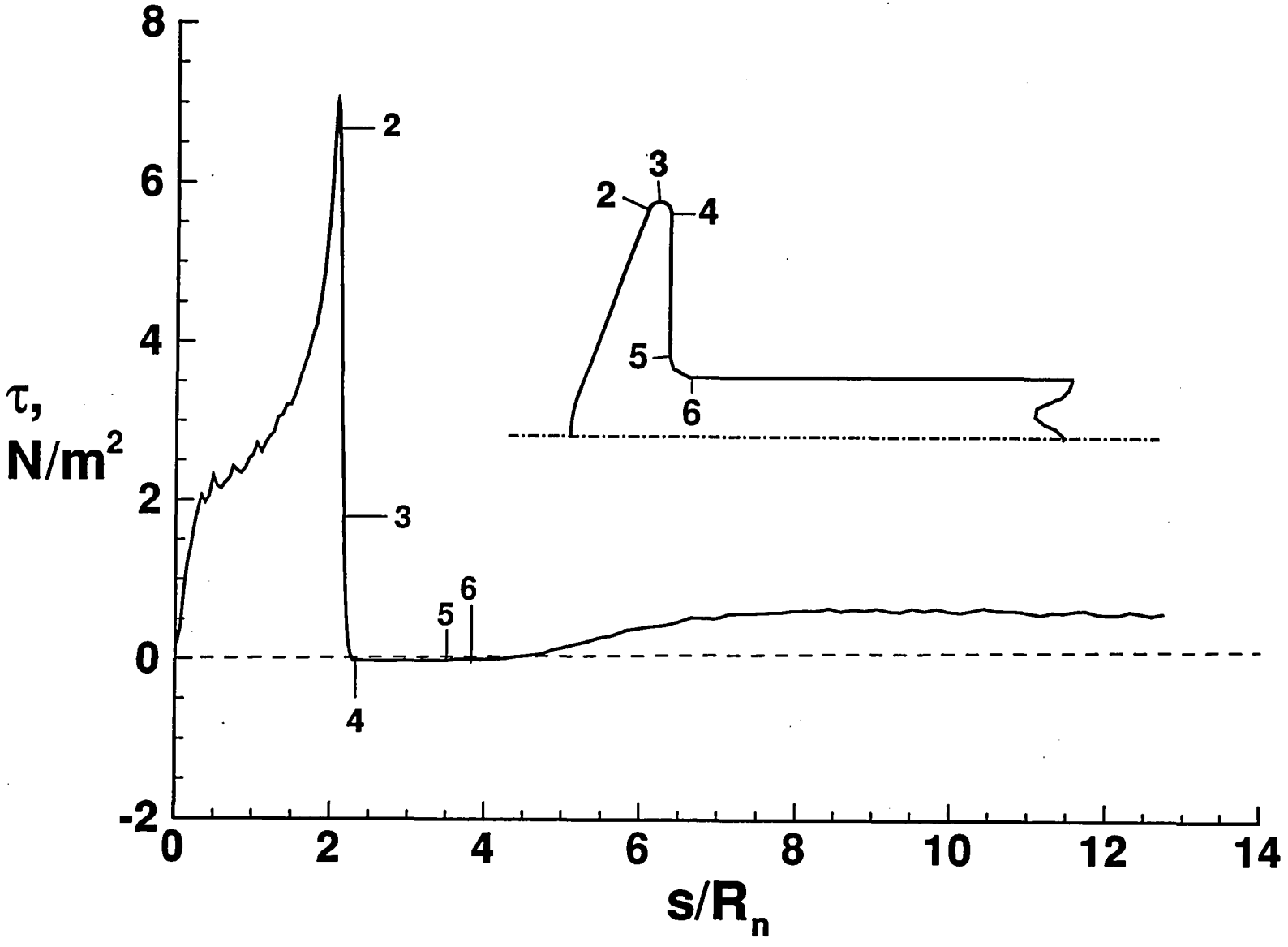

Fig. 13 Skin friction distribution for Case 1.

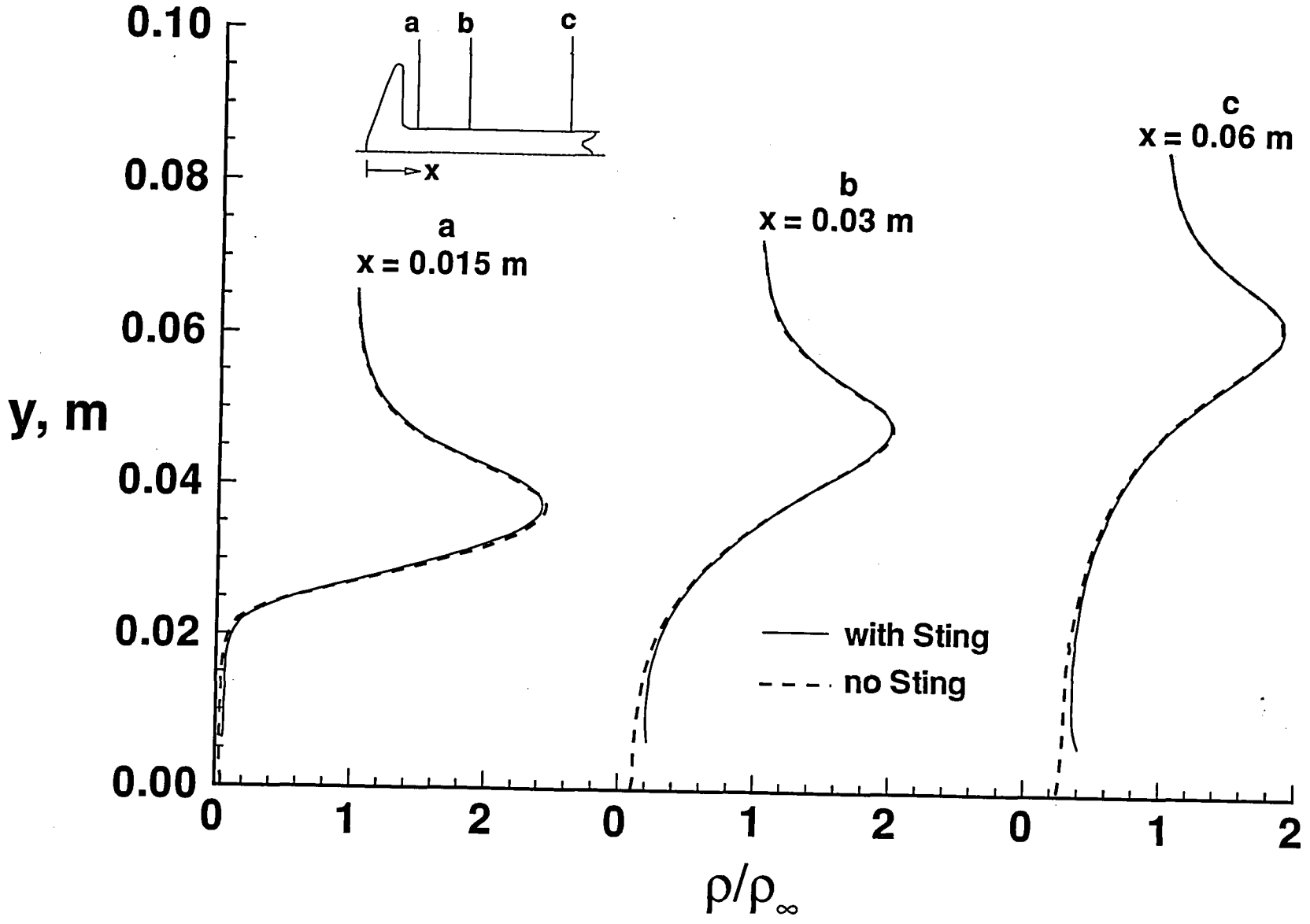

(a) Wake density profiles

Fig. 14 Effect of afterbody sting on wake results for Case 1

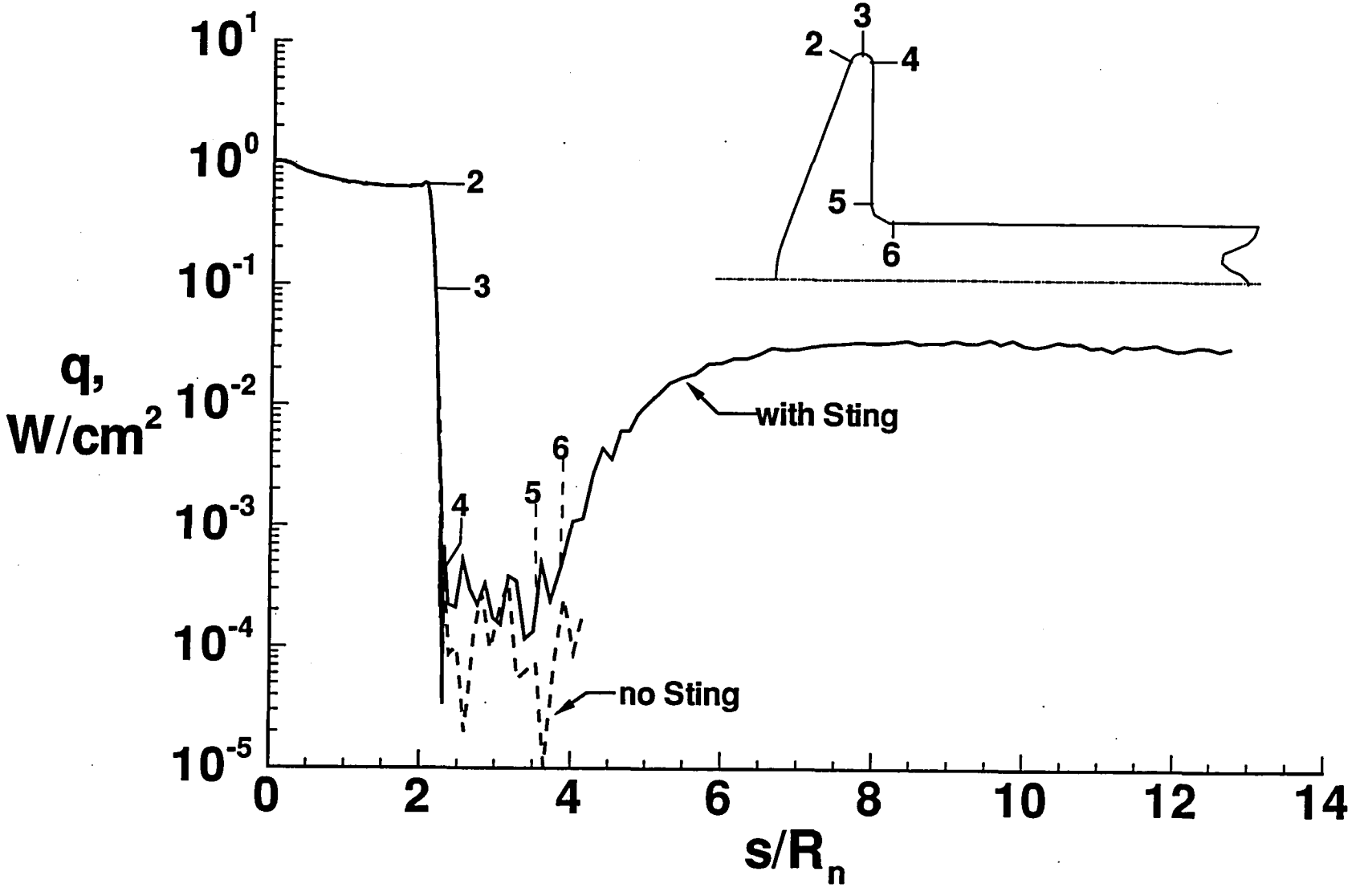

(b) Surface heating rate distribution

Fig. 14 Concluded.

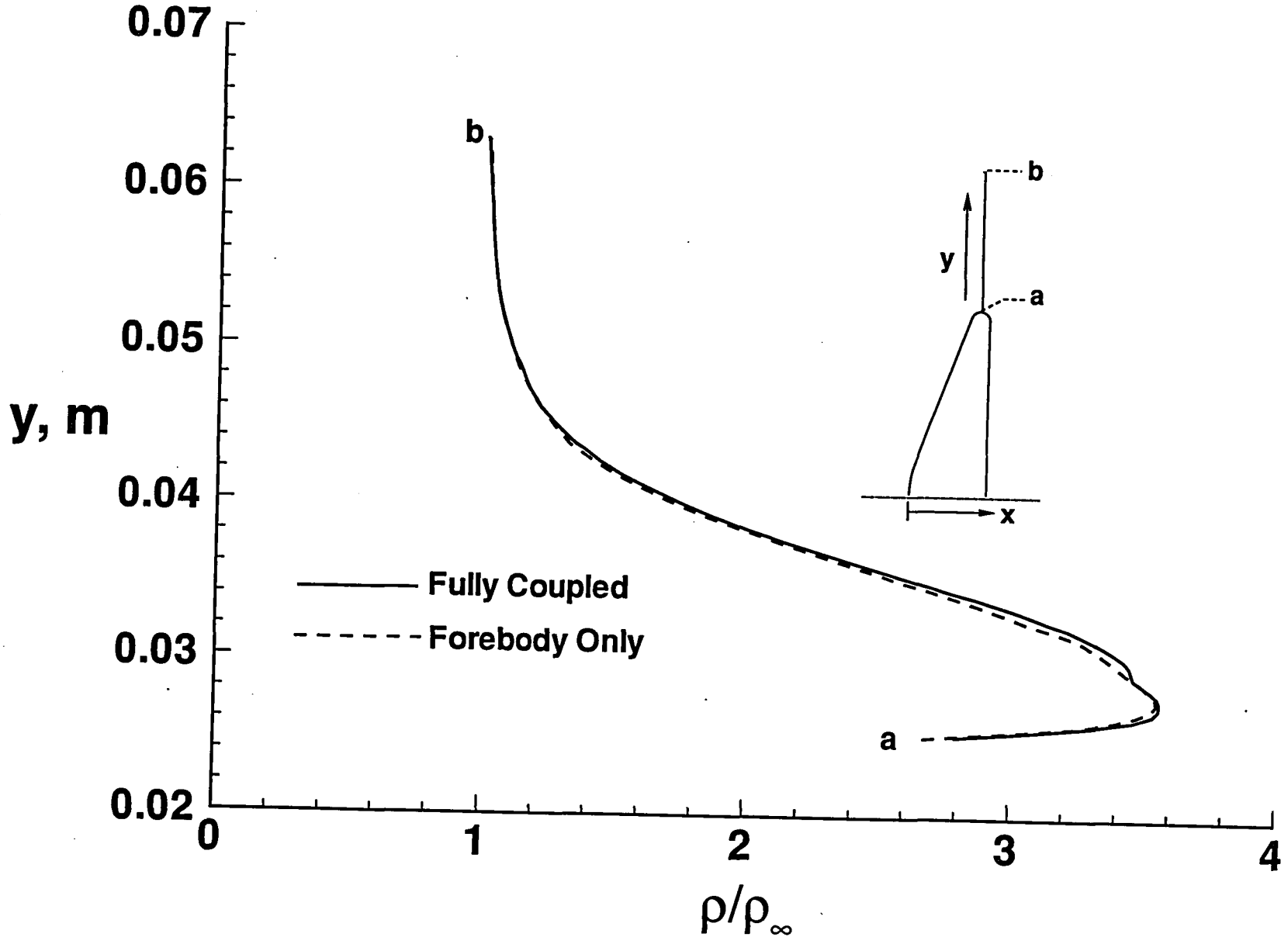

(a) Density profiles

Fig. 15 Effect of wake on forebody results for Case 1.

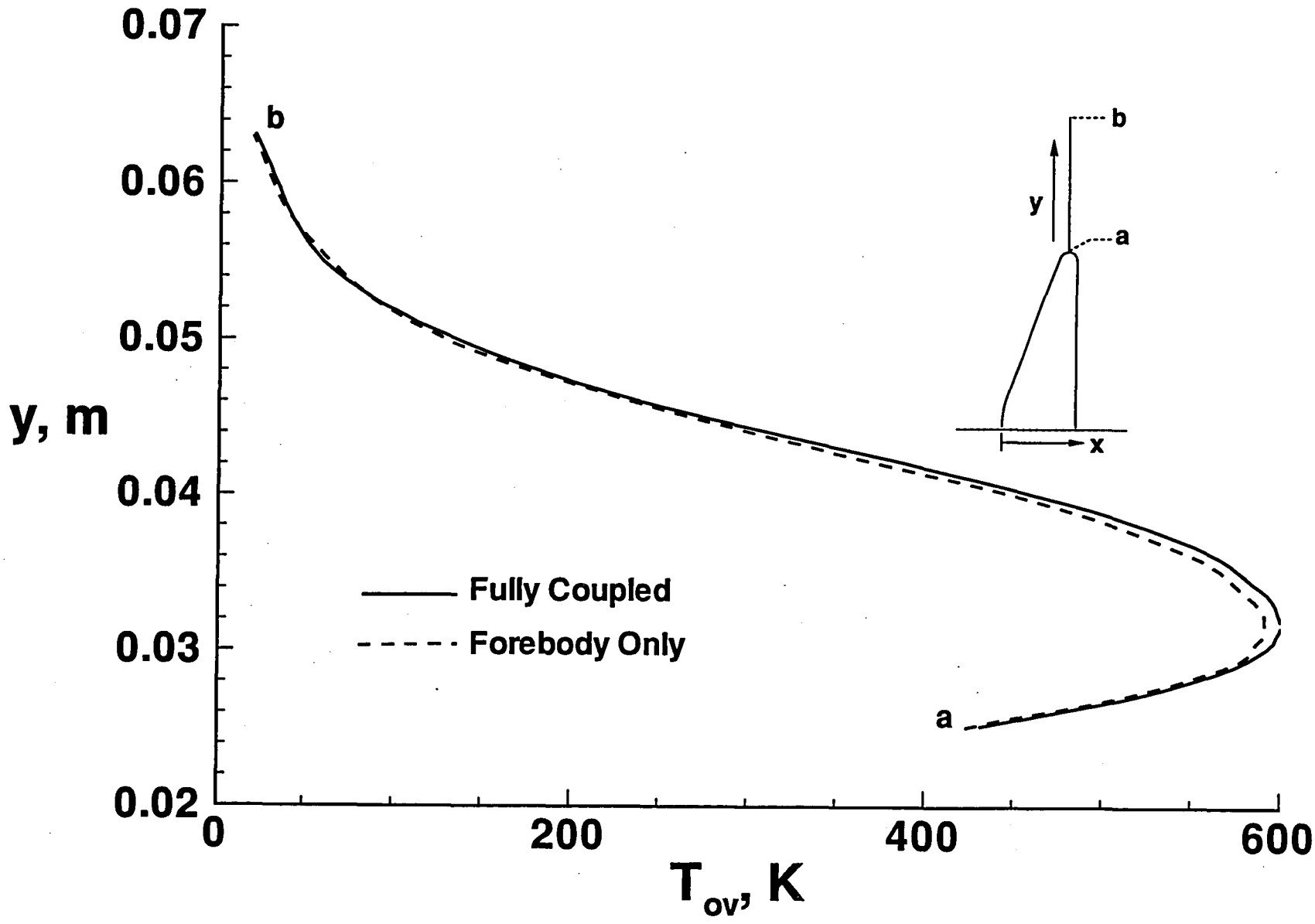

(b) Overall temperature profiles

Fig. 15 Continued.

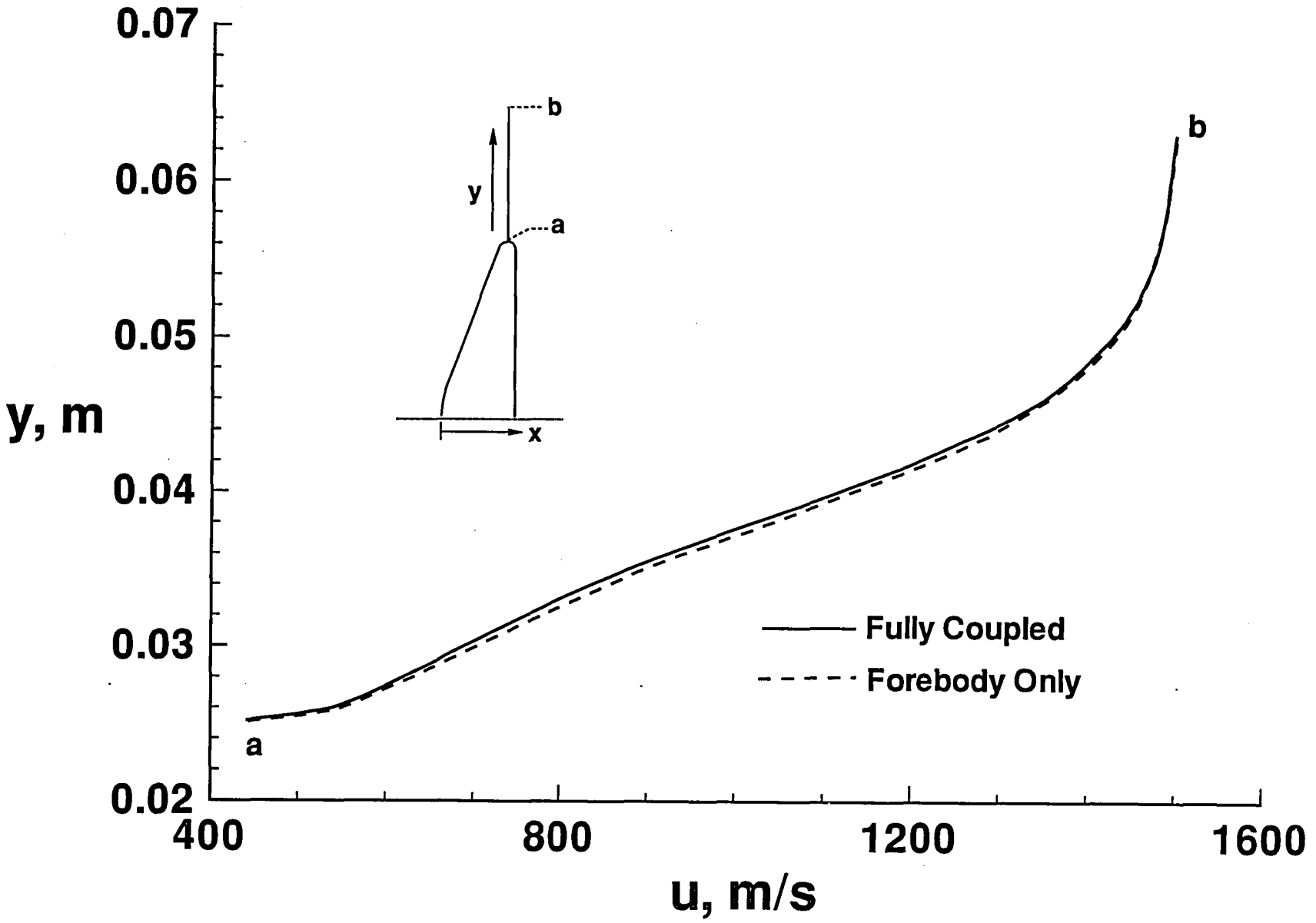

(c) Axial velocity profiles

Fig. 15 Continued.

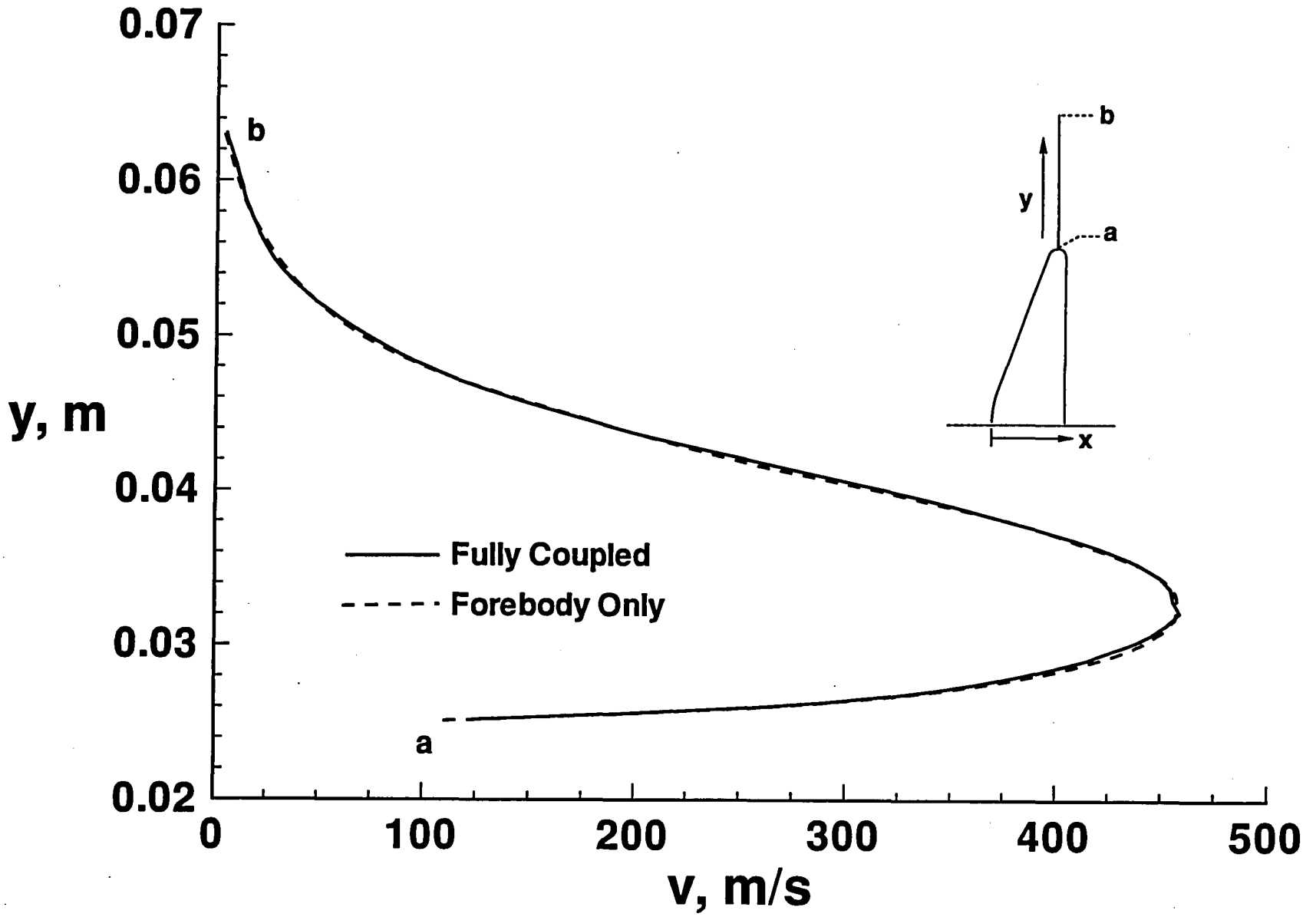

(d) Radial velocity profiles

Fig. 15 Concluded.

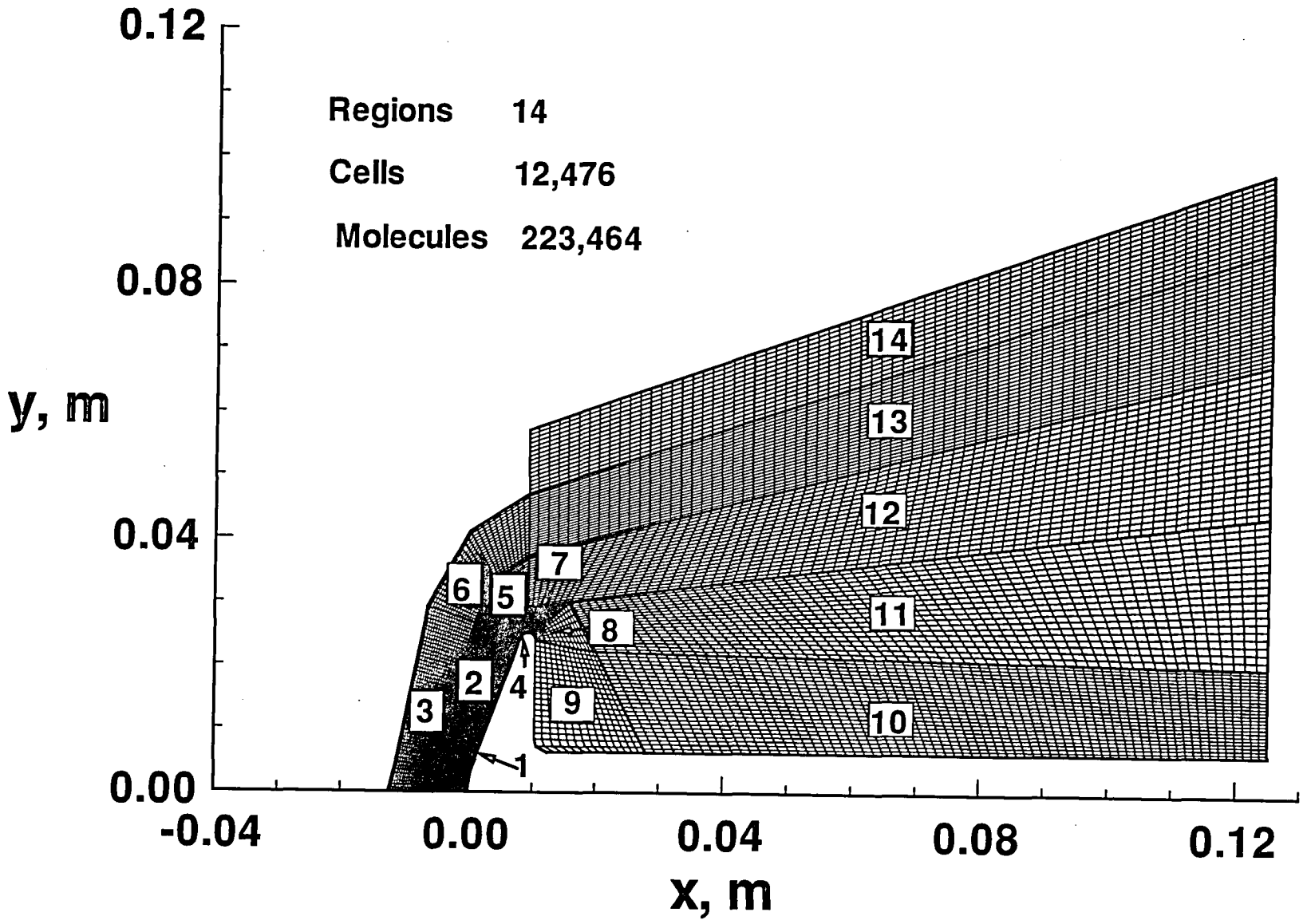

(a) Overall grid

Fig. 16 Computational domain and grid for Case 2.

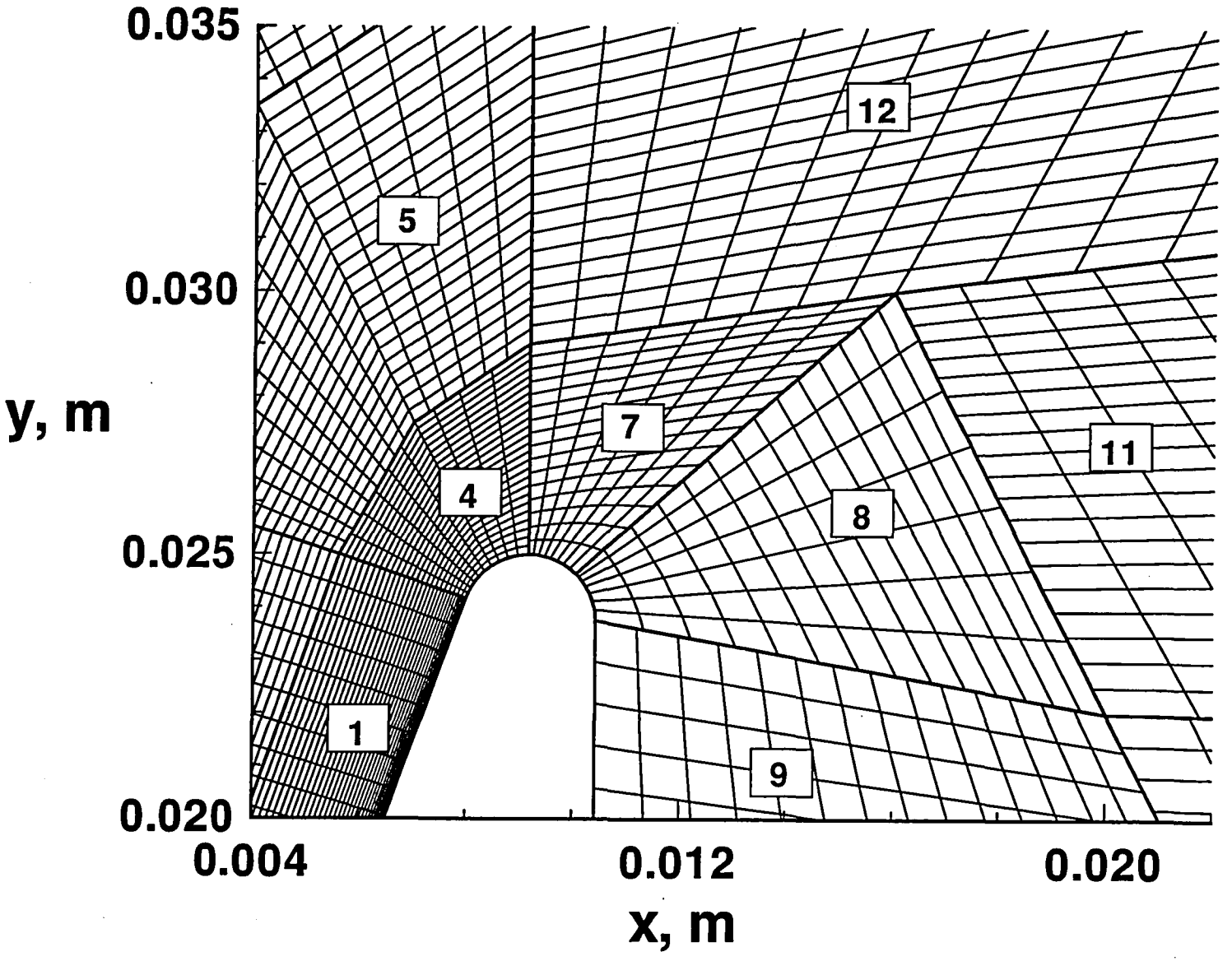

(b) Exploded view of grid for corner expansion.

Fig. 16 Concluded.

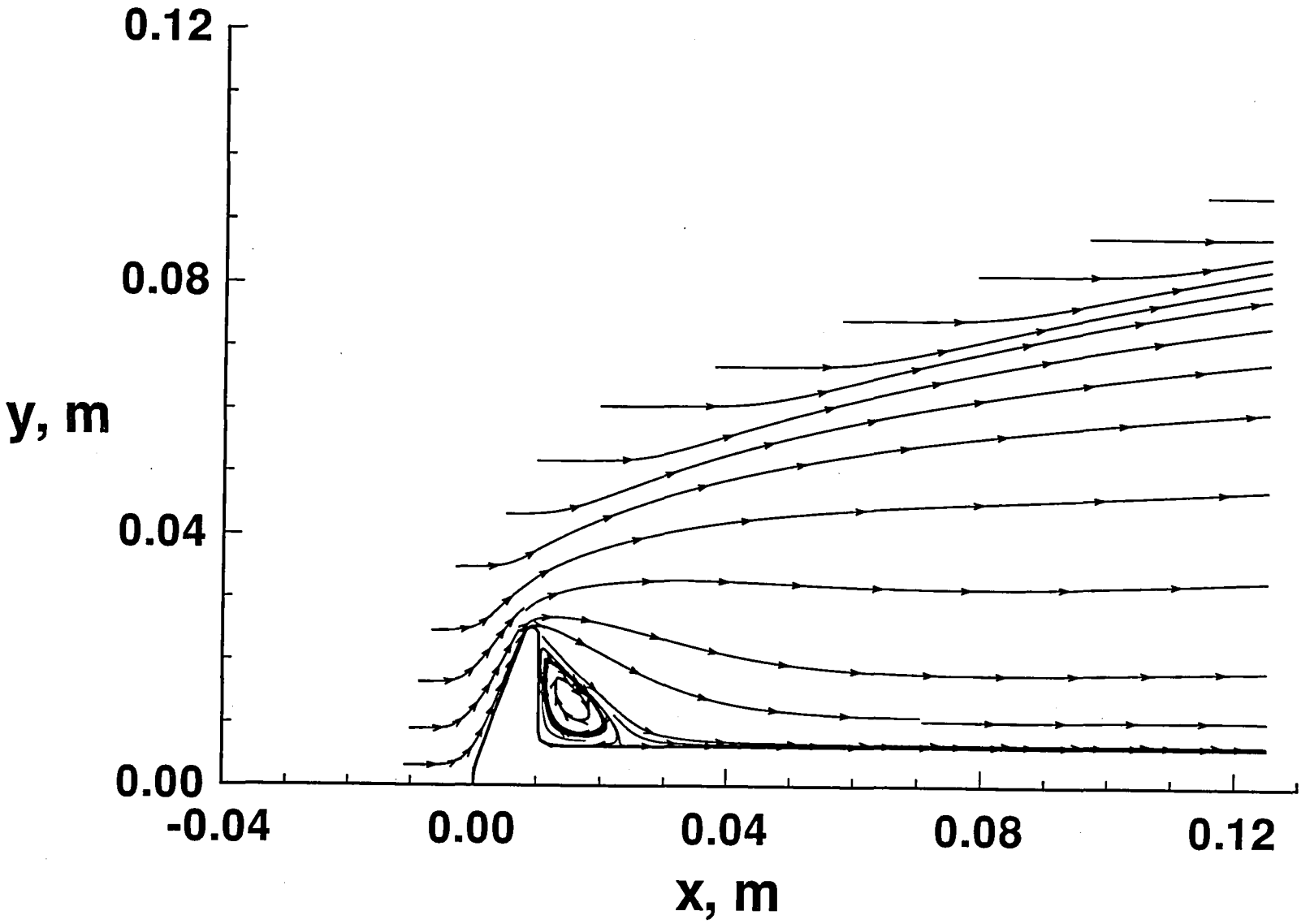

(a) With sting

Fig. 17 Particle traces for Case 2.

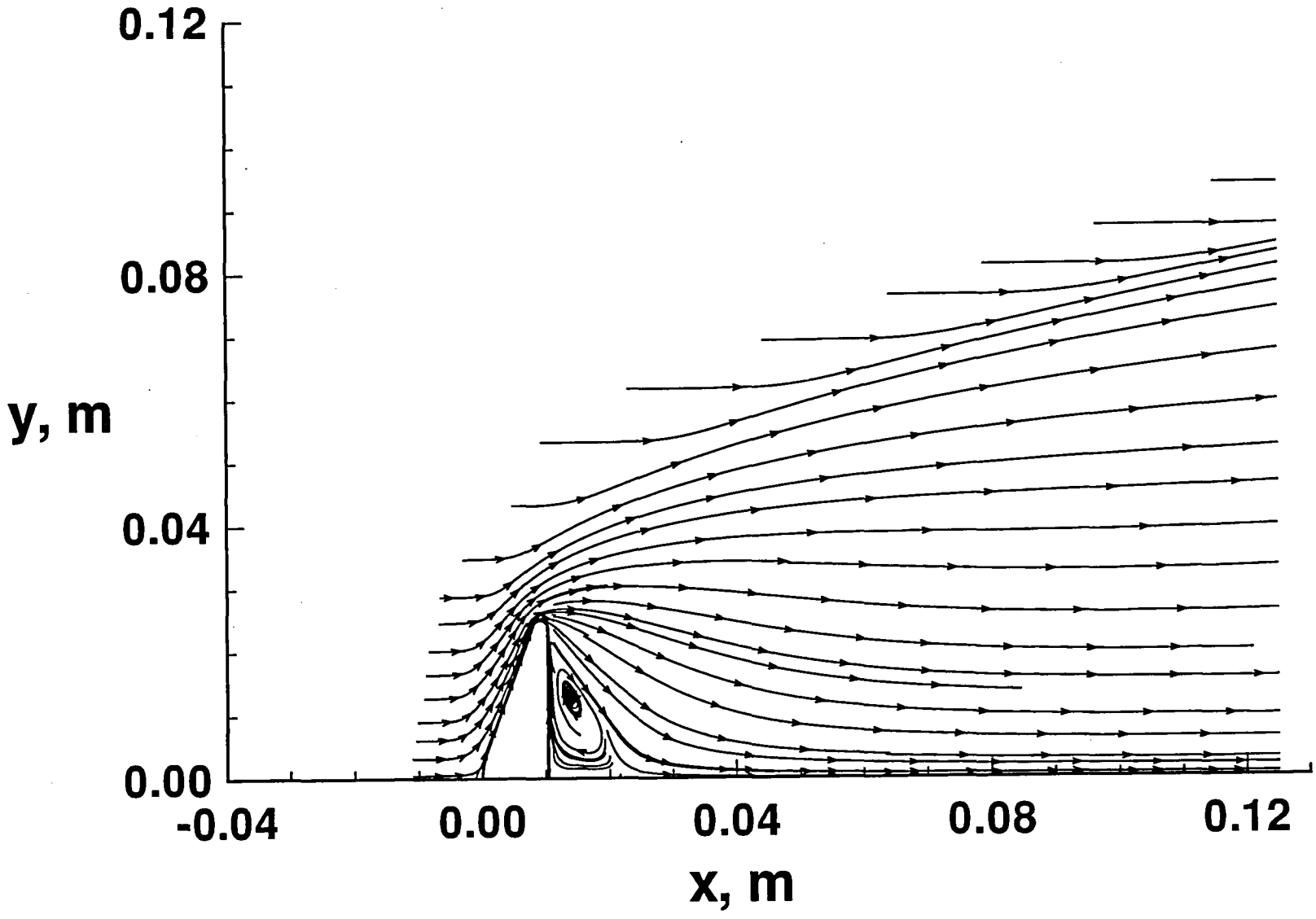

(b) Without sting

Fig. 17 Concluded.

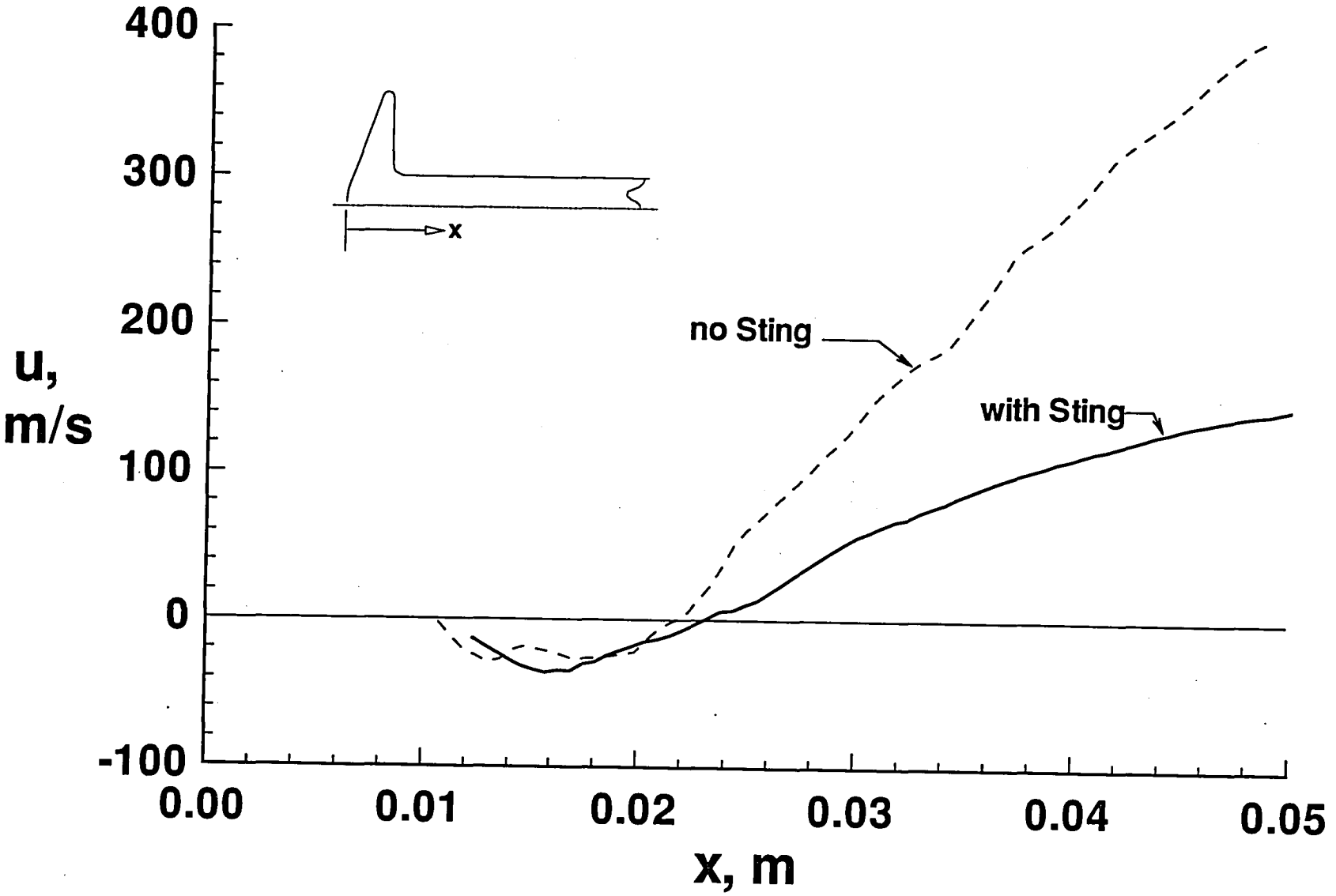

Fig. 18 Axial velocity for Case 2 along symmetry axis (no sting) and in cells adjacent to surface (with sting).

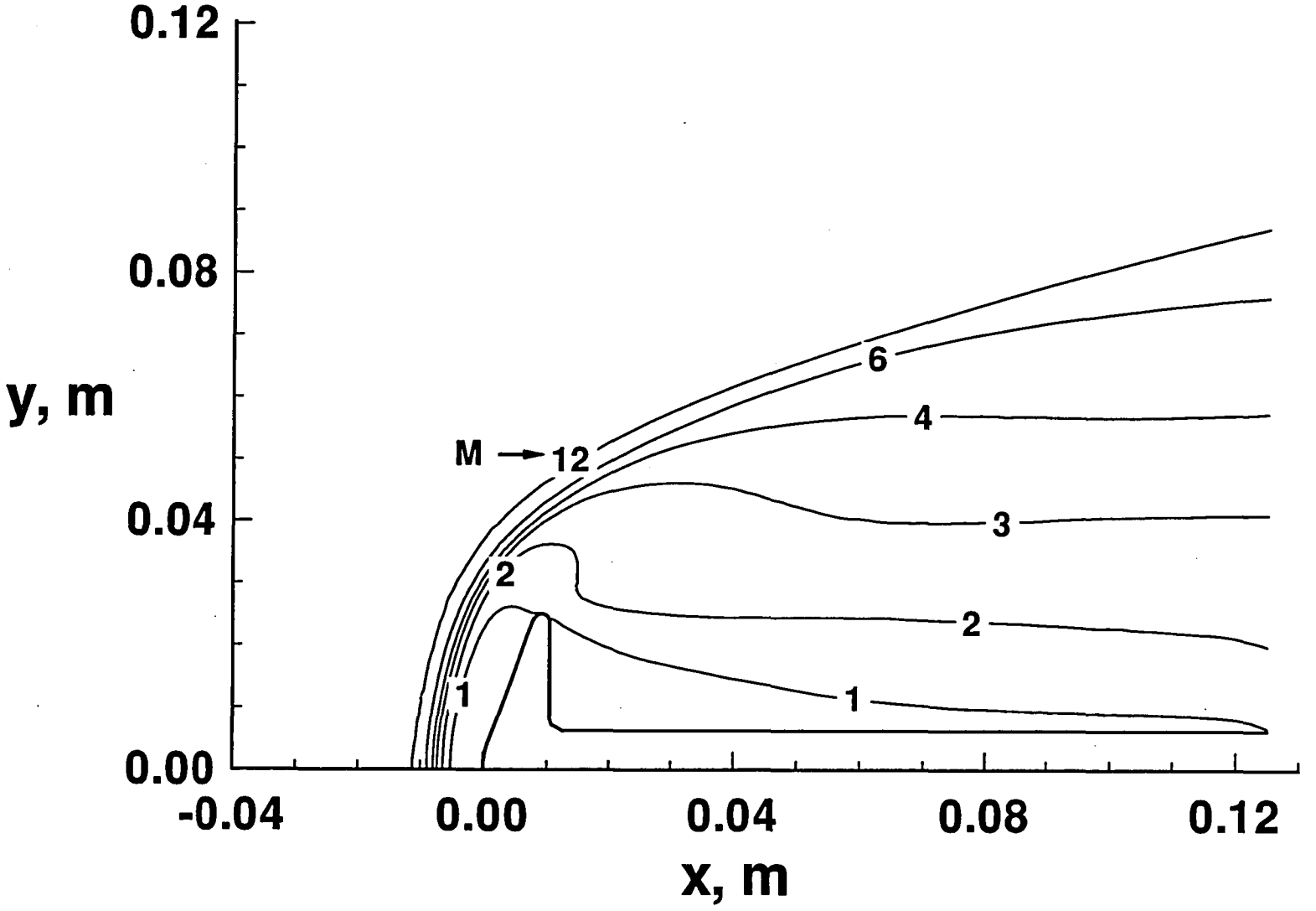

Fig. 19 Mach contours for Case 2.

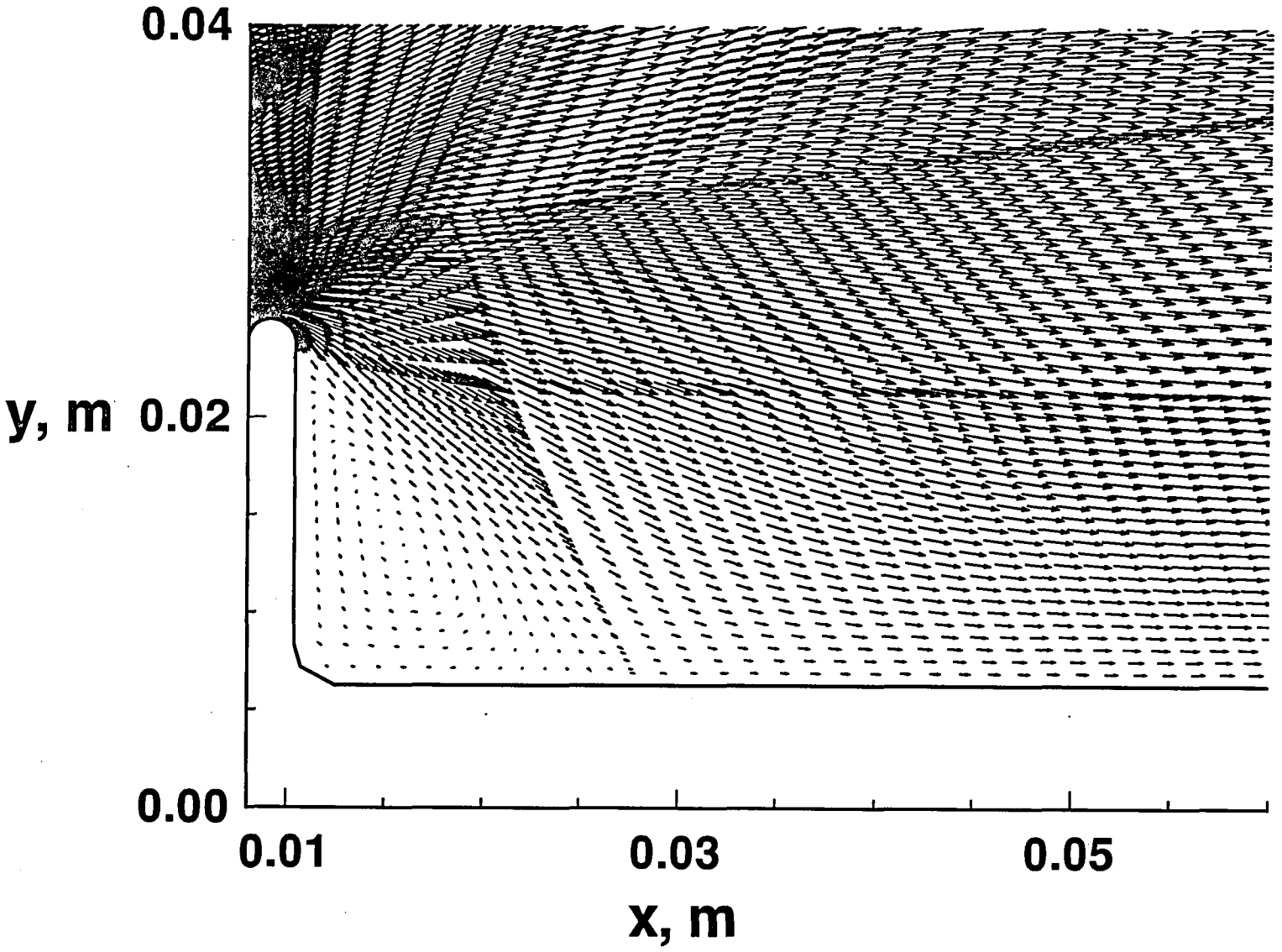

Fig. 20 Velocity vectors in near wake region

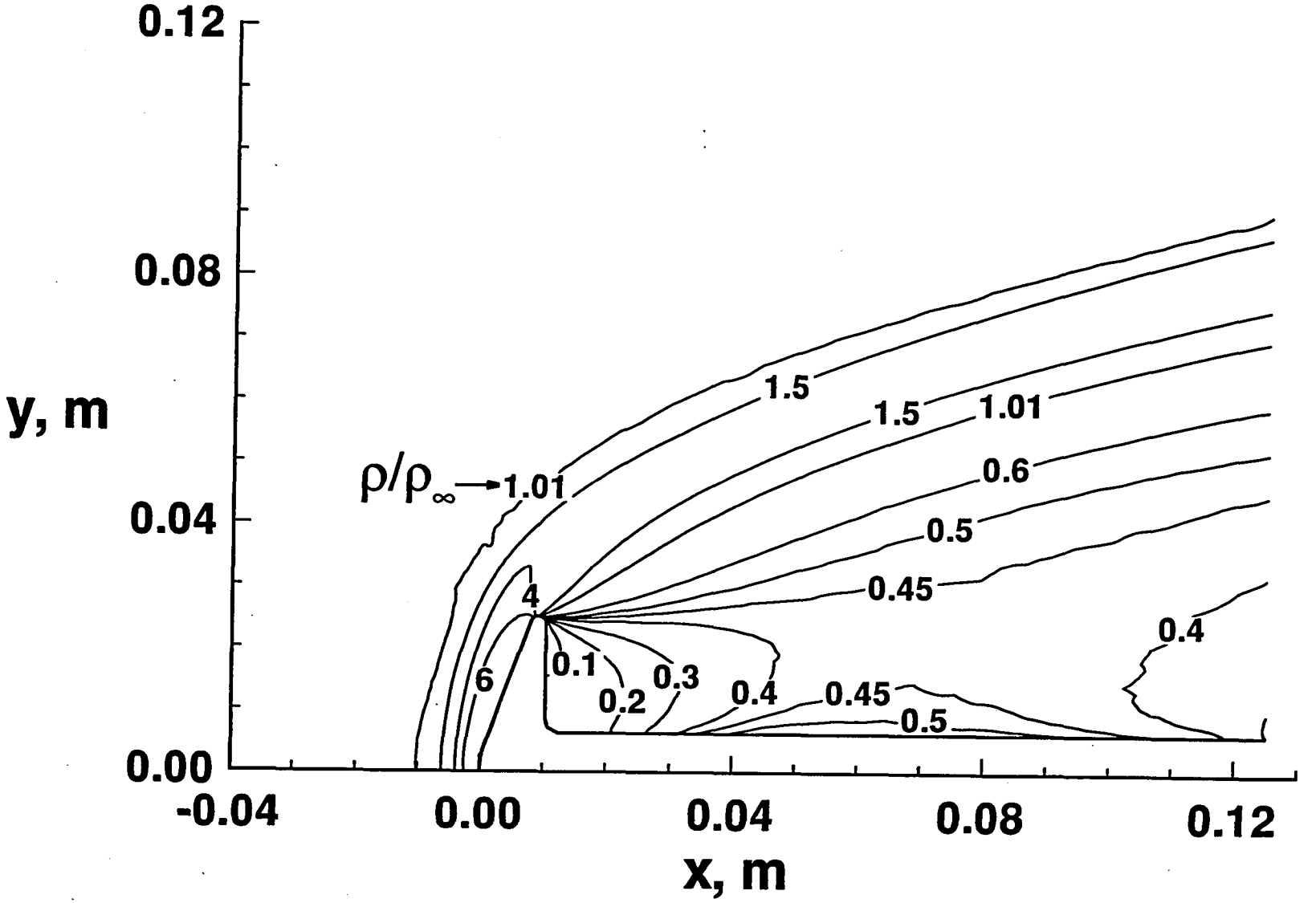

(a) Overall view

Fig. 21 Nondimensional density contours for Case 2 ($\rho_\infty = 5.192 \times 10^{-5}$ kg/m^3).

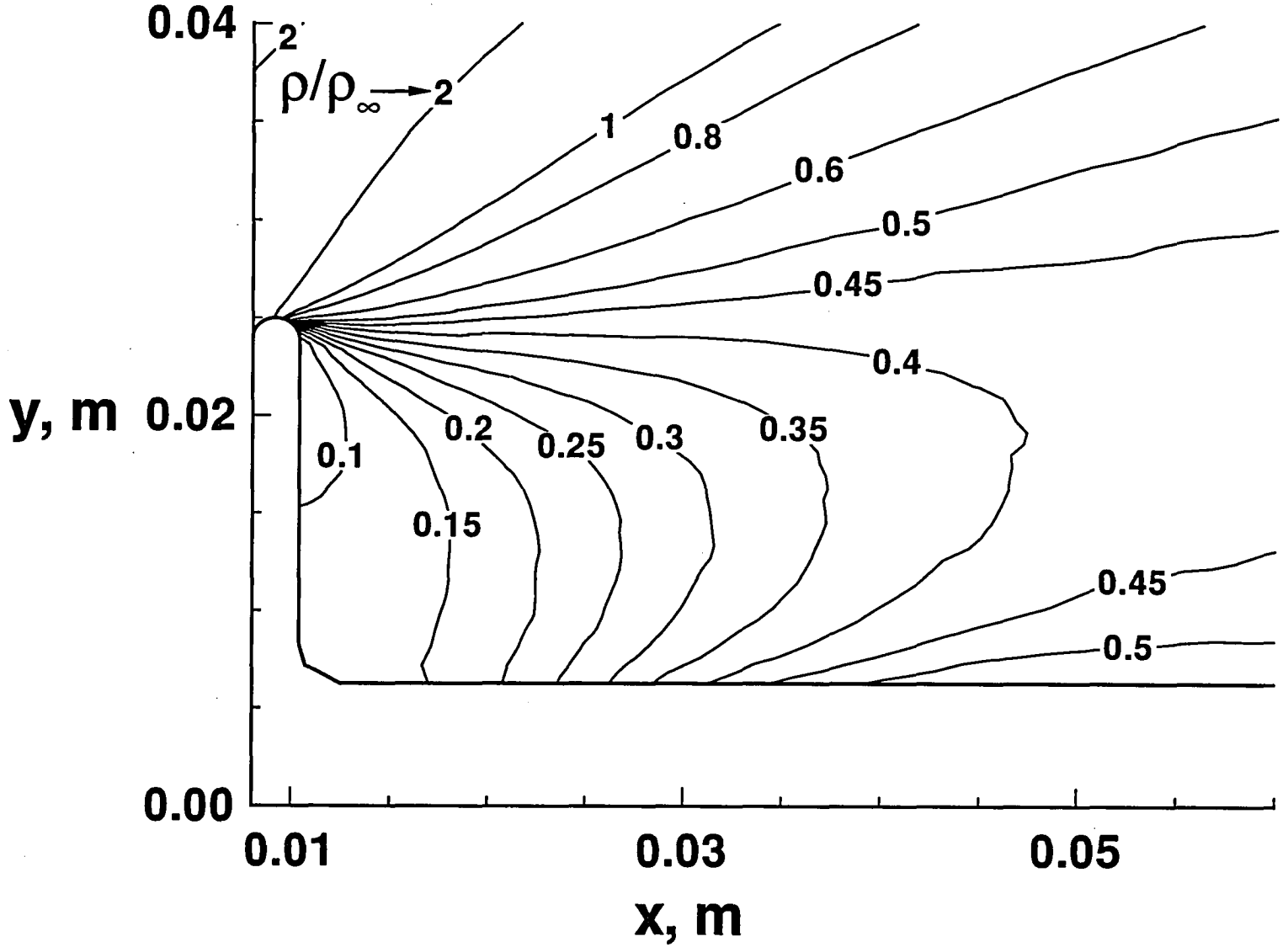

(b) Near wake region

Fig. 21 Concluded.

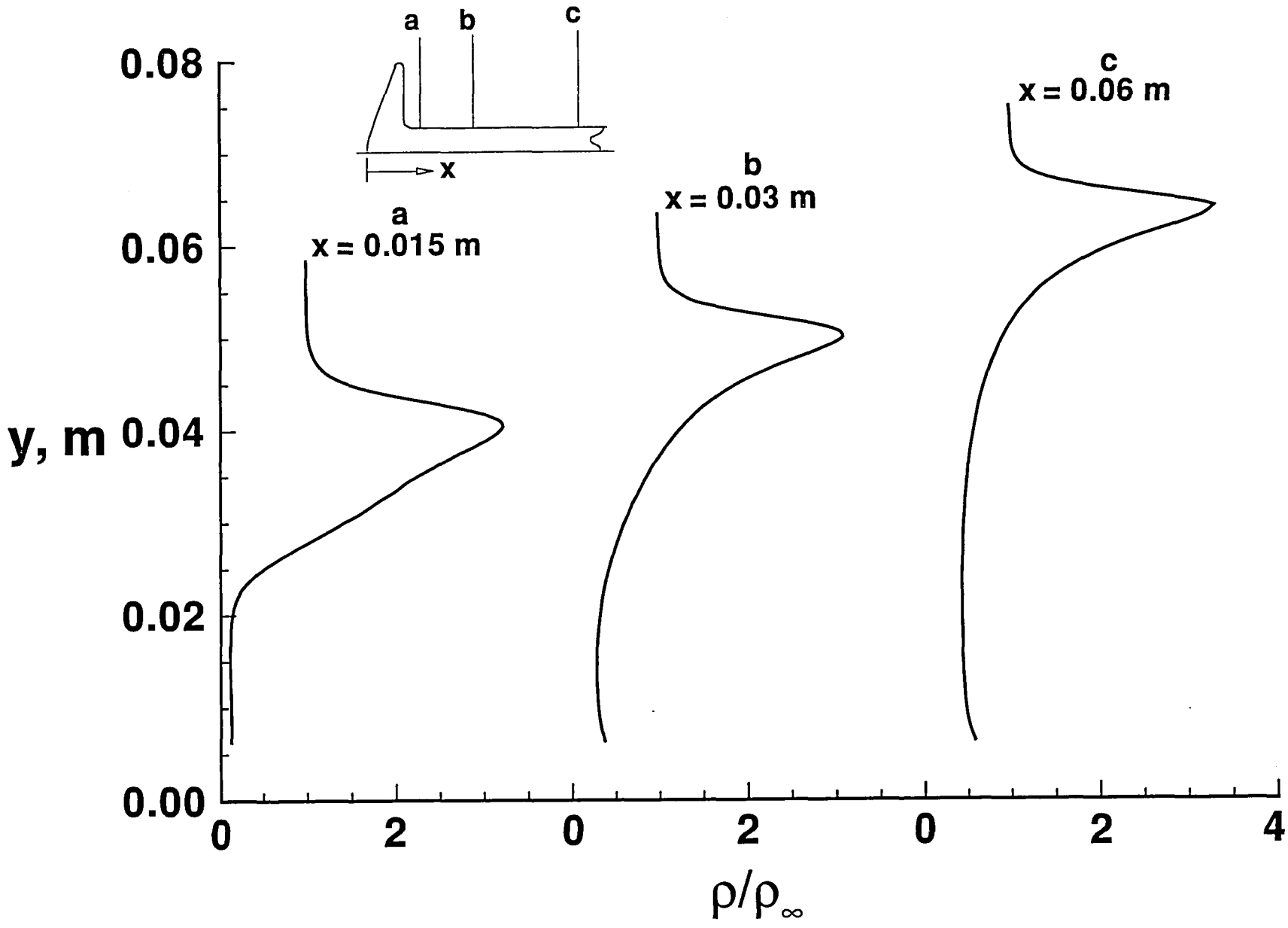

Fig. 22 Wake density profiles for Case 2 (base plane is located at x = 0.0104m).

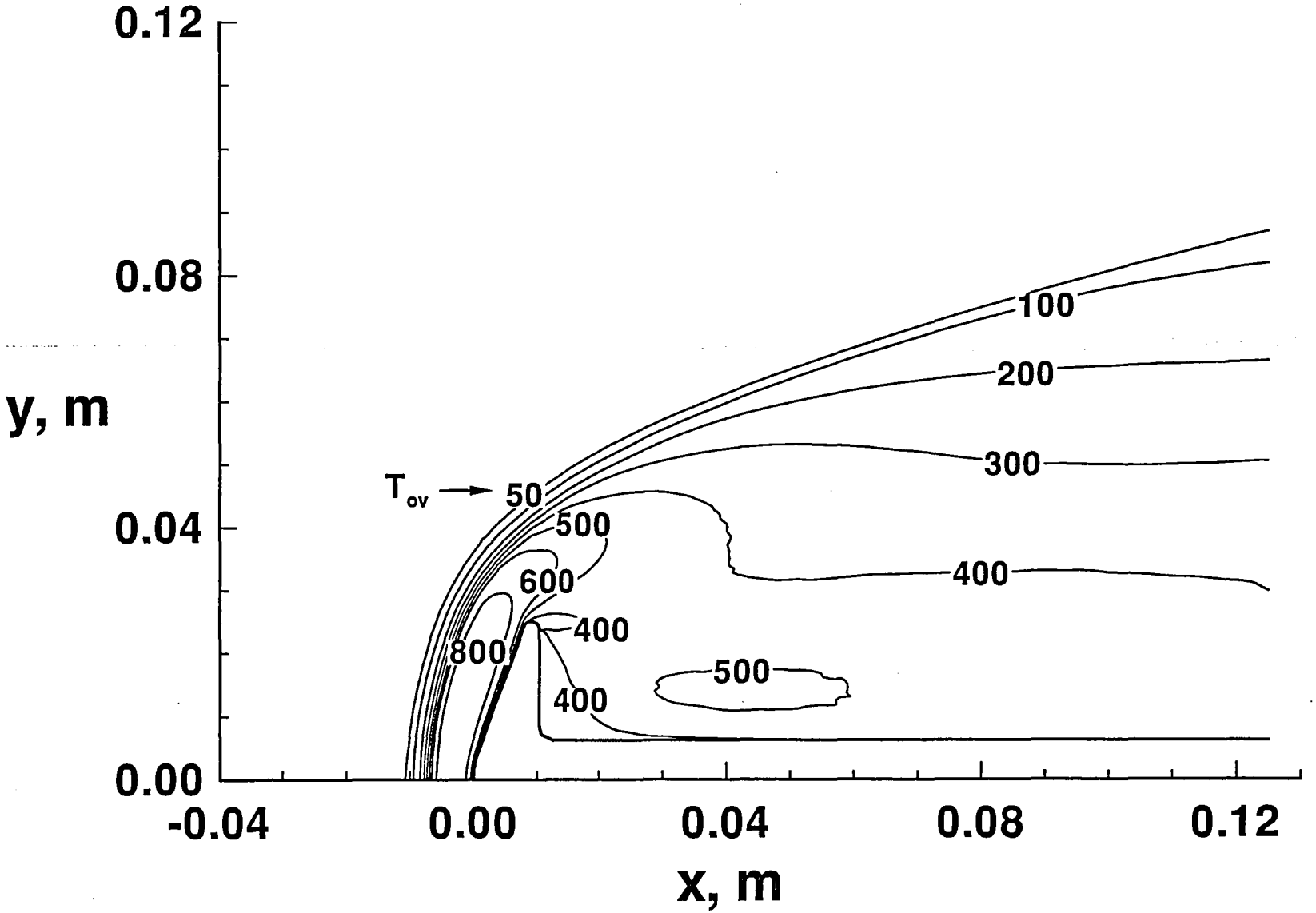

(a) Overall kinetic temperature

Fig. 23 Temperature contours for Case 2.

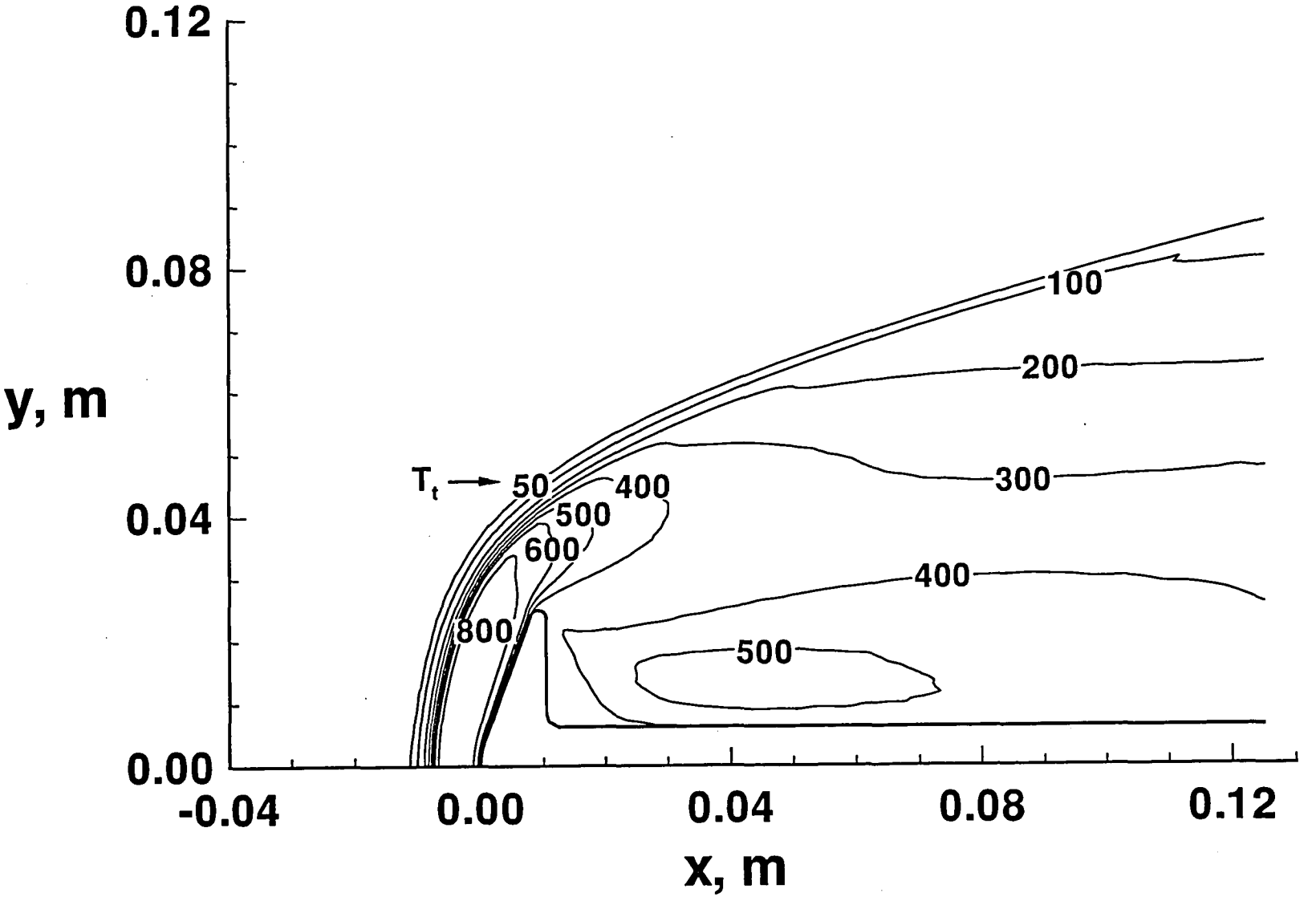

(b) Translational temperature

Fig. 23 Continued.

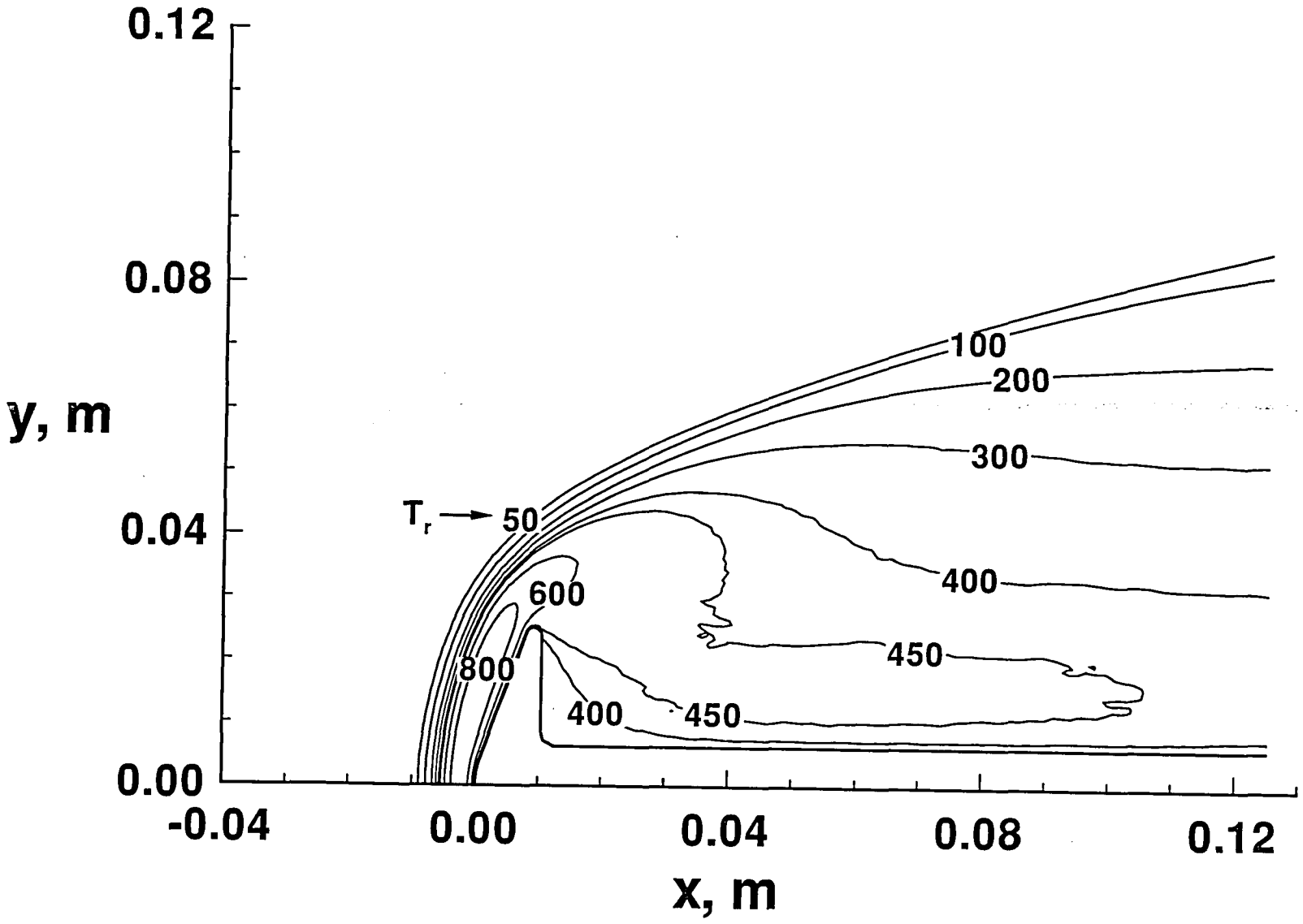

(c) Rotational temperature

Fig. 23 Concluded.

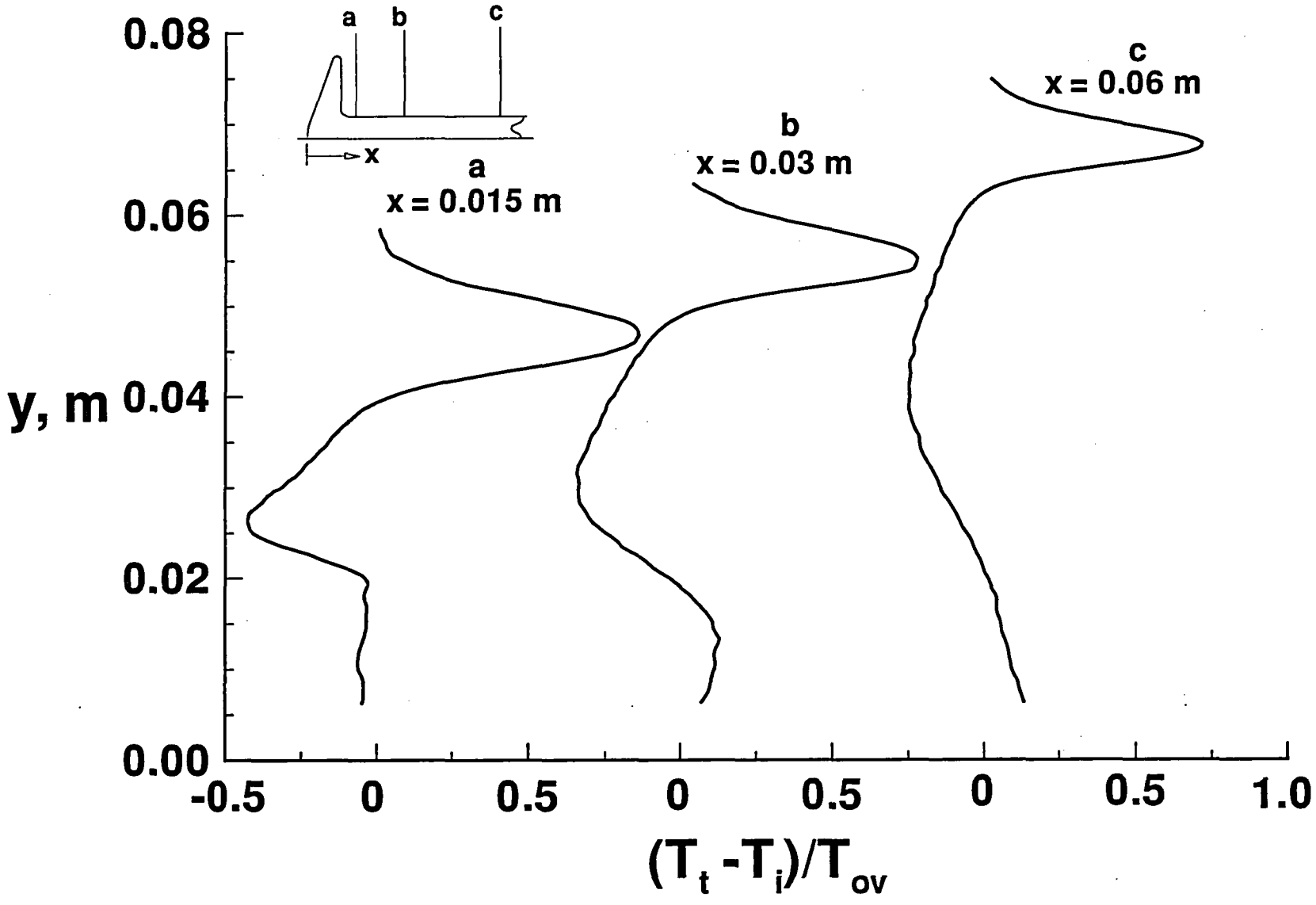

(a) Extent of thermal nonequilibrium

Fig. 24 Wake profiles for Case 2.

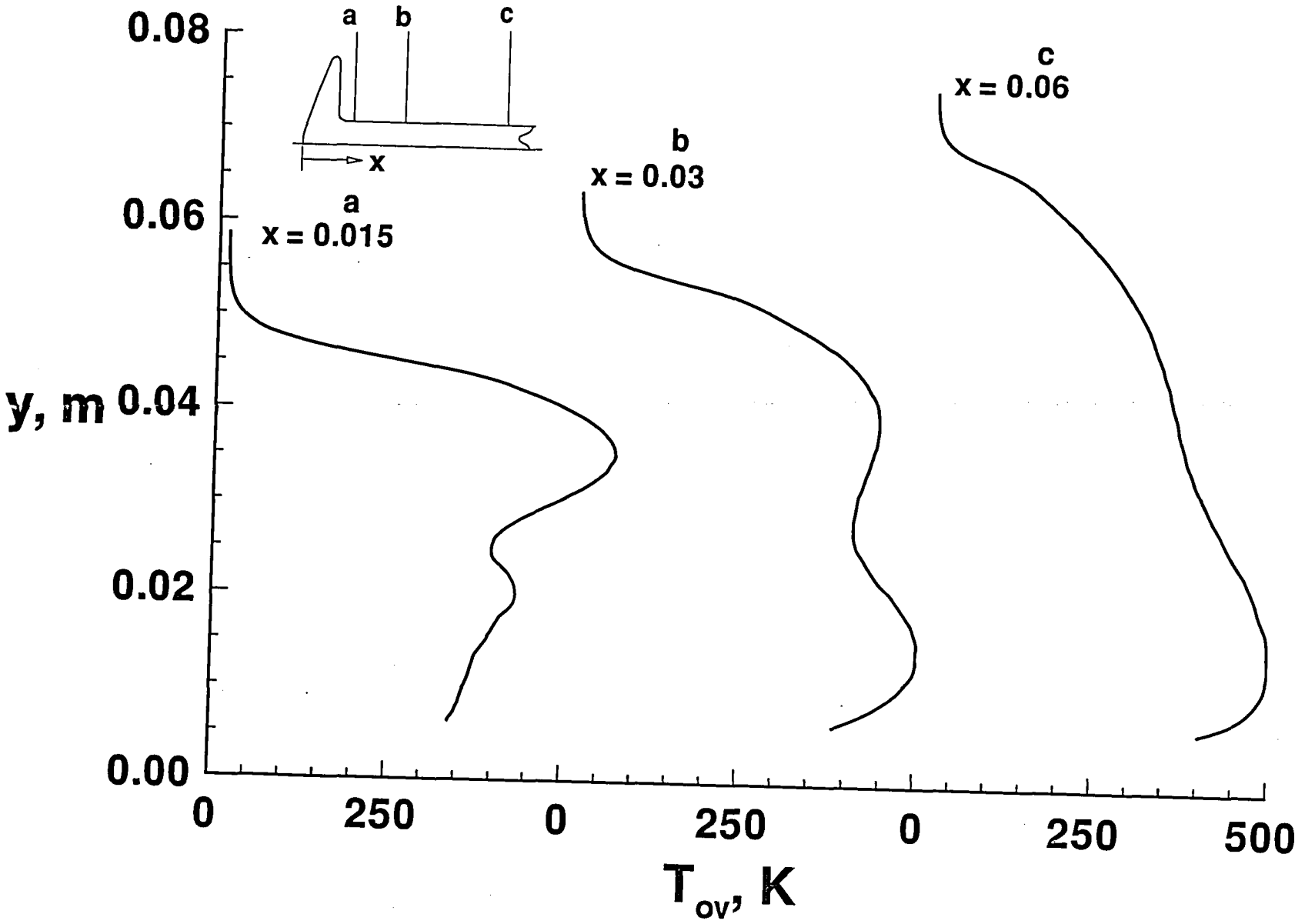

(b) Overall kinetic temperature

Fig. 24 Continued.

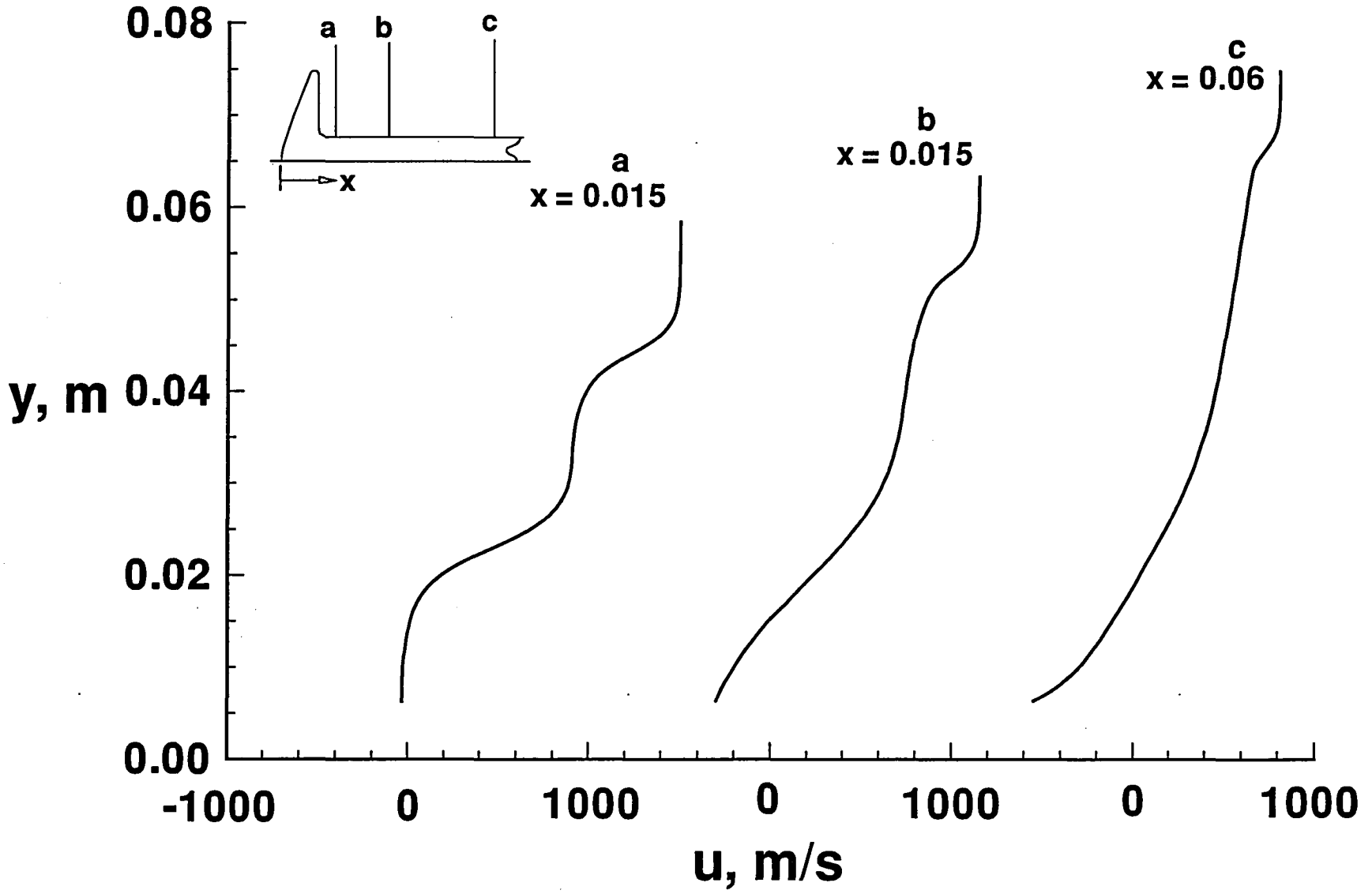

(c) Axial velocity

Fig. 24 Concluded.

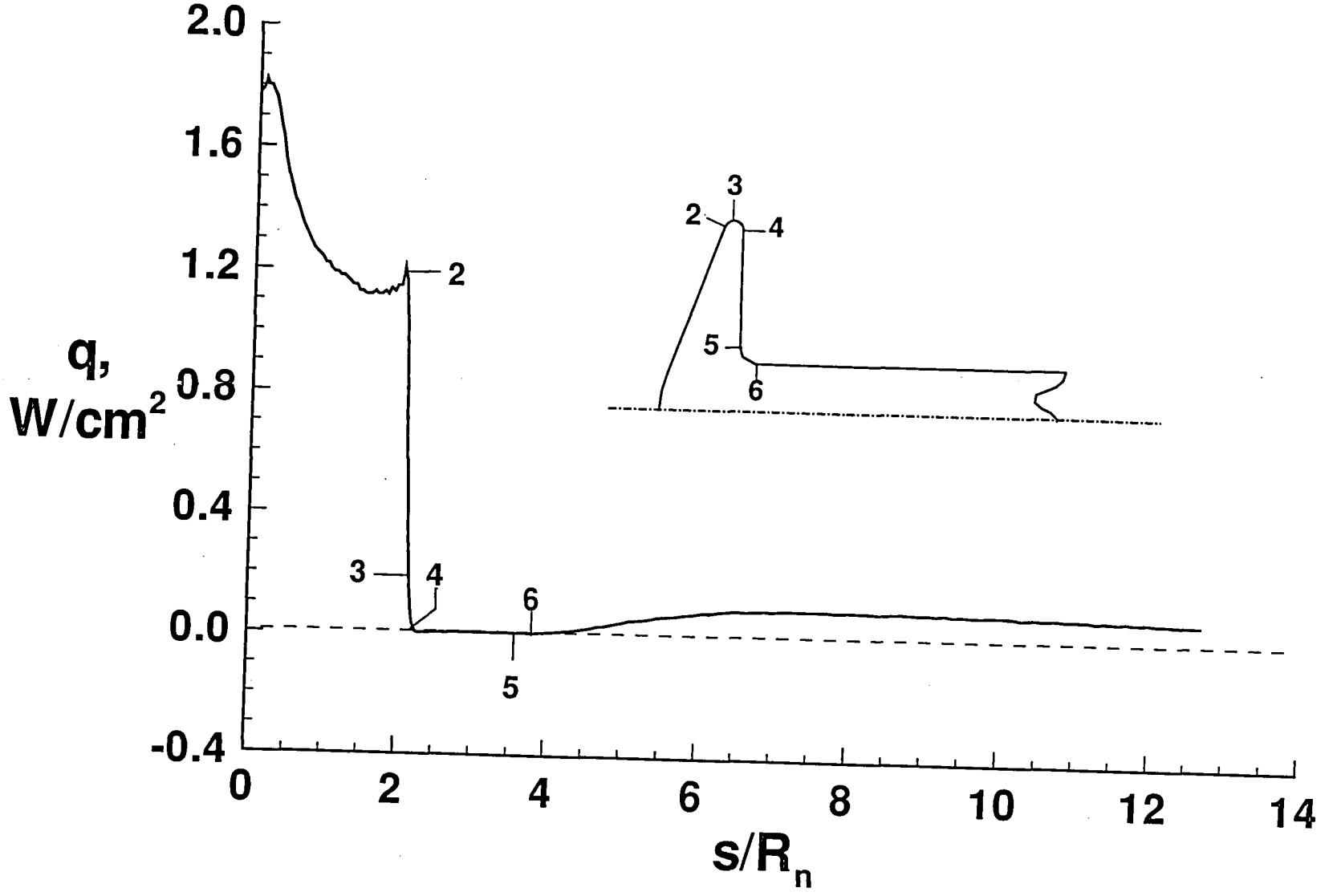

(a) Cartesian plot

Fig. 25 Surface heating rate distribution for Case 2.

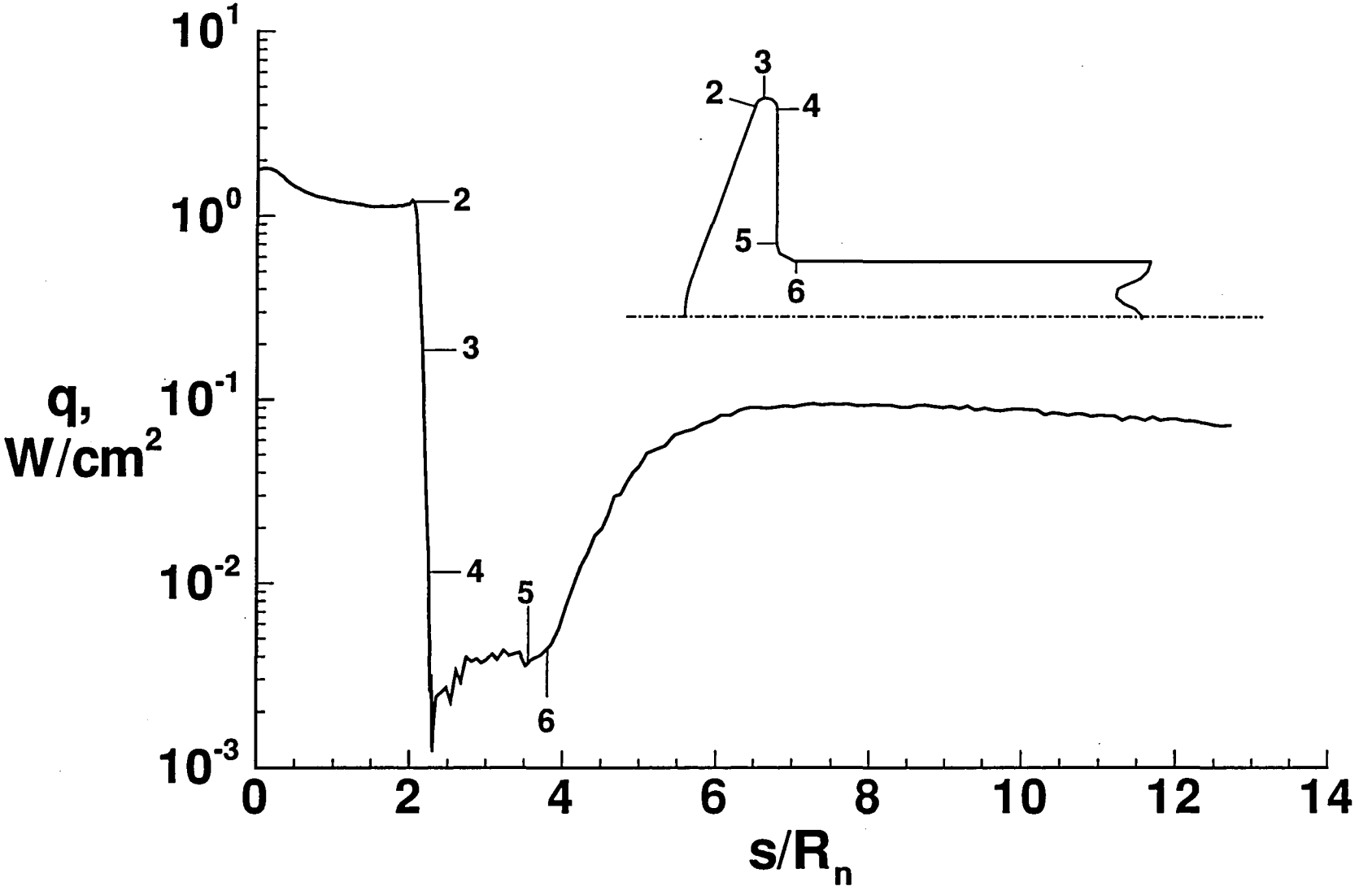

(b) Semilog plot

Fig. 25 Concluded.

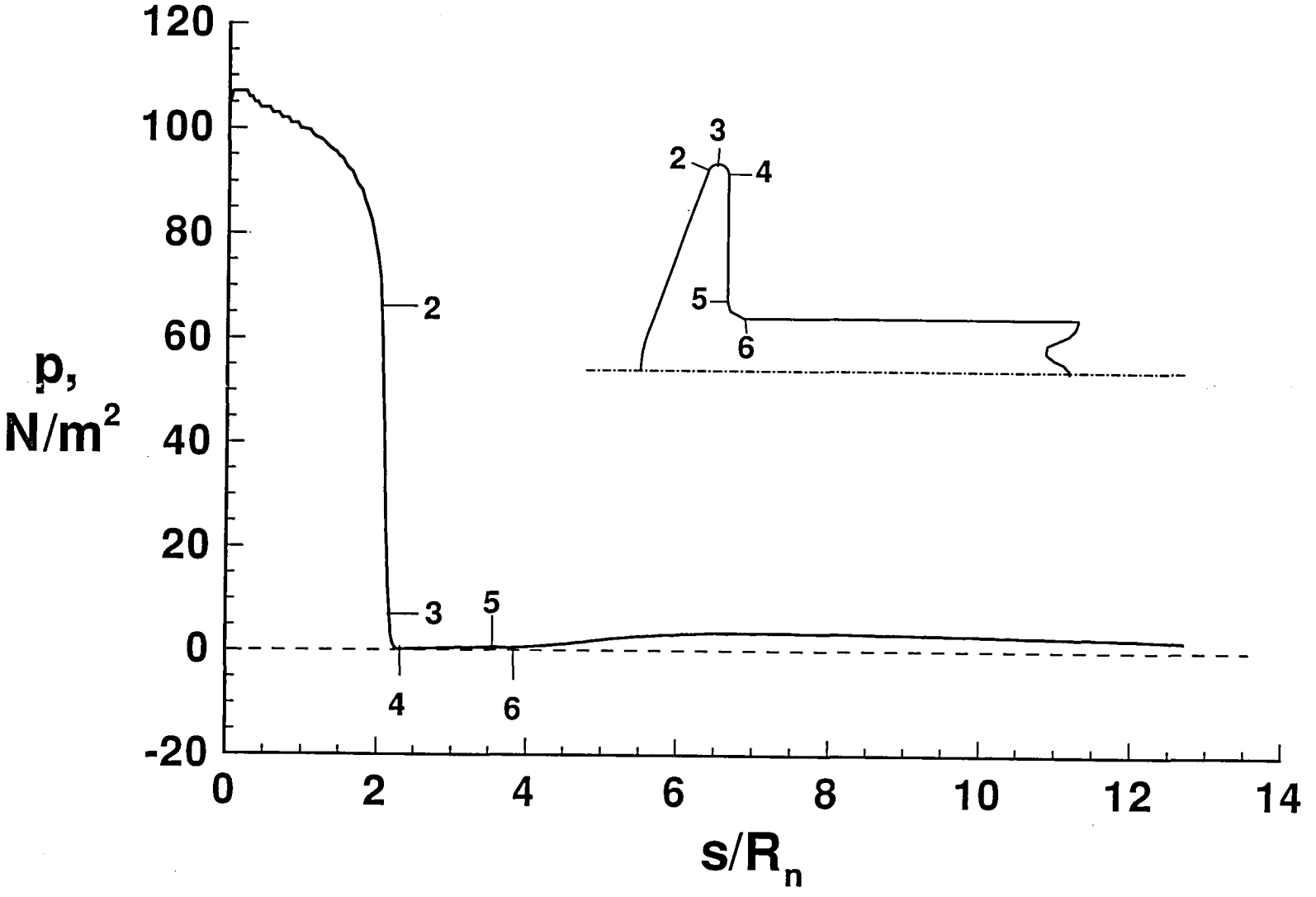

(a) Cartesian plot

Fig. 26 Surface pressure distribution for Case 2

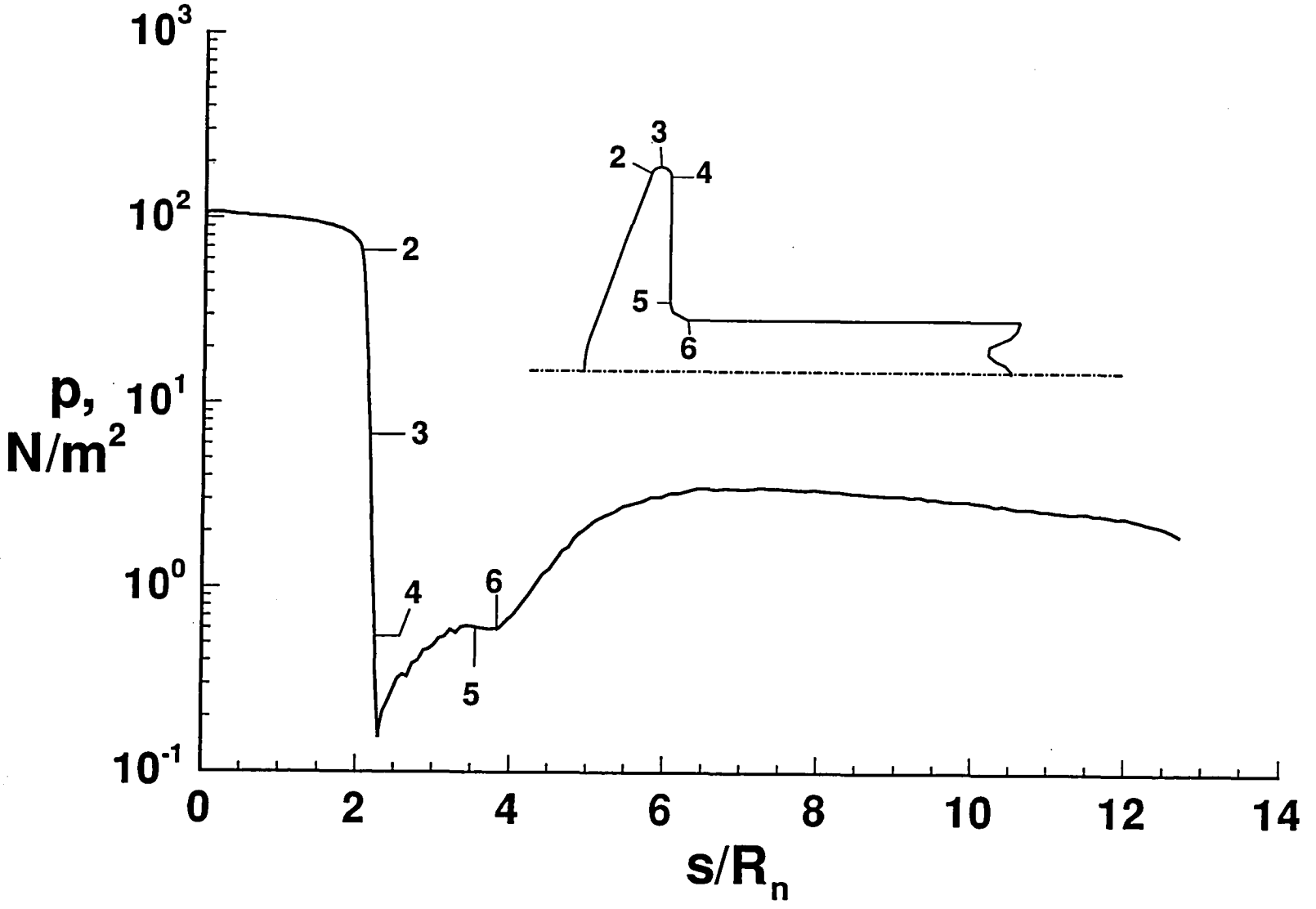

(b) Semilog plot

Fig. 26 Concluded.

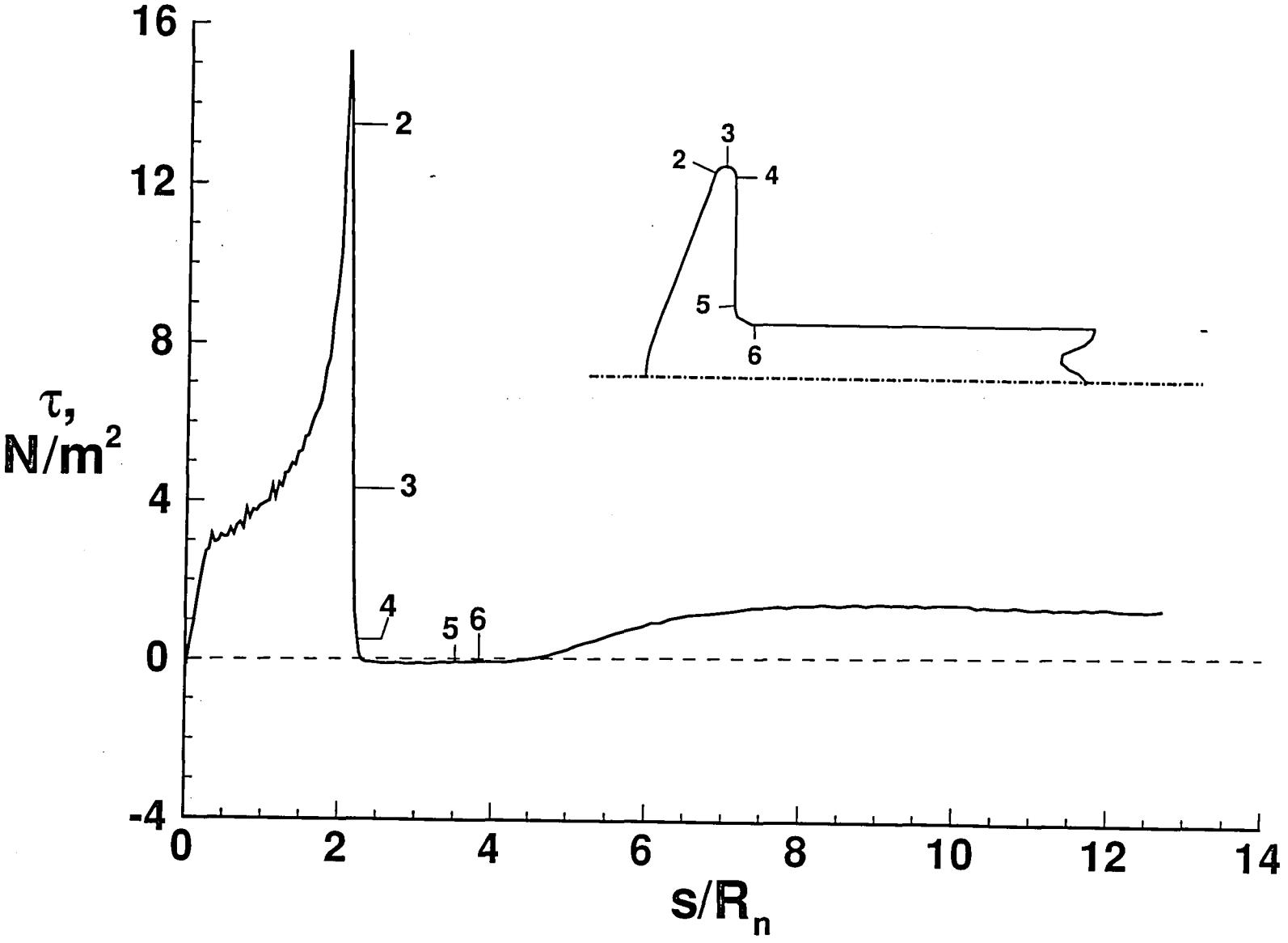

Fig. 27 Skin friction distribution for Case 2.

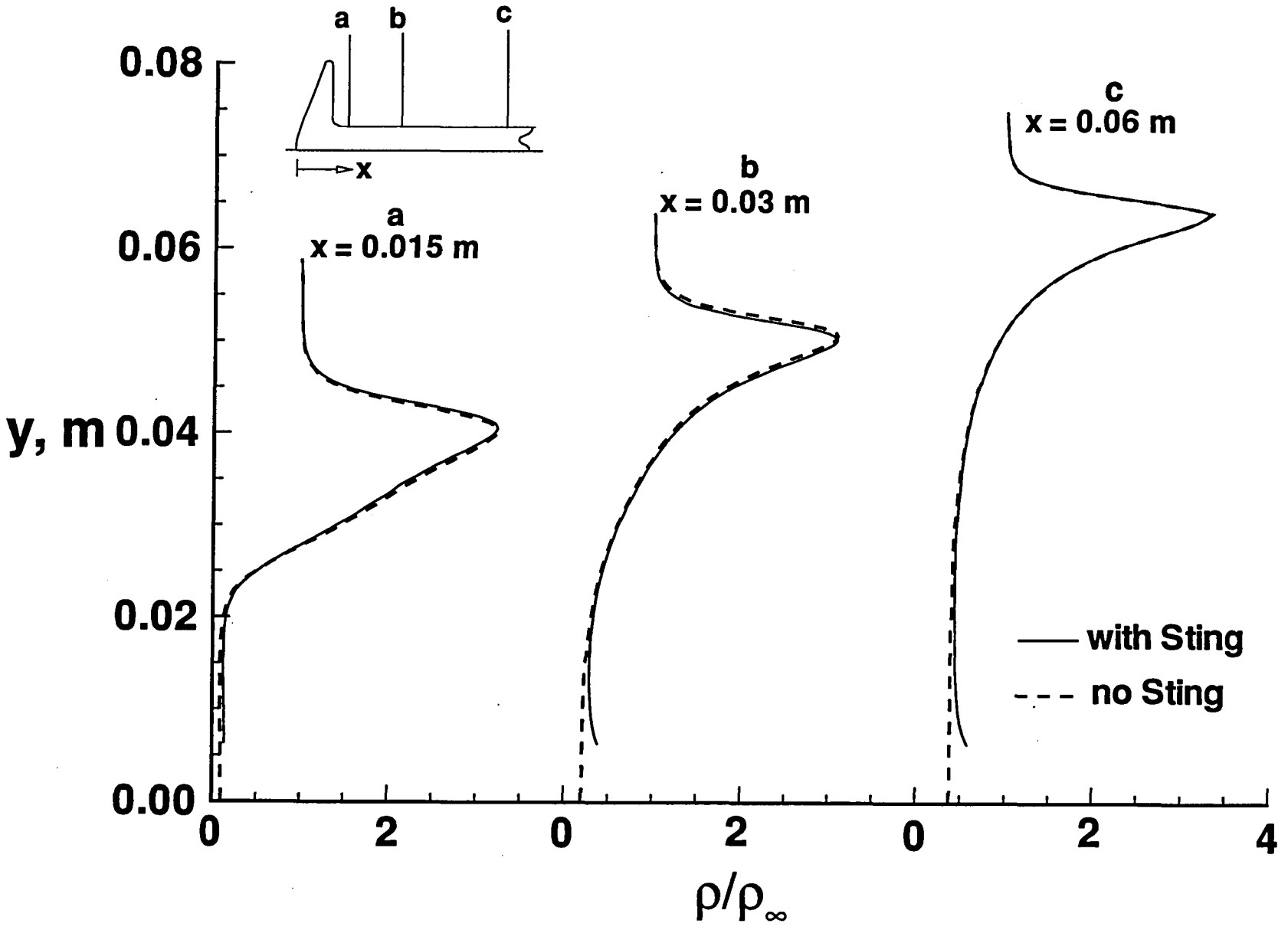

(a) Wake density profiles

Fig. 28 Effect of afterbody sting on wake results for Case 2.

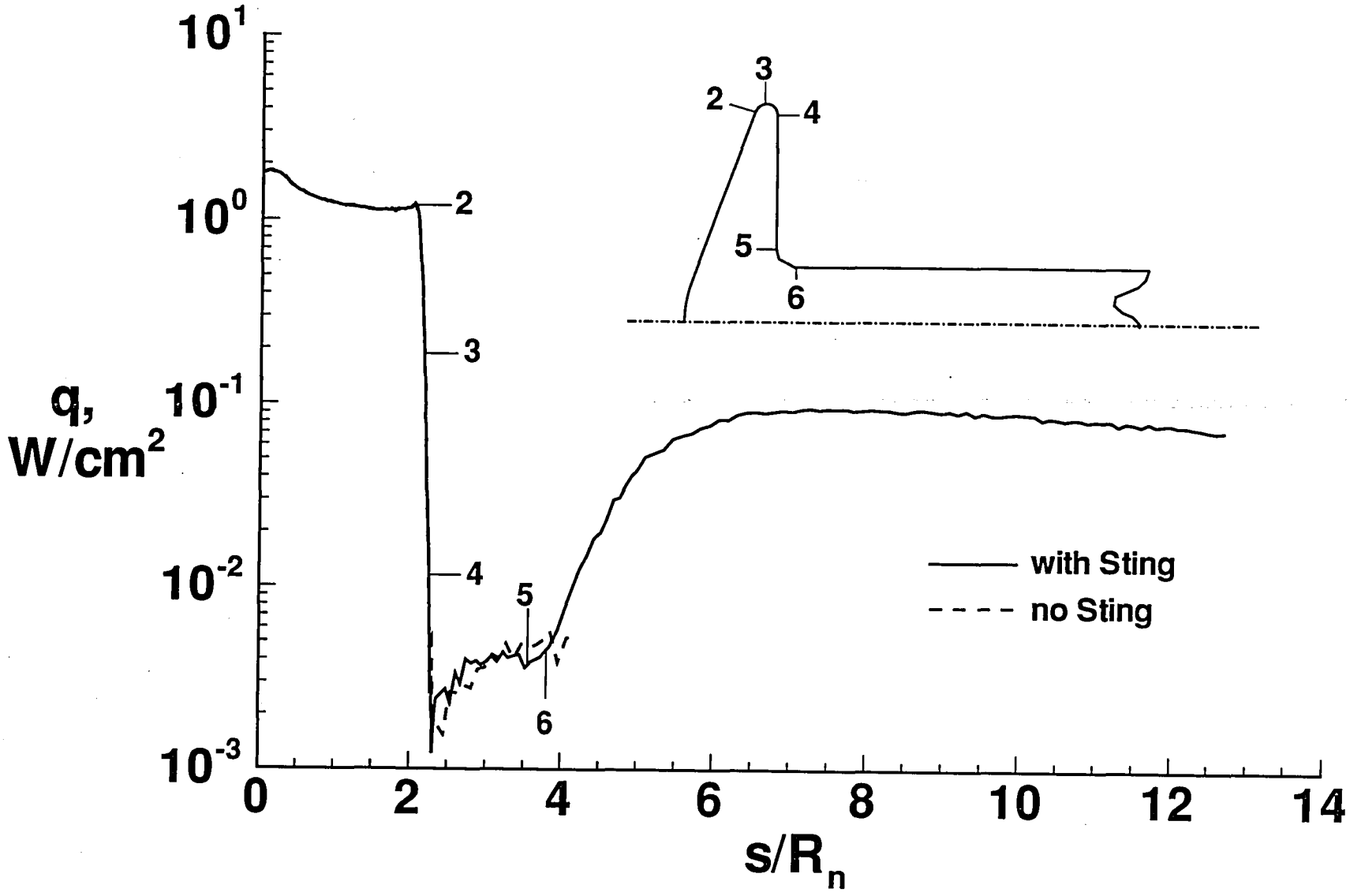

(b) Surface heating rate distribution

Fig. 28 Concluded.

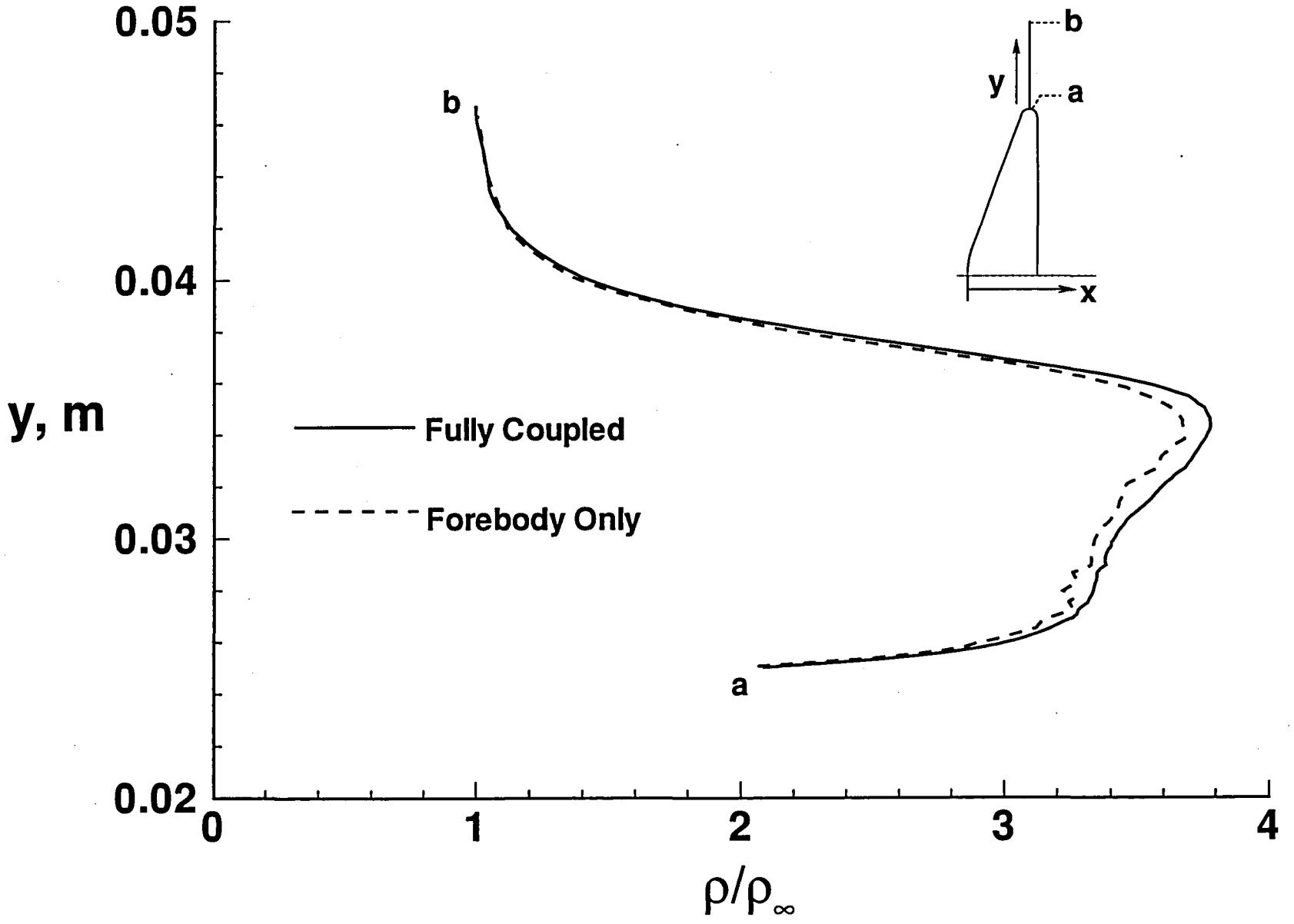

(a) Density profiles

Fig. 29 Effect of wake on forebody results for Case 2.

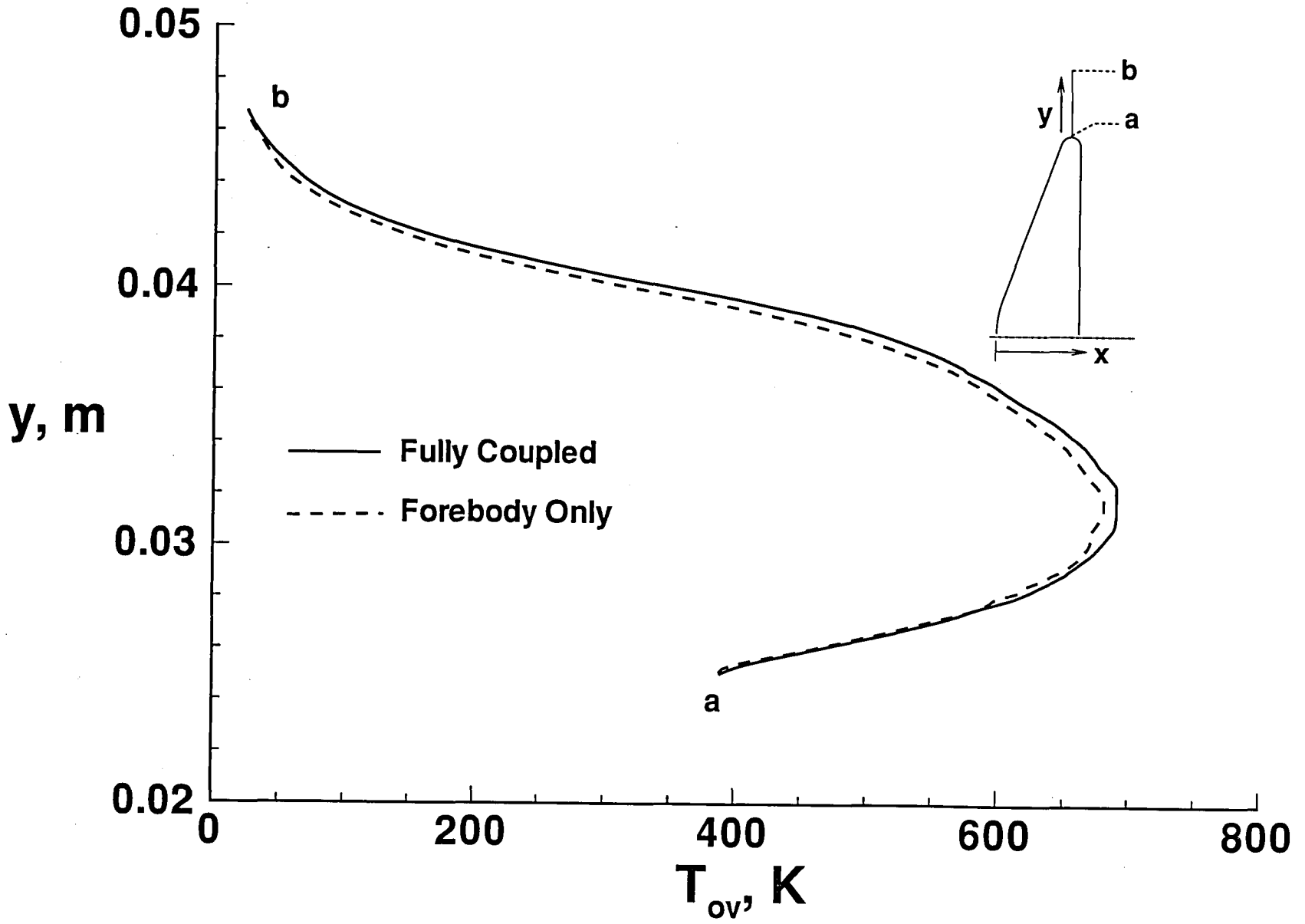

(b) Overall temperature profiles

Fig. 29 Continued.

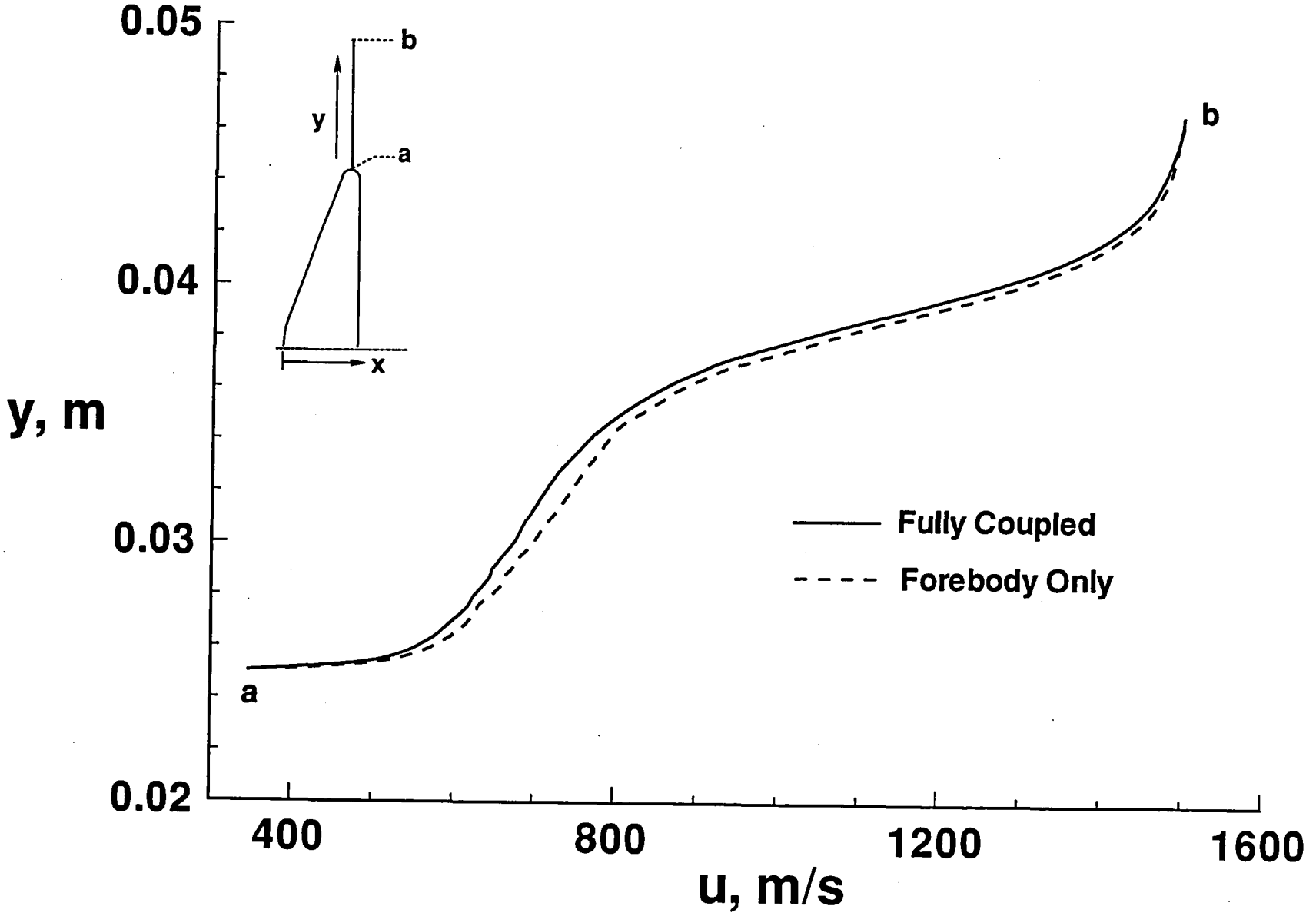

(c) Axial velocity profiles

Fig. 29 Continued.

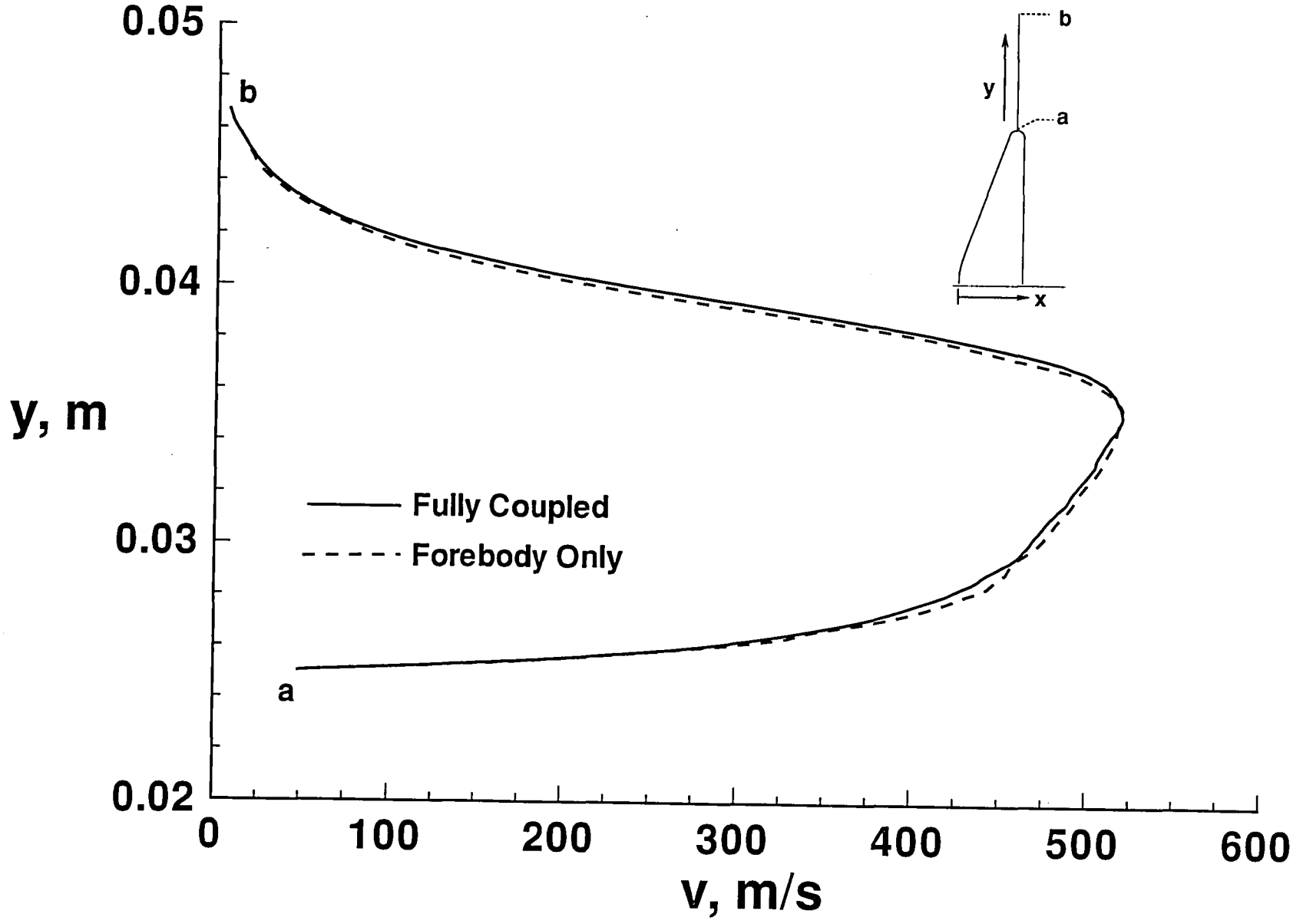

(d) Radial velocity profiles

Fig. 29 Concluded.

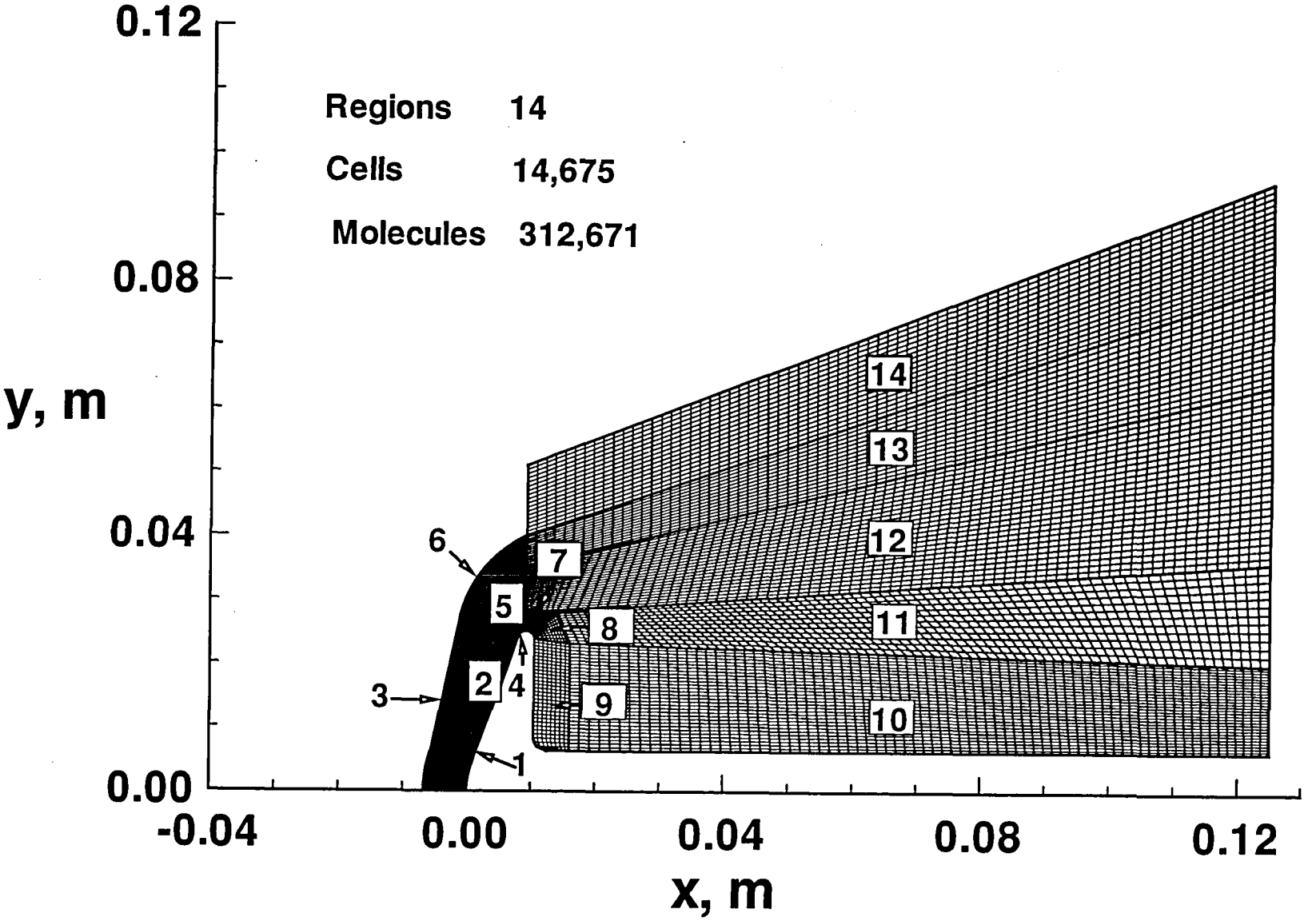

(a) Overall grid

Fig. 30 Computational domain and grid for Case 3.

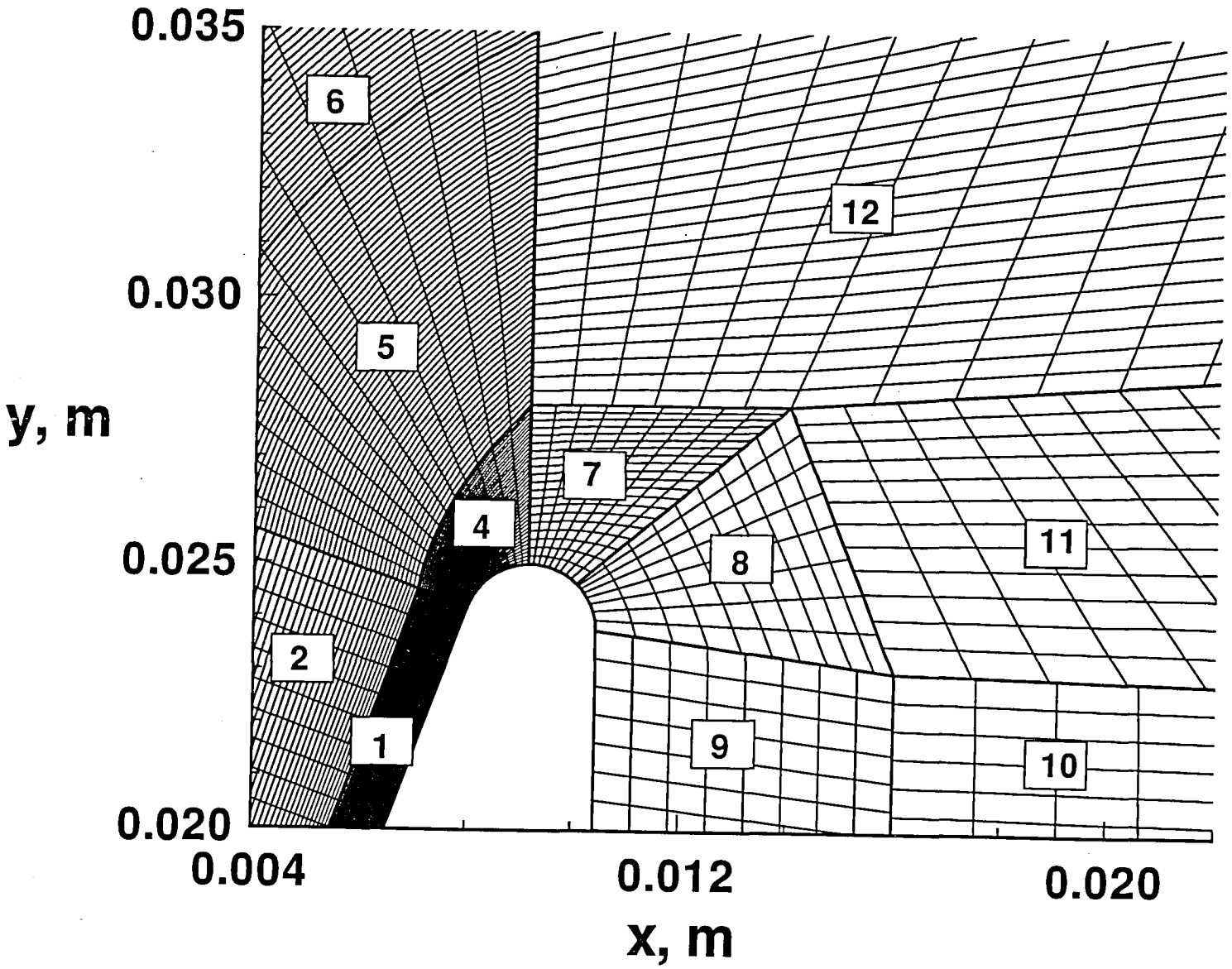

(b) Exploded view of grid for corner expansion.

Fig. 30 Concluded.

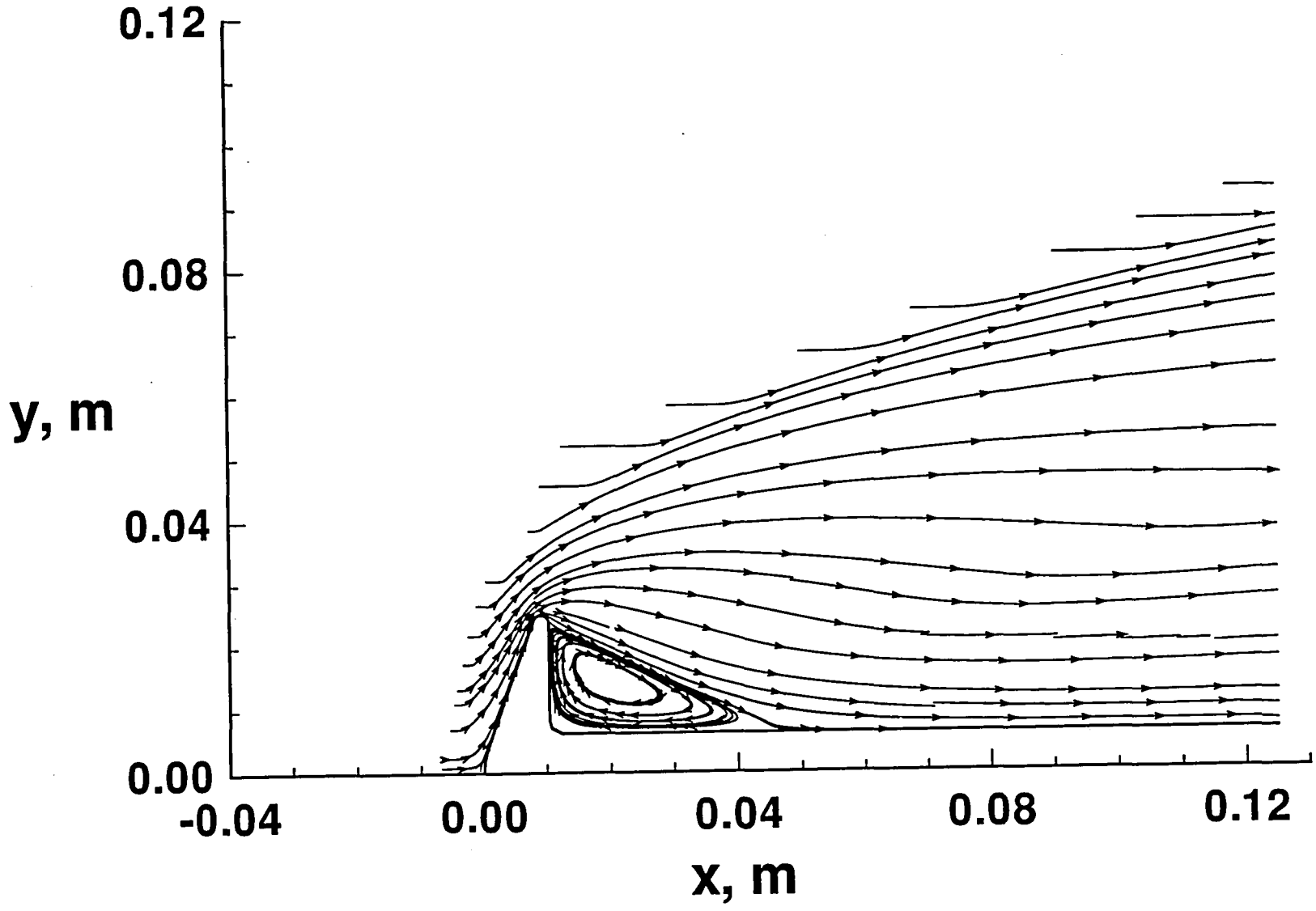

(a) With sting

Fig. 31 Particle traces for Case 3.

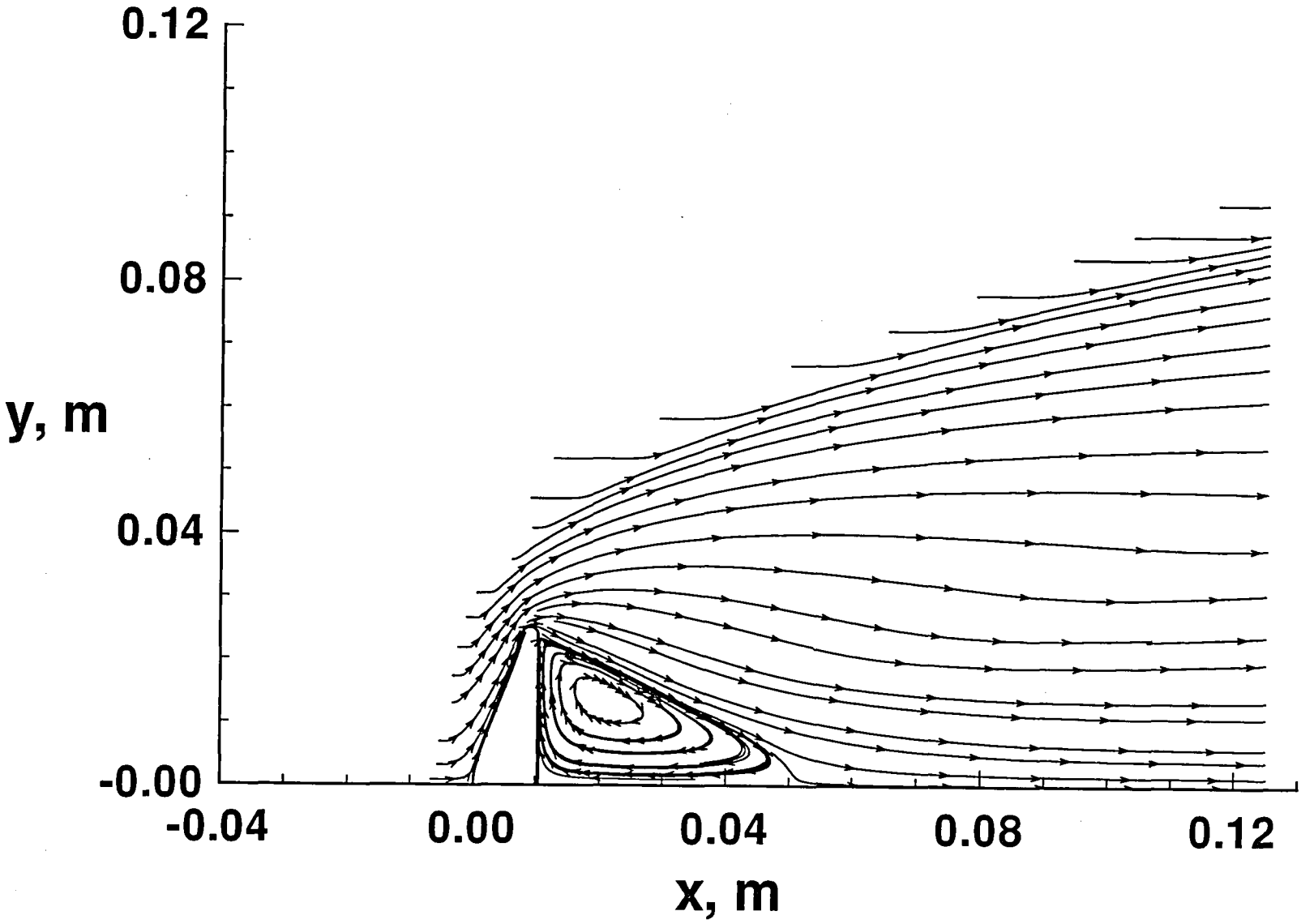

(b) Without sting.

Fig. 31 Concluded.

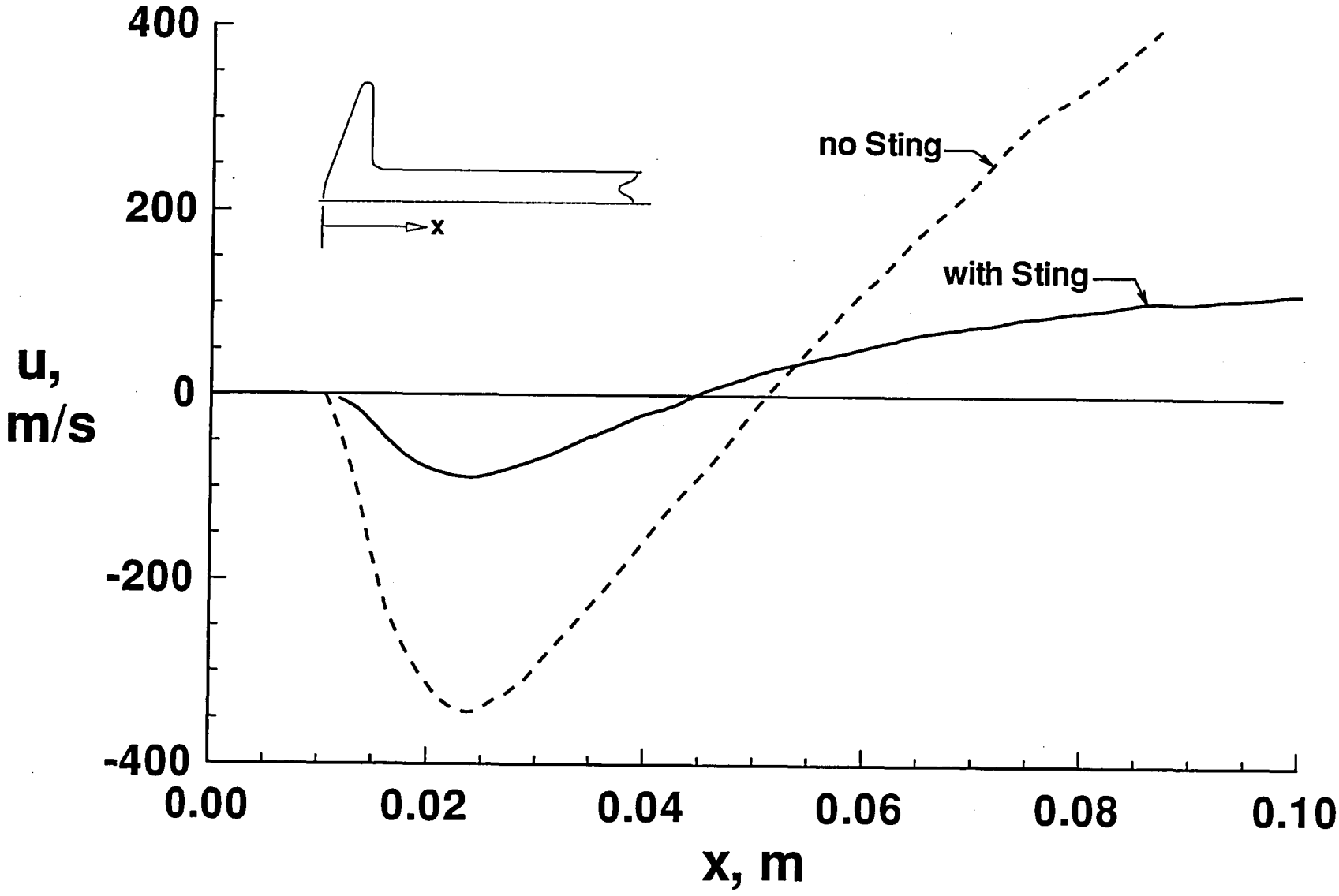

Fig. 32 Axial velocity for Case 3 along symmetry axis (no sting) and in cells adjacent to surface (with sting).

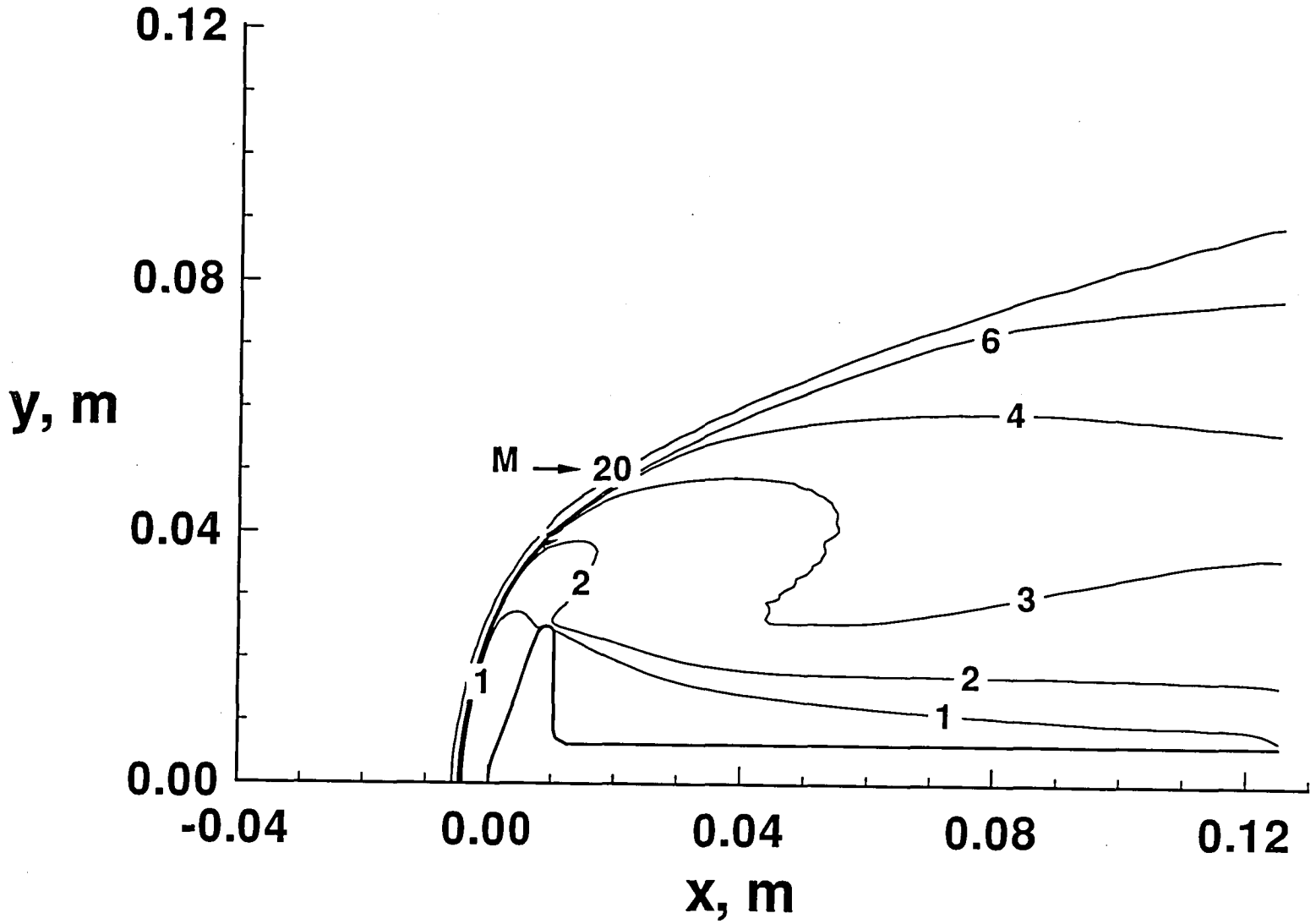

Fig. 33 Mach contours for Case 3.

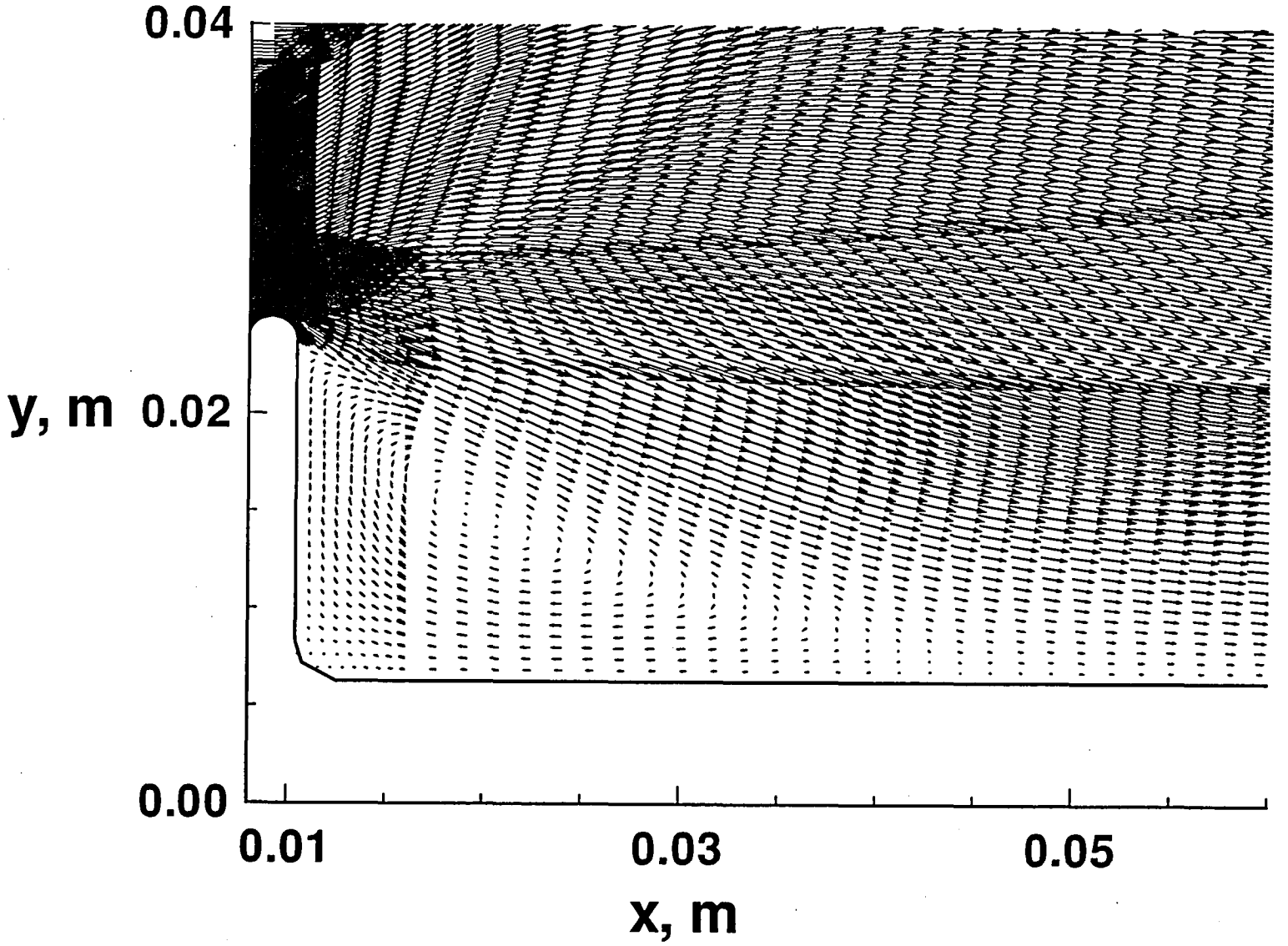

Fig. 34 Velocity vectors in near wake region for Case 3.

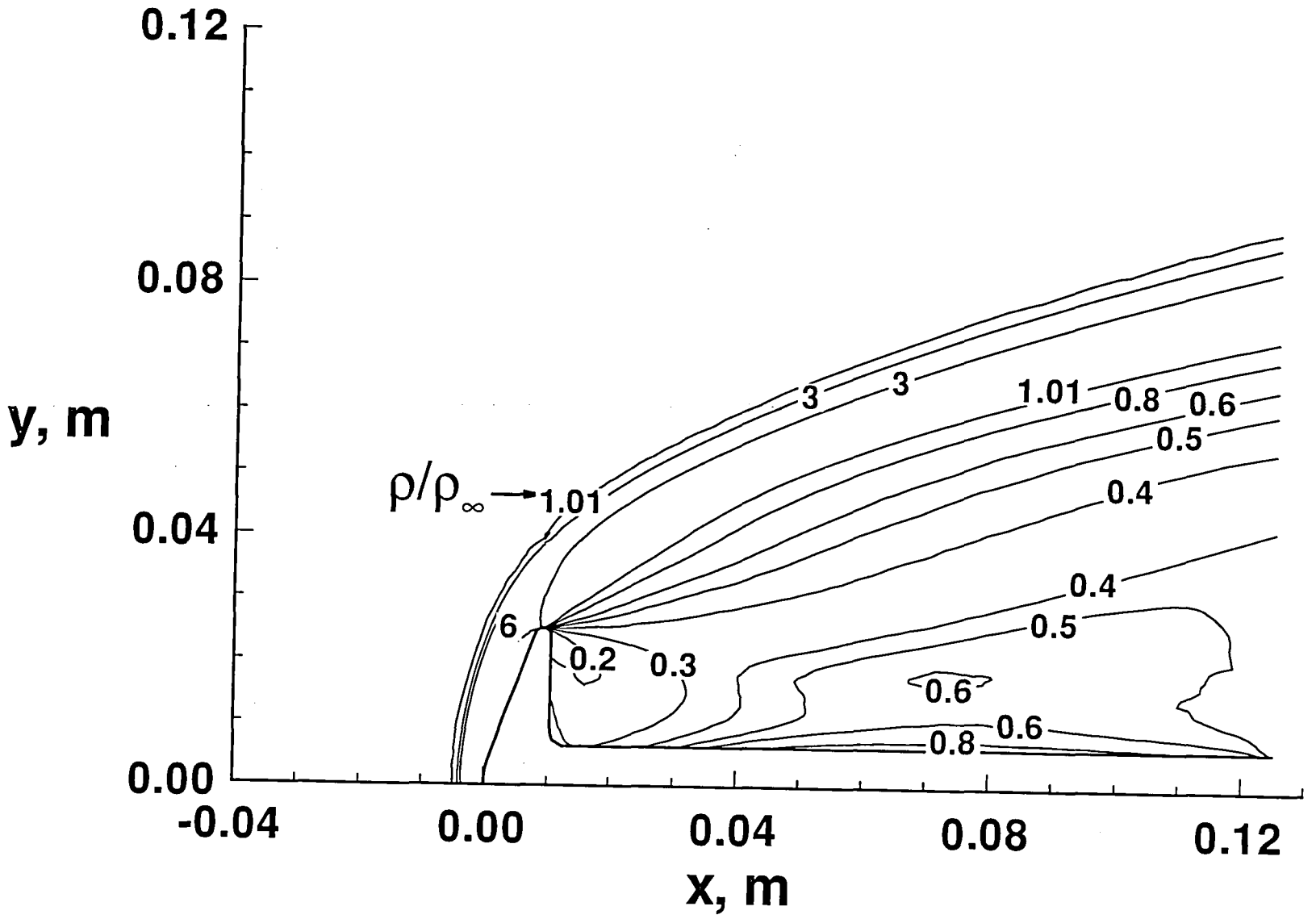

(a) Overall view.

Fig. 35 Nondimensional density contours for Case 3 (ρ_∞ = 46.67 x 10^{-5} kg/m^3) .

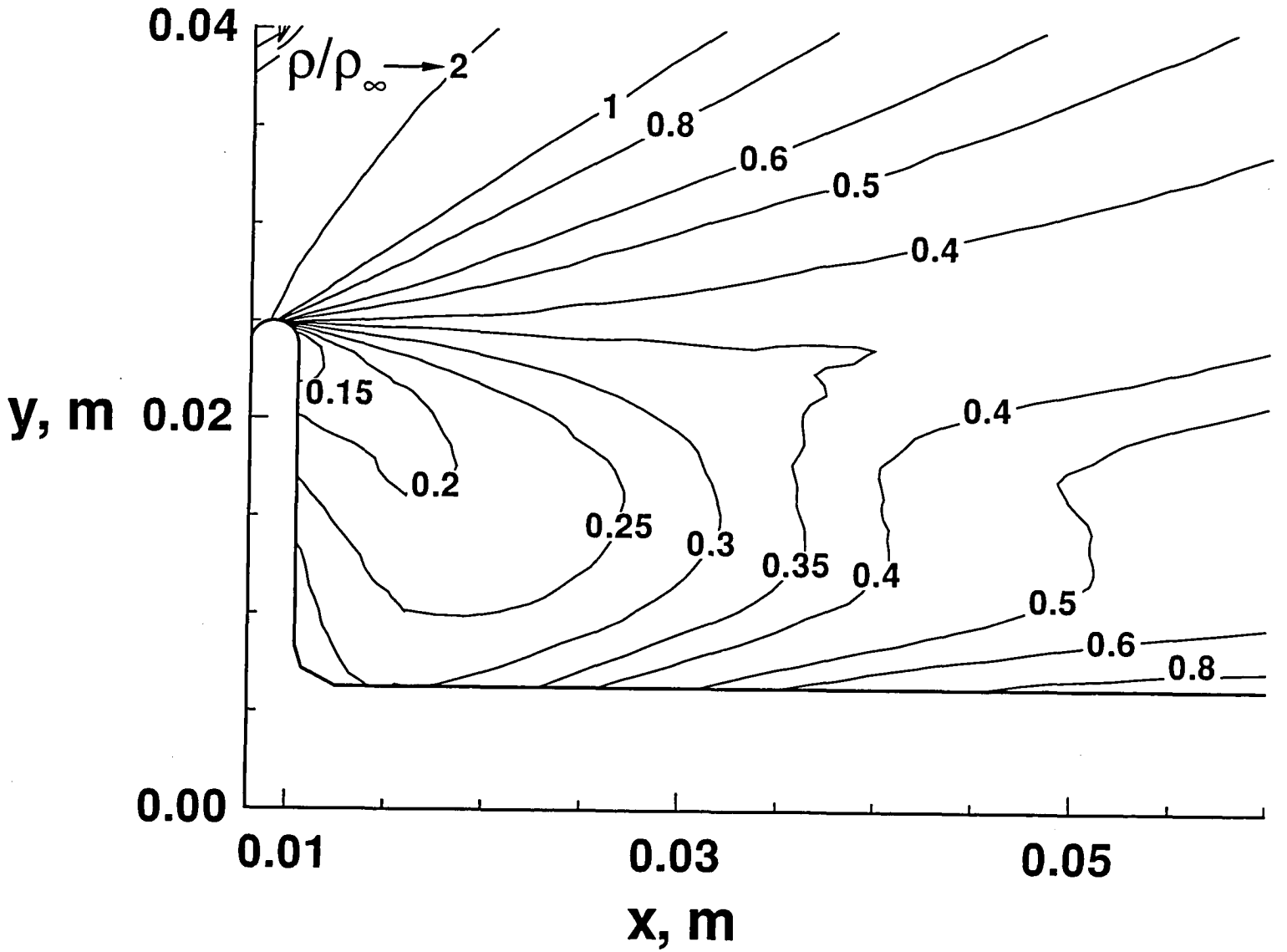

(b) Near wake region

Fig. 35 Concluded.

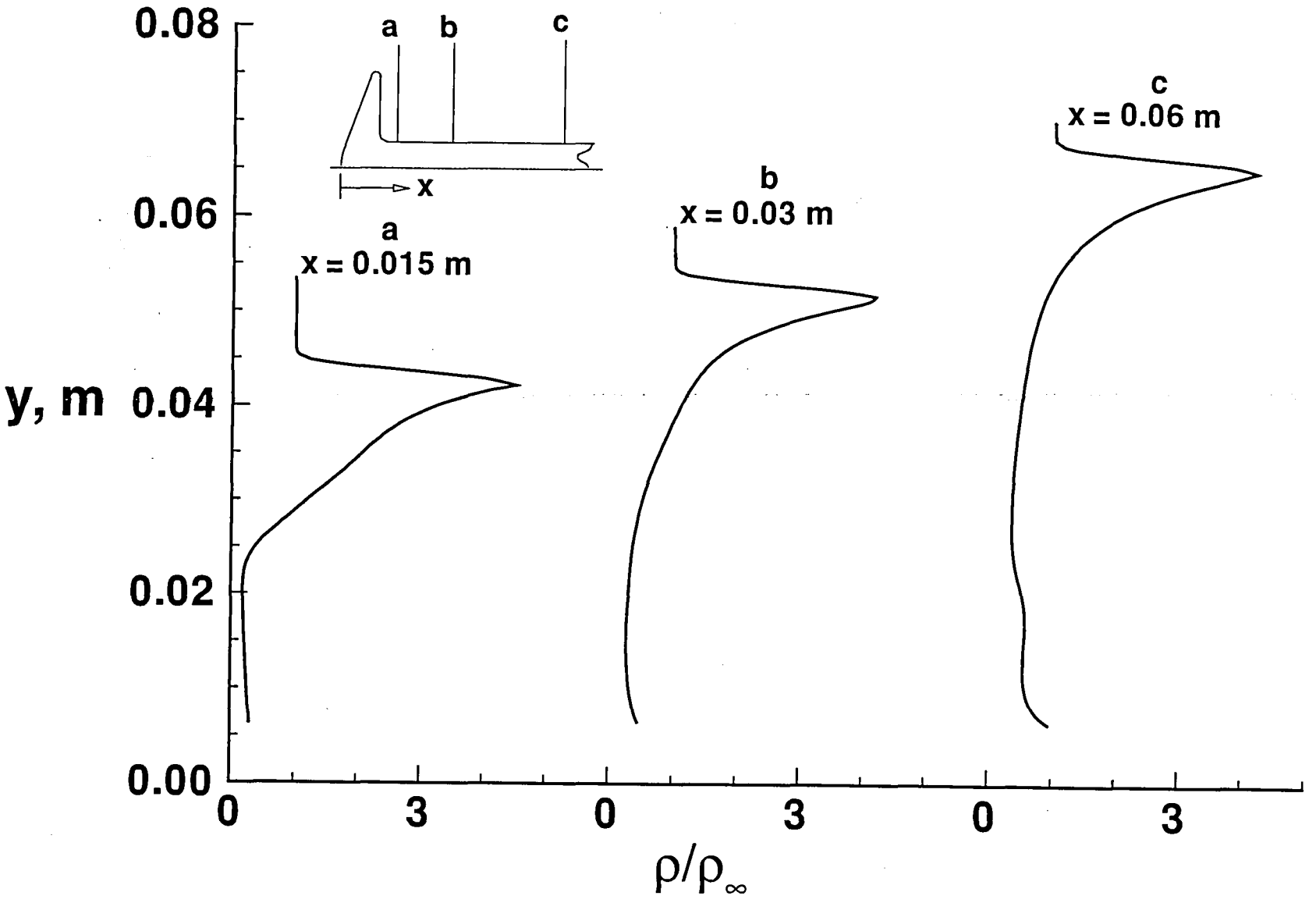

Fig. 36 Wake density profiles for Case 3 (base plane is located at x = 0.0104 m).

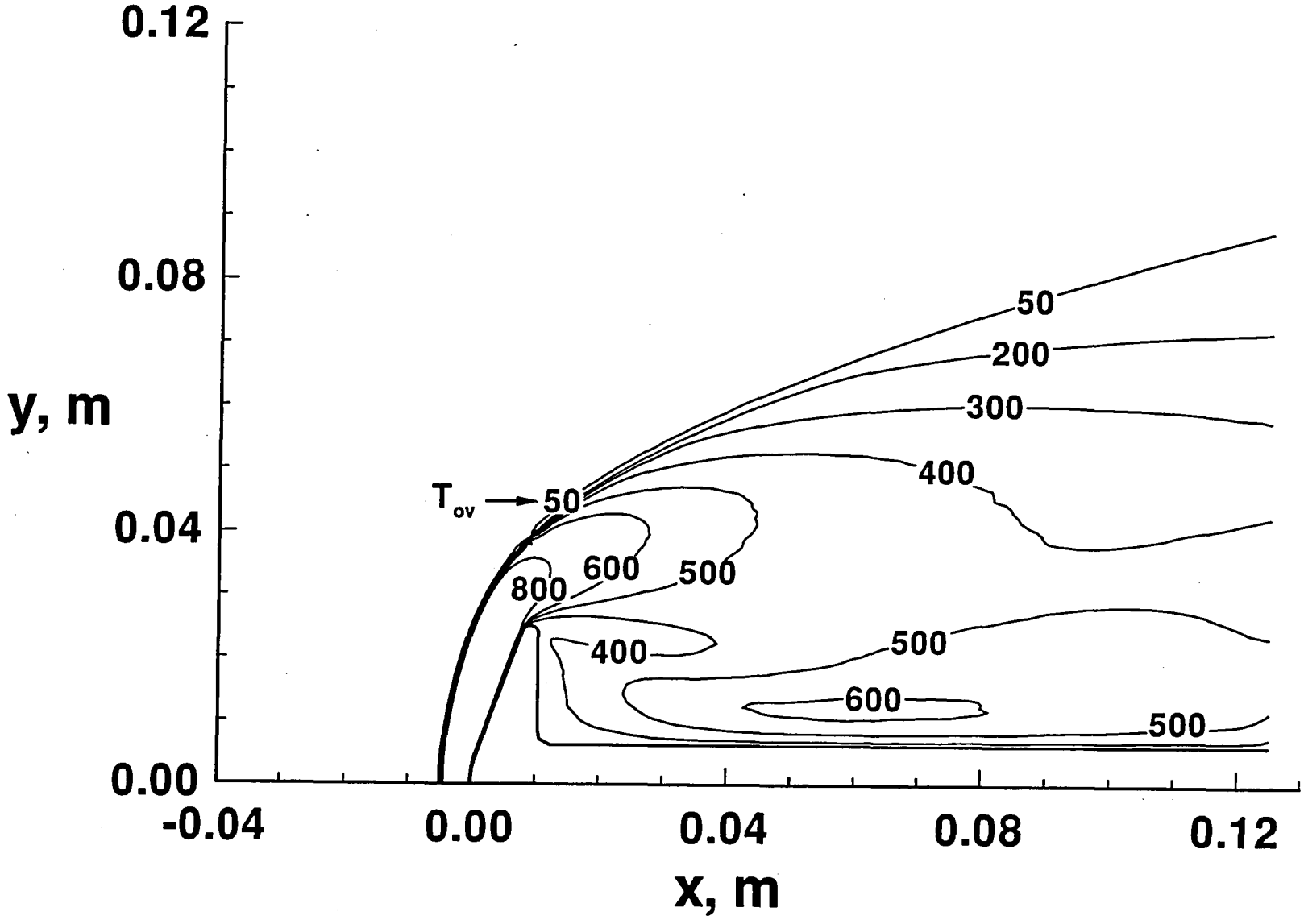

(a) Overall kinetic temperature

Fig. 37 Temperature contours for Case 3.

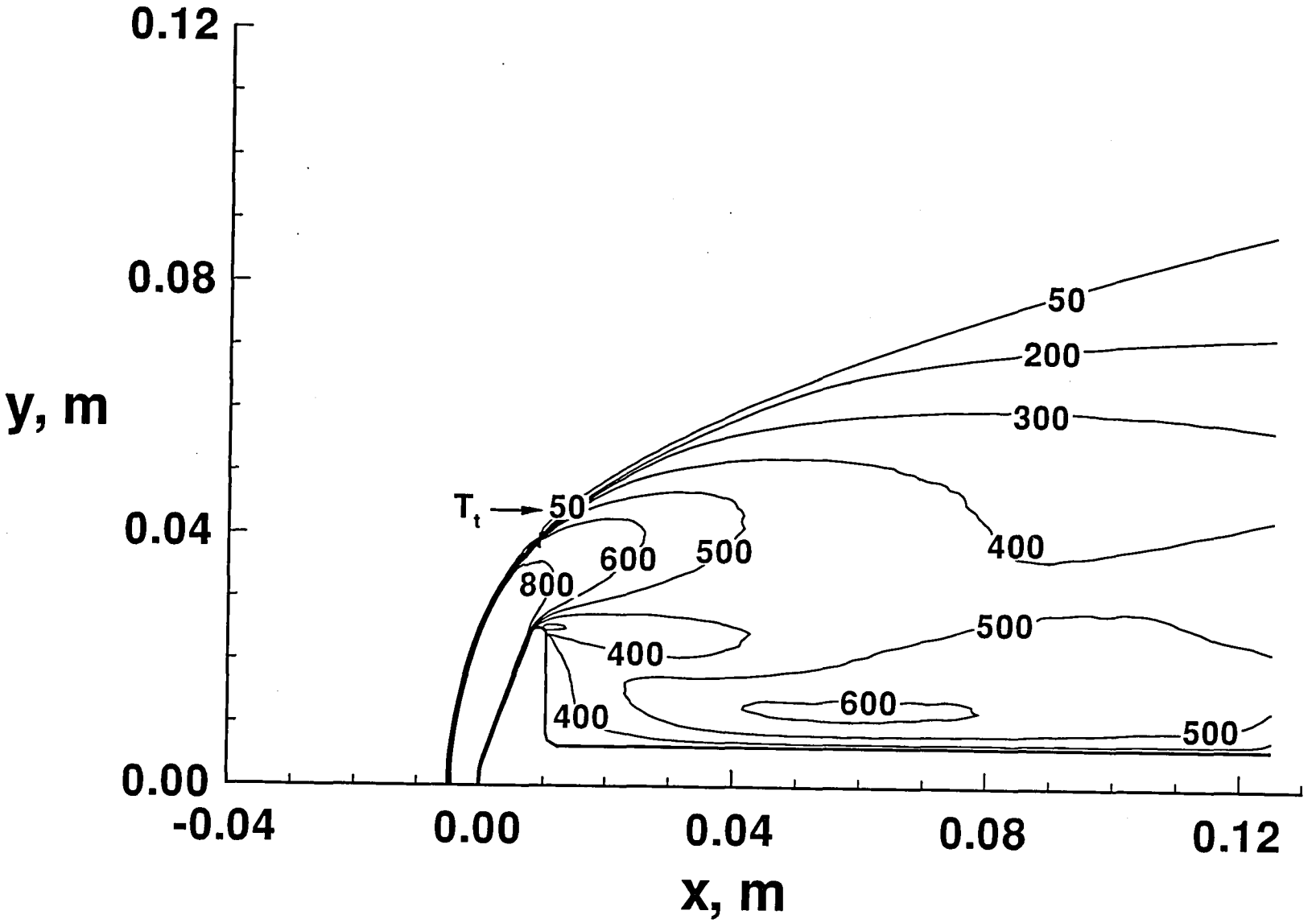

(b) Translational temperature

Fig. 37 Continued.

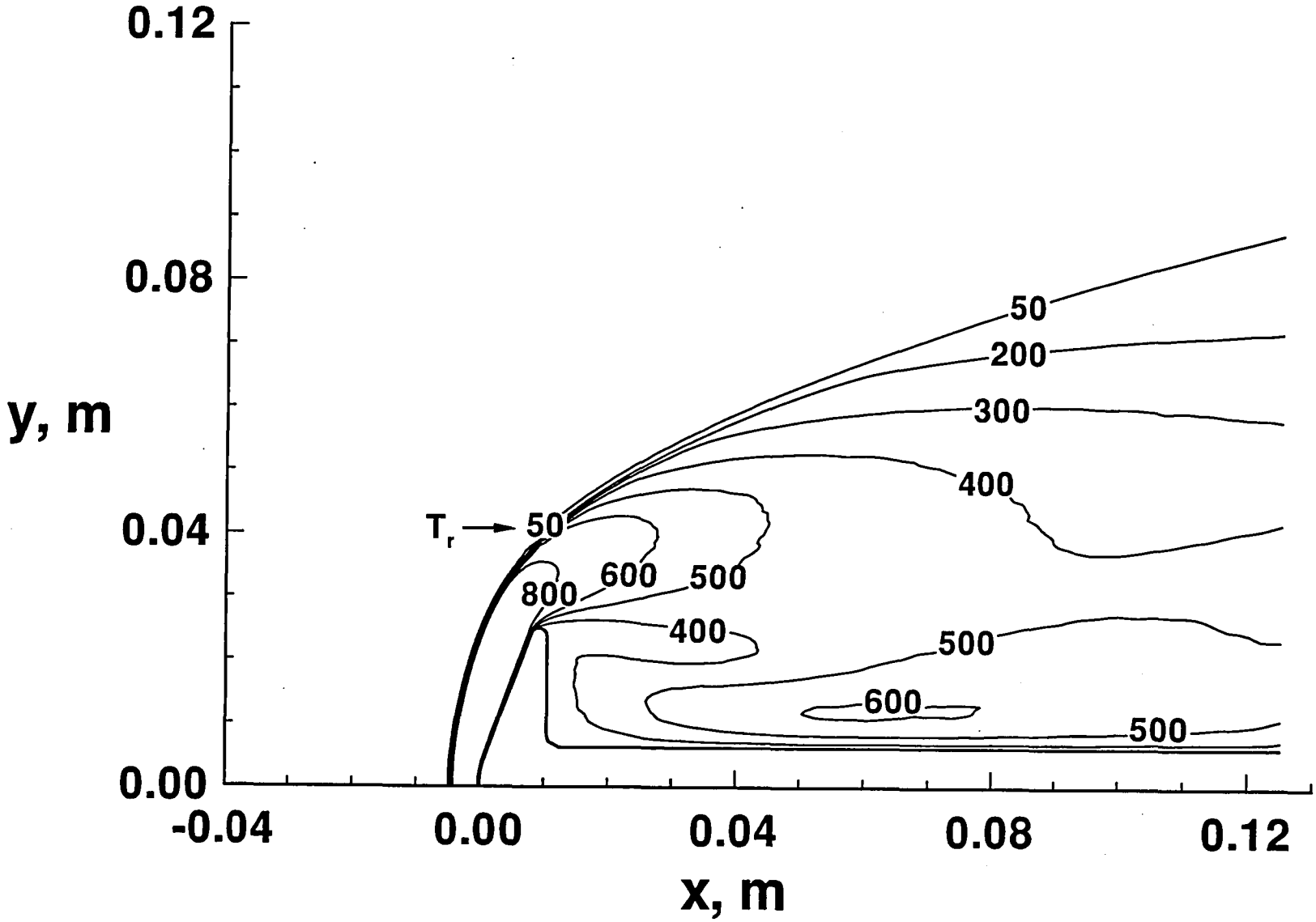

(c) Rotational temperature

Fig. 37 Concluded.

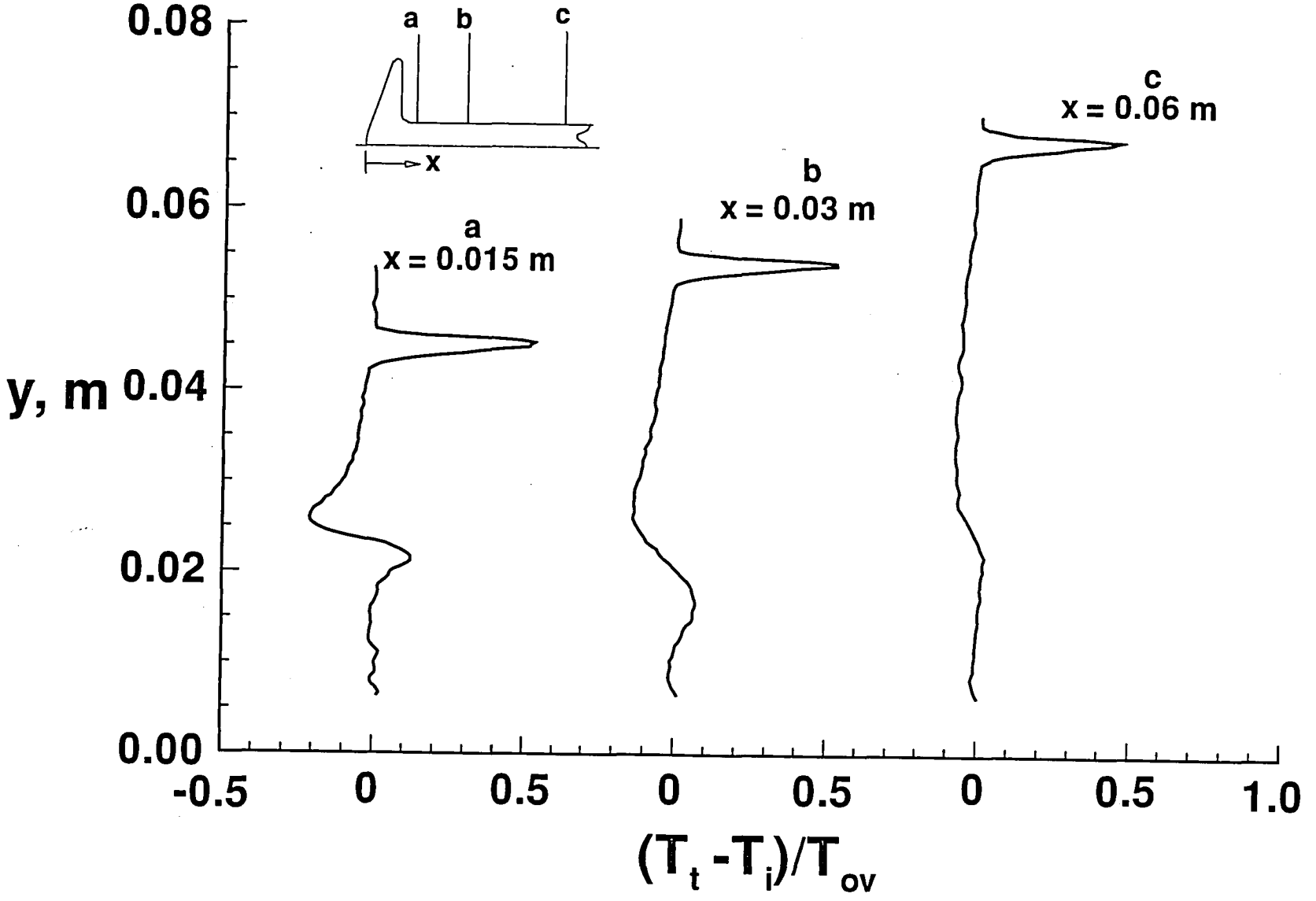

(a) Extent of thermal nonequilibrium

Fig. 38 Wake profiles for Case 3.

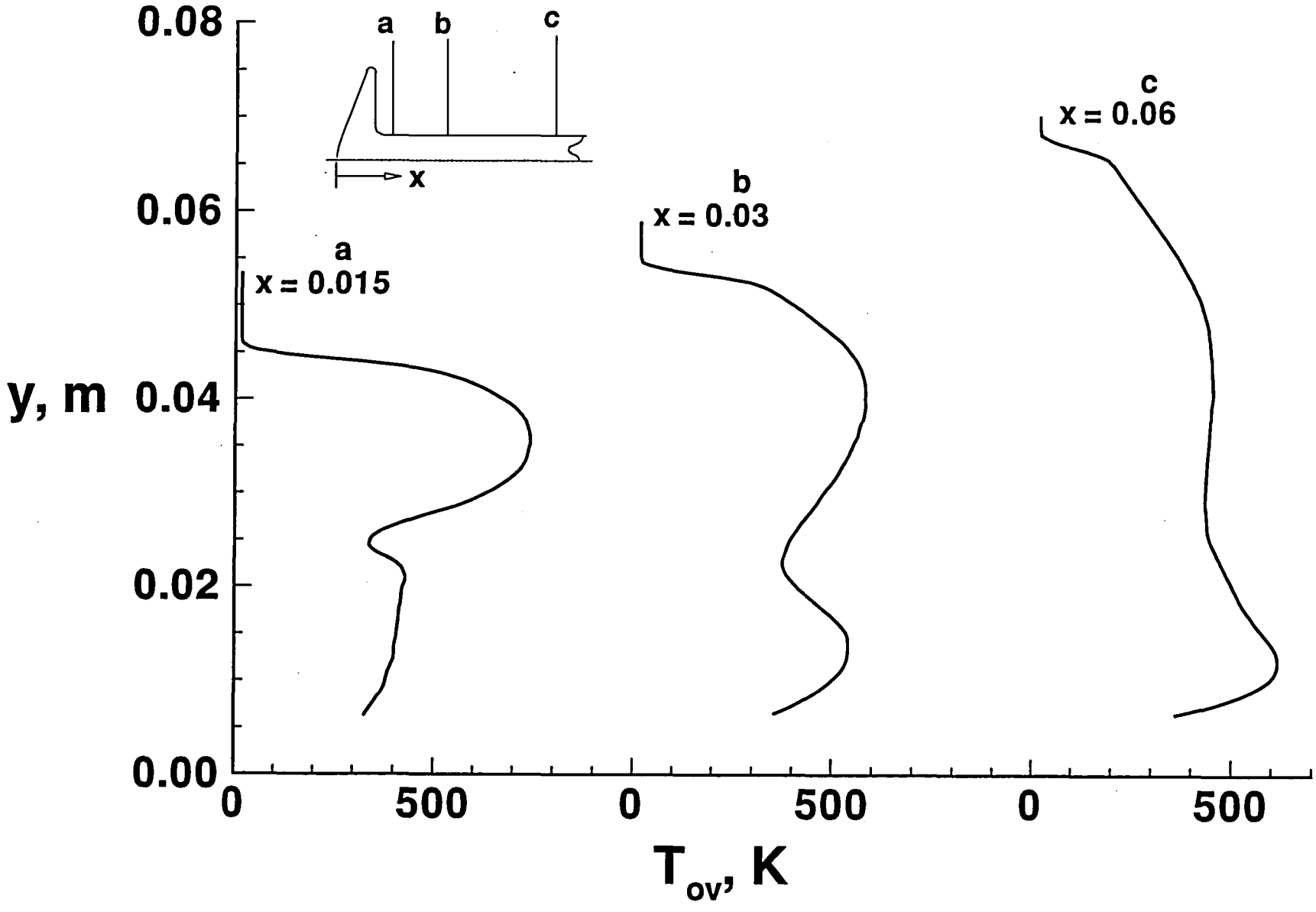

(b) Overall kinetic temperature

Fig. 38 Continued.

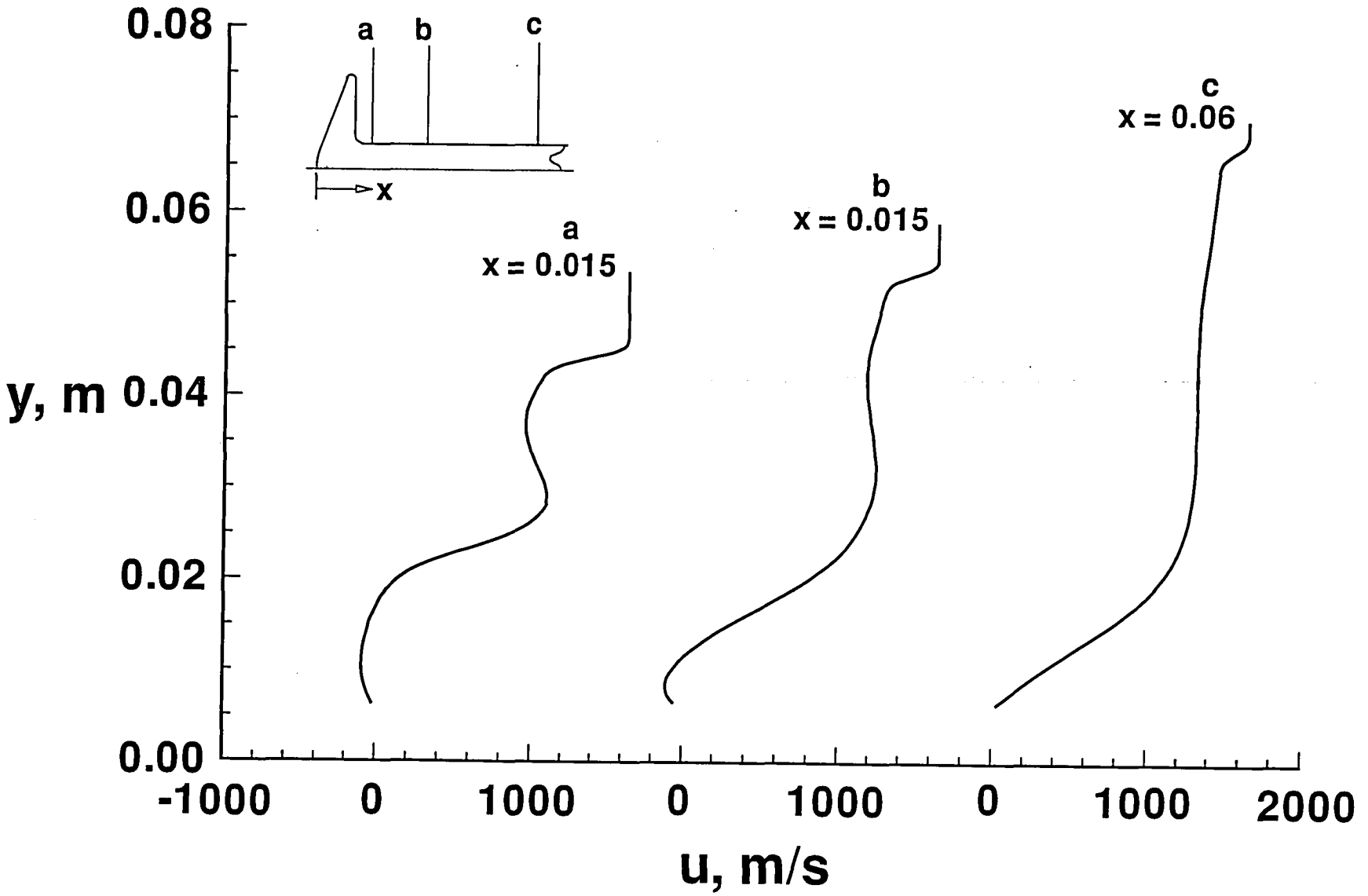

(c) Axial velocity

Fig. 38 Concluded.

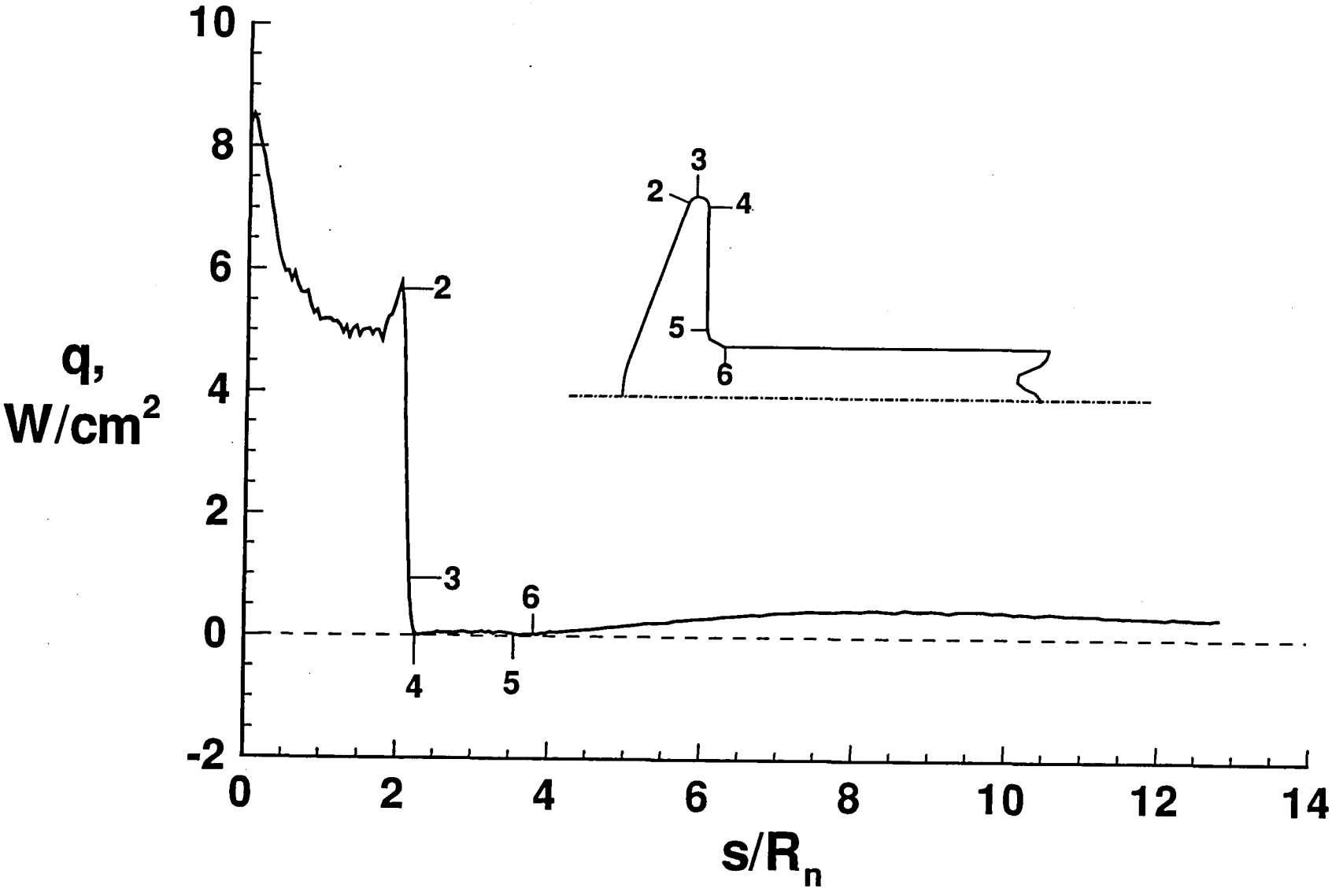

(a) Cartesian plot

Fig. 39 Surface heating rate distribution for Case 3.

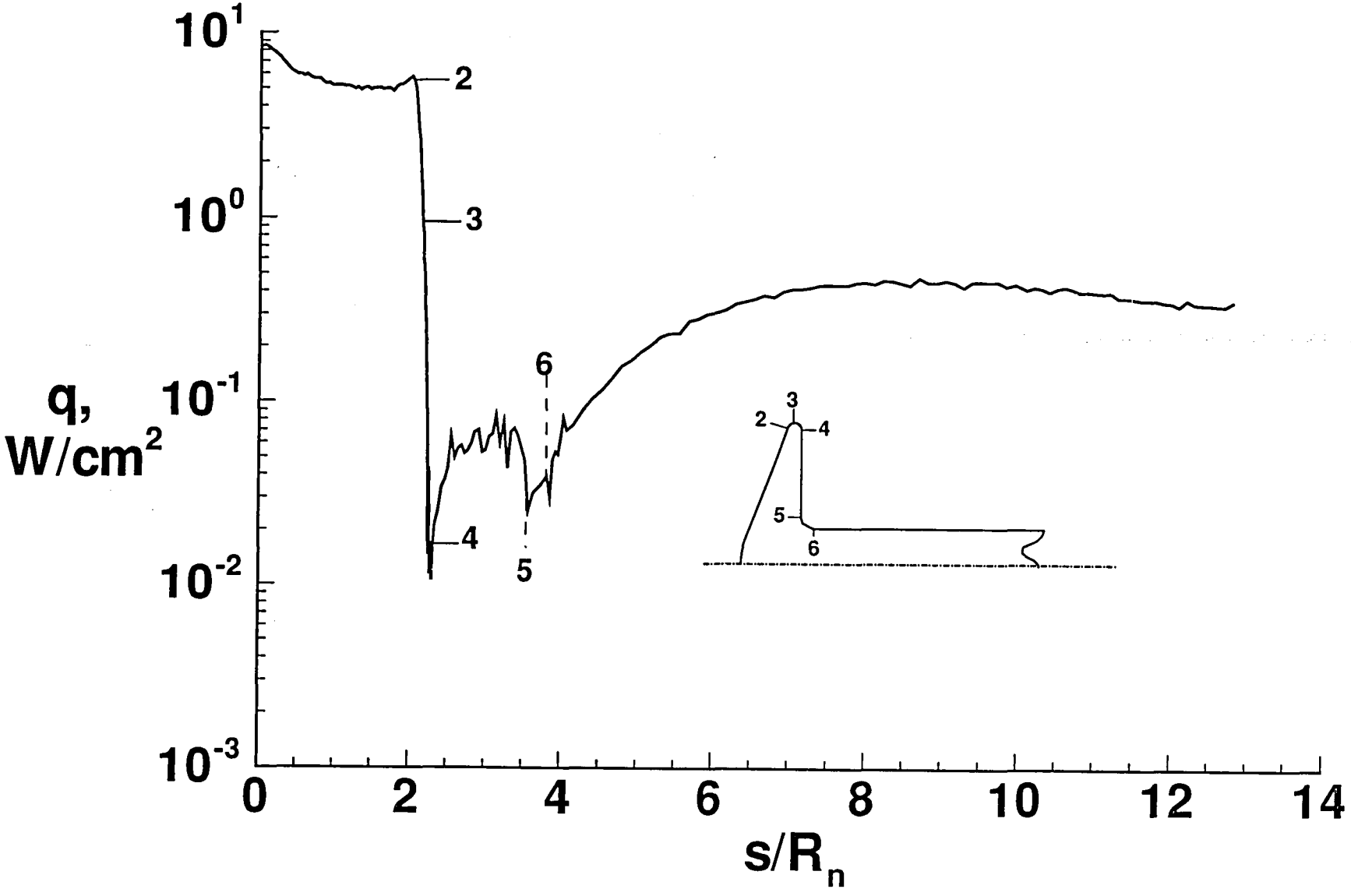

(b) Semilog plot

Fig. 39 Concluded.

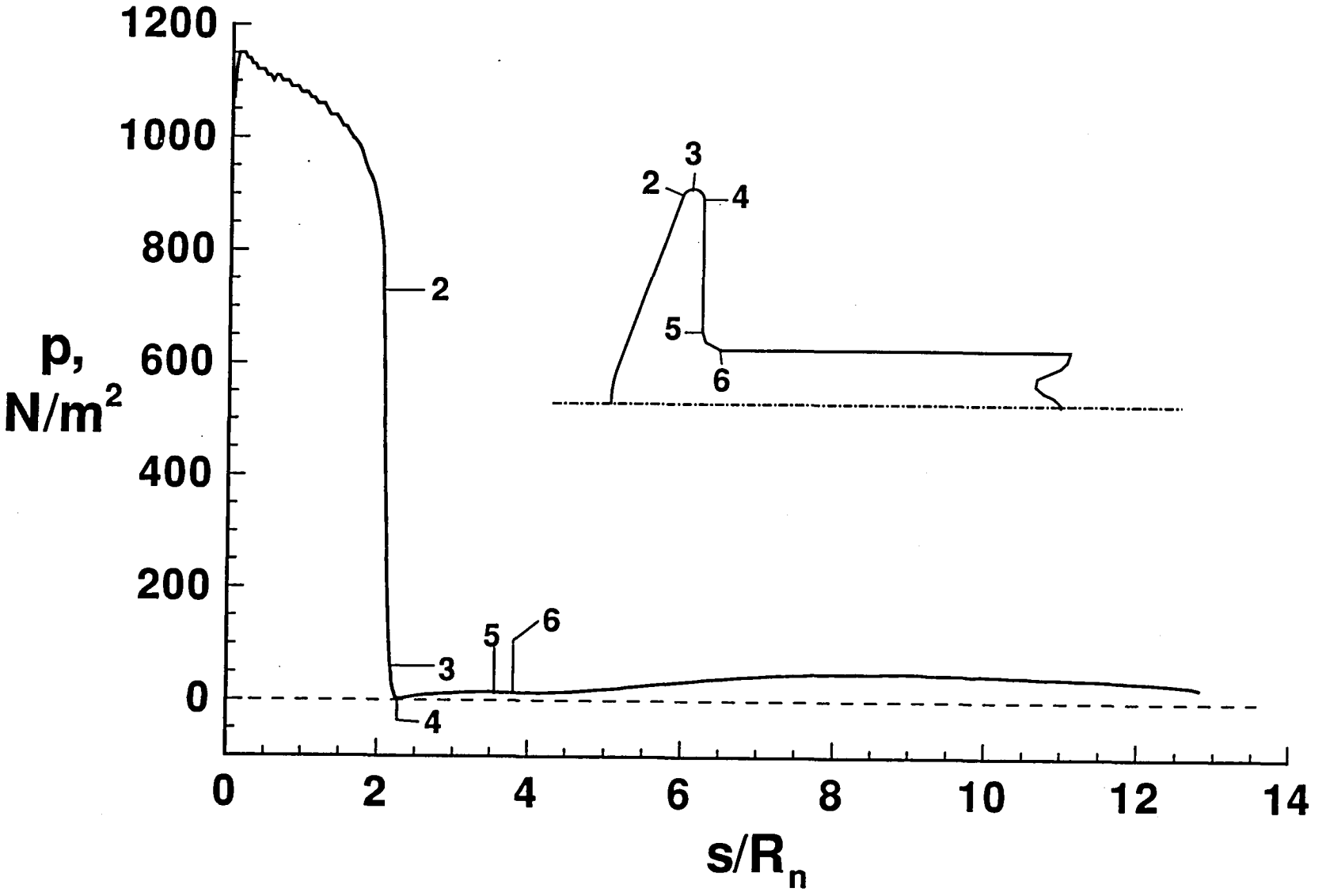

(a) Cartesian plot

Fig. 40 Surface pressure distribution for Case 3.

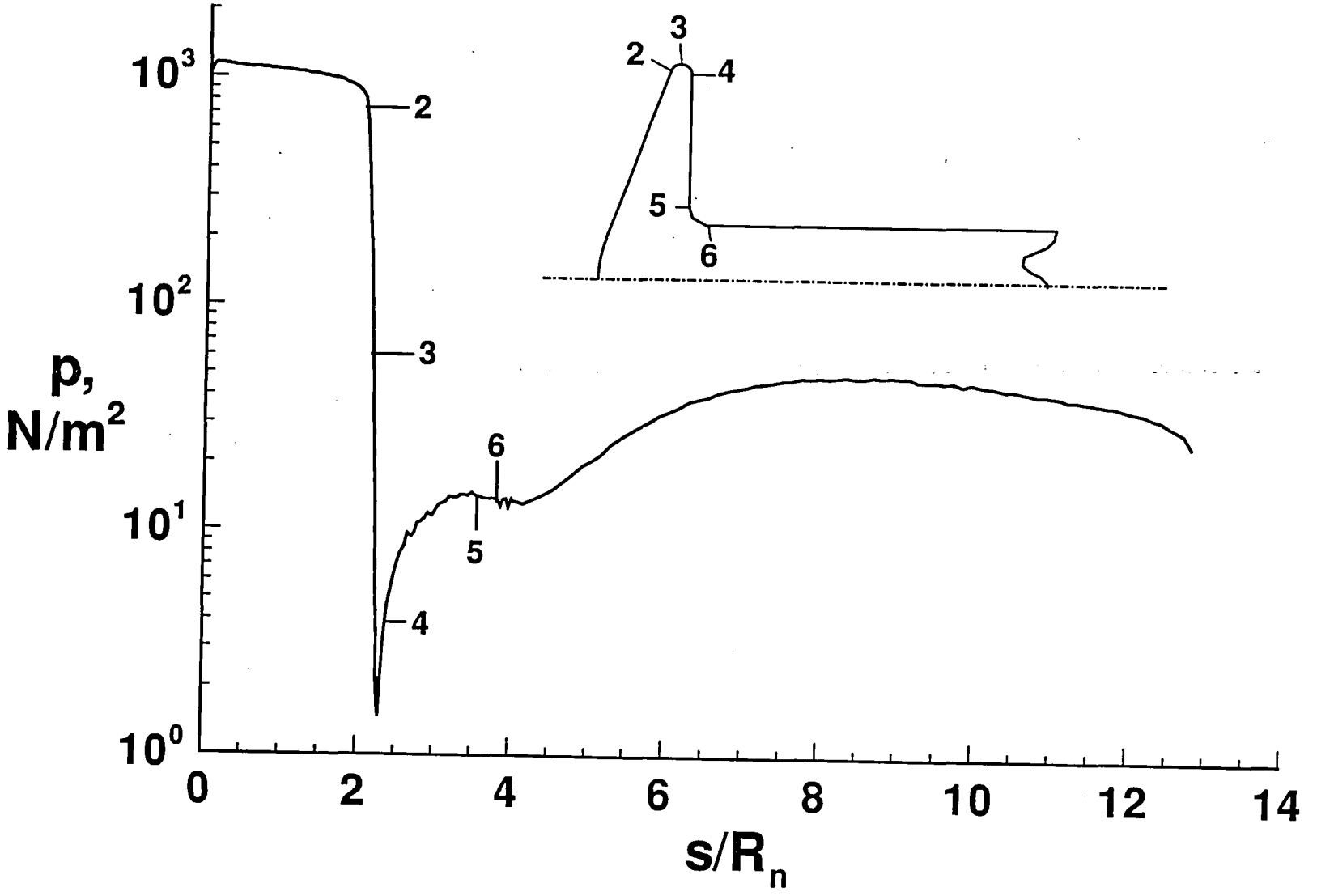

(b) Semilog plot

Fig. 40 Concluded.

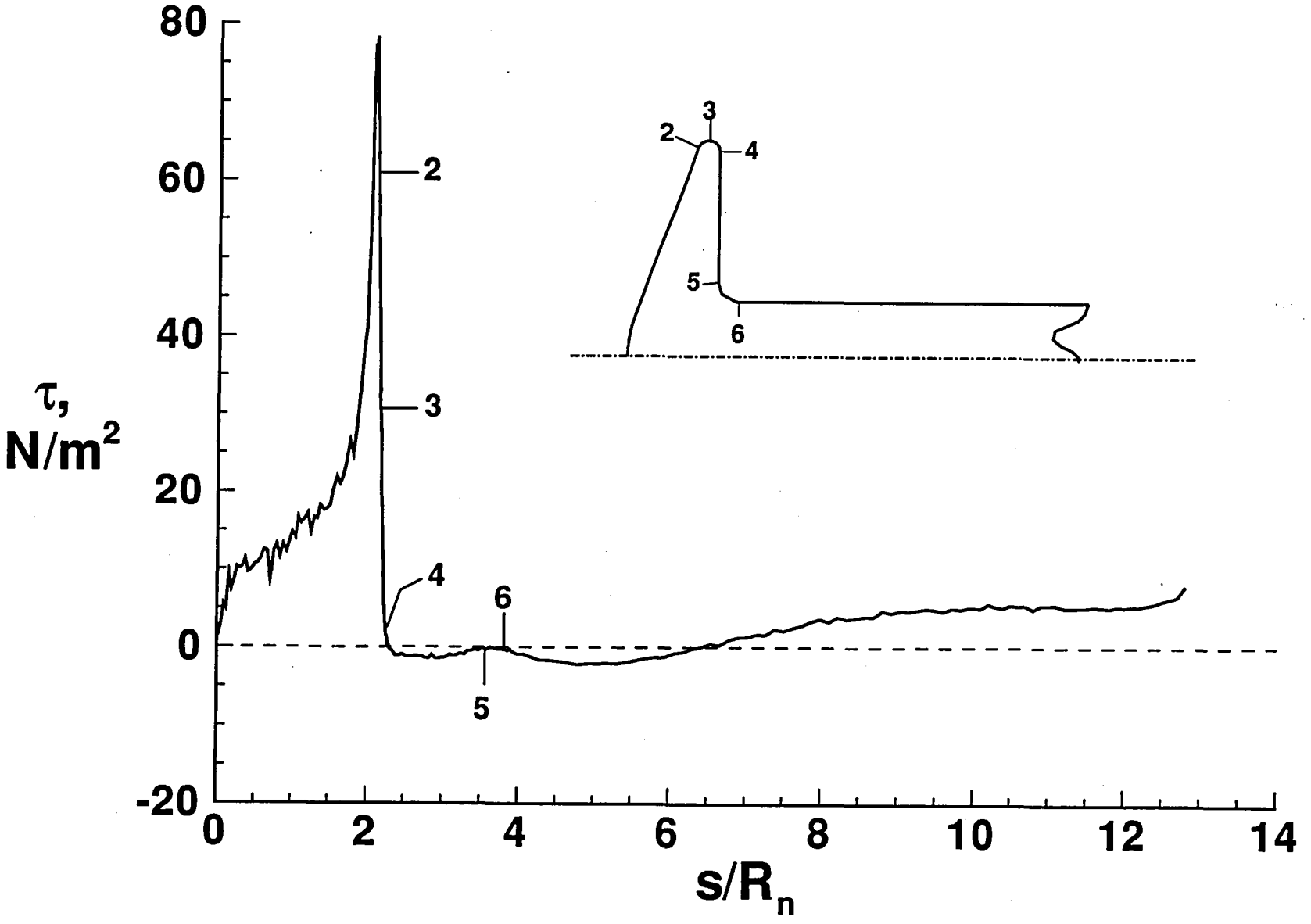

Fig. 41 Skin friction distribution for Case 3.

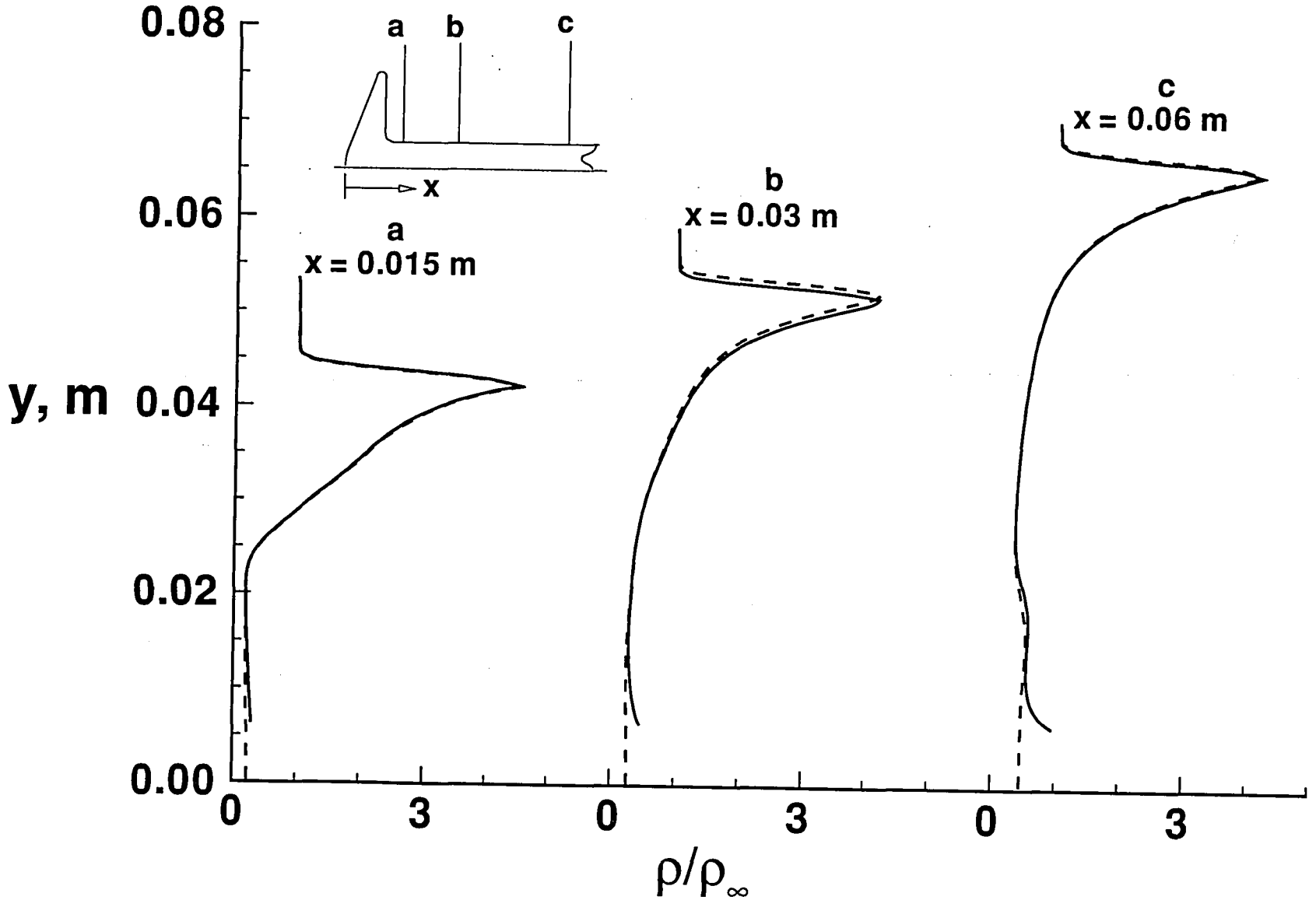

(a) Wake density profiles

Fig. 42 Effect of afterbody sting on wake results for Case 3.

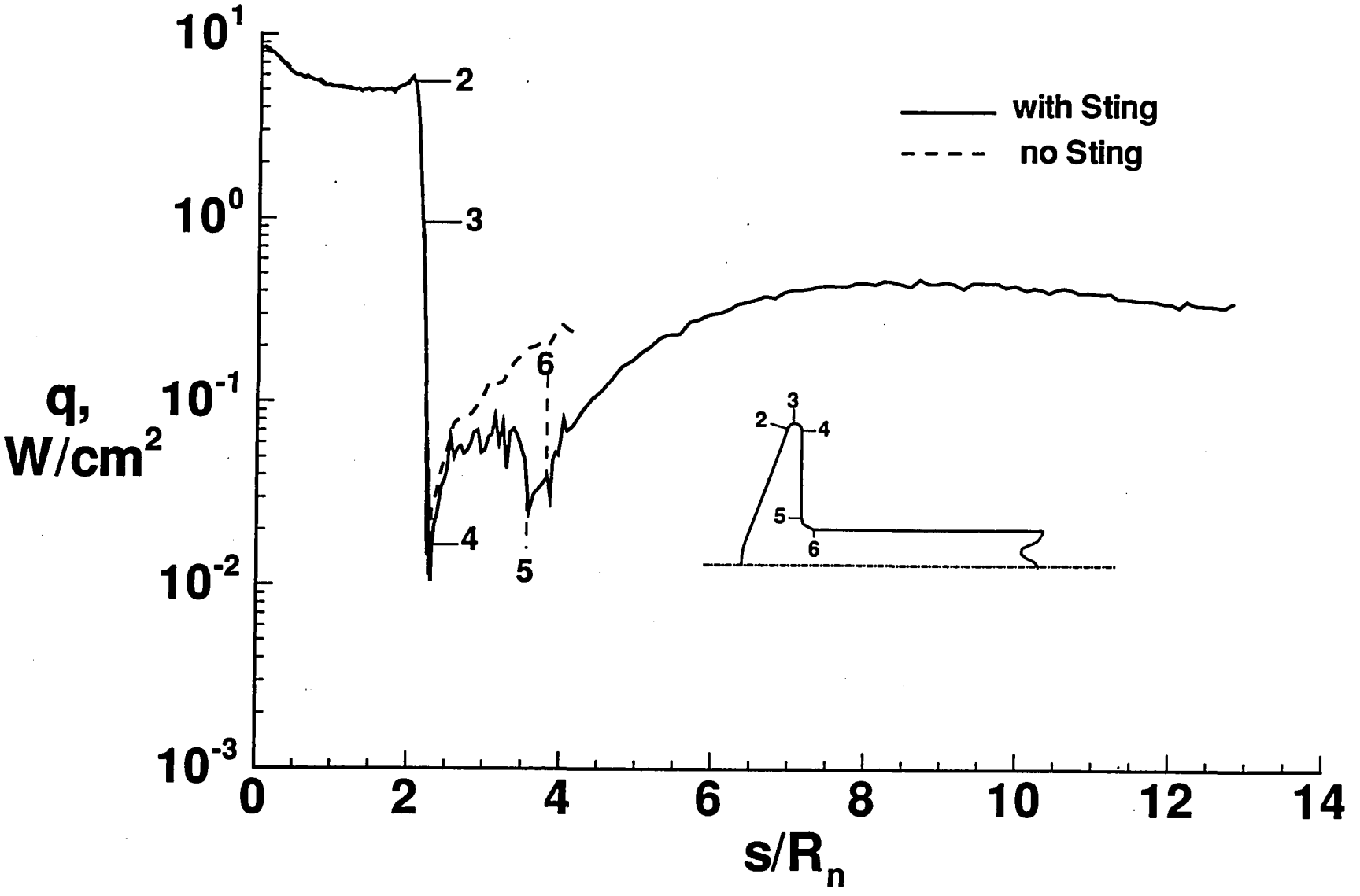

(b) Surface heating rate distribution

Fig. 42 Concluded.

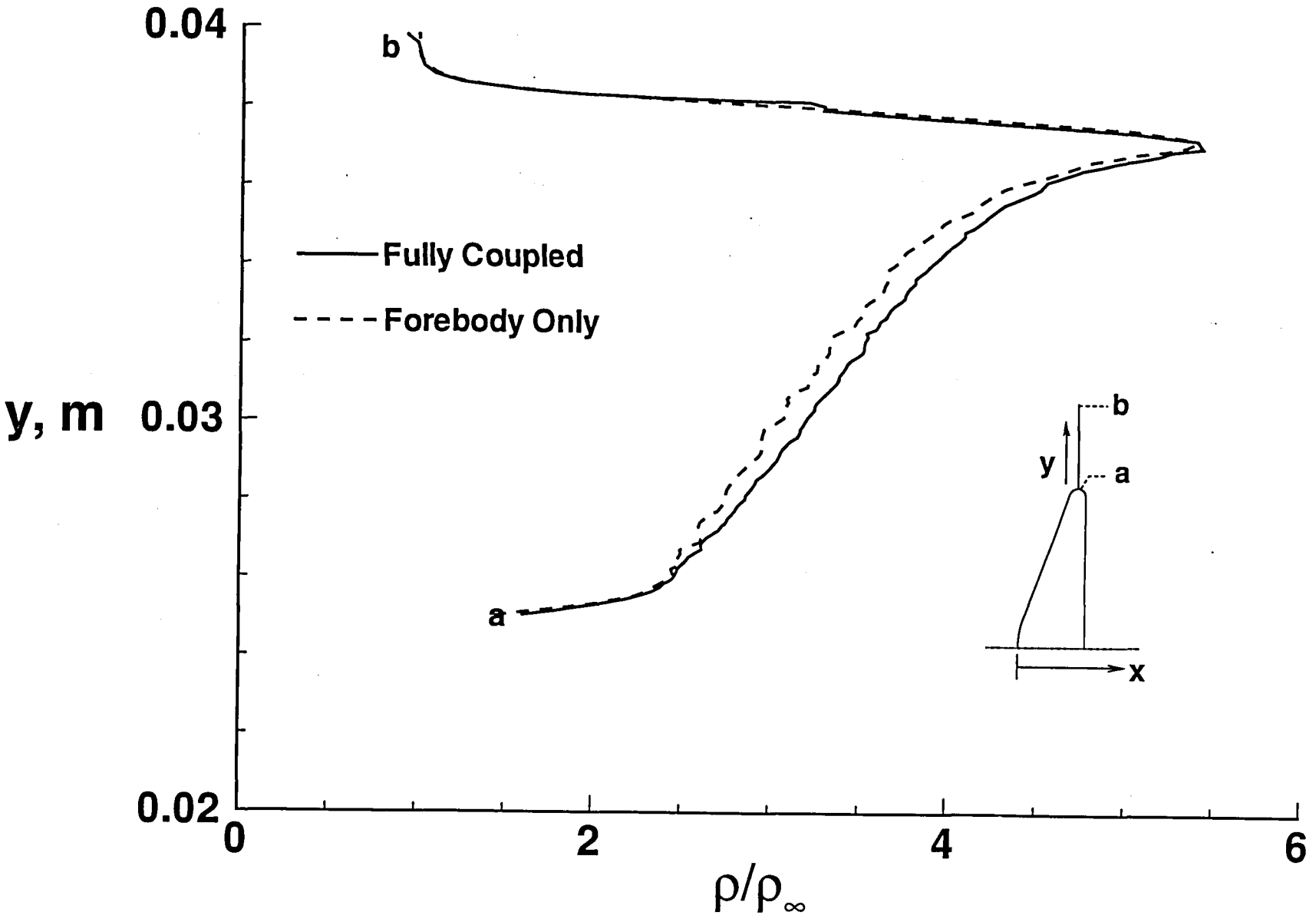

(a) Density profiles

Fig. 43 Effect of wake on forebody results for Case 3.

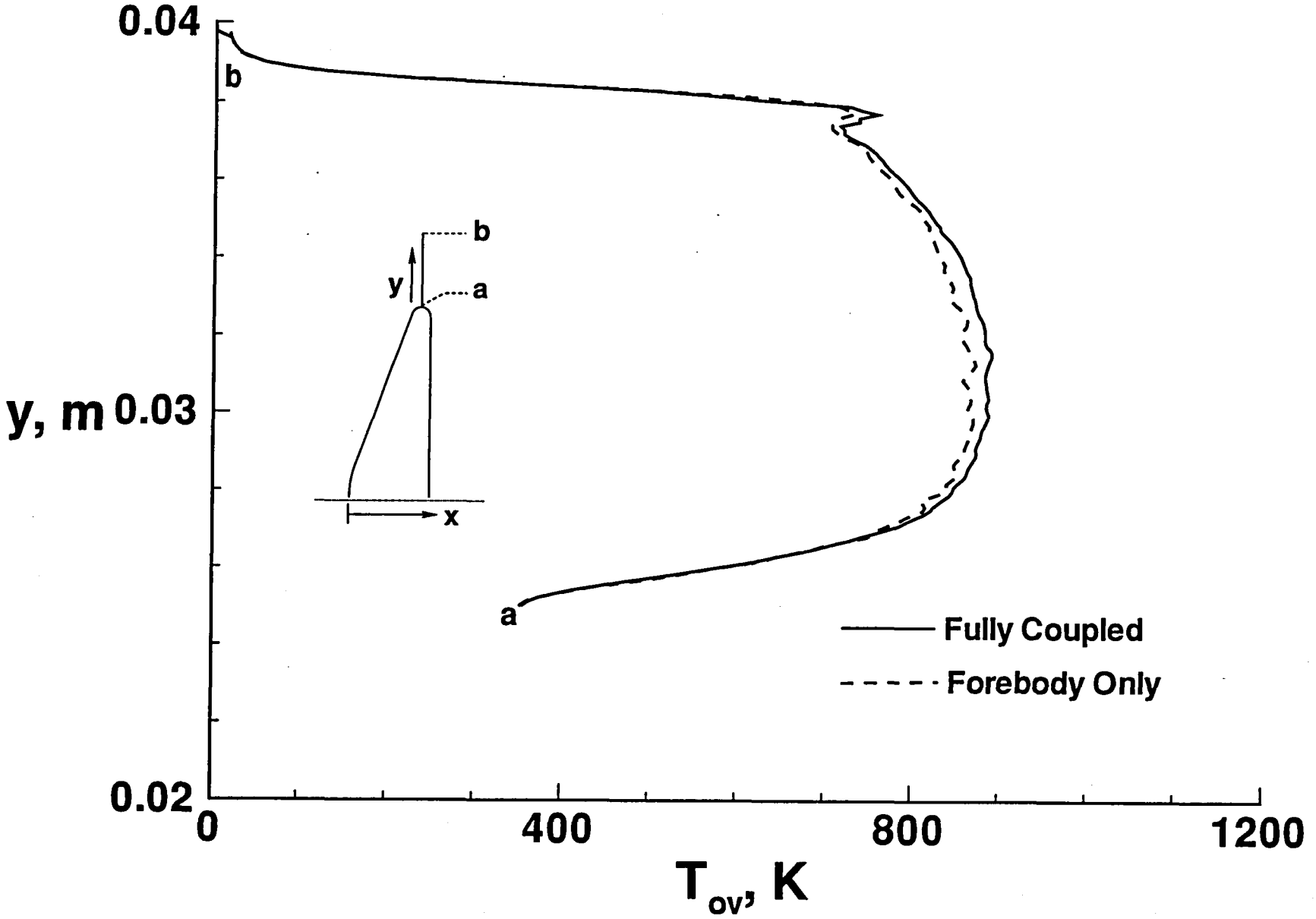

(b) Overall temperature profiles

Fig. 43 Continued.

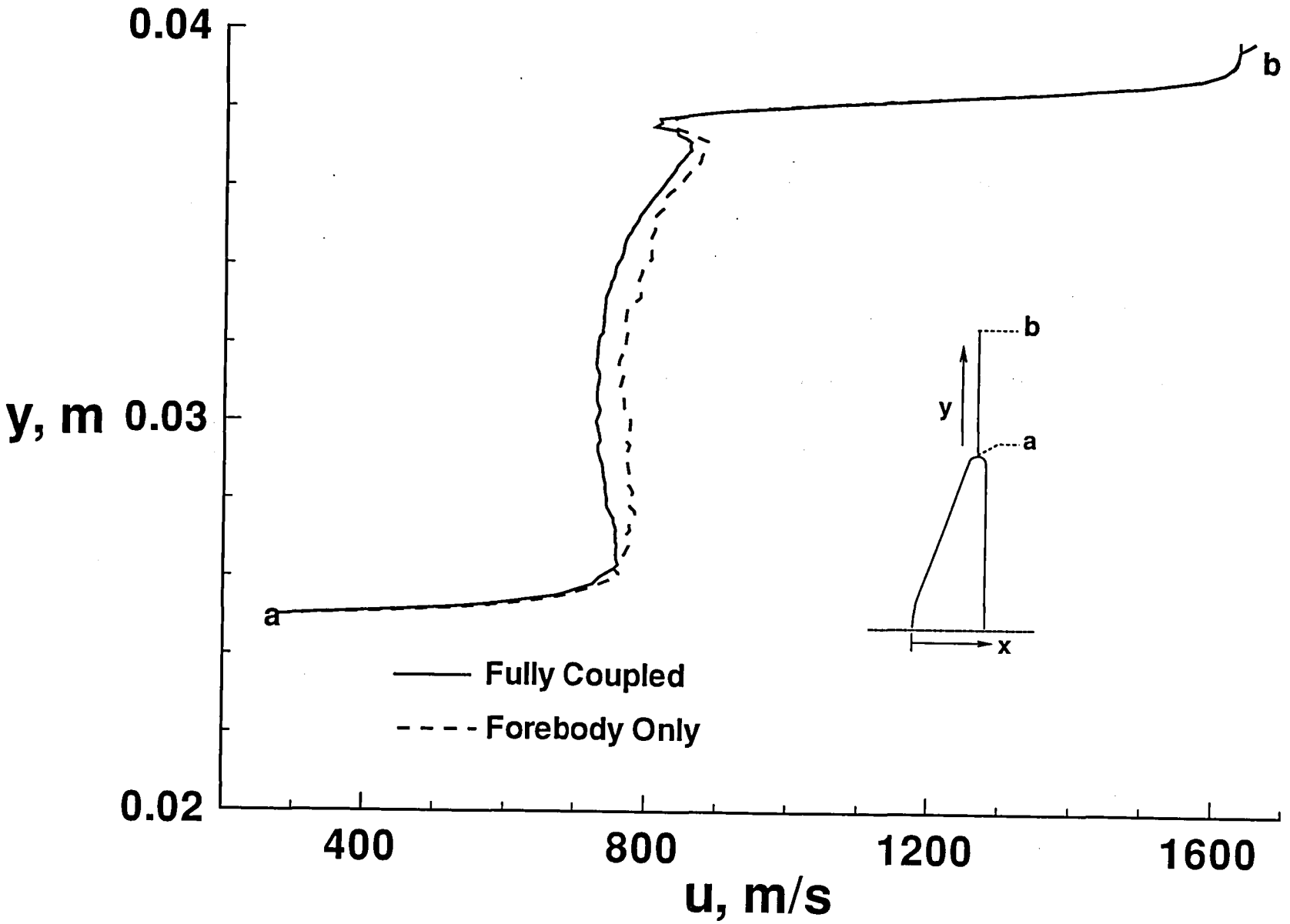

(c) Axial velocity profiles

Fig. 43 Continued.

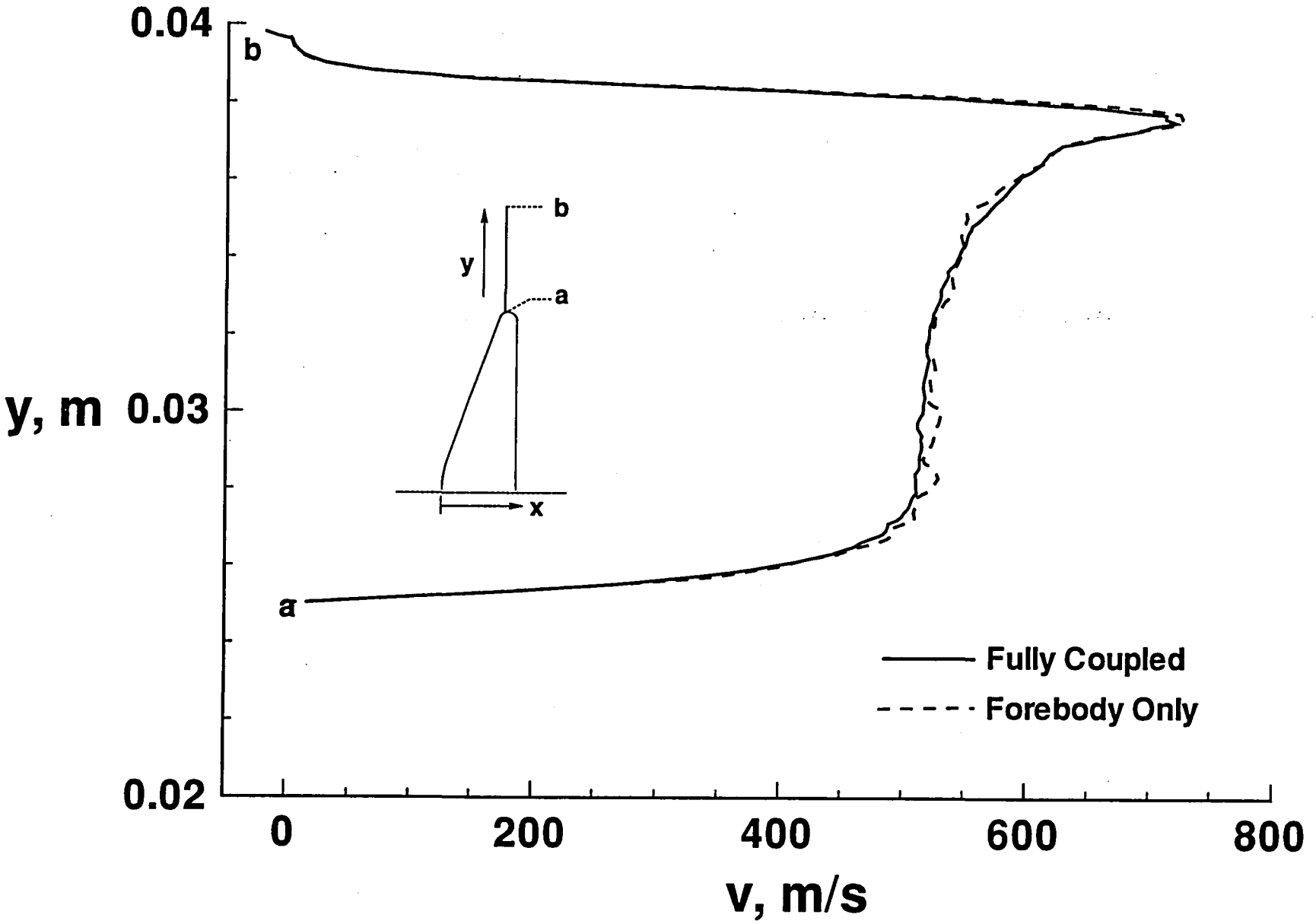

(d) Radial velocity profiles

Fig. 43 Concluded.

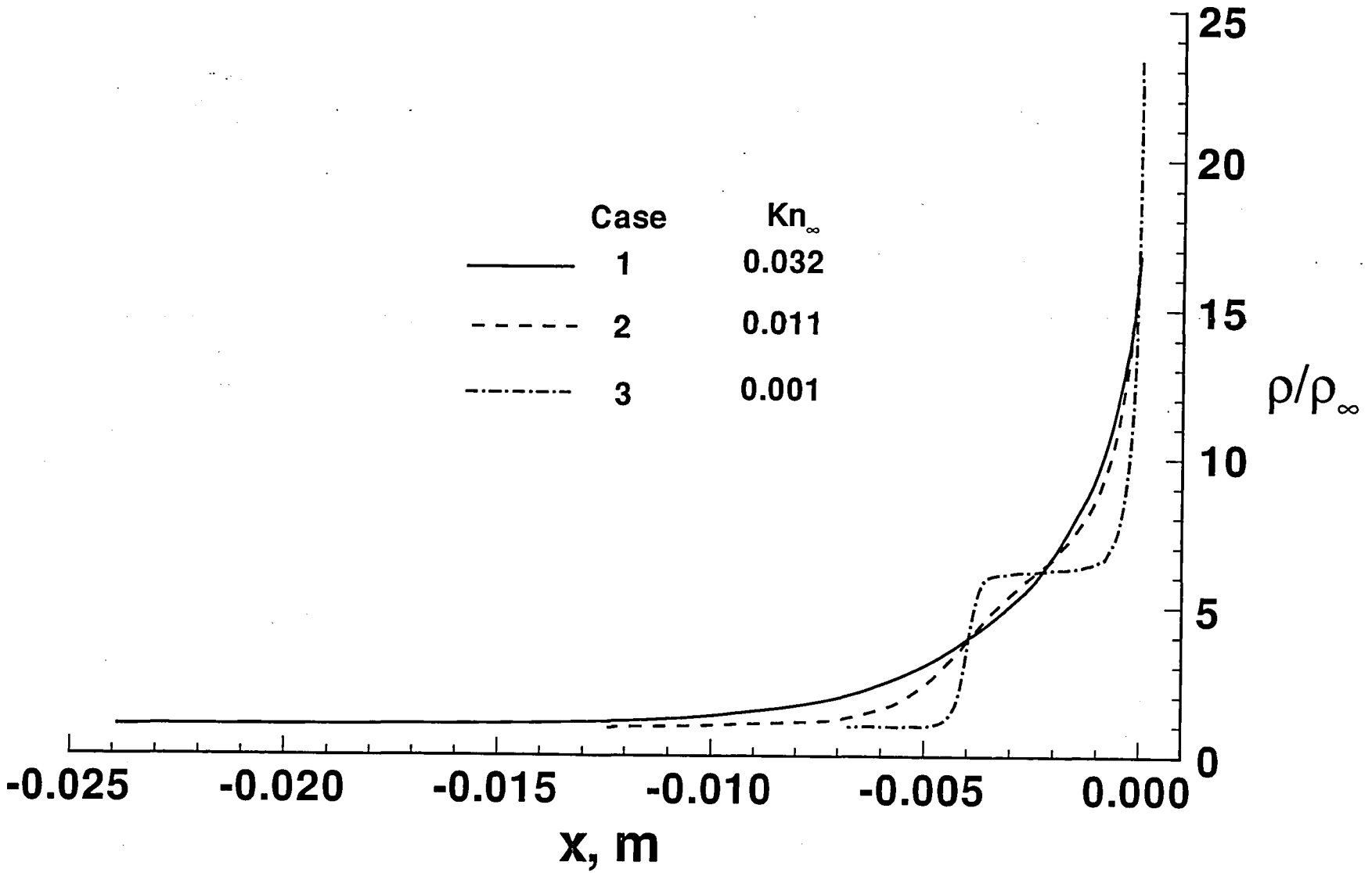

Fig. 44 Effect of rarefaction on the stagnation streamline density profiles.

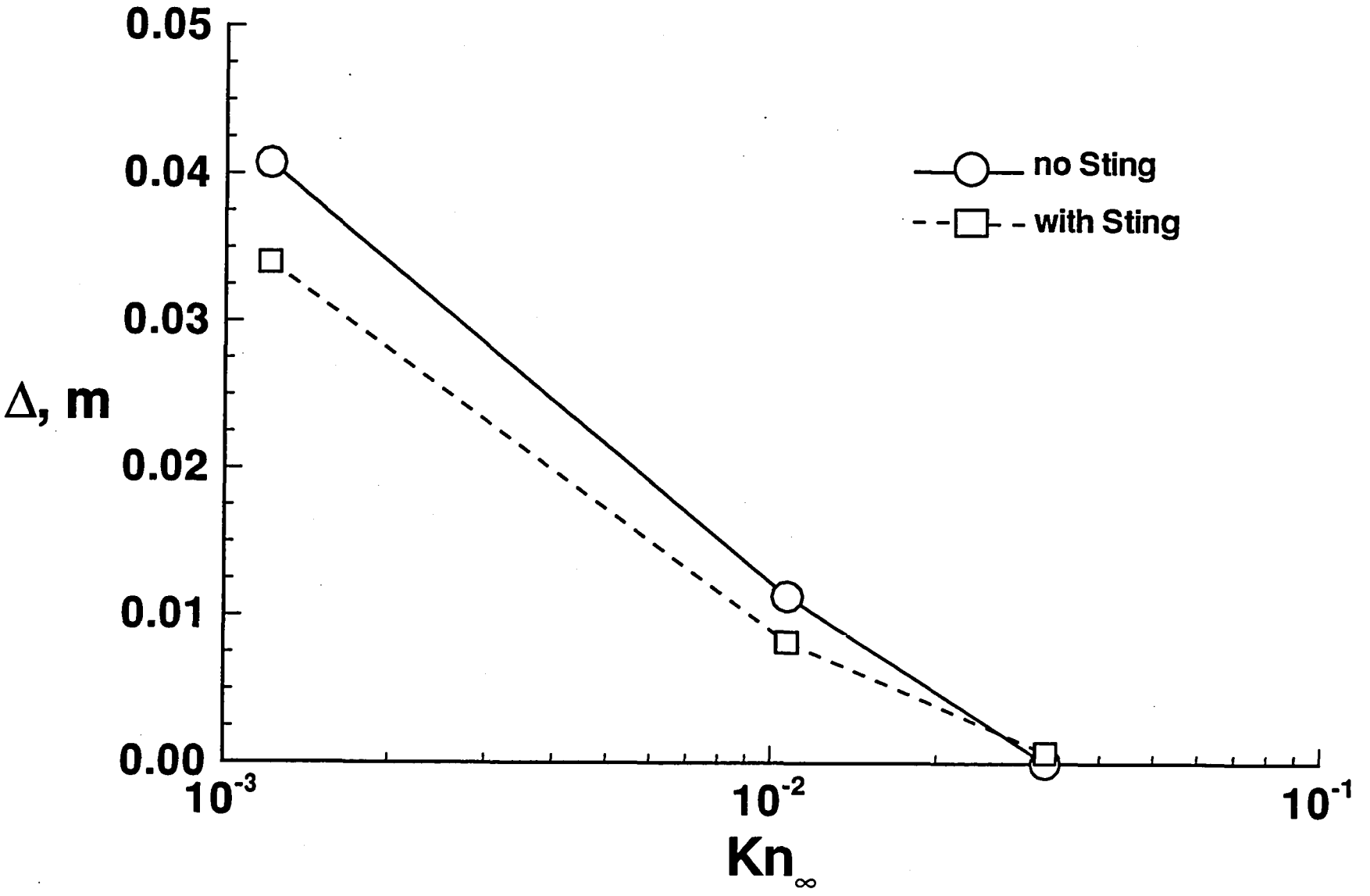

Fig. 45 Vortex size as function of Kn_∞.

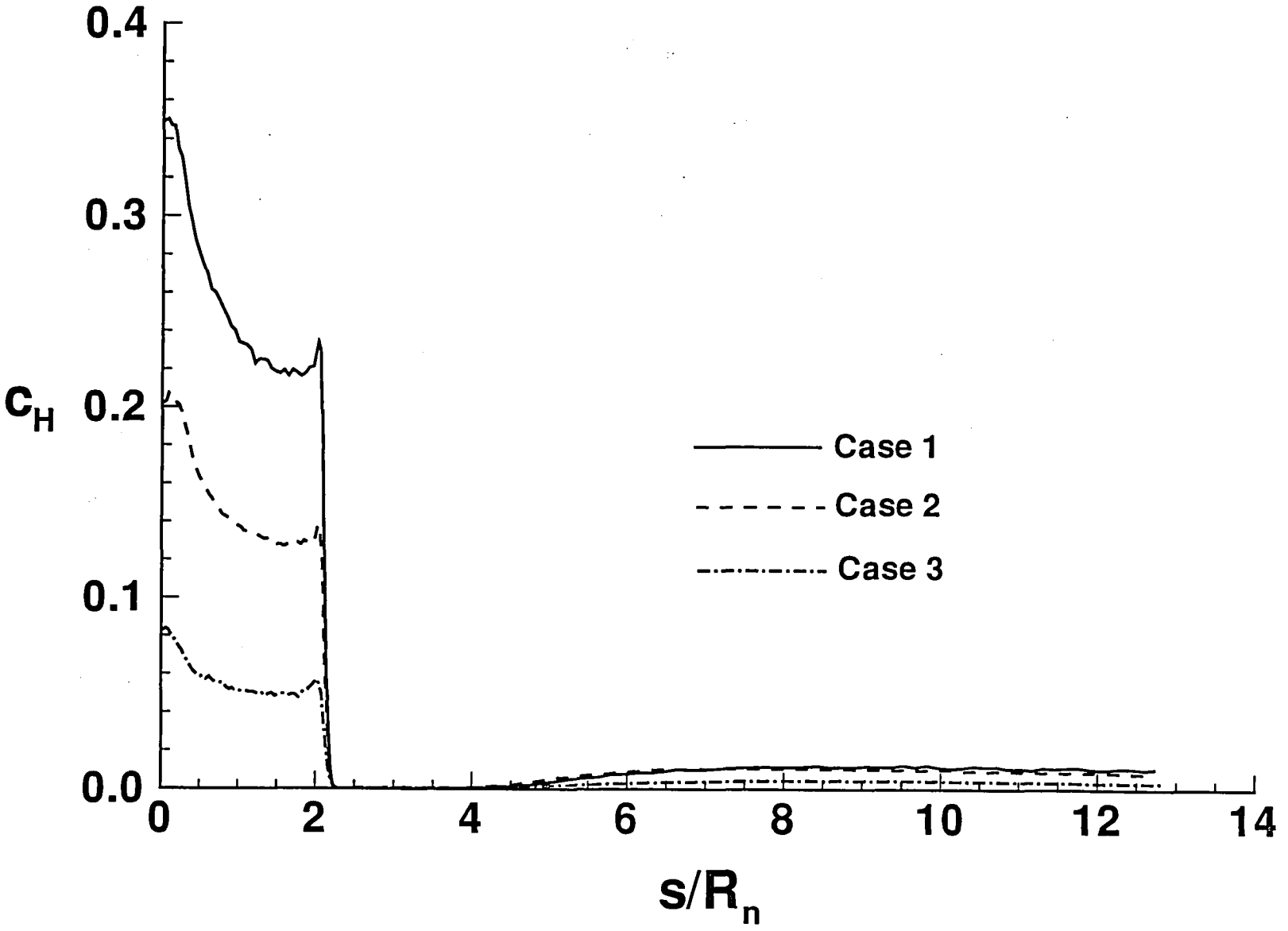

(a) Cartesian plot

Fig. 46 Effect of rarefaction on surface heating rate coefficient distribution.

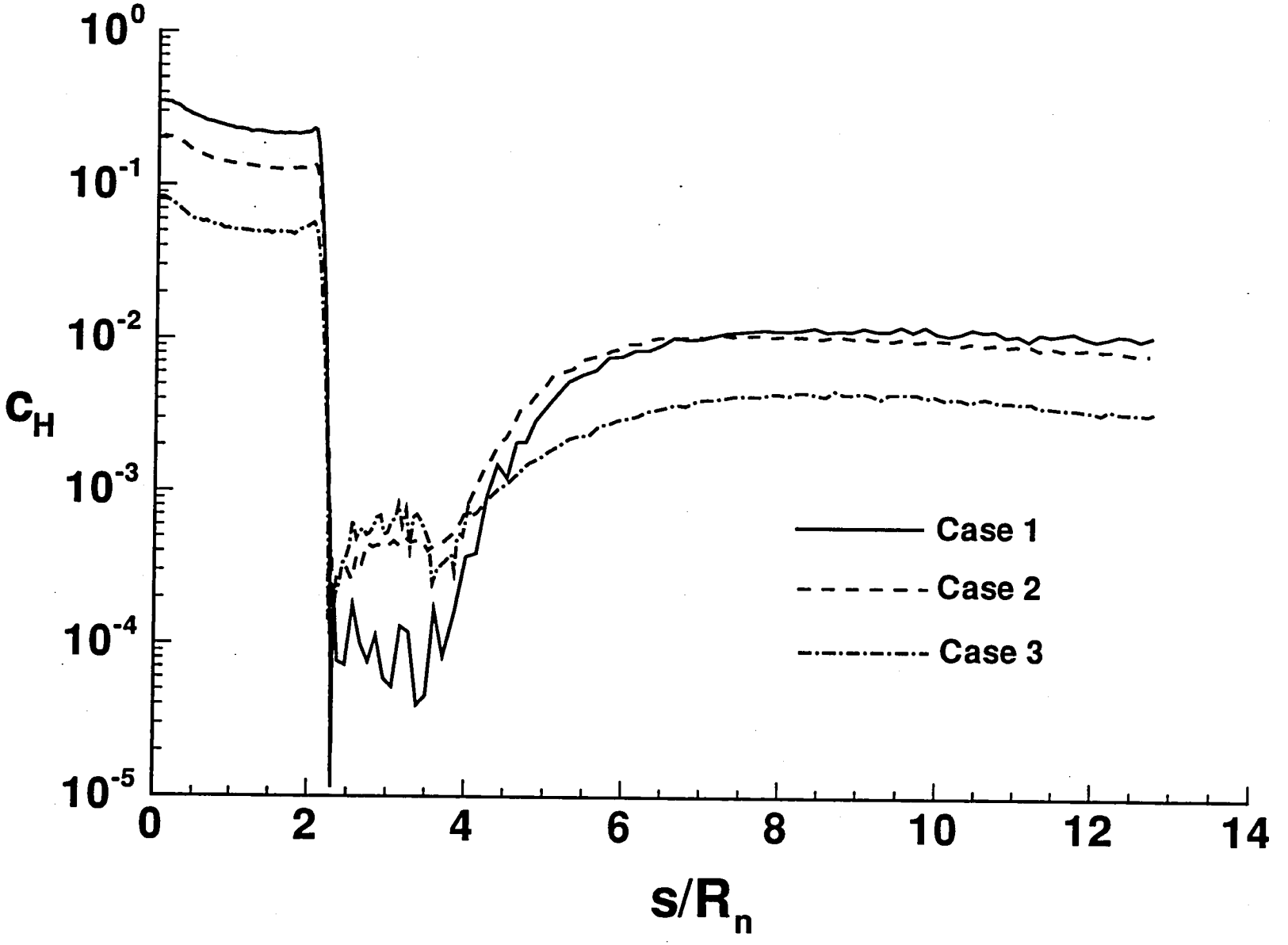

(b) Semilog plot

Fig. 46 Concluded.

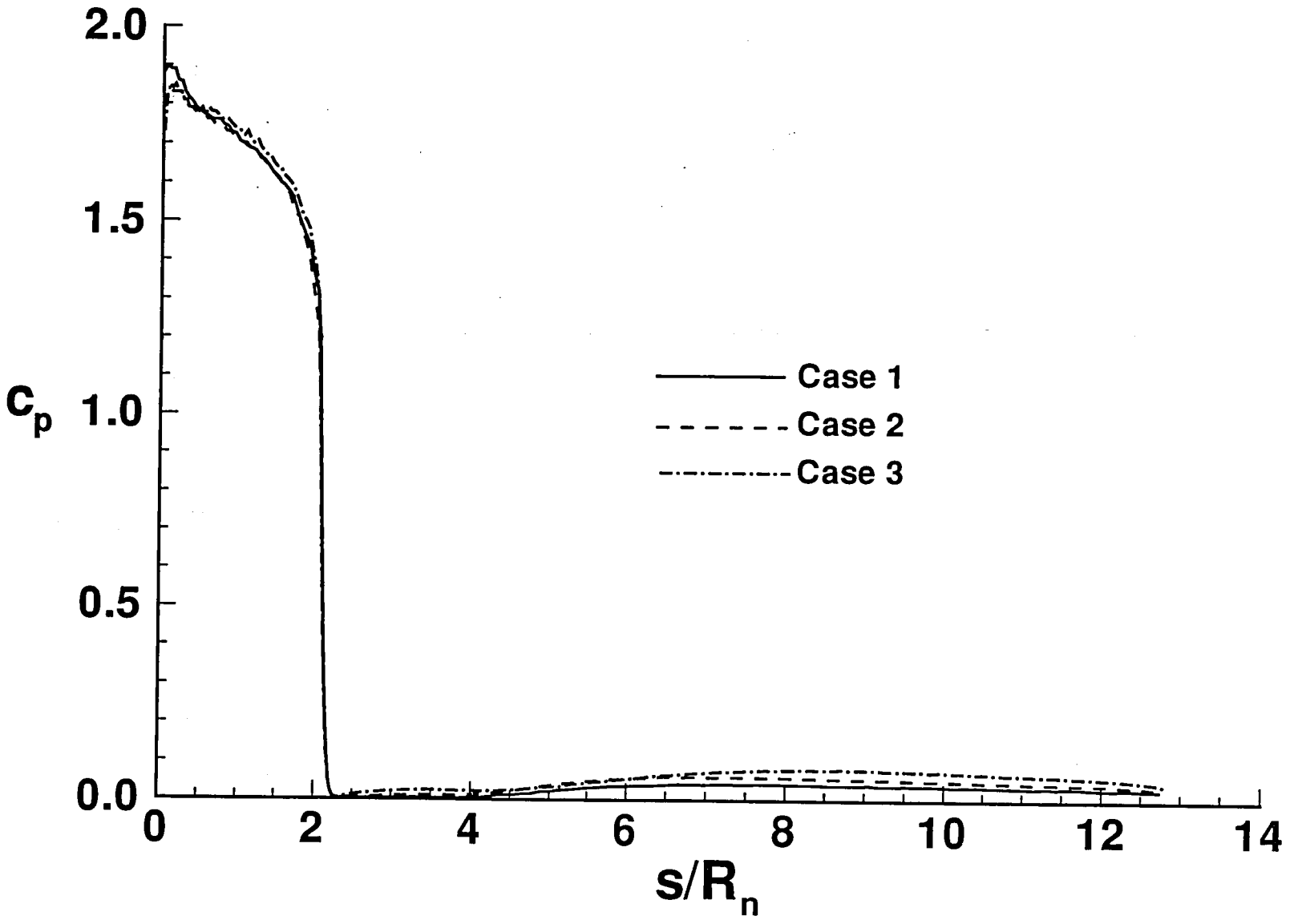

(a) Cartesian plot

Fig. 47 Effect of rarefaction on surface pressure coefficient distribution.

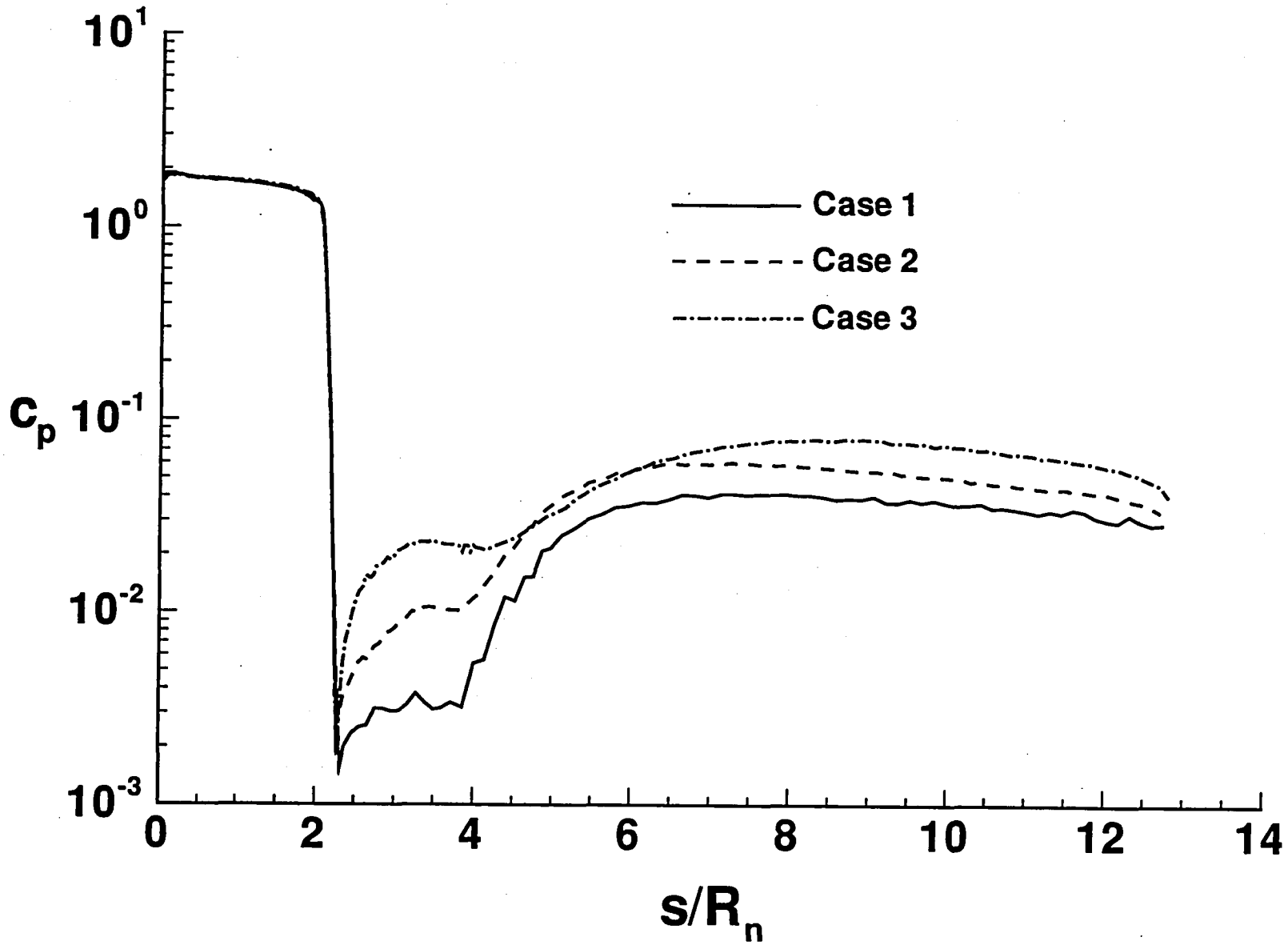

(b) Semilog plot

Fig. 47 Concluded.

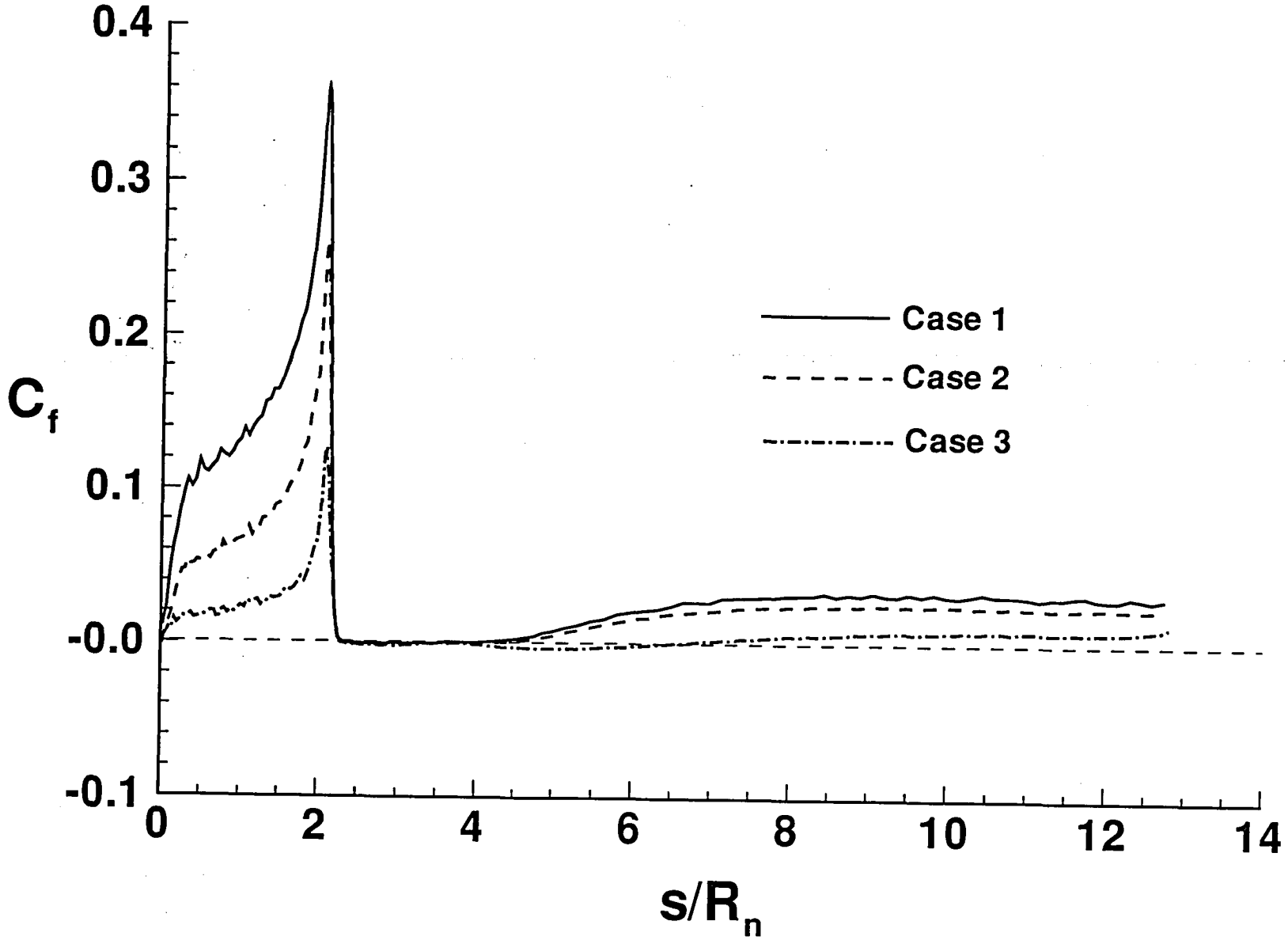

Fig. 48 Effect of rarefaction on skin friction distribution.

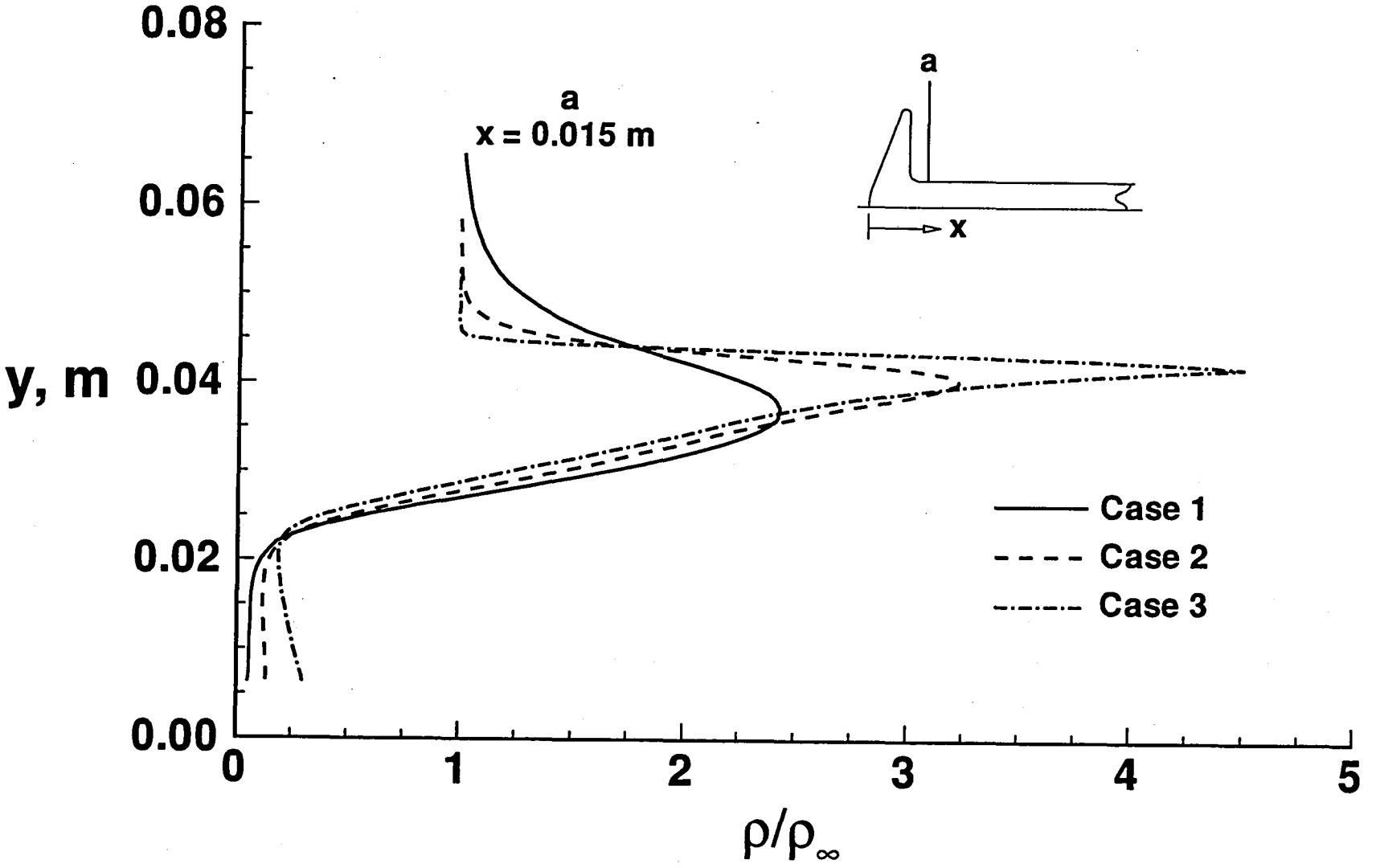

(a) Density profiles

Fig. 49 Effect of rarefaction on radial wake profile quantities 4.1 mm downstream of base plane.

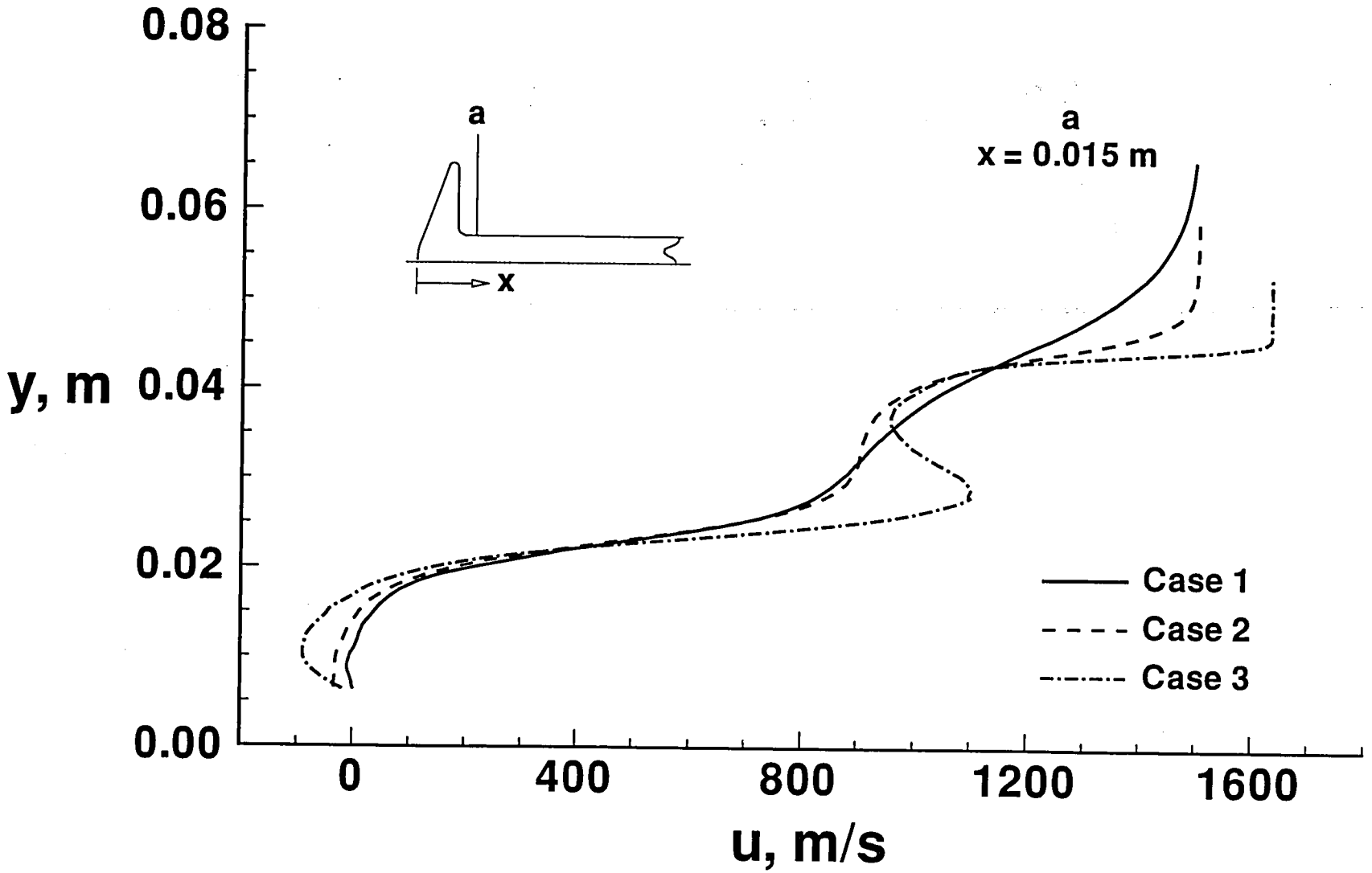

(b) Axial velocity profiles

Fig. 49 Continued.

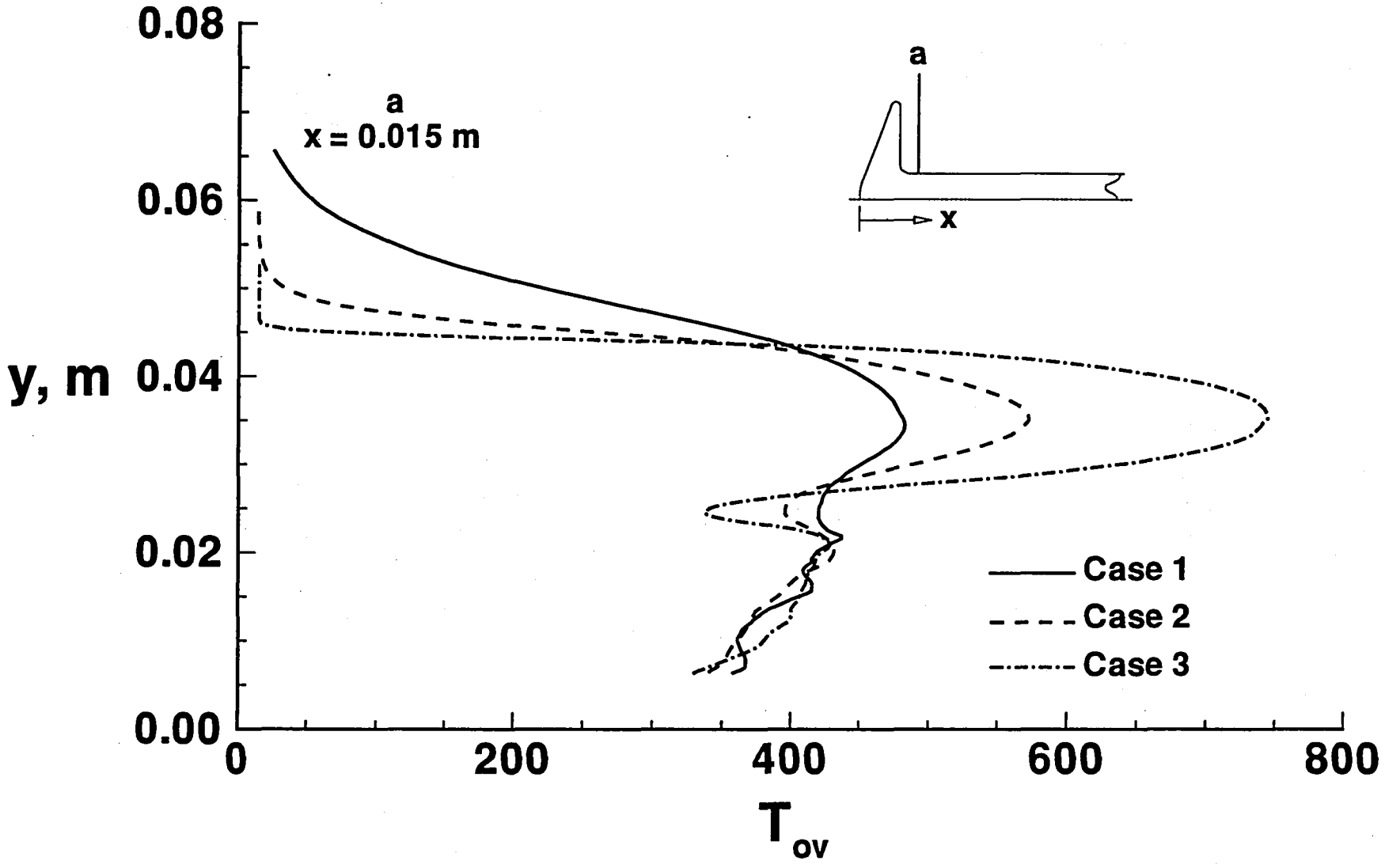

(c) Overall kinetic temperature profiles

Fig. 49 Continued.

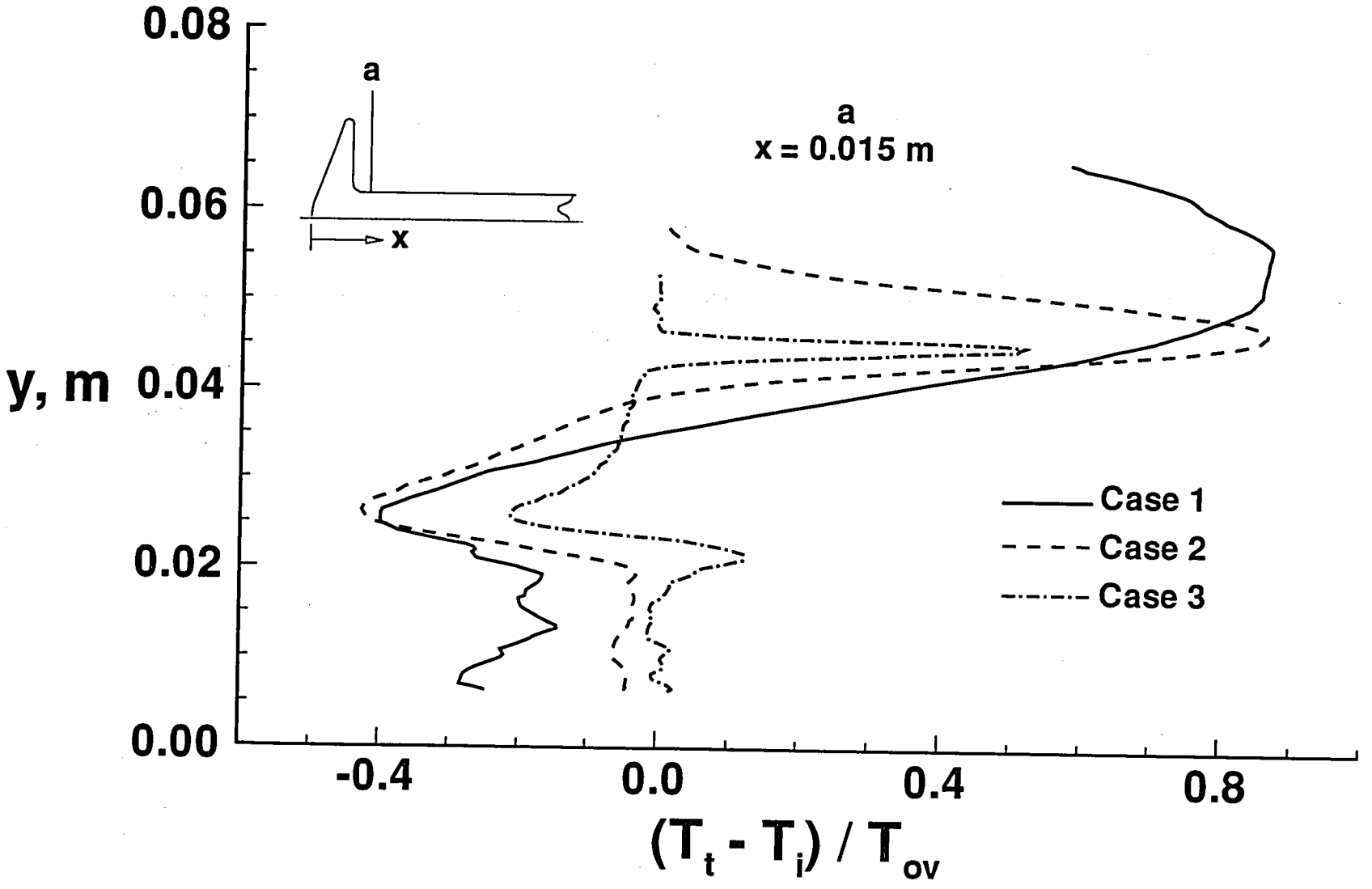

(d) Extent of thermal nonequilibrium

Fig. 49 Concluded.

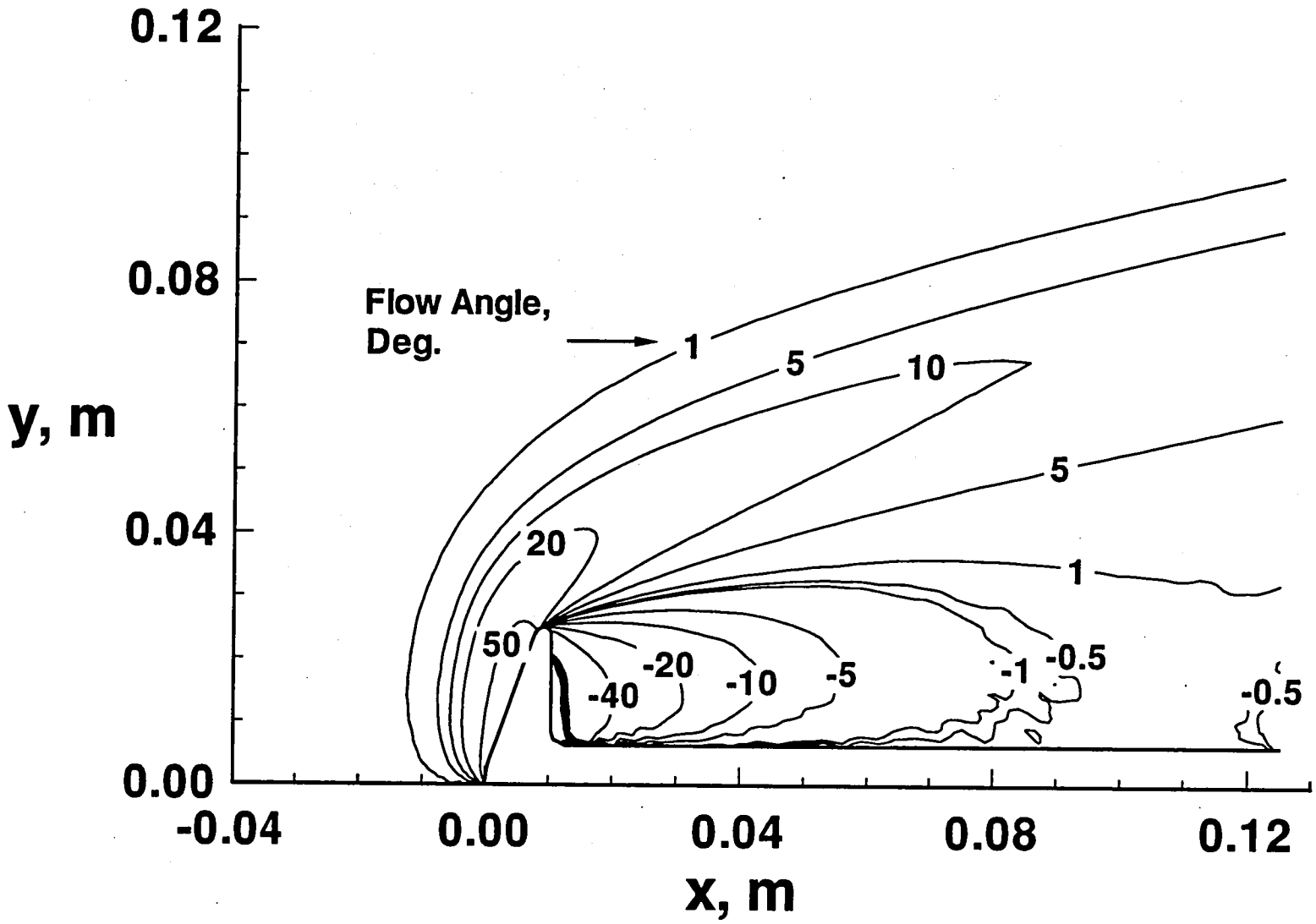

(a) Forebody and wake

Fig. 50 Flow angle contours for Case 1.

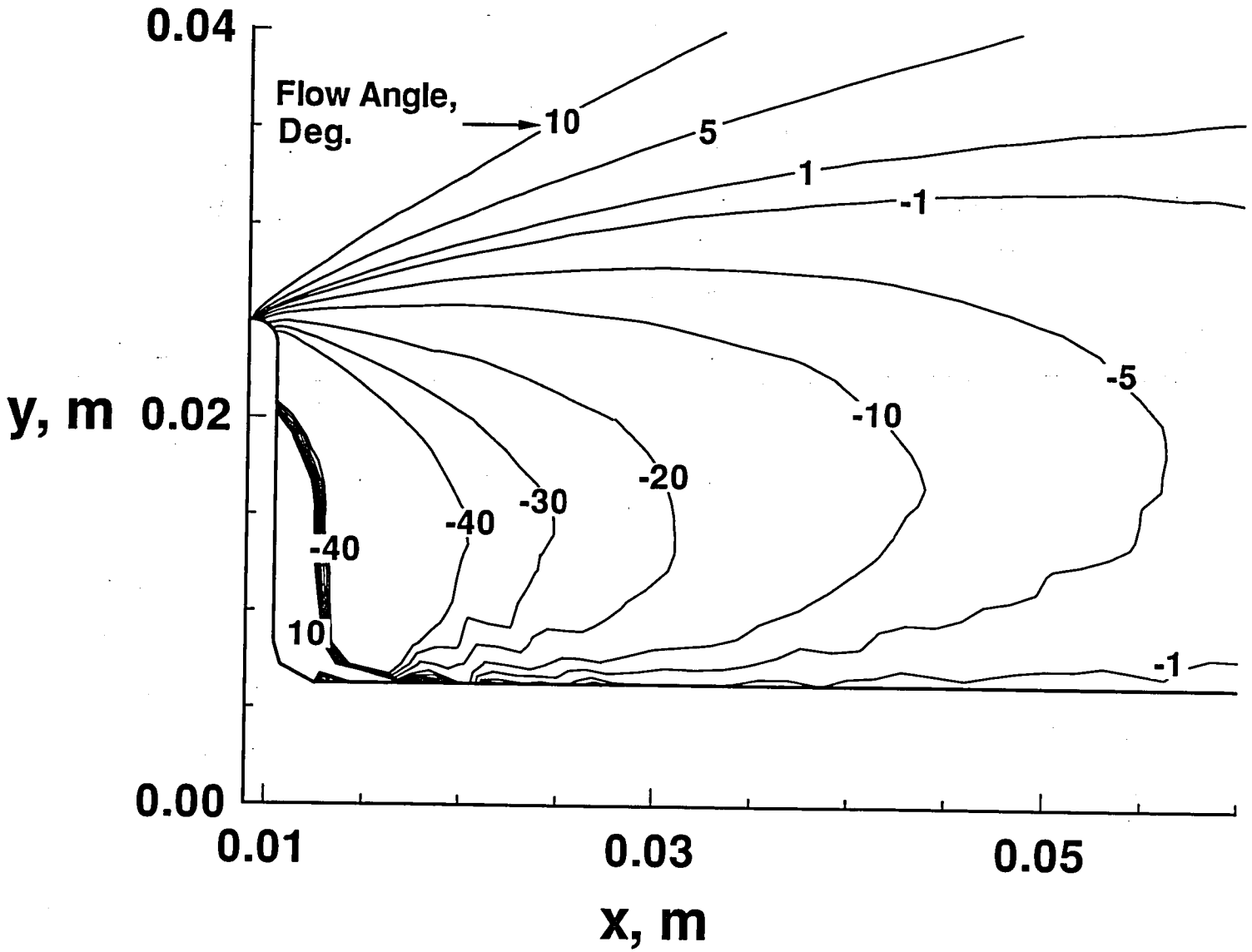

(b) Near wake

Fig. 50 Concluded.

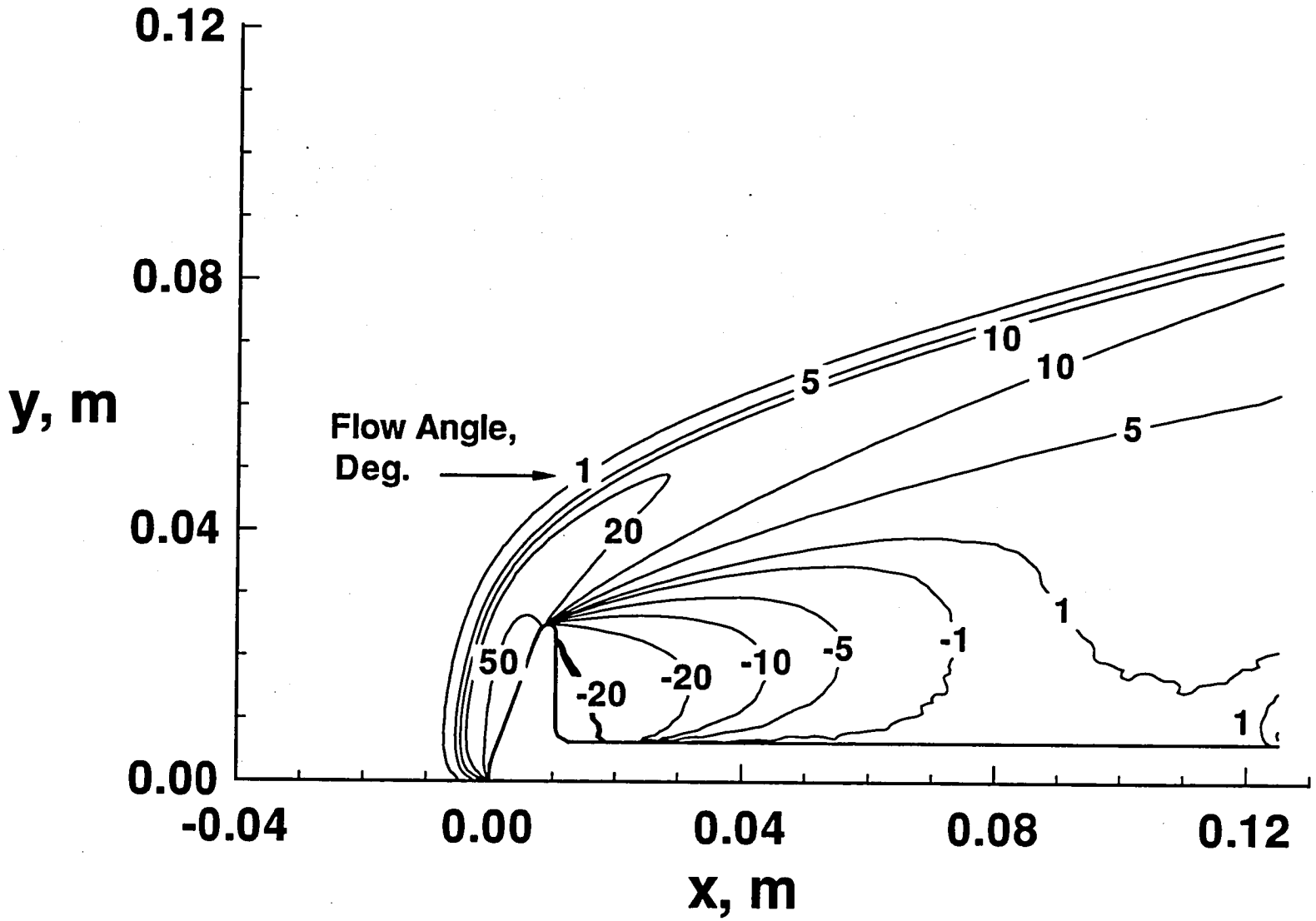

(a) Forebody and wake

Fig. 51 Flow angle contours for Case 2.

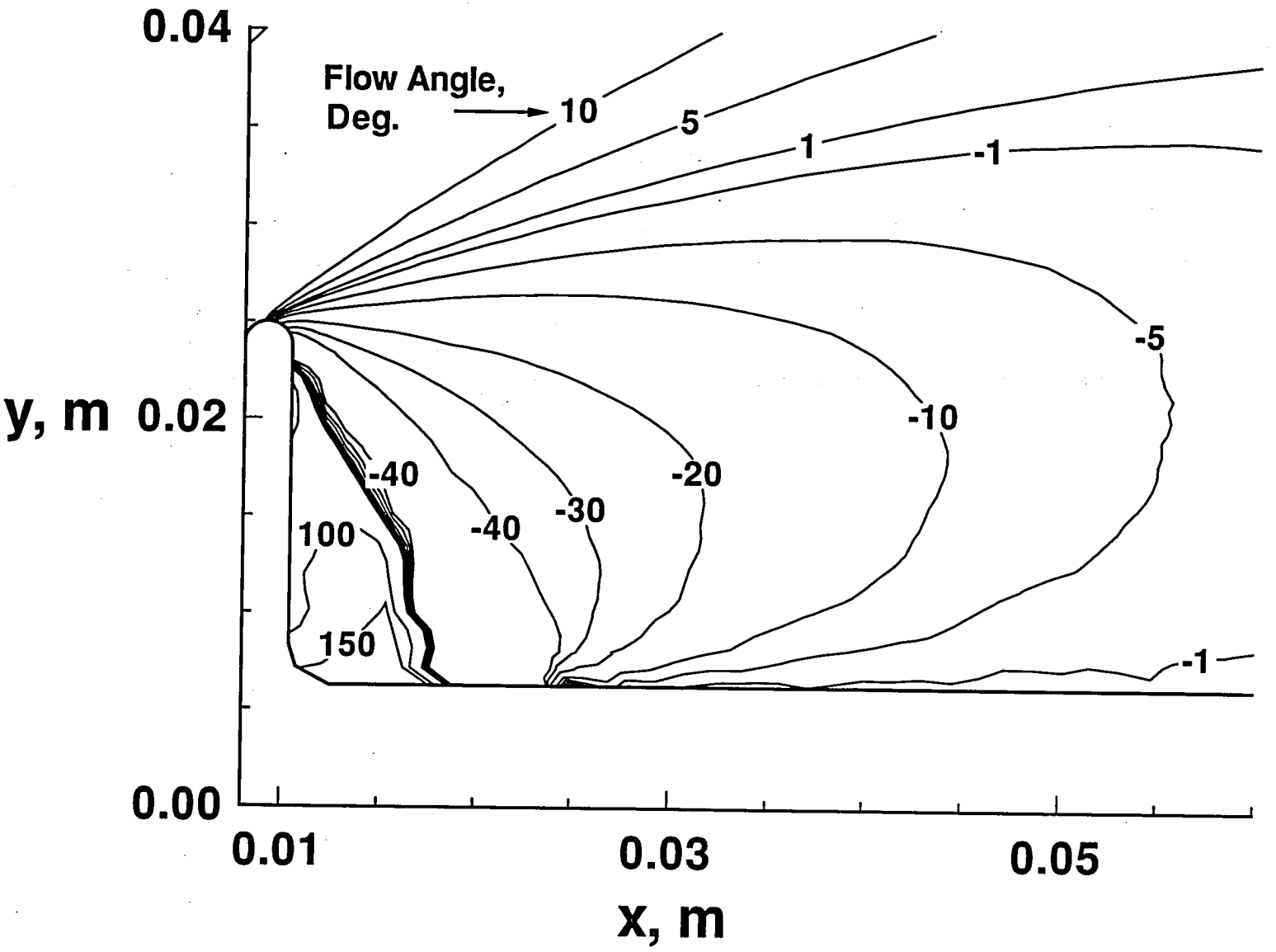

(b) Near wake

Fig. 51 Concluded.

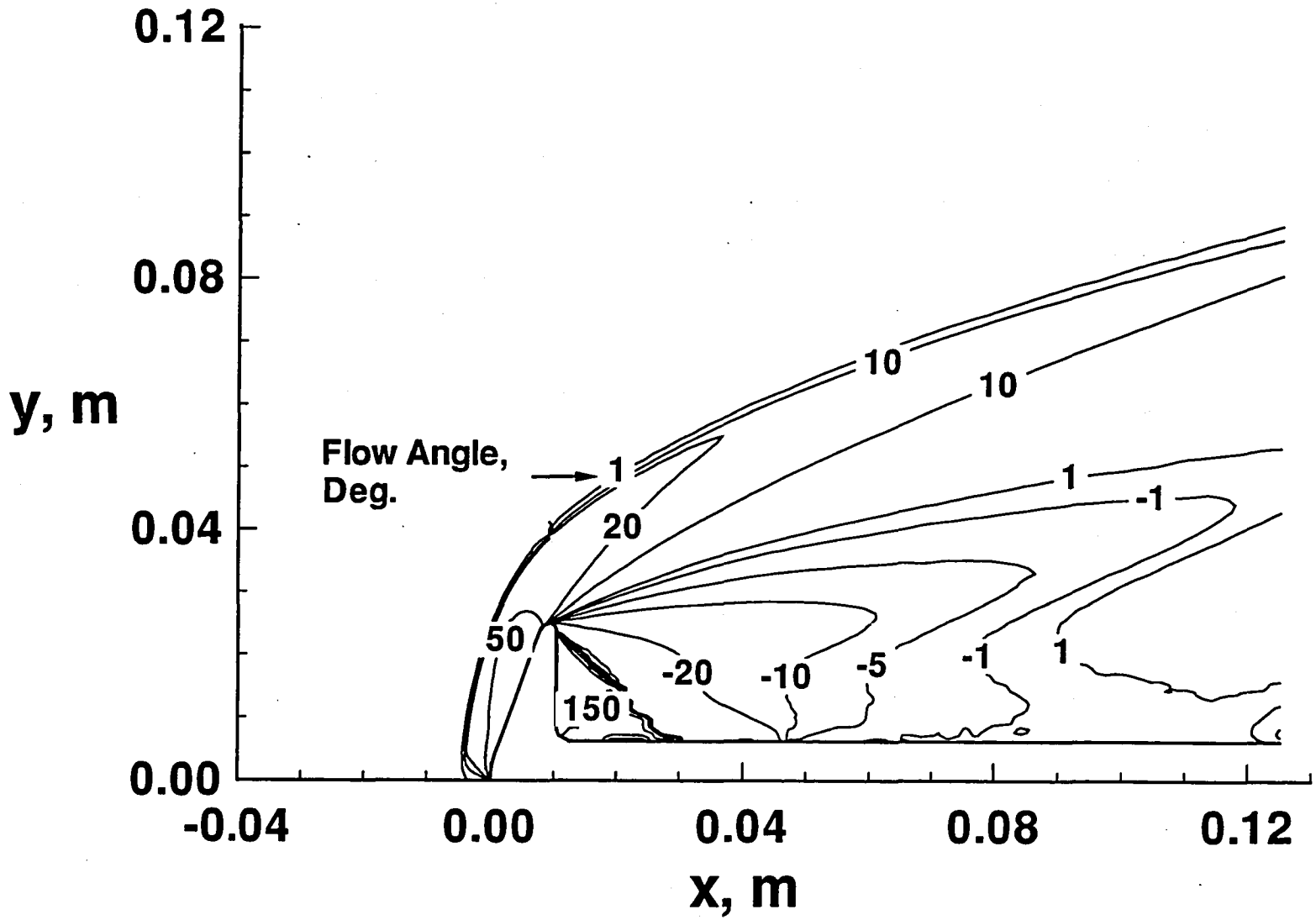

(a) Forebody and wake

Fig. 52 Flow angle contours for Case 3

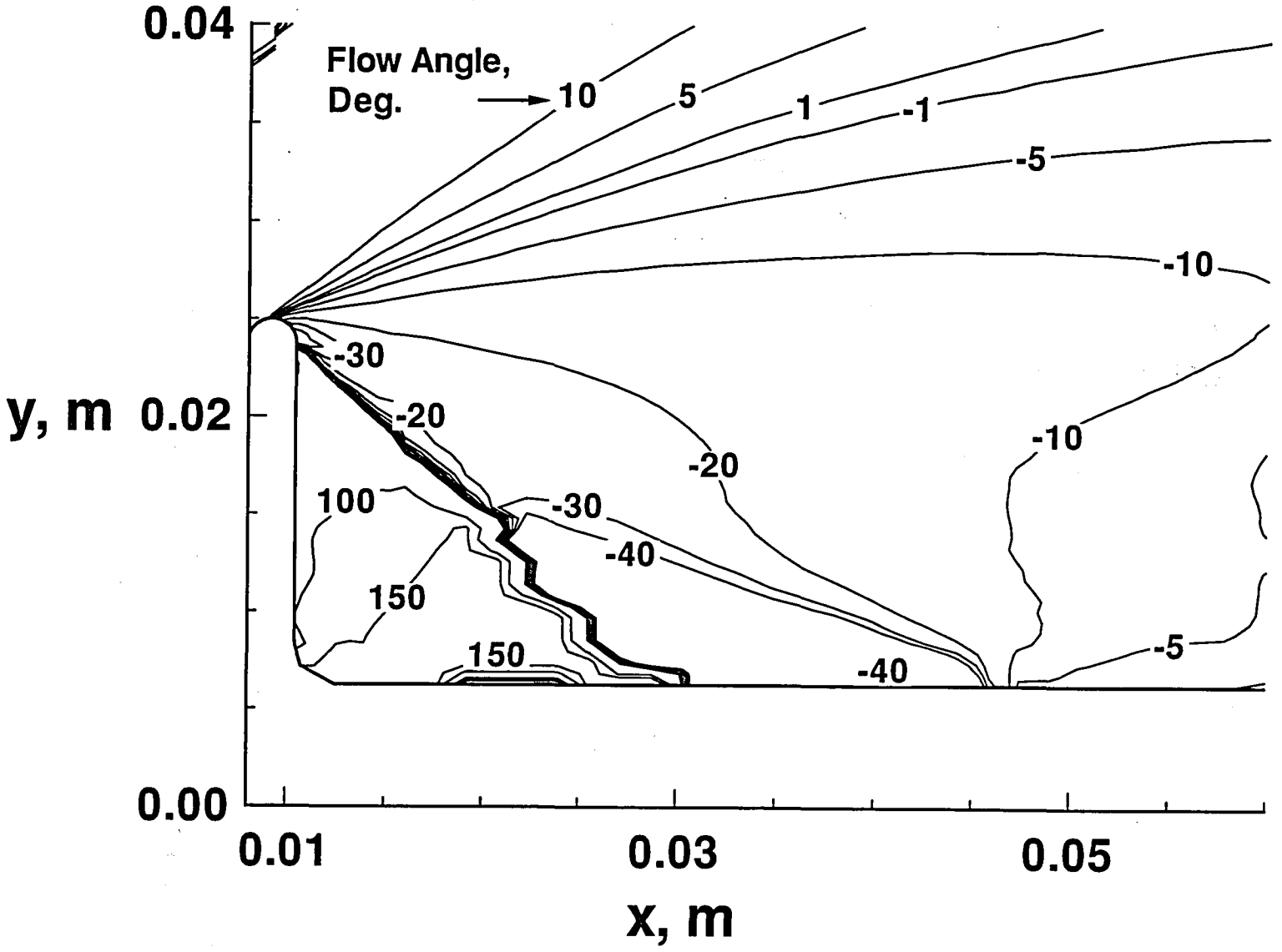

(b) Near wake

Fig. 52 Concluded.

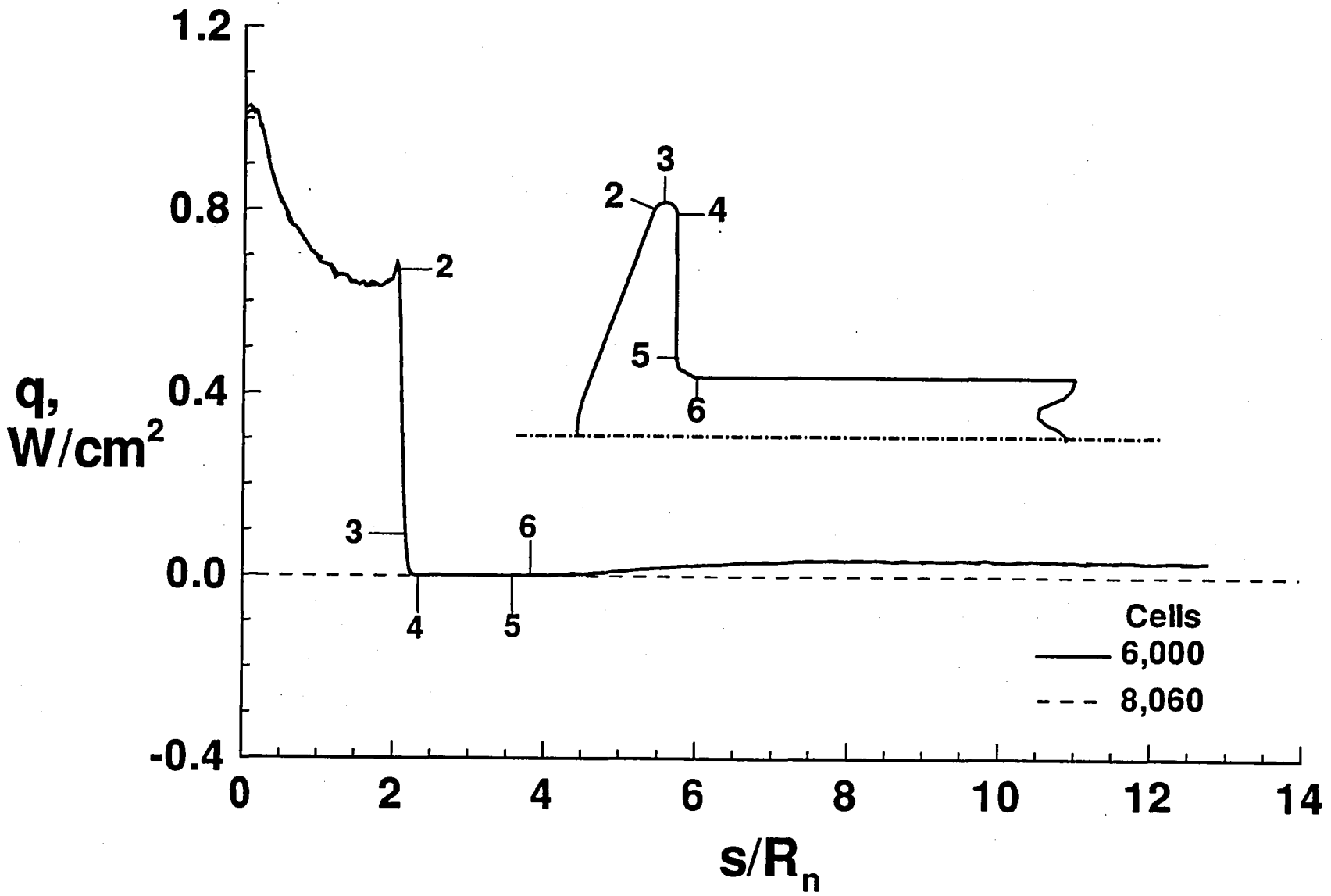

Fig. A1 Effect of grid refinement on surface heating rate distribution (Case 1).

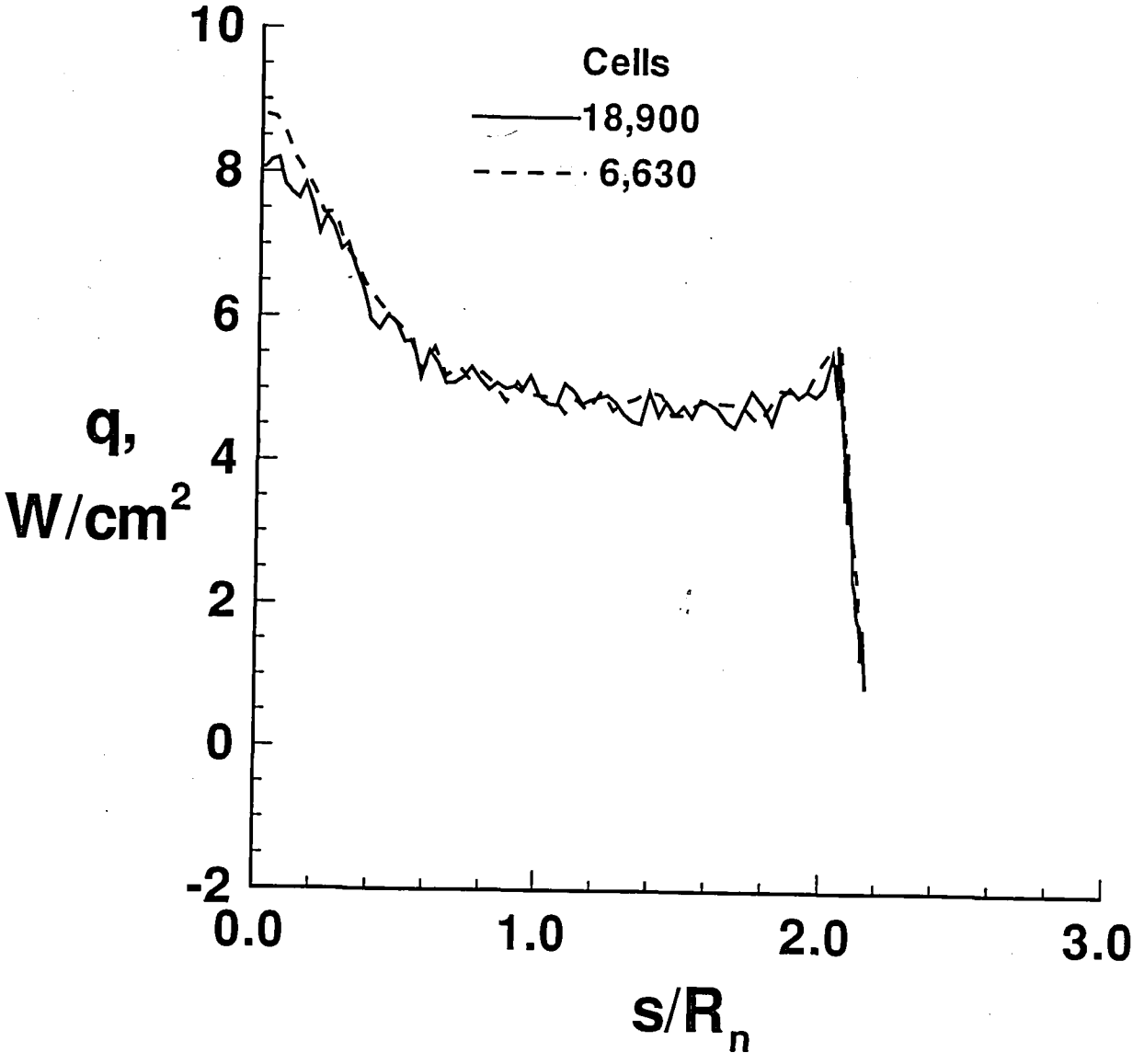

Fig. A2 Effect of grid refinement on surface heating rate distribution (Case 3).

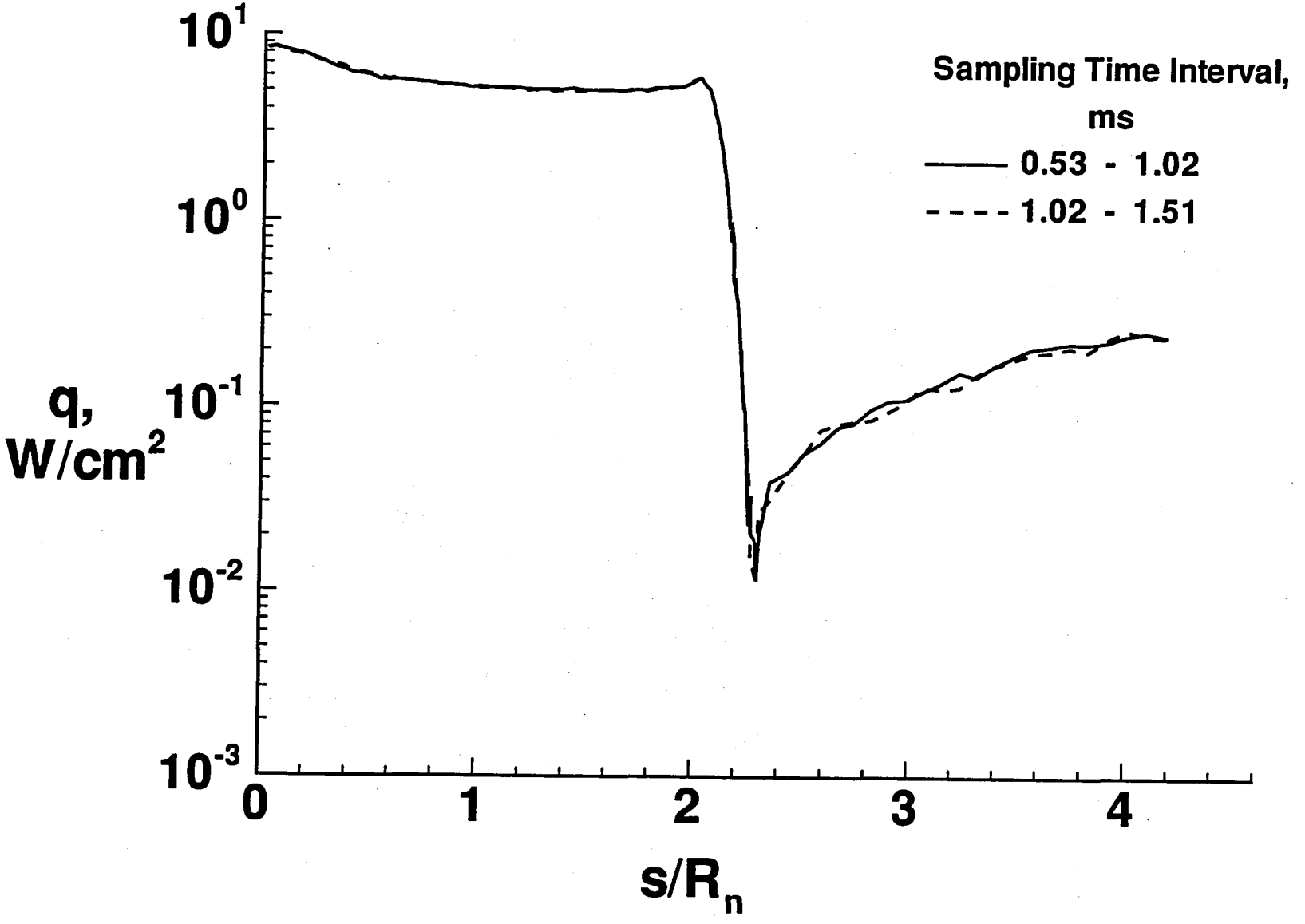

Fig. A3 Comparison of surface heating rate results for two consecutive time (time shown for region 1) sampling intervals for Case 3 (without sting).

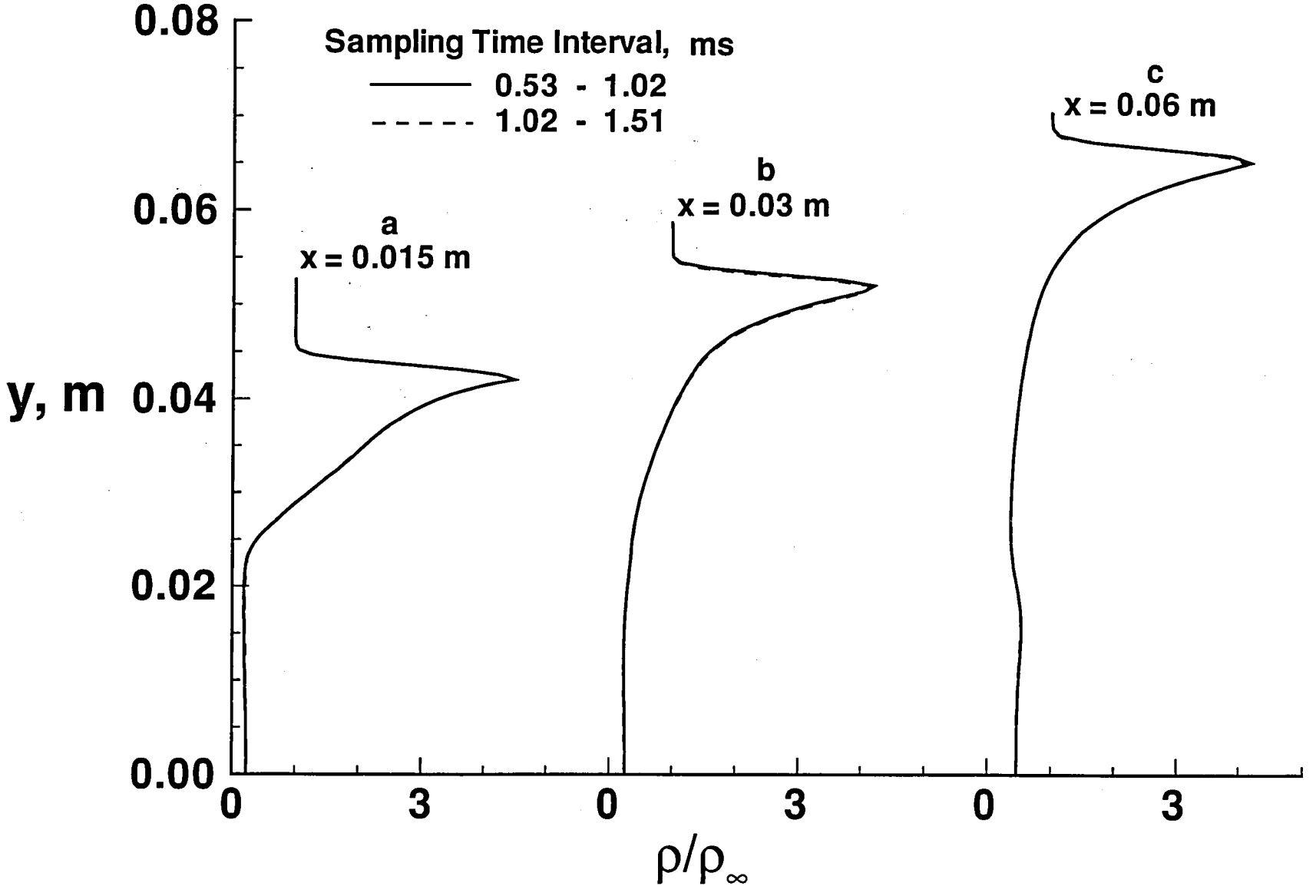

Fig. A4 Comparison of near wake density profiles at two consecutive time (time shown for region 1) sampling intervals for Case 3 (without sting).

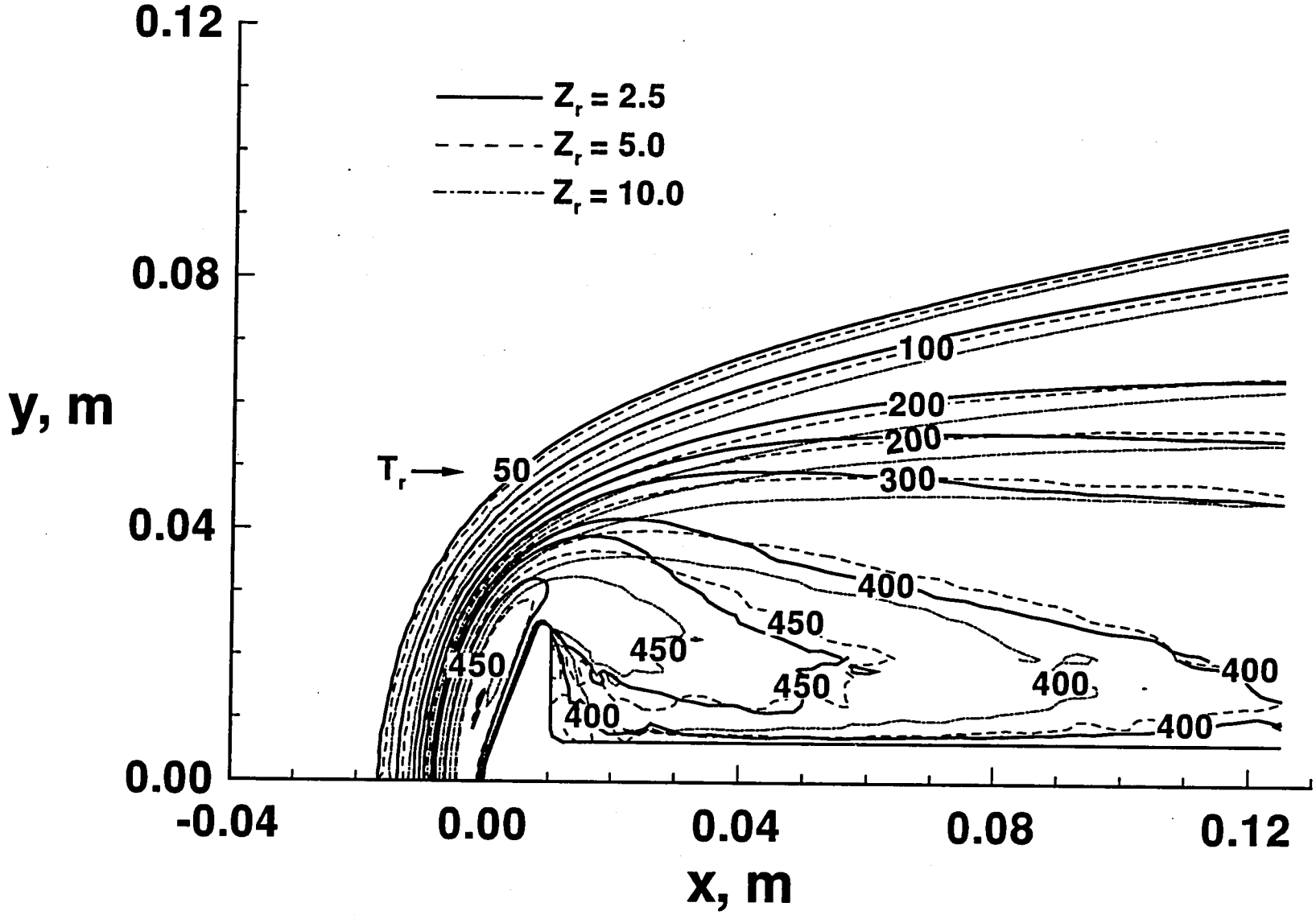

Fig. A5 Effect of rotational collision number, Z_r, on rotational temperature contours (Case 1).

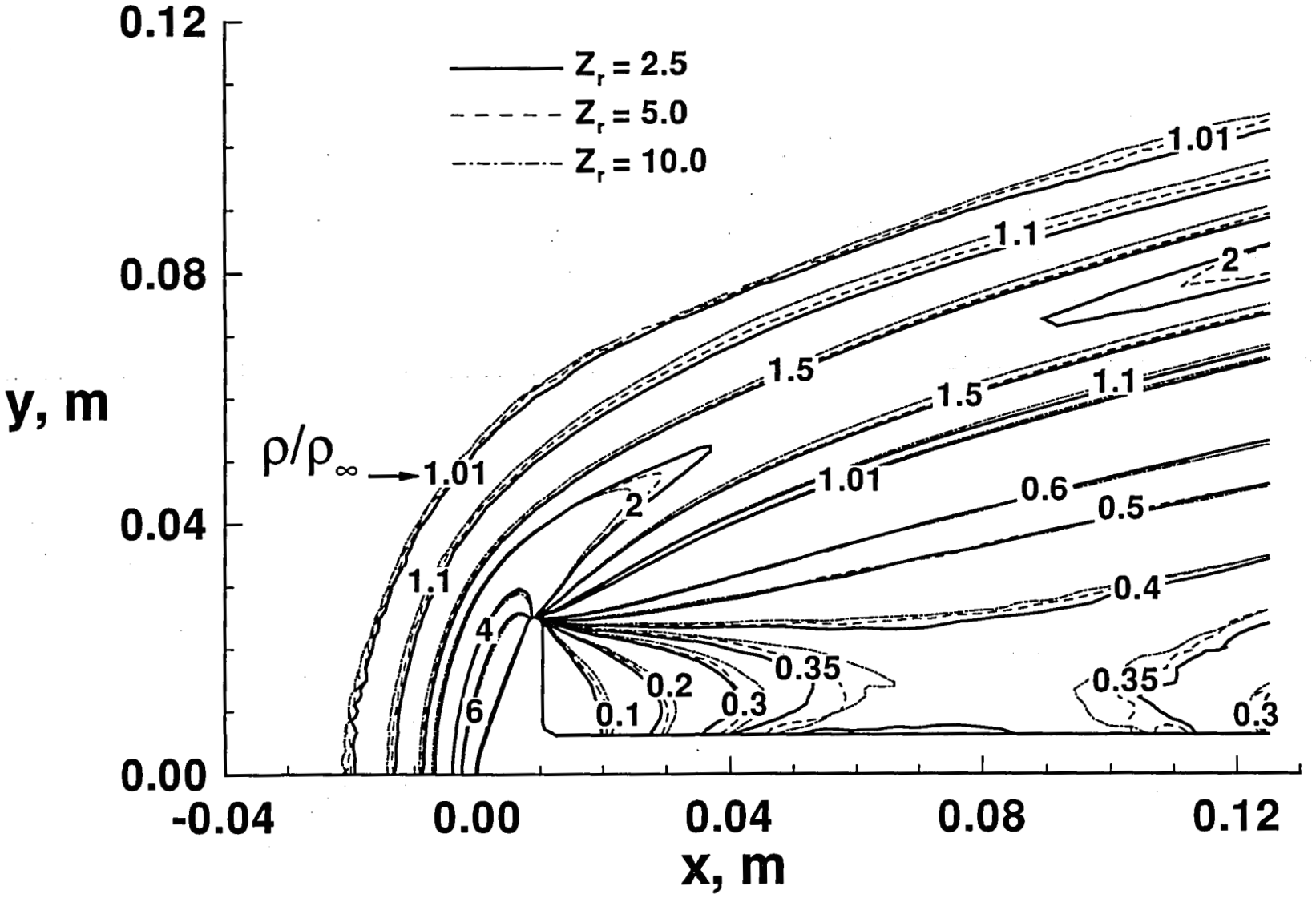

Fig. A6 Effect of rotational collision number, Z_r, on density contours (Case 1).

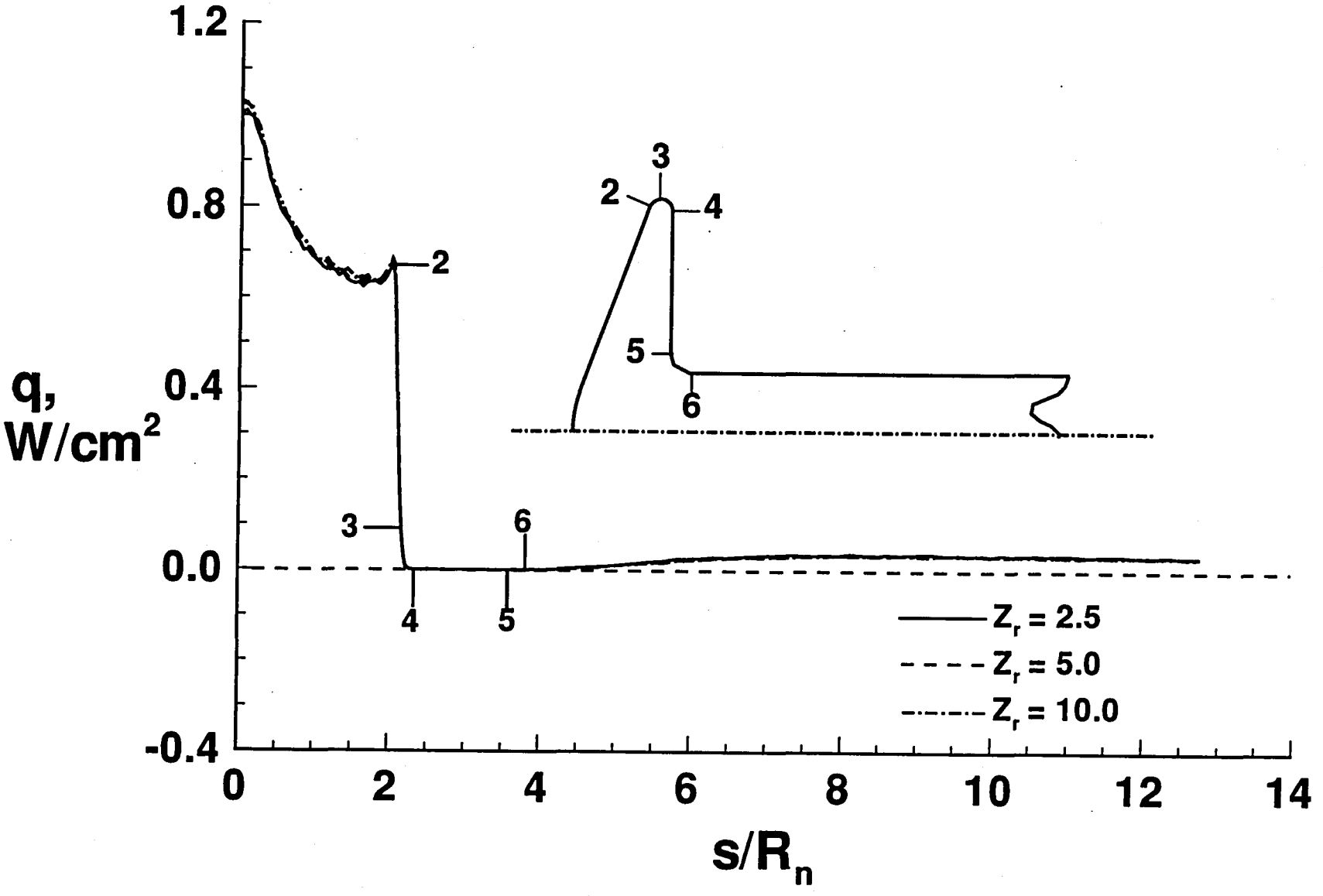

(a) Cartesian plot

Fig. A7 Effect of rotational collision number, Z_r, on surface heating predictions (Case 1).

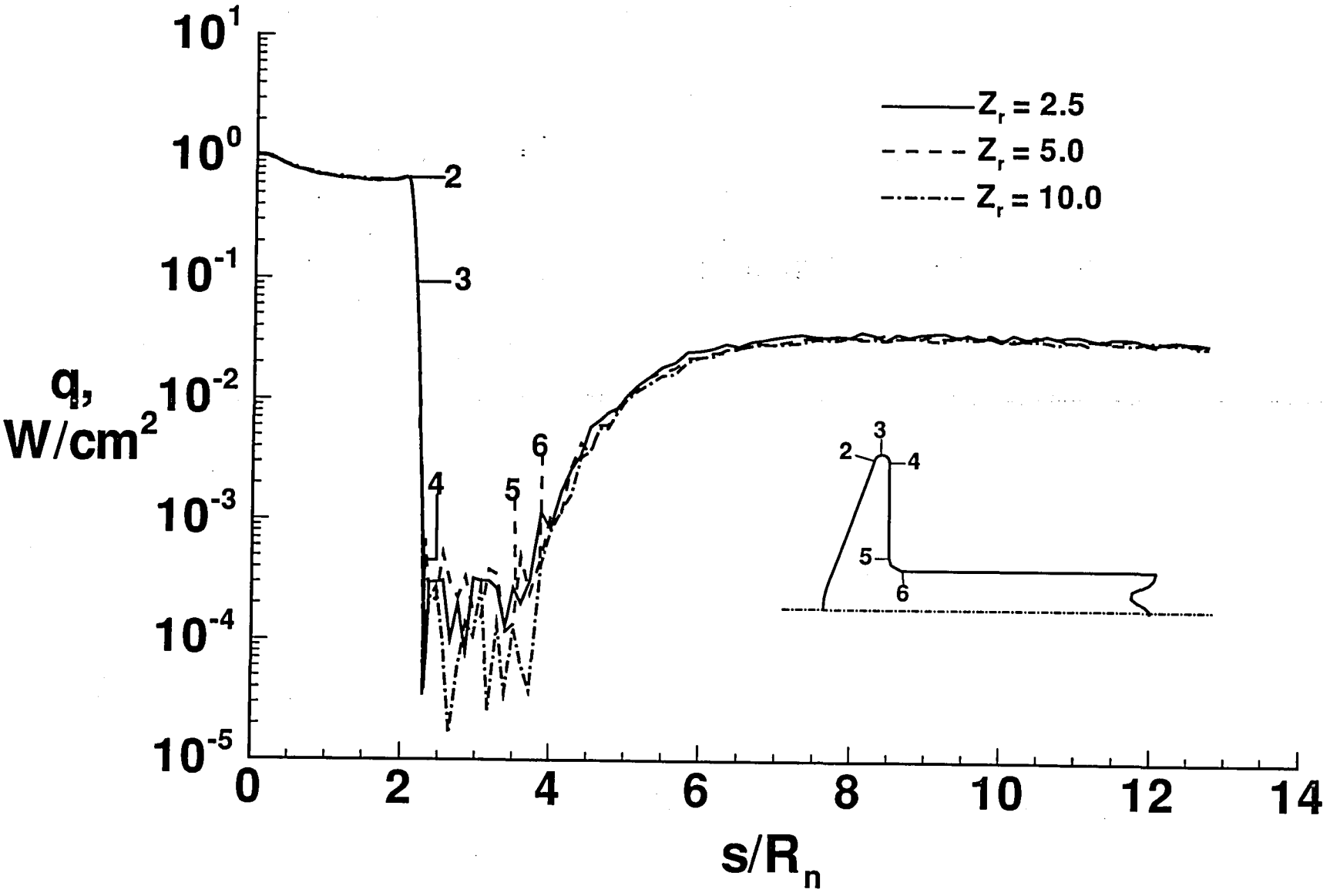

(b) Semilog plot

Fig. A7 Concluded.

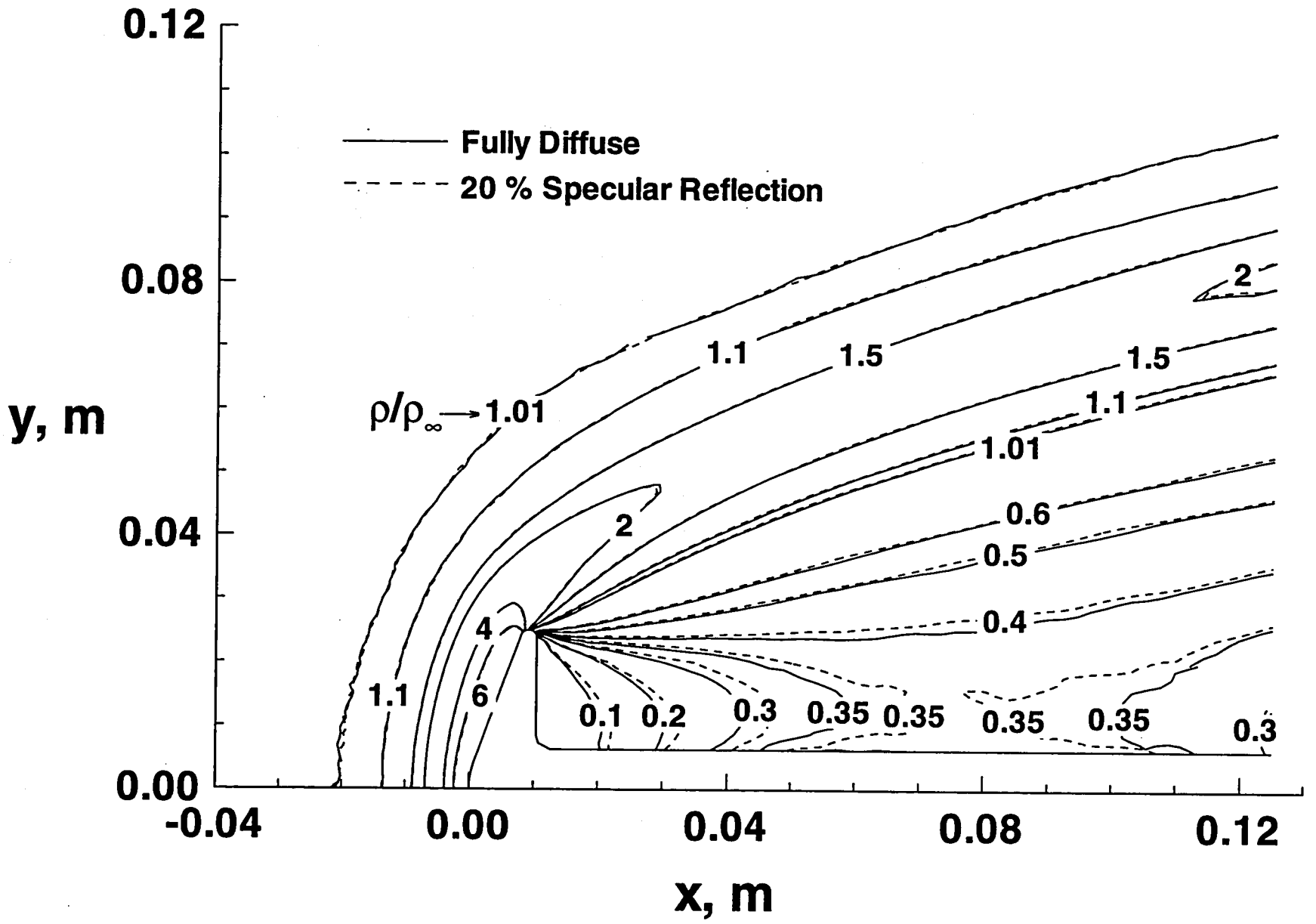

Fig. A8 Effect of surface reflection on density contours (Case 1).

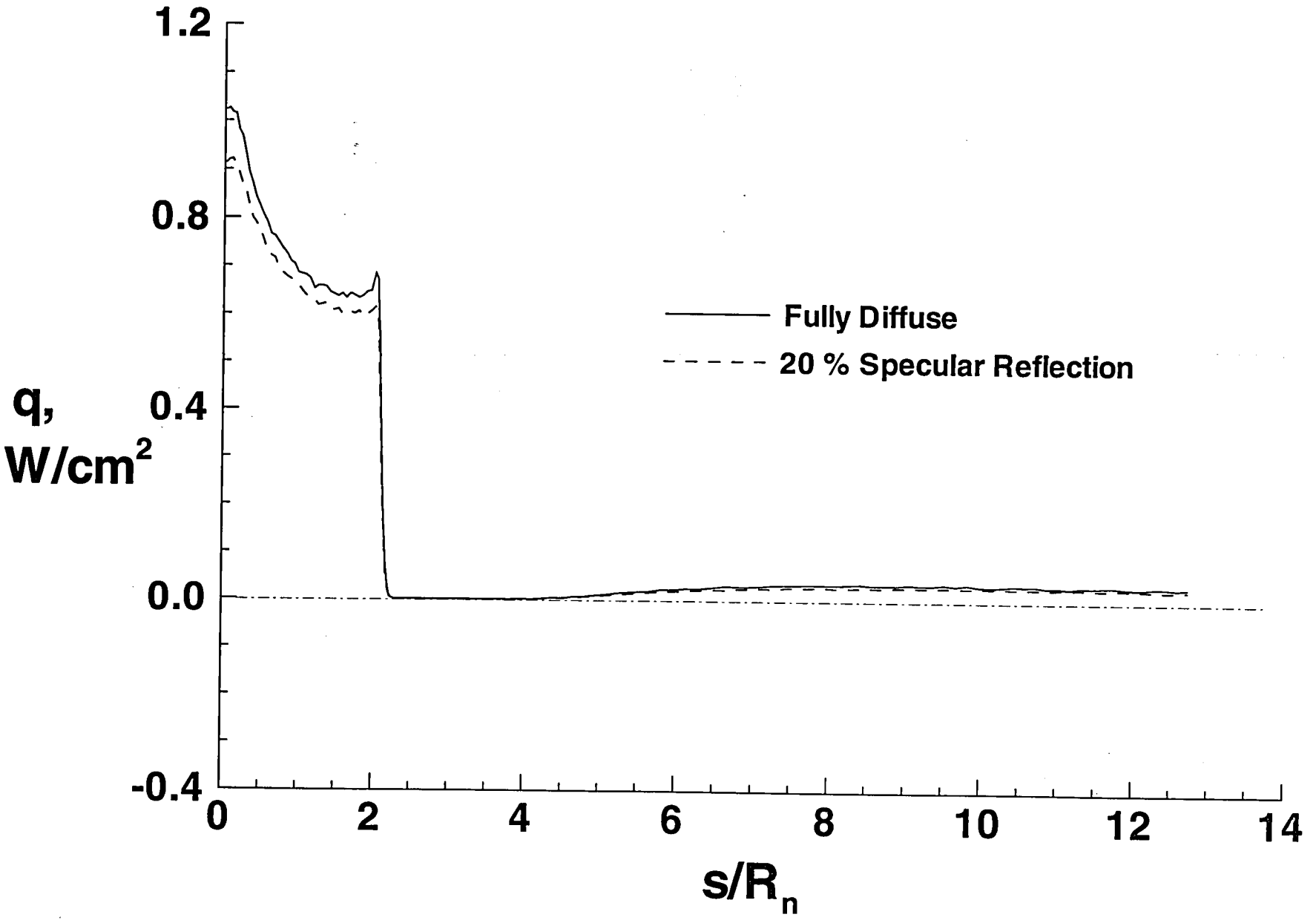

(a) Cartesian plot

Fig. A9 Effect of surface reflection on surface heating predictions (Case 1).

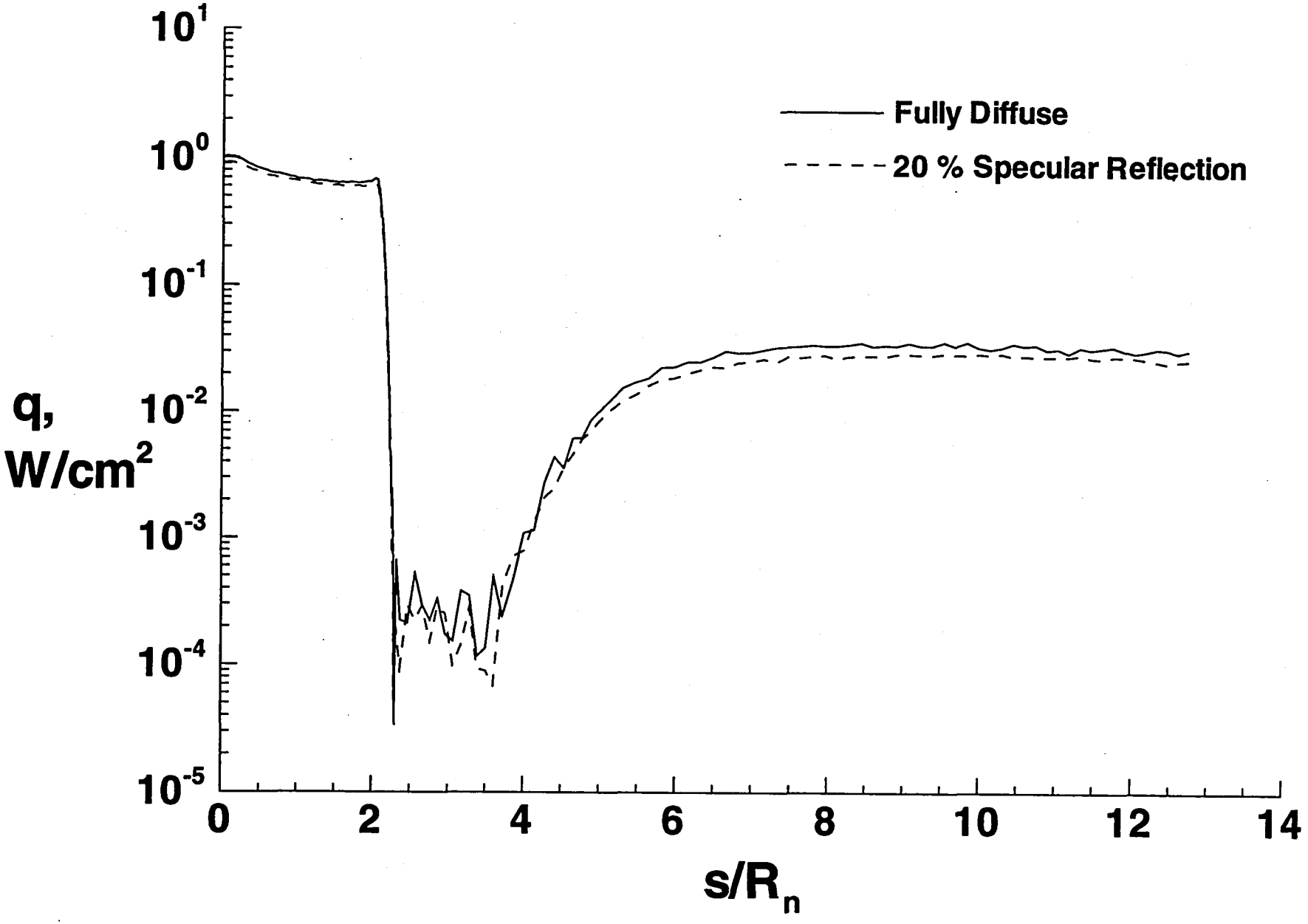

(b) Semilog plot.

Fig. A9 Concluded.

REPORT DOCUMENTATION PAGE

Form Approved
OMB No. 0704-0188

1. AGENCY USE ONLY (Leave blank)	2. REPORT DATE	3. REPORT TYPE AND DATES COVERED
	August 1993	Technical Memorandum

4. TITLE AND SUBTITLE

DSMC Simulations of Mach 20 Nitrogen Flows About a 70° Blunted Cone and its Wake

5. FUNDING NUMBERS

506-40-91-03

6. AUTHOR(S)

James N. Moss, Virendra K. Dogra, and Richard G. Wilmoth

7. PERFORMING ORGANIZATION NAME(S) AND ADDRESS(ES)

NASA Langley Research Center
Hampton, VA 23681-0001

8. PERFORMING ORGANIZATION REPORT NUMBER

9. SPONSORING/MONITORING AGENCY NAME(S) AND ADDRESS(ES)

National Aeronautics and Space Administration
Washington, DC 20546-0001

10. SPONSORING/MONITORING AGENCY REPORT NUMBER

NASA TM-107762

11. SUPPLEMENTARY NOTES

Moss: Langley Research Center, Hampton, VA; Dogra: ViGYAN, Inc., Hampton, VA; and Wilmoth: Langley Research Center, Hampton, VA.

12a. DISTRIBUTION/AVAILABILITY STATEMENT

Unclassified-Unlimited

Subject Category 34

12b. DISTRIBUTION CODE

13. ABSTRACT (Maximum 200 words)

Numerical results obtained with the direct simulation Monte Carlo (DSMC) method are presented for Mach 20 nitrogen flow about a 70-deg blunted cone. The flow conditions simulated are those that can be obtained in existing low-density hypersonic wind tunnels. Three sets of flow conditions are simulated with freestream Knudsen numbers ranging from 0.03 to 0.001. The focus is to characterize the wake flow under rarefied conditions. This is accomplished by calculating the influence of rarefaction on wake structure along with the impact that an afterbody has on flow features. This data report presents extensive information concerning flowfield features and surface quantities.

14. SUBJECT TERMS

direct simulation Monte Carlo (DSMC), blunted cone, Knudsen numbers, and flowfield

15. NUMBER OF PAGES

157

16. PRICE CODE

A08

17. SECURITY CLASSIFICATION OF REPORT	18. SECURITY CLASSIFICATION OF THIS PAGE	19. SECURITY CLASSIFICATION OF ABSTRACT	20. LIMITATION OF ABSTRACT
Unclassified	Unclassified		